FORSCHUNGSZENTRUM
ROSSENDORF e.V.
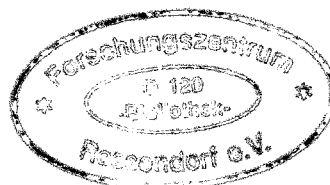
FZR

Archiv-Ex.:

$F2R - 32$

INSTITUTE OF BIOINORGANIC
AND RADIOPHARMACEUTICAL
CHEMISTRY

Annual Report 1993

Editor: B. Johannsen

CONTENTS

I.
INTRODUCTION

The *Institute of Bioinorganic and Radiopharmaceutical Chemistry of the Research Center Rossendorf Inc. (FZR)* herewith presents its 1993 Annual Report to document research activities in the second year of its existence.

The Institute's research programme and profile are derived from an awareness of the very important advances taking place in modern nuclear medicine. Based on sophisticated radiotracers and focused on the molecular level, nuclear medicine offers unique opportunities for studying tissue functions and translating the findings into ways of caring for sick people. For full exploitation of its potential, this discipline of *in vivo* chemistry requires great commitment to interdisciplinary research into radiotracers and a thorough appreciation of the complexity involved. Contributions from radiochemistry, organic and inorganic chemistry, radiopharmacy, radiopharmacology, physics, biology and medicine have all to be combined and merge in tracer design. The Institute's profile is such that it is prepared for the challenge of sophisticated interdisciplinary work in order to gain deeper insights into the fundamentals of the chemistry and biobehaviour of biochemical tracers.

With the emphasis on biochemical processes, positron emission tomography (PET) is the essential modality for assessing the global and regional functional status of the brain, heart or other organs of interest.
The task of establishing a PET centre - which calls for substantial scientific, financial and administrative commitment - has so far dominated the activities of the Institute.

Since single photon emission computed tomography (SPECT) continues to be the principal way of translating PET advances into broad clinical practice, specific SPECT tracers are one of the main subjects of research. An analogue concept of rational tracer design makes it possible to go from ^{11}C or ^{18}F PET tracers to ^{123}I SPECT tracers. A similar straightforward concept of development of biochemical tracers does not exist for ^{99m}Tc, the workhorse of nuclear medicine. Technetium has an intricate coordination chemistry that does not go well with the organic nature of biochemical substrates. Overcoming this problem as fast as possible by gaining a better insight into technetium chemistry and exploiting its versatility is a crucial task.

With this aim in mind our Institute's SPECT tracer group has been concentrating on the chemistry of new radiopharmaceutically relevant technetium compounds. Research has focused in particular on the reaction of technetium with sulphur-donor ligands and the corresponding products. They are considered to be of special value for a new generation of spe-

cific ^{99m}Tc tracers. Analogous rhenium compounds have also been studied in view of their therapeutic potential.

The two working directions - PET and SPECT tracer research - will be closely combined in the hope that they mutually stimulate each other and that biochemical tracer concepts of PET can be transferred to technetium compounds, going from PET to SPECT.

The subjects of our work in 1993 are described in this volume in 41 reports dealing with various aspects of radiotracers for nuclear medicine.

This first part describes synthetic work on ^{11}C-tracers and precursors. These studies have proved the usefulness of our concept of labelling substances in metabolically stabile positions. Some first tracers labelled in this way accordingly are presented. Preparatory to undertaking PET studies on patients, radiopharmaceutical procedures for the preparation and quality control of [^{18}F] FDG have been established.

The papers on technetium /rhenium chemistry describe our efforts to gain a deeper insight into the reactions taking place in intricate Tc/Re-ligand systems, to design more suitable and variable chelate units, and to start functionalizing these complexes in order to make them mimics of biochemical substrates or drugs.
Progress has been achieved in the complexation of SH-containing peptides, mainly by the introduction of N-alkylation, which remarkably influences the properties of the complexes, by systematic alteration of the peptide chain length and derivatization.
As for novel chelate units, the concept of mixed-ligand complexes has led to a variety of small-sized neutral compounds. They are characterized by diffent cores (Tc^{V}O vs. Tc^{III}) and versatility in respect of substituents, which makes it possible to adjust charge, lipophilicity and specific reactivity.
Some first steps have been undertaken towards the development of Tc/Re receptor-binding substances, with complexes functionalized with a substituent of the dopamine D$_2$ receptor-binding drug spiperone.

Binding studies using rat brain sections or homogenates have been carried out to characterize candidates for receptor-binding compounds, particularly for the dopamine D$_2$ receptor.
The biological and biochemical section of this report also provides information on methodological work for rat brain microvessel preparation, which should provide suitable models for evaluation of tracers capable of penetrating the blood-brain barrier.
The uptake of metal nuclides into normal and tumour cells has been studied to obtain insights into the uptake mechanism of tumour-affine radiopharmaceuticals.

Miscellaneous topics include ^{123}I labelling and quality control procedures, reports on the cyclotrone "Cyclone 18/9" and physical quality control of the PET camera, improvement of ^{99m}Tc-kit preparation procedures and a radioecological study on ^{14}C radioactivity in needles of a *Picea spec.*

II.
RESEARCH REPORTS

1. SUBSTANCES LABELLED IN METABOLICALLY STABLE POSITIONS:
2. THE SYNTHESIS OF [1-11C]NITROBENZENE

P. Mäding, J. Steinbach, H. Kasper, F. Füchtner

Introduction

The aim of the synthesis of 11C-ring-labelled aromatics, especially benzene derivatives, is described in [1]. The principle of this synthesis is the reaction of the precursor 5-di-methy-laminopenta-2,4-dienylidene-dimethylammonium perchlorate with a 11C-synthone containing a C-H-acid methyl group, e.g. [11C]nitromethane in the presence of a base catalyst in a suitable solvent at increased temperatures according to the following equation:

$$O_2N\overset{*}{-}CH_3 + [(CH_3)_2N \diagup\!\!\diagdown\!\!\diagup\!\!\diagdown\!\!\diagup\!\!\diagdown N(CH_3)_2] ClO_4 \xrightarrow[\substack{-HN(CH_3)_2 \\ -Base\cdot HClO_4}]{+Base} O_2N \diagdown\!\!\diagup\!\!\diagdown\!\!\diagup\!\!\diagdown\!\!\diagup\underset{*}{} N(CH_3)_2 \rightleftharpoons$$

$$HN(CH_3)_2 +$$
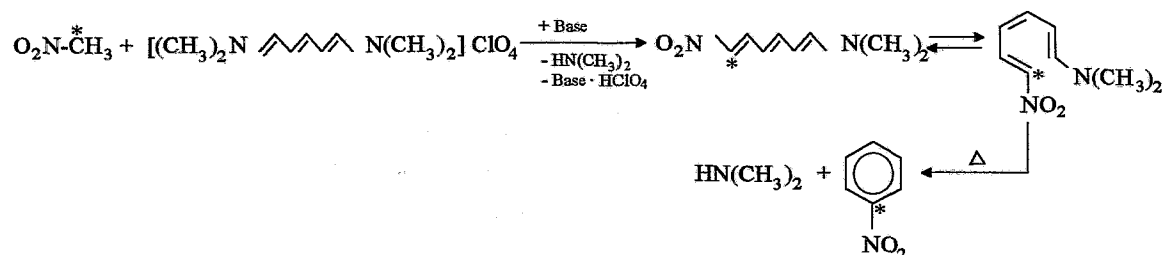
$$* \equiv {}^{11}C$$

Even the first attempts at cyclization using [11C]nitromethane indicated that the conditions worked out on an inactive scale [1] are not suitable for fast synthesis with 11C. NEt$_3$, the base used proved to be too weak. The experiments performed to adapt the synthesis are described in the following.

Experimental conditions and results

Various nonradioactive attempts at cyclization were carried out to test the much stronger base potassium tert.butylate in various aprotic solvents (e.g. MeCN, DMF, DMSO, di-oxane, THF, HMPT) at various temperatures (80 °C, 110 °C, 150 °C, 170 °C). The extent of conversion was investigated by HPLC analysis. The optimized conditions were successfully transferred to the radioactive scale.

[11C]CH$_3$NO$_2$ was synthesized according to [2] by a gas-solid reaction of [11C]CH$_3$I with AgNO$_2$. The required [11C]methyliodide was prepared by the classical one-pot method involving the reduction of [11C]carbon dioxide with LiAlH$_4$ to lithium aluminium-[11C]-methylate, hydrolysis of this intermediate organometallic complex and subsequent iodization of the [11C]methanol with hydrogen iodide [3]. Using a nitrogen gas flow (40 ml/min) the

[^{11}C]methyliodide generated was forced through a heated glass column (i.d. 3 mm, length 4 cm, oven temp. 80 °C) containing silver nitrite (0.4 g). The [^{11}C]nitromethane thus produced was trapped in a cooled vessel containing the solvent , the precursor and the base. Cyclization/ aromatization to [1-^{11}C]nitrobenzene was achieved by heating this vessel.

To determine the extent of conversion and the radiochemical purity, an HPLC system (Merck-Hitachi) was used, including a pump, a Rheodyne injector with a 20 μl loop, a Separon SGX C18 column (RP-18, 5μm, 150 x 3.3 mm, LP Prague) and a DAD detector coupled in series with a radioactivity detector. The mobile phase consisted of phosphate buffer according to Sörensen (2.6 mM NaH$_2$PO$_4$ + 5.1 mM Na$_2$HPO$_4$; pH 7) and acetonitrile at a flow rate of 0.5 ml/min with the following linear gradient of the eluents (Tab.1):

Table 1: Linear gradient of the eluents

Time [min]	buffer [%]	MeCN [%]
0	70	30
10	0	100
20	0	100

Another way to synthesize [^{11}C]CH$_3$NO$_2$ is by conversion of [^{11}C]CH$_3$I with silver or sodium nitrite in polar solvents [4]. We also tested this method with AgNO$_2$ in DMF at 100°C. In comparison with the on-line column method mentioned above this procedure is more expensive, because the [^{11}C]CH$_3$NO$_2$ produced has to be distilled into another reaction vessel containing the reagents for cyclization. Another advantage of the column method is the fact that the column containing the silver nitrite can be reused up to 20 times without loss of reactivity.

The best results in terms of extent of conversion and reaction time were obtained when the synthesis of [1-^{11}C]nitrobenzene was carried out under the following conditions:

Solvent: 250 μl HMPT
Precursor: 8 mg pentamethinium salt (5-dimethylaminopenta-2,4-dienylidene-
                              dimethylammonium perchlorate)
Base: 3.5 mg t-BuOK (as a solid)
Reaction temperature: 170 °C
Reaction time: 7 min

In this way [1-^{11}C]nitrobenzene was prepared with a radiochemical purity of about 92%. The reproducible radiochemical yields (half-life corrected) are in the range of 85±5 %, within an overall synthesis time from EOB of 25 min.

5

An HPLC chromatogram by detection of radioactivity is shown in Fig. 1, the results are listed in Table 2.

Fig. 1: HPLC chromatogram obtained from the reaction mixture of the [1-^{11}C]nitrobenzene synthesis

Tab. 2: Results of the HPLC chromatogram

peak	product	radioactivity [%] (decay-corrected)
A	unidentified product, probably [^{11}C]CH$_3$ONO [2]	2.81
B	[^{11}C]CH$_3$OH	5.33
C	[1-^{11}C]nitrobenzene	91.86

References
[1] Mäding, P., et al., FZR 93 - 12 (1992) 18
[2] Schoeps, K.-O. et al., Appl. Radiat. Isot. **40** (1989) 261
[3] Crouzel, C. et al., Appl. Radiat. Isot. **38** (1987) 601
[4] Schoeps, K.-O. et al., J. Lab. Comp. Radiopharm. **25** (1988) 749

2. SUBSTANCES LABELLED IN METABOLICALLY STABLE POSITIONS:

3. THE SYNTHESIS OF [1-^{11}C]ANILINE - A ^{11}C-RING-LABELLED SYNTHONE

P. Mäding, J. Steinbach, H. Kasper

Introduction

The synthesis of [1-^{11}C]nitrobenzene is described in [1]. A crucial step for synthesizing other ^{11}C-ring-labelled substances such as phenylalanine according to [2] is the reduction of [1-^{11}C]-nitrobenzene to ^{11}C-ring-labelled aniline. The appropriate diazonium salt is chosen to be the labelled synthone for further reactions.

Experimental conditions and results

The required [1-^{11}C]nitrobenzene was prepared in a special cyclization/ aromatization reaction [3] by conversion of [^{11}C]CH$_3$NO$_2$ with 5-dimethylaminopenta-2,4-dienylidene-dimethylammonium perchlorate in the presence of t-BuOK in MeCN, DMF or HMPT according to the following equation:
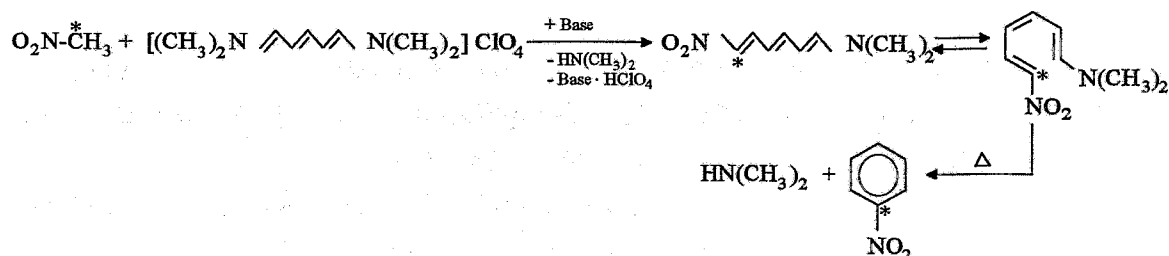
$* \equiv {}^{11}C$

Starting from the above reaction mixture, the following reduction was carried out by addition of a suitable reducing agent and heating:
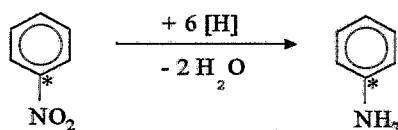
To determine the extent of conversion and the radiochemical purity, an HPLC system (Merck-Hitachi) was used, including a pump, a Rheodyne injector with a 20 μl loop, a Separon SGX C18 column (RP-18, 5μm, 150 x 3.3 mm, LP Prague) and a DAD detector coupled in series with a radioactive detector. The mobile phase consisted of phosphate buffer according to Sörensen (2.6 mM NaH$_2$PO$_4$ + 5.1 mM Na$_2$HPO$_4$; pH 7) and acetonitrile at a flow rate of 0.5 ml/min with the following linear gradient of the eluents (Table 1).

Table 1: Linear gradient of the eluents

Time [min]	buffer	MeCN
0	70 %	30 %
10	0 %	100 %
20	0 %	100 %

In the first experiments for reduction of [1-^{11}C]nitrobenzene, using $Na_2S_2O_4$ in DMF/H_2O at 110°C, [1-^{11}C]aniline was only obtained as a radioactive by-product. The main radioactive products were ionic compounds, probably consisting of N-phenylsulphamic acid and aminobenzene sulphonic acid [4].

Following this, many nonradioactive experiments were carried out in order to test other reducing agents (e.g. $Na_2S_2O_5$, $SnBr_2/HBr$, $NaBH_4$, $LiAlH_4/THF$, $FeSO_4/NaOH$, $PhNHNH_2$, H_2NNH_2, Na_2S) in suitable solvents (e.g. DMF, MeCN, THF, dioxane, DMSO, HMPT) at various temperatures (110 °C, 150 °C, 170 °C). The extent of conversion was investigated by HPLC. The conditions of successful nonradioactive reductions were transferred to the radioactive scale:

- Experiments using $SnBr_2/HBr$ in MeCN, DMF or HMPT at 110 °C or 170 °C produced an ^{11}C-labelled reaction product which was probably bound as a colloid, because the main activity was at the top of the HPLC column and resisted elution.

- An incomplete conversion of [1-^{11}C]nitrobenzene to [1-^{11}C]aniline with many by-products was achieved in a further experiment using phenylhydrazine in HMPT at 170 °C.

- The use of $THF-LiAlH_4$ solution in HMPT at 110 °C yielded about 60 % [1-^{11}C]aniline and two by-products, probably [^{11}C]azoxybenzene and [^{11}C]azobenzene [5, 6].

- The best results with regard to extent of conversion and reaction time were obtained by a synthesis of [1-^{11}C]aniline using Na_2S as follows:

In a one-pot process [1-^{11}C]nitrobenzene, synthesized from [^{11}C]CH_3NO_2, 8 mg of 5-dimethylaminopenta-2,4-dienylidene-dimethylammonium perchlorate and 3.5 mg of t-BuOK in 250 μl HMPT at 170 °C (see [1]), was reduced by adding to the reaction mixture a solution of 8 mg of $Na_2S \cdot 5$ H_2O in 100 μl H_2O and heating at 170 °C for 10 min. In this way [1-11C]aniline was prepared with a radiochemical purity of about 83 %. The reproducible radiochemical yields (half-life corrected) are in the range of 80±5 %, within an overall synthesis time from EOB of 37 min.

An HPLC chromatogram by detection of radioactivity is shown in Fig. 1, the results are listed in Table 2.
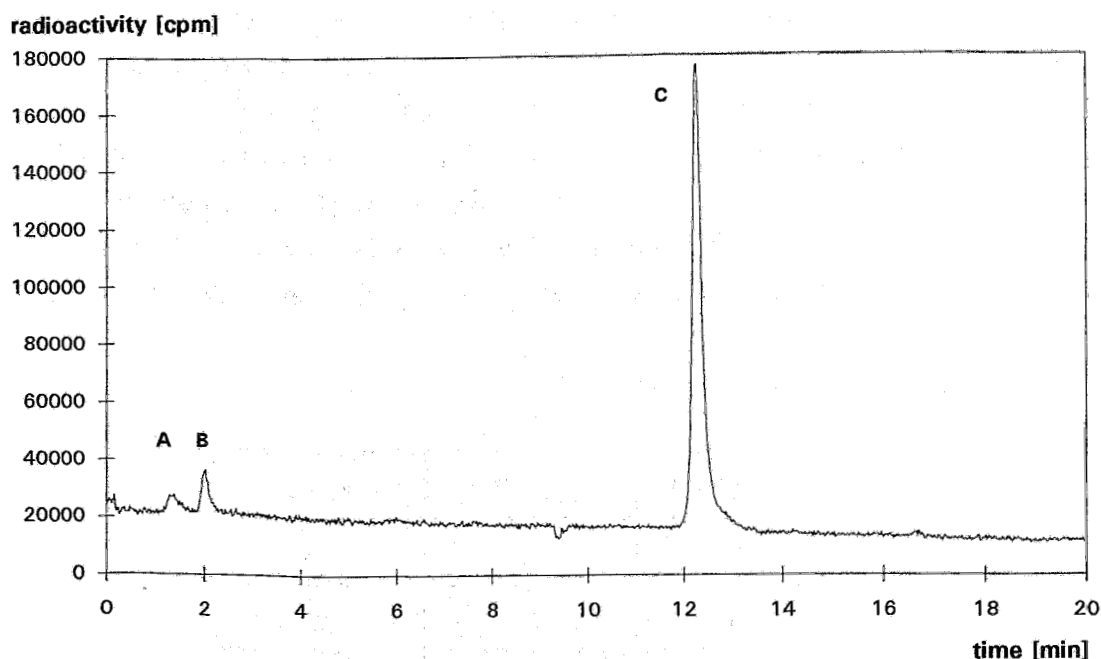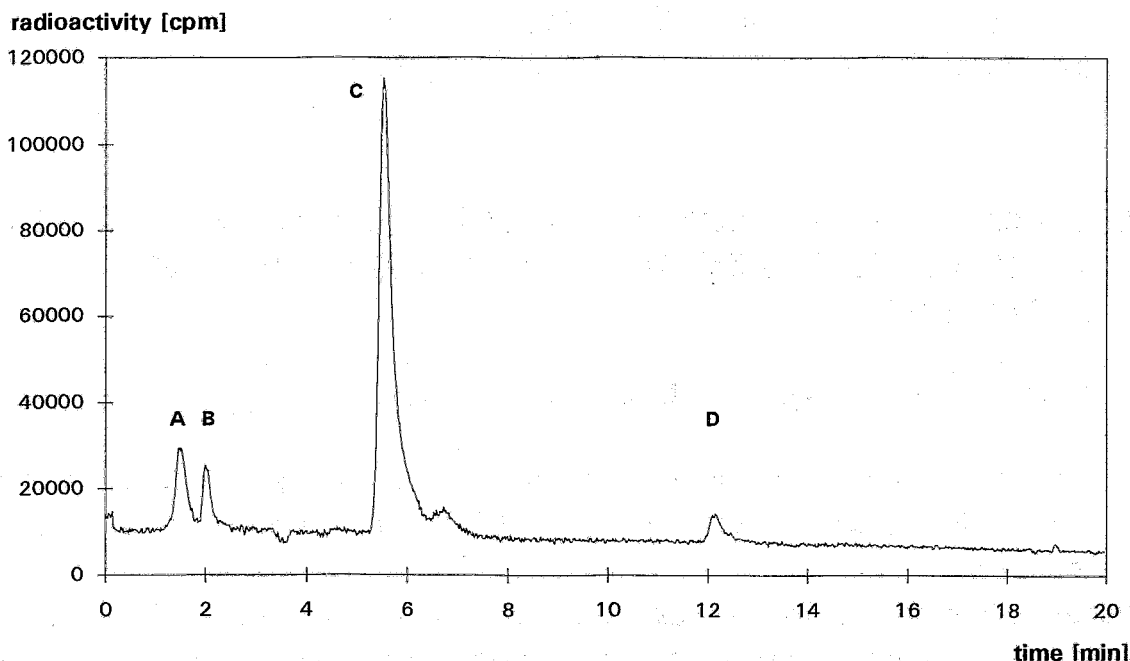
radioactivity [cpm]

Fig. 1: HPLC chromatogram obtained from the reaction mixture of the [1-^{11}C]aniline synthesis

Table 2: Results of the HPLC chromatogram

peak	product	radioactivity [%] (decay-corrected)
A	unidentified product, probably [^{11}C]CH$_3$ONO [7]	7.78
B	[^{11}C]CH$_3$OH	4.56
C	[1-^{11}C]aniline	82.76
D	[1-^{11}C]nitrobenzene	4.89

For further conversions, the [1-^{11}C]aniline should be separated from all inactive and radio-active by-products. The separation of [1-^{11}C]aniline and the testing of the further synthesis route to ^{11}C-ring-labelled phenylalanine according to [2] will be carried out in the near future.

References

[1] Mäding, P. et al., this report, p. 4

[2] Mäding, P. et al., FZR 93 - 12 (1992) 18

[3] Jutz, Ch. et al., Angew. Chem. **84** (1972) 299

[4] Houben-Weyl, Methoden der Organischen Chemie, 1957, Vol. XI/1, p.437

[5] Nystrom, R. F. et al., J. Am. Chem. Soc. **70** (1948) 3738

[6] Corbett, J. F., Chem. Comm. (1968) 1257

[7] Schoeps, K.-O. et al., Appl. Radiat. Isot. **40** (1989) 261

3. SUBSTANCES LABELLED IN METABOLICALLY STABLE POSITIONS: 4.PRECURSOR SYNTHESIS FOR ^{11}C-RING-LABELLED PYRIDINE DERIVATIVES

K. Chebani, P. Mäding, W. D. Habicher, J. Steinbach

Heterocyclic compounds, in particular derivatives of pyridine, participate in biological processes such as redox reactions. Appropriate labelled compounds could be useful for tracer studies.

Within the framework of our work on metabolically stable ^{11}C-labelled cyclic compounds, such as aromatics, the generation of [^{11}C]pyridine derivatives (I) is the first attempt to synthesize such heterocyclic tracers.
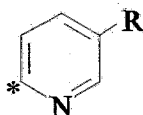
General synthetic route

Synthesis of these [^{11}C]pyridine derivatives was planned, starting with a malein-dialdehyde dimethylacetale (II) as the precursor and [^{11}C]-nitromethane according to equations (1) and (2):

$$(H_3CO)_2 CH\text{-}\overset{\overset{R}{|}}{C}\text{=}CH\text{-}CHO \;+\; [^{11}C]CH_3NO_2 \;\xrightarrow{\;-H_2O\;}\; (H_3CO)_2 CH\text{-}\overset{\overset{R}{|}}{C}\text{=}CH\text{-}CH\text{=}\overset{*}{C}H\text{-}NO_2$$

$* : \,^{11}C$
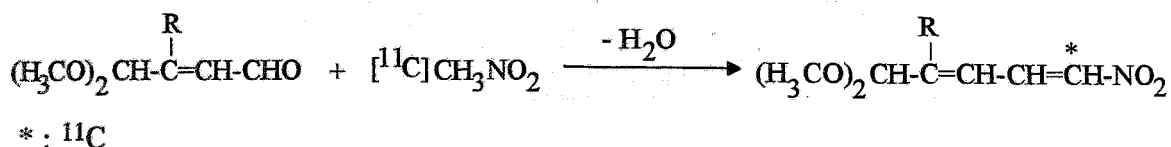
[^{11}C]nitromethane can be formed from [^{11}C]methyliodide and silver nitrite [1].

The ^{11}C-labelled compound (III) must be reduced to its amino analogue (IV).

The following intramolecular cycliztion reaction has to be expected simultaneously (equation 2):

$$(H_3CO)_2 CH\text{-}\overset{\overset{R}{|}}{C}\text{=}CH\text{-}CH\text{=}\overset{*}{C}H\text{-}NO_2 \;\xrightarrow{\;red.\;}\; [(H_3CO)_2 CH\text{-}\overset{\overset{R}{|}}{C}\text{=}CH\text{-}CH\text{=}\overset{*}{C}H\text{-}NH_2] \;\xrightarrow{\;H^+\;} \qquad (2)$$

(III)   (IV)   (I)
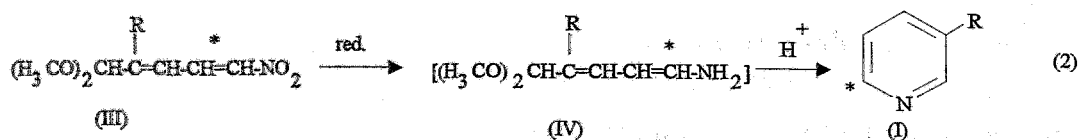
Originally we planned to synthesize [11C]nicotinamide (VI) according to equation (1) with R=CN. The idea was to generate [11C]pyridine-3-carbonitrile (V) and to hydrolyse it to nicotinamide (VI) (equation 3):

(V) → (VI)   hydrolysis H+   (3)
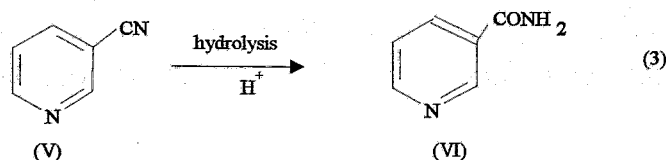
For the synthetic route described above the precursor "II" with R = CN (MeO)$_2$CH-C(CN)=CH-CHO (VII) had to be synthesized:

The following synthetic routes were studied for generating VII:

(4)

(H$_3$CO)$_2$ CH-C=CH-CHO
(VII)
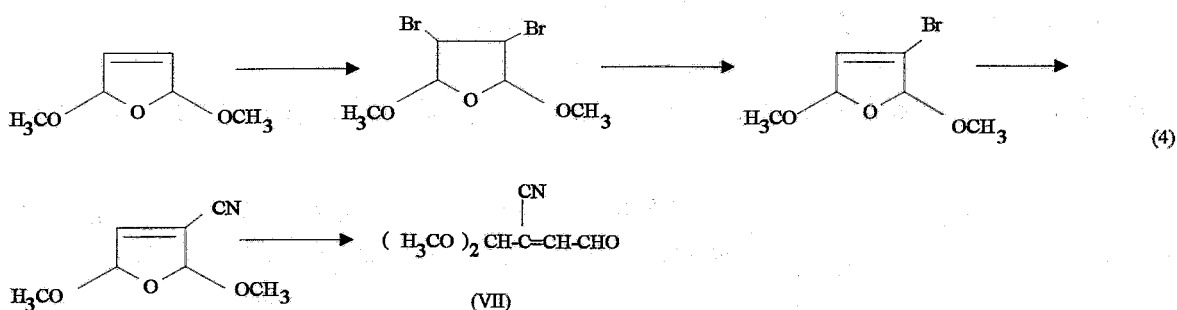
1. Synthesis was started with 2,5-dimethoxy-2,5-dihydrofuran (VIII). This compound reacts with bromine to 3,4-dibromo-2,5-dimethoxytetrahydrofuran (IX) according to [2].

(VIII)   + Br$_2$ →   (IX)   (5)

HBr is eliminated by potassium t-butoxide in tert-butyl alcohol as the solvent at 80 °C and under a nitrogen atmosphere:

(IX)   + K$^+$ $^-$OC(CH$_3$)$_3$ →   (X)   +KBr+HOC(CH$_3$)$_3$ (6)
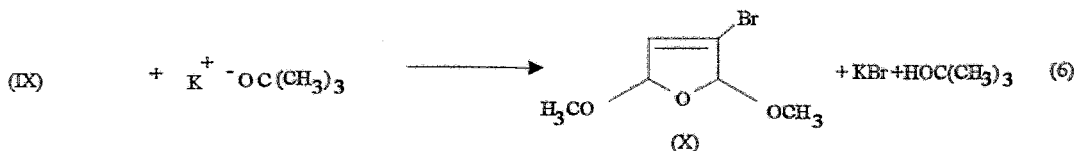
The yield was some 80 %. The structures of IX and X were proved by ^{1}H NMR spectra.
The 3-bromo-2,5-dimethoxy-2,5-dihydrofuran (X) formed was distilled as a colourless liquid at 78 °C / 1.4-1.6 kPa (11-12 Torr).
Various CN-Br exchange reactions were tried to obtain the 3-cyano-2,5-dimethoxy-2,5-dihydrofuran.

- One attempt was reaction of (X) with KCN in the presence of the cobalt-cyano-complex $K_3[Co(CN)_6]$ under a hydrogen atmosphere and reaction with copper(I) cyanide in DMF at various temperatures. IR and NMR spectroscopic investigations of the reaction products showed the exchange between the bromine and cyano groups to be difficult. The cyano compound obtained is probably instable. Similar statements have been made also in respect of other compounds with Br in α-position of an olefinic double bond [3].

- Another attempt was a Br-for-CN exchange on 3,4-dibromo-2,5-dimethoxy-tetrahydrofuran (IX) in order to synthesize the 3-bromo-4-cyano-2,5-dimethoxy-tetrahydrofuran, with subsequent HBr elimination. The substance (IX) was treated with KCN or Cu(I)CN in DMF at various temperatures. But the IR and NMR spectroscopic investigations showed that there was practically no Br-CN exchange.

2. The following synthetic route offers another possibility of producing the precursor (VII):
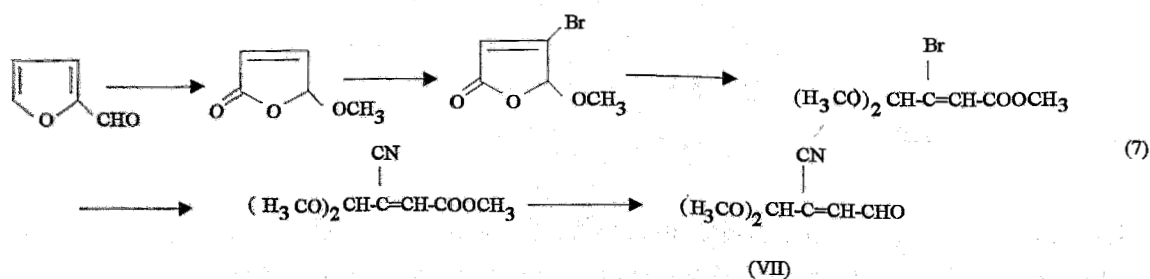
5-Methoxy-2(5H)-furanone (XI) was prepared by photooxidation of furfural in methanol [4] with a yield of about 50%.
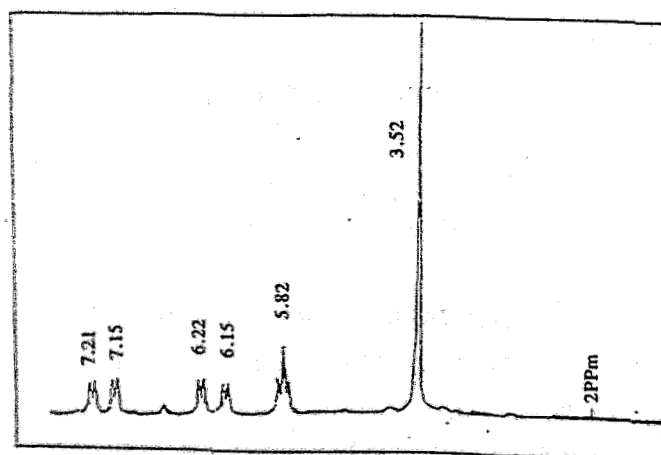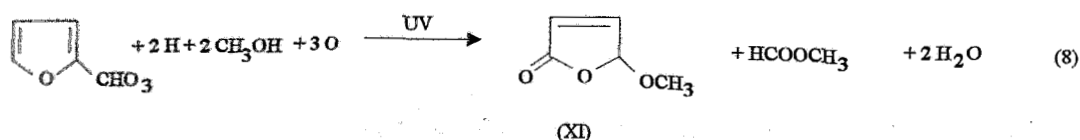
Fig.1: ^{1}H-NMR-spectrum of 5-methoxy-2(5H)-furanone

Compound (XI) was converted to 4-bromo-5-methoxy-2(5H)-furanone (XII) by bromination according to [5]:

$$(XI) \quad + \quad Br_2 \quad \longrightarrow \quad \text{(XII)} \qquad (9)$$

(XII)

Acidic hydrolysis of (XII) in methanol according to [6] leads to the Z and E isomers of methyl-3-bromo-4,4-dimethoxy-2-butenoate (XIII) in a yield of 80 %.

$$(XII) \quad \xrightarrow{CH_3OH/H^+} \quad (H_3CO)_2 CH\text{-}C\text{=}CH\text{-}COOCH_3 \qquad (10)$$

(with Br substituent)

(XIII)

Compound (XIII) was intended to be transformed into methyl-3-cyano-4,4-dimethoxy-2-butenoate (XIV). The ester group of (XIV) had to be reduced selectively to precursor (VII) in the presence of the cyano group :

$$(XIII) \quad \longrightarrow \quad (H_3CO)_2 CH\text{-}C\text{=}CH\text{-}COOCH_3 \qquad (11)$$

(with CN substituent)

(XIV)

Conversion of XIII to XIV was not successful, i.e. instead of XIV we found polymeric products. This result suggests that XIV cannot be isolated. This is in agreement with [7]. We have to change the substituent R in II.

References

[1] Schoeps, K.- O. et al, J. Lab. Comp. Radiopharm. **25** (1988) 749
    Schoeps, K.- O. et al, Appl. Radiat. Isot. **40** (1989) 261

[2] Houben-Weyl, Methoden der Organischen Chemie. Stuttgart: Verlag Georg Thieme,1960, Vol. V/4, p.60
    Sheehan, J. C. et al., J. Am.Chem. Soc. **74** (1952) 3825

[3] Houben-Weyl, Methoden der Organischen Chemie. Stuttgart, New York: Verlag Georg Thieme,1985, Band E-5, Teil (1), p. 1450

[4] Schenk, G.O., Justus Liebigs Ann. Chem. **584** (1954) 156

[5] Todd, A.R. et al., J. Chem. Soc. (1946) 628

[6] Farina, F. et al., Synthesis (1977) 642

[7] Prochazka, M.,et al., Collect. Czech. Chem. Commun. **48** (1983) 1765

4. SETTING UP AN APPARATUS FOR ROUTINE PREPARATION OF [18F]FDG

F. Füchtner, J. Steinbach, E. Lösel, R. Lücke

Introduction

The most widely used radiopharmaceutical in positron emission tomography (PET) studies is 2-[18F]fluoro-2-deoxy-D-glucose ([18F]FDG). The method commonly applied to prepare [18F]FDG is based on nucleophilic substitution using a phase-transfer catalytic reaction [1]. Having initially been restricted to a Ne-target for preparation of [18F]F_2, we used the electrophilic reaction. The version described by Bida [2] and adapted by Steinbach [3] proved to be a simple and very reliable procedure. Even with the new IBA PET-cyclotron "CYCLONE 18/9" and the nucleophilic [18F]FDG synthesis based on water-target-produced [18F]F^- now being available, this electrophilic method represents a useful stand-by and complementary procedure to the nucleophilic approach.

An apparatus for routine use of [18F]FDG based on electrophilic reaction has therefore been set up.

Experimental

The schematic layout of the [18F]FDG-preparation unit is shown in Fig. 1. The device consists of two main parts, the processing unit, situated inside the hot cell and its control unit. A pump, the radiation monitors and a recorder are additionally used. The arrangement is shown in Fig. 2. All parts of the processing unit, such as the reaction vessel, purification columns, electro-magnetic and electric stream selection valves, fittings, tubes, a waste absorber, electrical and tube connectors, conductivity cells, radioactivity monitors (Geiger-Müller tubes, 70034, VacuTec) and the manometer, are mounted on a stainless steel housing. The processing unit is remote controlled by the control unit via a common 24-wire cabel. The tubes for the target gas, the compressed N_2 (for delivering the liquids), and the vessels containing the liquids needed for the synthesis, are connected to the synthesis unit by PTFE tubing and luer adapters.

[18F]F_2 is produced by the $^{20}Ne(d, ^4He)^{18}F$ reaction using the 13.5 MeV deuterons of the Rossendorf cyclotron U-120 with Ne + 0.2 % F_2 as target gas. The target gas is forced by its own pressure (20 bar at the beginning) through a column (d_i=3 mm, L=100 mm, OMNIFIT) filled with about 70 mm KOAc x 1.5 HOAc (extra pure, MERCK) [3]. This column is situated in a glovebox about 18 m away from the target. The [18F]F_2 reacts to form volatile acetylhypofluorite ([18F]AcOF), which is transported through a transporting tube (polyethylene; d_i=1.3 mm; d_o=1.8 mm, L appr 500 m). After being discharged from the target by its own pressure, the [18F]AcOF is transported to the synthesis unit using N_2 as a carrier gas with a pressure of 5 bar. In contrast to the previous

N₂ → N_2 70 kPa

1. Freon + TAG
2. HCl

from targetry

pump H_2O

manometer

NC
1 — NO

NC
5 — NO

6

7

8

2

4 3

1

reaction vessel

heating with a
thermocoulpe

purification column

stream selection valve

9

alumina cartridge

conductivity measurement
luer adapter
sterile filter
electro magnetic valve
inline check valve
radioactivity measurement

1 M NaOH

waste
absorber

product 2

product 1

foreruns

Fig. 1: Schematic representation of apparatus for routine production of [^{18}F]FDG
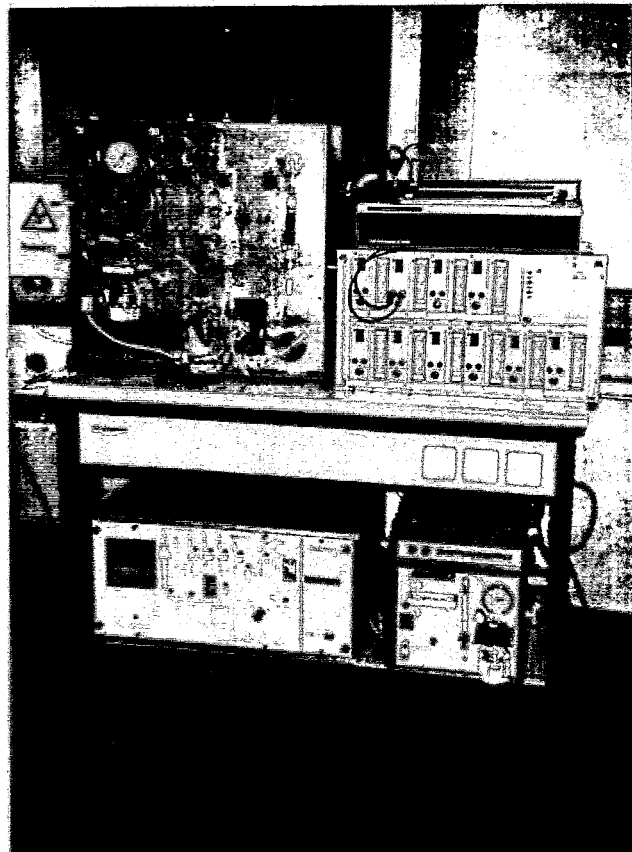
Fig. 2: Laboratory system used for routine production of [^{18}F]FDG

procedure [3], the [^{18}F]AcOF is directly absorbed in the reaction vessel containing a solution of 30 mg tri-O-acetyl-D-glucal (TAG, for synthesis, MERCK - Schuchardt) in 20 ml trichlorofluoromethane (CFCl$_3$, for synthesis, MERCK - Schuchardt). Under these conditions the reaction between TAG and the gaseous [^{18}F]AcOF occurs, forming tetraacetylated [^{18}F]FDG. The volume of the solvent is reduced to about 5 ml by evaporation during the adsorption. This step takes about 15 minutes. After the adsorption of the radioactivity the remaining solvent is evaporated by increasing the temperature and blowing in gaseous N$_2$. During evaporation the temperature of the reaction vessel is increased to 125 °C to reach the conditions for hydrolysis. After evaporation 2 ml of 1 M HCl (Titrisol, MERCK) is added and the hydrolysis takes place to form [^{18}F]FDG. The temperature and time of hydrolysis were optimized before so as to minimize unhydrolysed intermediate products and decomposition products by analysing the synthetic mixture by HPLC [4]. The synthetic mixture is purified by a combination of columns. The first column (d$_i$=10 mm, L=200 mm, OMNIFIT) is filled with 10 ml bifunctional ion exchange resin (AG 11A8, BIO-RAD) to retain the ionic components. On a second column (SEP PAK cartridge ALUMINA A, Millipore) the remaining [^{18}F]F$^-$ is separated from the mixture. The [^{18}F]FDG is eluted from the columns with sterilized water (aqua ad iniectabilia, Serum-Werk Bernburg). Fractionation of the eluent in the foreruns, product 1 and product 2, is carried out by monitoring radioactivity on the outlet of the last column and by switching the stream selection valve accordingly. The main radioactive peak (product 1) is always fractionated in the same way so that the volume is always the same. This made it possible for us to add in advance the neccessary amount of NaCl (extra pure, MERCK) in order to reach an isotonic solution. The sterilization of the final product is achieved by sterile filtration (microporous membrane cellulose acetate, 0.22 μm, ALLTECH).

All parts of the equipment which come into contact with the precursors and the radiopharmaceutical are newly assembled for each production cycle from sterilized glassware and tubing. Before using the equipment, the liquid system and especially the chromatographic columns are cleaned by washing with sterilized water to ensure that the system is free of endotoxins (apyrogenicity).

Results

So far we have only been able to test the described device with a radioactivity of [^{18}F]AcOF up to 50 MBq because we have not yet received permission to work with a higher activity level. Under these conditions the device works very well and reliably. The optimum time and temperature of hydrolysis were found to be 15 minutes at 125 °C. In the 6 ml of product 1 more than 95 % of the radioactivity is usually found. The product has been chemically characterized by HPLC [4]. The total preparation time after EOB is about 40 minutes. Taking into consideration the splitting of the [^{18}F]F$_2$ radioactivity into [^{18}F]AcOF and [^{18}F]NaF, the transporting losses (about 20 to 50 % of the [^{18}F]AcOF)

16

and the synthesis and chromatographic yields the total yield of [^{18}F]FDG is between 15 and 25 % EOB. In order to transport the [^{18}F]AcOF over a distance of 500 m, the transporting tube must be preconditioned with cold F_2 and AcOF to increase the transport yield. The yield of the preparation itself lies between 60 and 75 %. The preparation unit is designed to enable us to prepare [^{18}F]FDG twice a day without having to handle directly the synthesis unit in the hot cell.

Prior to application of the thus prepared [^{18}F]FDG to humans, the system must be proved to meet the recognized quality criteria in at least three runs [5]. For quality assurance it is important to have in-line process control. The built-in quality control involves monitoring the temperature, radioactivity and conductivity from one step to the next throughout the synthetic procedure. With this control we can identify most of the problems at a very early stage.

With the same device set-up we have also prepared 2-[^{18}F]fluoro-2-deoxy-D-galactose ([^{18}F]FDGal), using tri-O-acetyl-D-galactal as a precursor.

References

[1] Hamacher, K., et al., J. Nucl. Med. **40** (1989) 433

[2] Bida, G.T., et al., J. Nucl. Med. **25** (1984) 1327

[3] Steinbach, J. et al., ZFK - 728 (1990) 76

[4] Füchtner, F. et al., this report, p. 17

[5] Meyer, G.-J. et al., "Quality assurance and quality control of short-lived radiopharmaceuticals for PET", in Stöcklin, G., et al., "Radiopharmaceuticals for PET", Kluwer Academic Publisher, Dordrecht, 1993, p. 91

5. DETERMINATION OF THE CHEMICAL AND RADIOCHEMICAL PURITY AND SPECIFIC RADIOACTIVITY OF [^{18}F]FDG BY HPLC

F. Füchtner, K. Neubert, J. Steinbach

Introduction

According to the rules of good manufacturing practice (GMP) [1], quality control of the final product is an essential part of the quality assurance of (radio)pharmaceutical production. In the case of radiopharmaceuticals labelled with the short-lived PET radionuclides, special restrictions are imposed on quality testing:

- time limitations between production and application,

- analysis of small sample volumes and of extremely small concentrations and

- handling at high radioactivity levels.

In previous work at Rossendorf, quality control for [18F]FDG comprised determination of sterility, apyrogenicity, pH and radiochemical purity by TLC [2].

High performance liquid chromatography (HPLC) in combination with the radioactivity detection is the best control method for the radiochemical purity of [18F]FDG [3]. An anion exchange separation mechanism allows isocratic separation of carbohydrates. Using a strong basic eluent, the weakly acid carbohydrates form anions and are therefore retained on the anion exchange resin.

The chemical and radiochemical purity and specific radioactivity can be determined simultaneously by including in the chromatographic system a mass detector sensitive, enough for quantitative determination of the product species.

Experimental

These requirements are met by combination of electrochemical (pulsed amperometric) detection (ECD) with a diode-array detection (DAD). The electrochemical principle is a very sensitive and selective detection method for carbohydrates, about two orders of magnitude more sensitive than the refractive index. If only a common amperometric detector (single potential) is used, the detector response decreases as the electrode surface becomes fouled due to the oxidation process. Pulsed amperometric detection overcomes this drawback [4]. DAD is an unspecific detector which provides a good overview and in some cases substances can be identified by means of spectroscopic data.

[18F]FDG produced at Rossendorf by electrophilic reaction [5] and [18F]FDG prepared by nucleophilic substitution sent to our group by other producers, was analysed using this chromatographic system.

Equipment

Chromatographic system:

- gradient pump	series 1050	Hewlett Packard
- autosampler	series 1050	Hewlett Packard
- column oven	column thermostat MISTRAL	Spark Holland
- DAD	1040 M	Hewlett Packard
- ECD	1049 A	Hewlett Packard
- radioactivity detector	A 120	Canberra Packard
- computer system	Vectra, 80486/33	Hewlett Packard
- 3^D-software	G1309A	Hewlett Packard

Dose calibrator:

- Aktivitätsmeßgerät	M 2311	Messelektronik Dresden

Reagents and standards

- 1 M sodium hydroxide   sodium carbonate < 0.02 % (w/v) Fluka
- glucose   Merck
- 2-fluro-2-deoxy-D-glucose   SIGMA

Chromatographic conditions

- column:	CarboPac PA 1 (4 x 250 mm)	Dionex
- guard column:	CarboPac PA 1 (4 x 60 mm)	Dionex
- column temperature:	30 °C	
- sample volume:	20 - 100 μl	
- eluent:	100 mM NaOH	
- flow rate:	1 ml/min	
- pressure:	about 14.5 MPa	

- ECD: electrochemical cell: - working electrode: gold electrode,
                                                - reference electrode: Ag/AgCl,Cl$^-$
                                                - auxiliary electrode: platinum,

potential and time set up:	[V]	[msec]
- sample oxidation:	-0.35 - 0.35	50
- electrode oxidation:	-0.65	200
- electrode reduction:	0.65	200

- DAD:	Signal = 230 nm, BW=60 nm,
	Refer. = 450 nm, BW=80 nm,
- A120	γ-flow cell, CaF$_2$, 100 μl, 0-1024 KeV

Monosaccharide separation is carried out with a NaOH eluent. To obtain stable retention times for the analytes, it is very important to prepare eluents from stock solution low in carbonate to minimize carbonate contamination of the column. In order to exclude carbon dioxide during ventilation of the eluent reservoir we used a tube filled with sodium hydroxide pellets.

After each analysis complete elution of all injected substances was checked by injection of an aliquot of the sample into the chromatographic system without the separation column. If the detector response is the same in both cases, all injected species are removed from the column.

To determine the optimum detector response, the detection potential was changed systematically from -0.35 to 0.35 V, using the chromatographic system with ECD. From time to time the working electrode surface has to be cleaned mechanically by polishing.

For determination of the specific radioactivity the radioactivity of an aliquot volume was measured with a dose calibrator.

Results

Fig. 1 shows the dependence of the ECD detector response on the working electrode potential. Since oxidation of the mobile phase and other electro-active substances occurs with increasing working electrode potential optimum sensitivity and selectivity are obtained where the signal-to-noise ratio reaches a maximum and the working electrode potential is minimized. For this reason the working electrode potential was set at -0.08 V. This value differs somewhat from the literature data with +0.05 V for FDG [4] and sugars in general [6].

detector response [μA x sec]

working electrode potential [V]

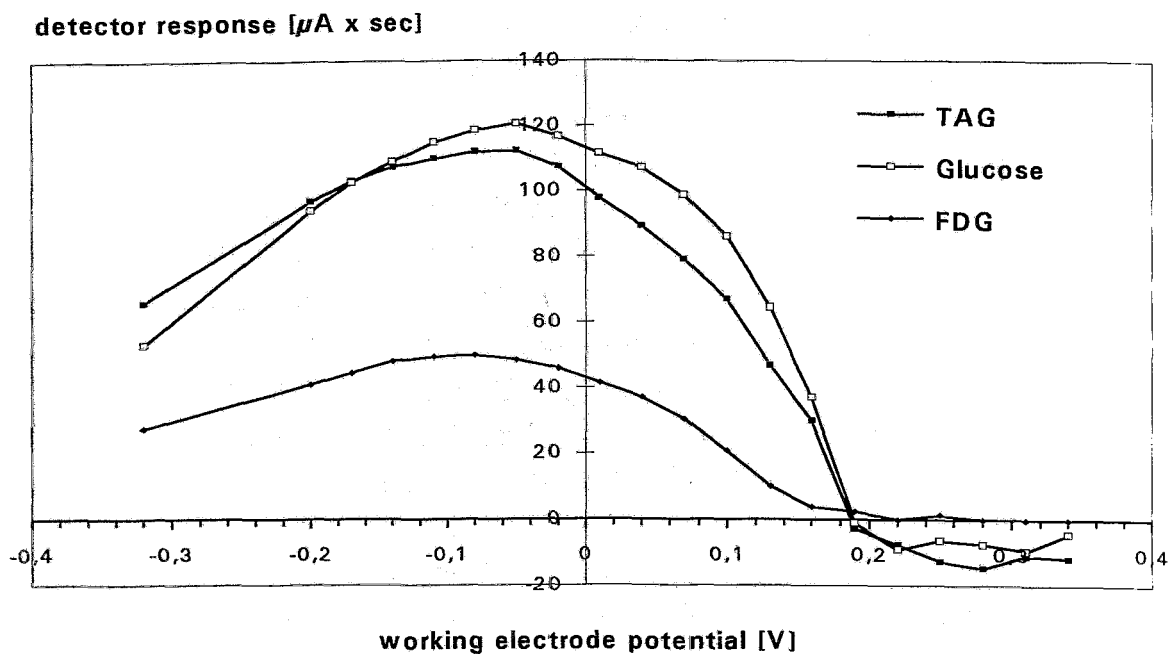Fig. 1: Dependence of the detector response of FDG, glucose and TAG on the
working electrode potential, injection volume: 10 μl,
concentration: 0.1 mM of each

Fig. 2 demonstrates the results of HPLC analysis of the final [^{18}F]FDG produced by electrophilic reaction. The chromatogram shows the separation of F$^-$, glucose, FDM, FDG, partially hydrolysed sugars and other initial, intermediate and final substances.
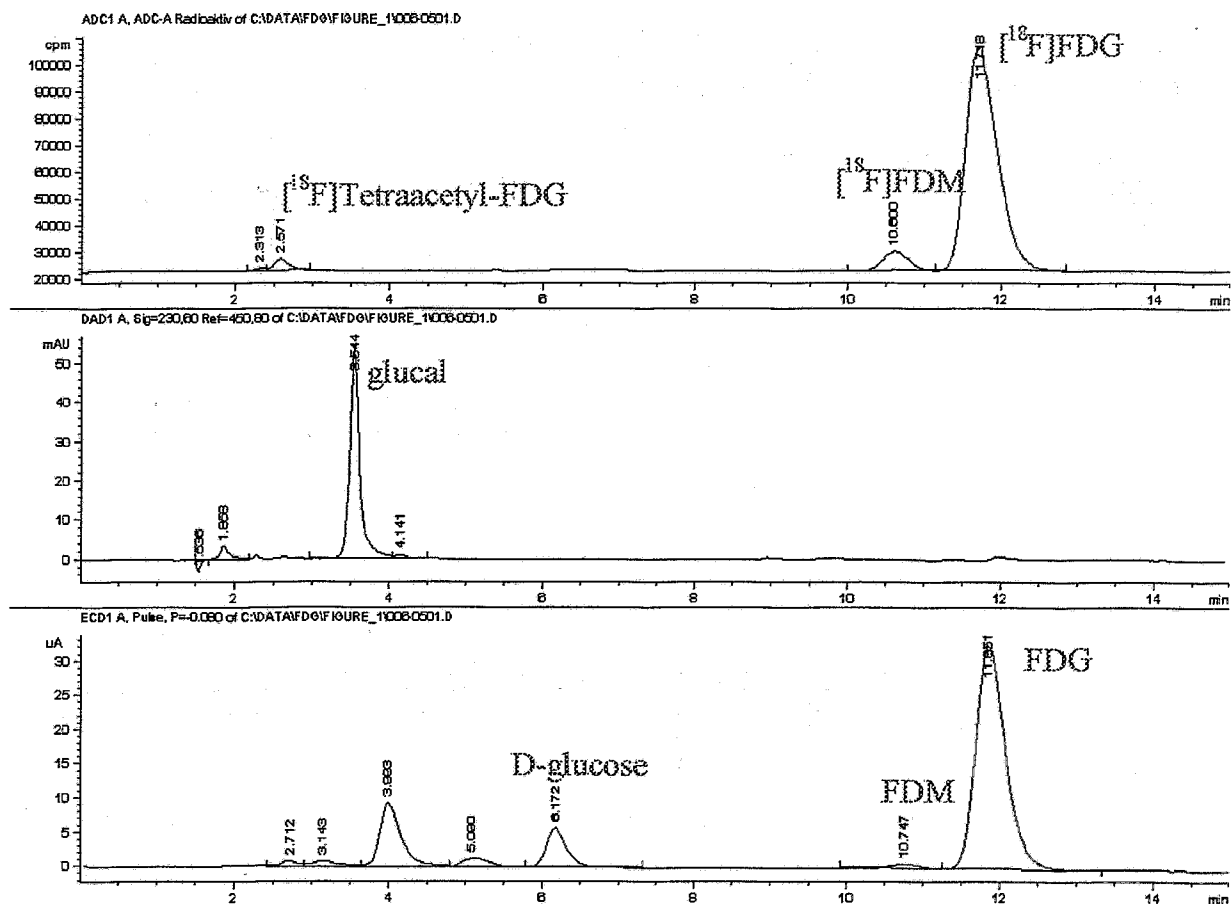
Fig. 2: Chromatogram of 50 μl of final product of [18F]FDG prepared by electrophilic reaction

In respect of *radiochemical purity* we can see that besides the main [18F]FDG peak in the chromatogram ($\approx$91 %) there are also its epimer 2-[18F]Fluoro-2-deoxy-D-mannose ([18F]FDM, $\approx$6 %), traces of [18F]F⁻ ($<$1 %) and partially acetylated [18F]FDG derivatives ($\approx$3 %).

To find out about *chemical purity* we determined the concentrations of the main components from the chromatograms of the DAD and ECD signals. Apart from the precursor tri-O-acetyl-D-glucal (TAG) (0.5 mM), D-glucose (0.3 mM) and the FDG (6.9 mM) and FDM (0.5 mM), there are some other peaks which do not correspond neither to the radioactive peaks nor to any known substances. Since no FDM standard is available, the concentration of FDM has to be estimated from the FDG/FDM peak ratio obtained in the analysis and from [4]. The other peaks in the chromatogram have not been identified up till now. Spectroscopic analysing methods such as MS and IR are required for this. In future traces of organic solvents in the final product will be determined by GC.

For *specific radioactivity* we found a value of 100 GBq/mmol. This value results from the FDG concentration determined and from the maximum radioactivity reached in former ex-

periments with our target design and running parameters [2]. The specific radioactivity determined is in accordance with literature data [3].
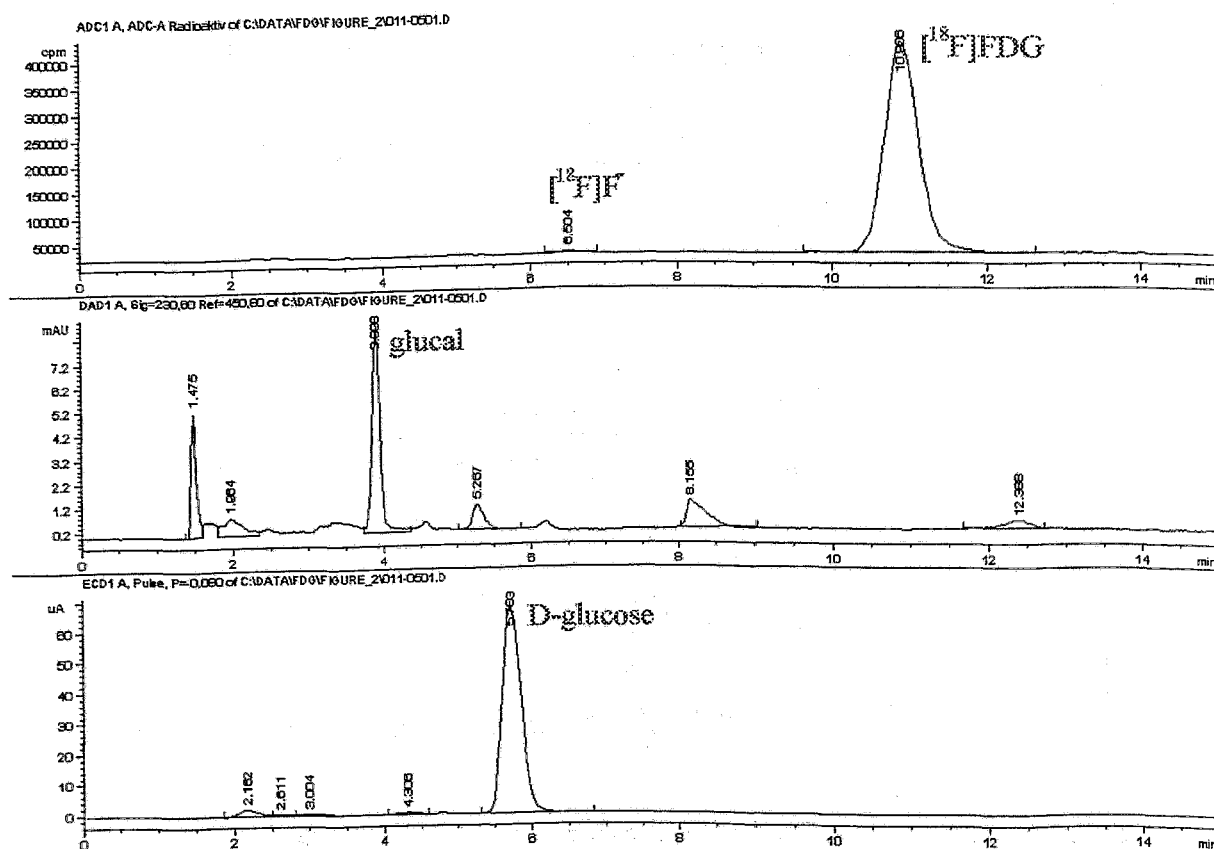
Fig. 3: Chromatogram of 20 μl of final product of [^{18}F]FDG synthetisized by nucleophilic substitution

Additionally we also analysed final [^{18}F]FDG synthetized by **nucleophilic substitution**. The results are shown in Fig. 3. In contrast to the electrophilic product we find a high degree of radiochemical purity ([^{18}F]FDG > 99 %) in which no FDM is observerd, in accordance with the principle of synthesis. The chemical composition is characterised by a high concentration of D-glucose (1.5 mM) and numerous unknown components. Since only a few samples were analysed, we were unable to determine the amount of FDG exactly. This concentration is near the detection limit of the method at about 1.5 μM. In two samples we determined about 3 μM of FDG whereas in another we did not find any. Using the first values a specific radioactivity of 0.1 TBq/μmol can be calculated. This value is similar to the results obtained by another group [7] but differs from the literature data of about 1 TBq/μmol, which was determined by the amount of ^{18}F introduced into the synthesis [3].

In conclusion it must be mentioned that in order to reach reproducible analytical results and a high system performance a major problem must be overcome. Since stronger retained anions in analytical samples or residual anions in the eluent itself (e.g. carbonate) are only

slowly eluated from the column by hydroxide ions, the retention time for analytes decreases steadily. To reduce this effect it is necessary:

- to avoid very high salt concentrations and organic solvents in samples and
- to use high hydroxide eluent concentrations.

Nevertheless, the column has to be regenerated between analytical sequences with 0.5 M NaOH when isotonic samples are analysed.

Analysing practice has shown that HPLC with the described detector configuration is suitable for simultanious determination of the chemical and radiochemical purity and specific radioactivity of $[^{18}F]FDG$. The results are available after about 20 minutes so that the analysis can be carried out before application of the radiopharmaceutical.

References

[1] Commission of the European Communities III/B/6, "The rules governing medical products in the European Community, Vol. IV; Guide to good manufacturing practice for medical products." No. III/3973/89-EN, (1990), Brussels, Belgium

[2] Steinbach, J. et al., ZFK - 728 (1990) 76

[3] Meyer, G.-J. et al., "Quality assurance and quality control of short-lived radiopharmaceuticals for PET", in Stöcklin, G., et al., "Radiopharmaceuticals for PET", Kluwer Academic Publisher, Dordrecht, 1993

[4] Dionex, Application Note 00 (1991)

[5] Füchtner, F. et al., this report, p. 14

[6] "Installation instructions", DIONEX, Document 08/27 (1991) 5

[7] Bergman, J., Åbo Akademi, Turku, Finland, private communication

6. DETERMINATION OF THE SPECIFIC ACTIVITY OF $[^{123}I]NaI$

C. Kretzschmar, R. Scholz, F. Füchtner, J. Steinbach

Introduction

In last year`s annual report we described a method for reproducible quality control of various iodine species in a non carrier added $[^{123}I]NaI$ solution [1]. The quality of the radioiodine is such that it can be used in labelling processes. The $[^{123}I]NaI$ solutions investigated were produced by the Karlsruhe Nuclear Research Centre.

The new method described enables us to determine radiochemical purity as well as specific activity. For this purpose the chromatographically determined iodine content of the solutions has to be quantified. The use of reference solutions of known iodine concentrations makes it possible to determine the iodine content in real $[^{123}I]NaI$ solutions in g/l.

Experimental

According to DAB 10 the specific activity of [^{123}I]NaI should be $\leq$ 5 Ci/mg iodine. With [^{123}I]NaI solutions of only 5 MBq, the analytical task is to determine iodine with a sensitivity of some 10 ng in an injection volume of 200 μl. The absolute radioactivity content was measured with the help of an isotope calibrator.

The method described in this paper for determination of the specific activity of [^{123}I]NaI is based on an ion chromatography with RP 18-columns modified with quarternary alkylammonium salts.

For the investigations a HPLC system (Merck-Hitachi) was used, including a pump, a manual injection valve with a 200 μl sample loop, a column thermostat with column and an UV/VIS, an electrochemical and a radioactivity detector.

As RP-18 support material we used LiChrospher (5μm). The glass columns (150 x 3.3 mm; LP-Prague) were filled with the support by a slurry technique. In order to achieve ion exchange properties, an acetonitrile/water solution of the quarternary ammonuim salt tetra-kis-ammonium bromide was pumped through the column up to equilibrium. The capacity of the ion exchange was determined by the UV break-through curve while modifying or equilibrating the column with a UV absorbing ionic solution.

As eluents we used Na$_2$SO$_4$ solutions with a concentration of 10 mmol/l. Detection was accomplished by measuring the UV absorption at 225 nm, or electrochemically by using a Ag electrode, or by measuring radioactivity with a β-flow-cell detector.

Results

The described ion chromatographic method was proved to be reproducible and sensitive enough to determine the total content of iodine ("hot" and "cold") and its various species in the solution. Both UV and electrochemical ion detection were suitable for detecting the undesirable "cold" iodine in the solutions being examined. For this purpose electrochemical detection is about 100 times more sensitive than UV detection.

Although the [^{123}I]NaI solutions are declared n.c.a. preparations, they might be improved with regard to labelling procedures.

The limit of detection in the order of 10 ng was achieved by the use of this method. The content in reference solutions was determined within this order of magnitude.

The content of iodine in the real [^{123}I]NaI solutions was determined quite well in this way.
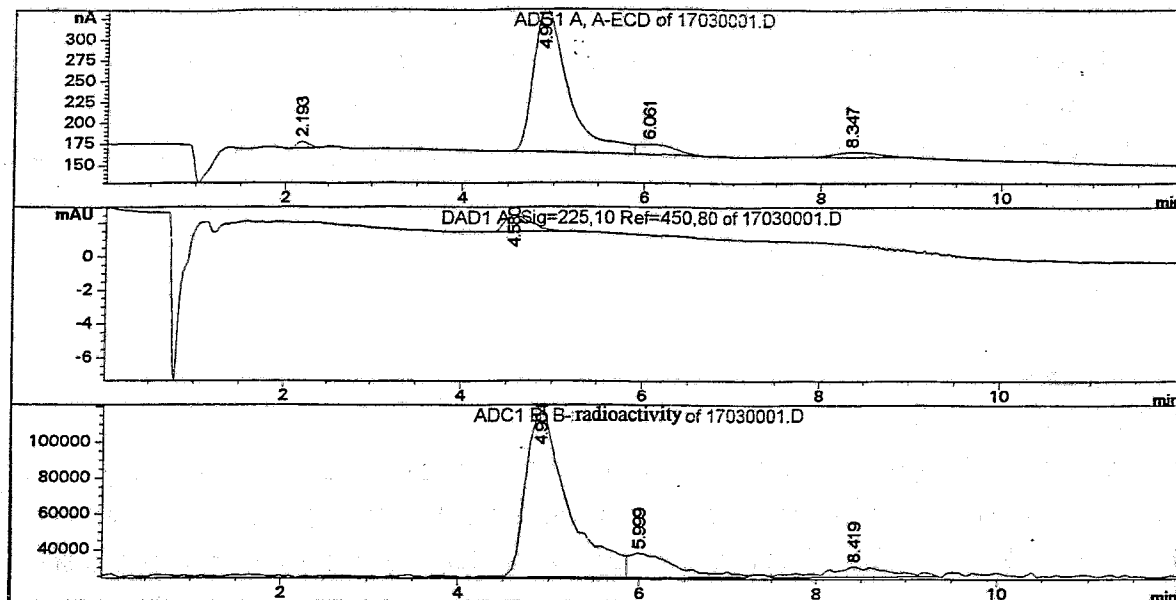
Fig. 1: Determination of iodide in a [^{123}I]NaI solution
a: electrochemical detection, b: UV detection with a diode array detector
c: radioactivity detection, retention time of iodide: 4.9 min;
column preparation analogous to [1]

References

[1] Füchtner, F. et al., FZR 93 - 12 (1993) 22

7. A NEW LABELLING METHOD FOR L-3-α-METHYLTYROSINE

C. Kretzschmar, R. Scholz, J. Steinbach

Introduction

Various procedures for the labelling of L-3-α-methyltyrosine (MTy) with [^{123}I]iodine by electrophilic oxydation have been described in the literature. The use of iodate or chloramin-T or labelling with iodogene often gives yields of only up to 60 %. The use of iodate also diminishes the specific activity of the product.

Because [^{123}I]NaI is a rather expensive starting material, the yield should be as high as possible. To increase the yield, we introduced a different method of exchange labelling for the synthesis of L-3-[^{123}I]Iodo-α-methyl tyrosine (^{123}I-MTy).

25

The precursor synthesis was carried out according to

$$MTy + Br_2 \xrightarrow{Fe} Br\text{-}MTy + HBr.$$
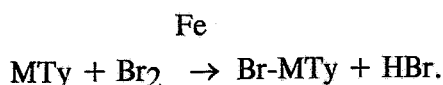
The labelling procedure is performed as a Finkelstein reaction by [^{123}I]iodine-for-bromine exchange:

$$Br\text{-}MTy + [^{123}I]I^- \rightarrow {}^{123}I\text{-}MTy + Br^-$$
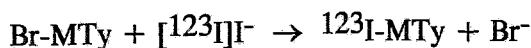
Experimental

1. Precursor synthesis

To a solution of 0.5 g methyltyrosine in 50 ml chloroform, a catalytic amount of Fe powder was added. The mixture was stirred at room temperature. Approx. 1 g Br_2 was added to the mixture drop by drop. The mixture was stirred for two hours at room temperature and then for 30 minutes at 40 °C.

After adding 100 ml 2N HCl was given to the mixture, the organic phase was separated. The aqueous phase was twice extracted with chloroform.

The aqueous solution was centrifuged at 6000 rpm to remove the catalyst. Separation was carried out by preparative column chromatography at ambient pressure. We used 0.15 N H_3PO_4 for elution. Process control was by TLC. The product in the eluate was detected by the ninhydrin reaction. The fractions containing the bromo amino acid were combined, and the water was evaporated to 2 ml. This solution was stored in the refrigerator for further use. The substance was characterized by UV spectra.

2. Labelling by exchange reaction

The labelling reaction used is analogous to the method described by Mertens [1] for radioiodination of p-I-phenylalanine.

100 μl of L-3-Br-methyltyrosine solution were added to 500 μl of a solution containing 5 mg gentisic acid, 7 mg citric acid and 1 mg tin(II)-sulphate in 1 ml water. Then 30 μl of a solution containing 32.5 mg $CuSO_4$ x 5 H_2O in 10 ml water were added. The active iodine was added to the reaction mixture as [^{123}I]NaI. The vial was closed and the reaction carried out at 100 ° or 150 °C for 30 minutes.

The product is purified by HPLC on RP 8 columns with 0.15 N H_3PO_4 as the eluent (Fig. 1). Quality control is ensured by the same chromatographic procedure at an analytical level.

Results

The precursor synthesis described is time consuming because of the preparative purification step. However we were able to produce enough substance for quite a few labelling procedures. The yield of the exchange reaction is approx. 100 % in each case.

The long reaction time of 30 min is a disadvantage in comparison with the usual method of electrophilic oxidation (the labelling occurs immediately).

The advantage of the method is the greater robustness against [^{123}I]NaI solutions of varying specific activities. The high yields obtained with various [^{123}I]NaI solutions were independent of their "cold" iodine content. Furthermore, a decrease of the specific activity is avoided.
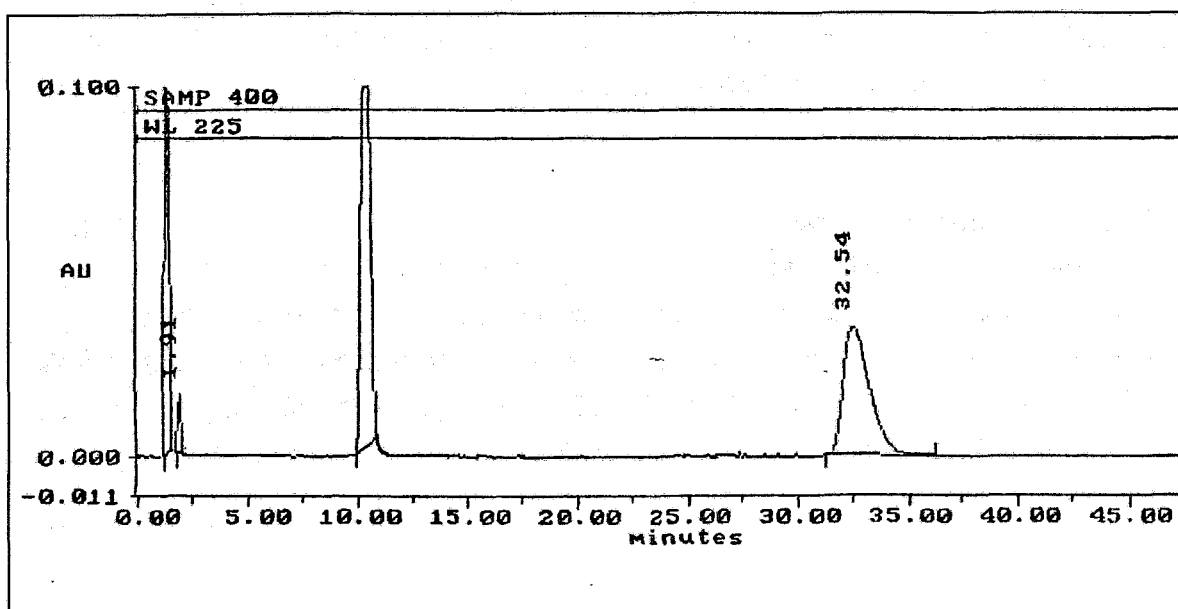
Fig. 1: Analytical control and preparative purification of L-3-[^{123}I]iodo-α-methyltyrosine

Column:	RP 8
Eluent:	0,15 N H$_3$PO$_4$
Retention times:	void volume - all ions
	10 min gentisic acid
	32 min L-3-[^{123}I]iodo-α-methyltyrosine

References

[1] Mertens, J. et al., Plenum Press, New York (1991)

8. THE ROSSENDORF PET CYCLOTRON "CYCLONE 18/9" - A STATUS REPORT

St. Preusche, J. Steinbach

An important component of the Rossendorf PET Centre is the production unit for PET radionuclides - the IBA PET cyclotron "CYCLONE 18/9". Preparations for its installation began in early 1992. Its main parameters are discribed in the 1992 annual report [1]. Details of the technical preparations for cyclotron installation at user's site are summarized in the present paper.

The building licence issued by the "Landratsamt Dresden" (Dresden Council Department) in April 1993 enabled us to start construction work. After partial demolition of the concrete shielding of the former Van de Graff accelerator vault these important steps could be done within the following 6 months.

1. Building the cyclotron vault

The thickness of the concrete walls and ceiling of the cyclotron vault has to meet all requirements concerning the shielding of direct n- and γ-radiation during operation of the cyclotron. Calculations were carried out by the supplier of the cyclotron (Siemens AG) with the computer programs MORSE and LEAKAGE [2]. The calculations using a predicted concrete density of 2.35 g/cm^3 and a free distance between targets and walls of 0.80 m gave the following results:

- outer walls (cellar level)   1.40 m
- wall to the control room   2.35 m
- ceiling (above ground)   1.90 m (see Fig. 1).

Our own estimations (based on [3]) are within the same range.

The "Materialprüfungsanstalt für das Bauwesen Dresden" (Material Research Laboratory/Building) determined an average concrete density of 2.55 g/cm^3 [4].

2. Conversion of rooms

Rooms formerly used for the cyclotron U-120 were converted into (see Fig. 1)
- control room (R001)   - hot lab (R001d)
- room for technical equipment (R001a)   - sluice (R001e).

3. Installation of 3 facilities for ventilation and climatization

To meet the the manufacturer's requirement in terms of room parameters 3 faclities for ventilation and climatization were installed including complete controlling and monitoring systems (see Table 1).

These facilities are planned to operate 24 houres a day. Three modes of operation are available (Automatic, Full Power, Half Power). During operation of the cyclotron an under pressure of 30 Pa will be guaranted in the vault. In case of a breakdown of the ventilation facility the operation of the cyclotron will be stopped by switching off the radio frequency (RF).

Table 1: Facilities for ventilation and climatization

Room	No. of ventilation facility	Current of air		Pressure conditions in the rooms (+)/(-)/(=)
		fresh air m^3/h	exhaust air m^3/h	
Control room (R001)	2	2.800	2.800	(=)
Room for techn. equipment (R001a)	2	350	350	(=)
Cyclotron vault (R001b)	1	1.000	1.000	(-) 30 Pa
Hot lab (R001d)	1 and 3	75	90 15: box 75: room	(-) 200 Pa in the box (-) in the lab

4. Installation of the gas supply system
The gas supply system will be used for:
- the gases needed for the operation of the cyclotron (H_2, D_2: ion sources, He: collimator cooling, N_2: venting)
- the gases and gas mixtures needed for the targets.

5. Installation of the compressed air system
Compressed air is needed for the pneumatic post system, the butterfly valves of the oil diffusion pumps and for the inflatable rubber tube of the door for closing the vault airtight.

6. Construction of the outer water cooling circuit
For the cooling circuit of the cyclotron the manufacturers stipulated an inlet temperature of the cooling water of (16 - 18) °C. To fulfil this condition a closed outer cooling circuit was planned. The inner and outer circuits are connected through a heat exchanger (capacity 50 kW) in room R001a.
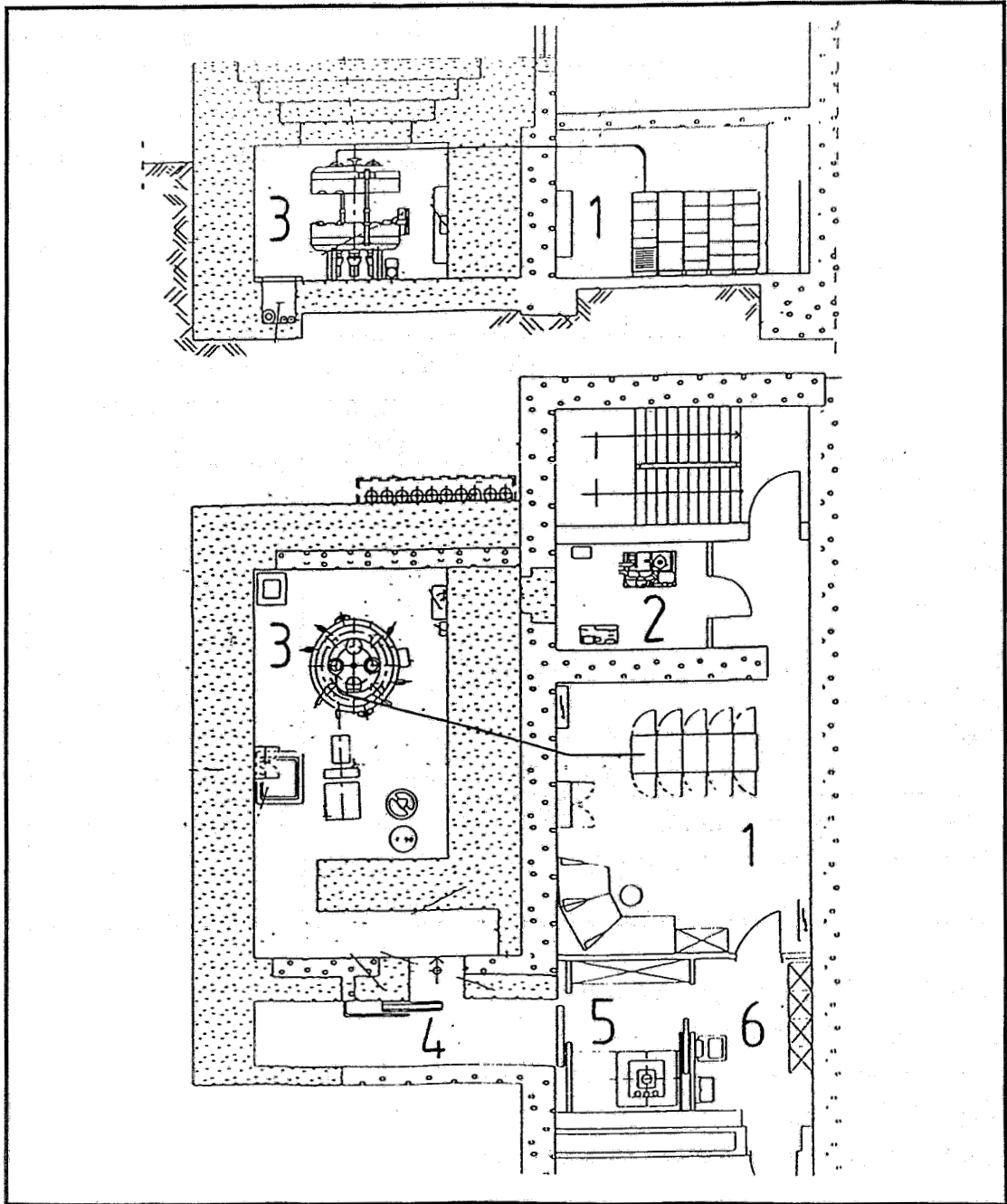
Fig. 1: The Rossendorf PET cyclotron: layout of the rooms

1 - control room (R001) 2 - room for technical equipment (R001a)
3 - cyclotron vault (R001 4 - entry room (R001c)
5 - hot lab (R001d) 6 - sluice (R001e)

7. Two doors for radiation protection

During operation of the cyclotron the cyclotron vault is closed with 2 doors for radiation protection, mainly for protection against neutron radiation. The door to room R001b is a sliding door made of a steel rack with a filling of interlaced polyethylene briks (thickness 16

cm). These briks are used for moderation of the fast neutrons. The back of this door is covered with cadmium sheet metal for absorption of the thermal neutrons. To create an under pressure of 30 Pa in the vault during operation of the cyclotron the door will be sealed airtight by an inflatable rubber tube which has to be filled with compressed air.

The door to room R001c is also a sliding door, but of two parts. With a steel rack this door is filled with polyethylene plates (thickness 3 cm) and the back is covered with 0.6 cm lead.

8. Construction of box 0 (hot cell)

The hot lab (R001d) with box 0 is the cyclotron-end terminal of the pneumatic post system between the cyclotron building and the radiopharmaceutical building. To handle the maximum activity of 92 GBq within box 0 the lead shielding of box 0 has a thickness of 10 cm to the front and 7 cm in all other directions. The loading unit for the pneumatic post as well as auxiliary equipment are placed inside this box.

9. Lengthening of the Rossendorf Activity Transport System (RATS)

It was necessary to lengthen the existing RATS (pneumatic post and gas transport system) for about 80 m from the former terminal in the cyclotron building to box 0 in the hot lab. The new pneumatic post system was tested with this result: for the 500 m distance the time of flight of a small pneumatic post box is around 1 minute. The gas transport system has also been tested.

10. Exhaust air emission measuring facility

The former exhaust air chimney of the cyclotron U-120 was replaced by a chimney for both cyclotrons. The so-called pick-up system for exhaust air is installed in this chimney. The ventilation facilities of both cyclotrons work independently of each other. The exhaust air tubing systems unite under the roof of the cyclotron building so that we only use one emission measuring facility for both cyclotrons.

The measuring facility consists of four main parts:
- a gas monitor for continuous monitoring of radioactive gases with a short half-life
- a continuous aerosol collector with a constant current of air
- a transportable gas collector unit
- an electronic system with switches for thresholds and a lot of possibilities for presentation
  of the measured values.

The "Sächsisches Staatsministerium für Umwelt und Landesentwicklung" (Saxon State Ministry of Environment and Regional Development) asked the TÜV Bayern Sachsen/TÜV Sachsen (TÜV = Association for Technical Inspection) for an expert opinion on our security report in compliance with the German Radiation Protection Regulations. One of the most important results was the statement that all our shielding measures were considered

adequate. Many of the TÜV's recommendations had already been fullfilled or were under consideration during the building phase respectivly. Other recommendations will be considered during installation of the cyclotron.

On October 6th 1993 our PET cyclotron was inserted into the vault. The installation of all components of the cyclotron is under way now. It is carried out by the manufacturers (IBA/Belgium), the supplier (Siemens AG) and the user (our PET-Tracer department) and will be finished within 6 months.

References
[1] Johannsen, B. et al., FZR 93 - 12 (1993)
[2] Information of Siemens AG, 1992
[3] Sauermann, P. F., Jül-751-PC, April 1971
[4] Prüfbericht Nr. 93-12-1775-01, 23.09.1993
    Materialprüfungsanstalt für das Bauwesen, Freistaat Sachsen, MPA Dresden

9. PHANTOM TESTS WITH THE PET CAMERA POSITOME IIIP

H. Linemann, E. Will

Introduction
Preparatory to using the PET-camera POSITOME IIIp [1] for studies on patients, we carried out phantom tests in order to explore the technical potentials, simulating the conditions applied during clinical investigations. The tests were carried out using the methods and the phantom set proposed by the EEC Task Group for the PET Instrumentation Program [2]. The head phantom of this set (20 cm diameter, 20 cm length) was used to test the brain camera.

The phantom tests also afforded us an opportunity to study the POSITOME programs and to write instructions for data acquisition and image reconstruction .

The sources used for the tests were filled with $[^{18}F]NaF$ or $[^{11}C]Na_2CO_3$ solution up to 50 MBq.

The tests performed and their results are described in this paper.

Spatial resolution
As the results for axial resolution were presented in the 1992 annual report [1], only transaxial resolution is described here.

Three glass capillaries (inside diameter 1 mm) were inserted into the phantom body parallel to the phantom axis in different radial positions (0, 4.5, 9 cm). The capillaries were filled with [18F]NaF solution (7 MBq/ml). This test was carried out both with and without water in the phantom.

Fig. 1 shows the profiles through the centres of the line sources for one of the three slices. The measured values of transaxial resolution (FWHM) are 1.2±0.1 cm for the 64*64 images and 1.15±0.05 cm for the 128*128 image. There was no significant difference between the results obtained for the water-filled phantom and that without. All measurements are with computed attenuation and scatter correction.

One test was carried out without attenuation correction for comparison (Fig. 1c). Under these conditions the two inner line sources show a significantly decreased tracer concentration but the FWHM values are almost unchanged.
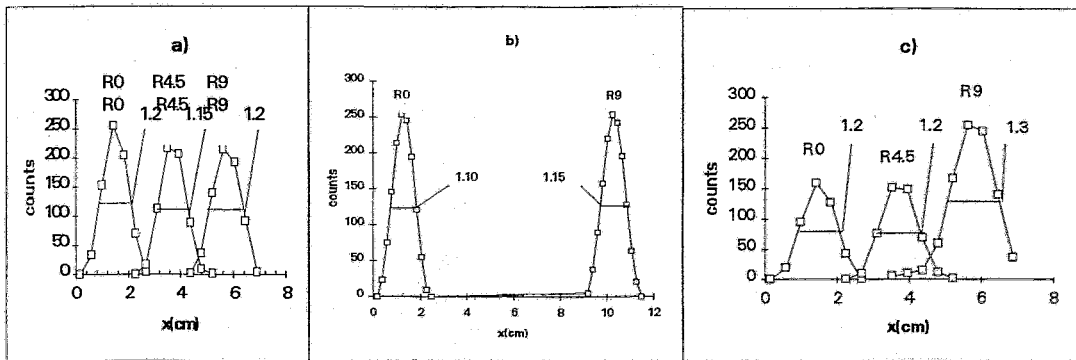
Fig.1: Transaxial resolution (water phantom, lower slice, projection on x-axis)

(a) 3 line sources, 64*64 image, computed attenuation correction

(b) 2 line sources (on x-axis), 128*128 image, computed attenuation correction

(c) 3 line sources, 64*64 image, no attenuation correction
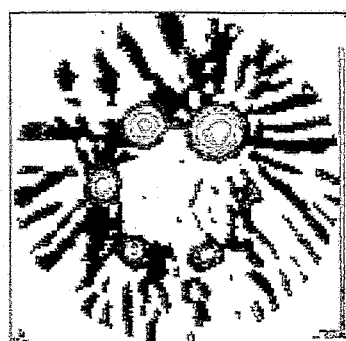
Recovery of 'hot' spheres

The objective of this procedure is to quantify the apparent decrease in specific activity of small objects. This decrease is expected when the dimensions in any direction are less than 3*FWHM (scanner resolution) [2]. The recovery coefficient (RC) of an active volume is defined as the measured activity concentration in the volume divided by the measured concentration in a large volume with all dimensions larger than 3* FWHM.

This test consists of two measurements. The first scan is made with 6 hollow spheres of different diameters. These spheres are filled with samples of equal specific activity and fixed in the water-filled head phantom. All spheres are arranged coplanar in the same radial position (Fig. 2a). The second scan is performed with the homogeneous head phantom filled with active solution. For both scans the measured specific activity divided by the injected

specific activity (measured with the dose calibrator) was estimated and inserted into the RC equation.

The apparent dimension of the spheres, wich is influenced by the spatial resolution of the camera, must be considered in close connection with the RC. Fig. 3a shows the relation between the measured diameters (the $FWHM_{SP}$ values in profiles through the images) and the real diameters of the 6 spheres. Due to the spherical form of the sources, the apparent dimensions decreases for smaller spheres. But with dimensions approximating the camera resolution of about 1 cm, the apparent diameters exceed the real ones.

The recovery coefficient is dependent on the region of interest (ROI) used for the sphere images. For a ROI dimension which is small in comparison with the object, the RC should be 1 for objects with all dimensions larger than 3*FWHM (spatial resolution) if the corrections for attenuation, scatter, and dead time have been made correctly. The tests reported here lead to an RC of 1.02 for the largest sphere (3.7 cm diameter) and a small ROI (0.6 cm diameter). Fig. 3b shows the RC values for ROI s equivalent to the apparent source dimensions and the camera resolution respectively. The first curve can be used to correct the measured specific activity of small spherical structures in realistic human studies.
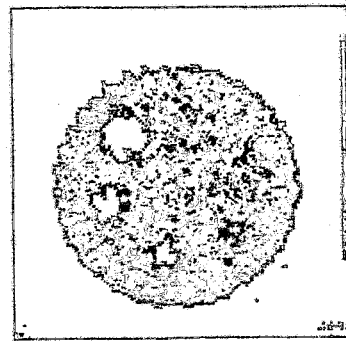
(a)   (b)

Fig. 2: Spheres (diameter: 3.7, 2.2, 1.7, 1.3, 1.0 cm) in head phantom
    (a) "hot" spheres ($[^{18}F]$NaF solution,100 kBq/ml) in water (scan time: 30. min)
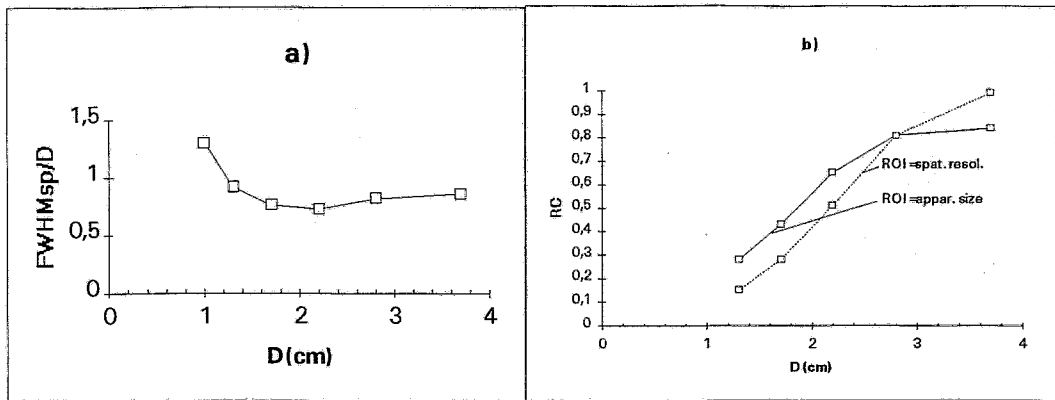   (b) "cold" spheres in $[^{18}F]$NaF solution (3 kBq/ml, scan time: 60. min)

Fig. 3: Recovery coefficient ("hot" spheres in water)
  (a) apparent diameter (FWHM$_{SP}$) as a function of the real sphere diameter D
  (b) RC as a function of the real sphere diameter D

'Cold' spheres

In contrast to the arrangement described above, in this test the 6 spheres were filled with water, with activity only in the phantom body. The correction conditions were the same as for the previous test.

Fig. 2b indicates that all spheres were detected. But compared with the pictures of 'hot' spheres the picture seems to be more deformed due to the restricted camera resolution. The different statistics of the two images must also be considered in this comparison.

The profiles through the images show a decrease in the measured tracer concentration to about zero only for spheres with a diameter greater than 2 cm. Smaller spheres with a diameter of about 1cm are correlated with minimal tracer concentrations of 40 % of the mean surrounding concentration.

Brain phantom

As a phantom with a nearly realistic structure the Hoffman Brain Phantom [3] was used in addition to the EEC phantom. In this phantom the grey substance is represented by a 12 mm thick slice and the white substance by a 3 mm thick slice filled with active solution. Ventricles and skull are represented by compact material without radioactive substances (Fig. 4a). These activity thicknesses are in the same relation as the metabolic rates of the substances represented [3]. The phantom should therefore produce realistic structures if the whole thickness is imaged.

A comparison of the measured picture (Fig.4b) with the phantom structures (Fig.4a) shows that only structures with transaxial dimensions greater than about 1 cm were imaged in nearly actual size. The measured activity concentration around the outer 'grey substance' is changed by a factor of 2 measured with a small ROI ($0.4*0.4$ cm^2). This variation is caused by the different width of this structure and the influence of the recovery coefficient.

(a)   (b)
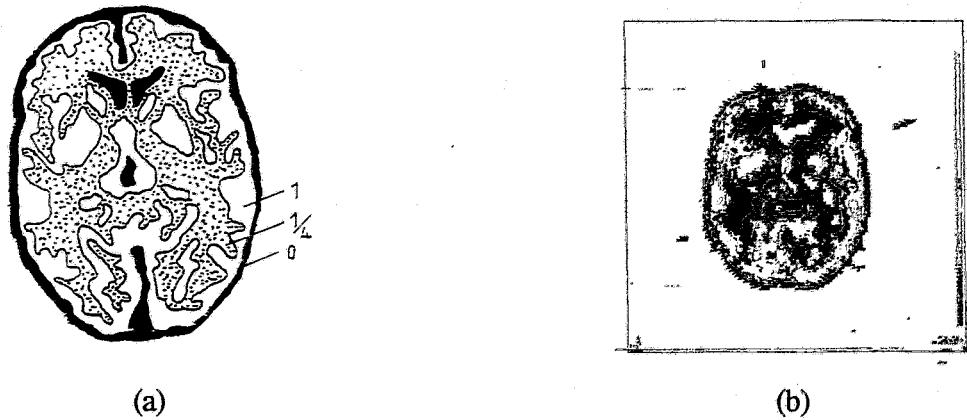
Fig.4: Hoffman Brain Phantom, (a) real structure, (b) measured picture ([^{18}F]NaF solution, 57 kBq/ml, scan time:15.min, computed attenuation correction)

Conclusion

After the POSITOME IIIp installation described in the last annual report [1] the phantom investigations demonstrated the correct functioning of the camera as well as of the programs for data aquisition and image reconstruction. In addition, they showed the influence of restricted spatial resolution.

References

[1] Enghardt, W. et al., FZR 93 -12 (1993) 16

[2] Guzzardi, R. et al., Ed.: EEC concerted action "PET Investigation of Cellular Regeneration and Degeneration", Brussels-Pisa (1990)

[3] Veklerov, E. et al., IEEE Transactions on Nucl. Science 35 (1988) 141

10. TECHNETIUM AND RHENIUM COMPLEXES DERIVED FROM SPIPERONE
1. SYNTHESIS OF A 4-FLUOROBUTYROPHENONE-CONTAINING NEUTRAL RHENIUM COMPLEX

H. Spies, St. Noll, B. Noll, K. Klostermann[1]

[1] Technische Universität Dresden

The question whether coordination compounds, preferably those of technetium, are able to imitate organic receptor-binding ligands is of basic interest for the design of a new generation of biospecific Tc tracers.

Investigations have therefore been undertaken to synthesize Tc and Re complexes showing structural analogies to the D_2 receptor-binding ligand spiperone and to study their binding affinity.

Although the spiperone molecule tolerates some structural modifications without any drastic change in its bonding properties [1,2], an early attempt by Ballinger et al.[3] to use ^{99m}Tc labelled spiperone dithiocarbamate as a potential radiopharmaceutical for dopamine receptor imaging did not produce the desired result. Complex formation of spiperone dithiocarbamate with the metal, probably resulting in a rather bulky 1:2 (metal to ligand) complex, obviously leads to complete loss of the receptor binding properties.

Our strategy in designing of "spiperone-like" coordination compounds involves substitution of nonessential parts of the receptor-binding molecule by a chelate unit in such a manner that the charge, molecular weight and general shape of the new compounds will not differ too much from those of the original receptor-binding molecule.

As a first step, rhenium complexes with partial structures of spiperone have been prepared. The resulting new class of compounds, which we call "rhenium spiperoids", consist of sulphur-coordinated oxorhenium(V) chelates combined with fluorobutyrophenone (as described here) or a more complete molecular part of spiperone (as will be described later) as a substituent.

The complexes are accessible by the "3+1" synthesis principle [4], which involves common action of both a tridentate and a monodentate ligand on an appropriate Re(V) precursor.

Here we describe the synthesis and properties of the first representative of the "spiperoides" (3-thiapentane-1.5-dithiolato)(p-fluorophenyl-1-oxobutanethiolato-4)oxorhenium(V) **3**.

The stable, crystalline compound has been characterized by elemental analysis and spectroscopic methods.
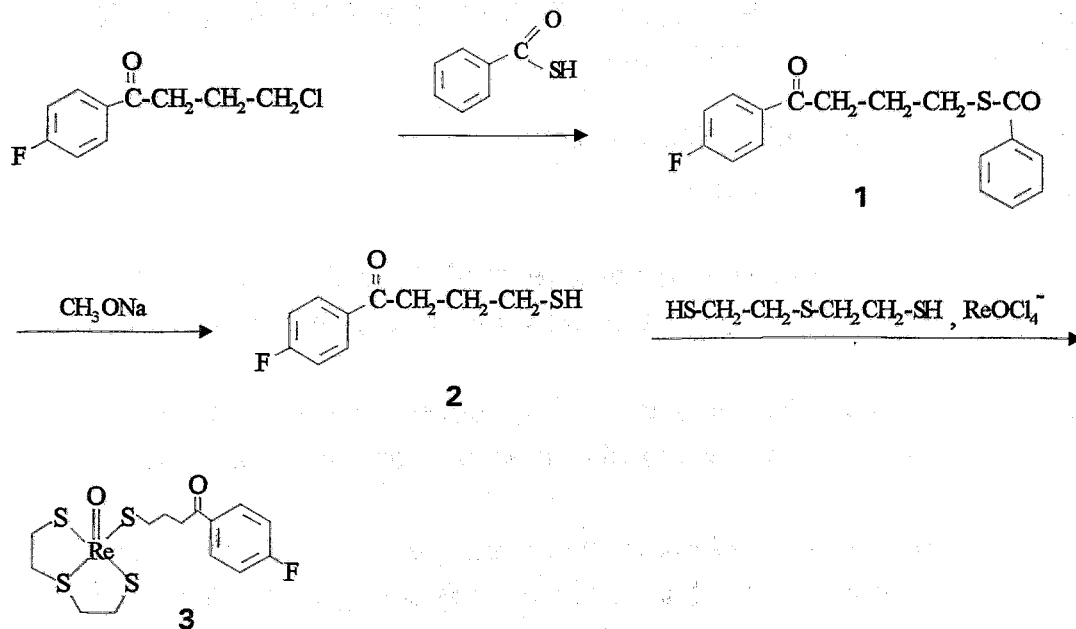
Synthesis follows the route as shown in Fig.1.

Fig.1: Reaction scheme of the preparation of **3**

4-Chloro-(p-fluoro)butyrophenone reacts with thiobenzoic acid to give 4-benzoylmercapto-(p-fluoro)butyrophenone **1**. Its hydrolysis results in 4-mercapto-(p-fluoro)butyrophenone **2**. An equimolar mixture of **2** and 3-thiapentane-1.5-dithiole is allowed to react with Re(V) gluconate in an aqueous/acetonic solution and produces the mixed ligand complex **3** together with several by-products. Separation of the resulting compound by semipreparative HPLC (Hypersil ODS 8 x 250, 0.1 % aq.tfa/0.1 % tfa in acetonitrile 50/50) yields pure **3** as dark brown needles mp.: 166 $^{\circ}$C (acetone/methanol). Yield: about 55 % (at 0.1 mmol-level). Elemental analysis: Calc. for $C_{14}H_{18}O_2S_4FRe$ (Mol.weight 551.75): C: 30.48, H: 3.29, S: 23.25 %; found: C: 29.42, H: 3.24, S: 23.64 %.

UV (acetonitrile/water): 240, 380 nm.

IR (KBr): 969 cm^{-1} Re=O; 1601 cm^{-1}, 1673 cm^{-1} C=O.

^{1}H NMR (CDCl$_3$): 4.35/4.21 ppm (2xd) 2 H, 4.0 ppm (m) 2 H, 3.0 ppm (m) 2 H, 2.0 ppm (m) 2 H -CH$_2$-CH$_2$-S-CH$_2$-CH$_2$-; 8.00 ppm (m) 2 H, 7.08 ppm (m) 2 H fluoro-phenyl; 3.97 ppm (t) 2 H, 3.12 ppm (m) 2 H, 2.37 ppm (m) 2 H -CH$_2$-CH$_2$-CH$_2$-.

The composition of **3** follows from elemental analysis, infrared, ^{1}H NMR and mass spectroscopy.

The IR spectrum shows the Re=O band at 969 cm^{-1} and the C=O vibration at 1673 cm^{-1}.

The ^{1}H NMR spectrum of **3** correponds in general with the proposed structure. The observed spectrum is rather complicated due to the presence of several methylene groups in the molecule and refers to nonsymmetry of the two parts of the tridentate ligand.

The most intense peak in the electron impact mass spectrum (Fig. 2) at m/z = 552 is due to the molecular ion with the ^{187}Re isotope (natural abundance of about 63 %), while that at m/z = 550 corresponds to the molecular ion with the isotope ^{185}Re (about 37 % abundance). Fragments such as m/z = 534 (M-F) and m/z = 165 ($-(CH_2)_3-CO-C_6H_4F$) confirm the assumed composition.
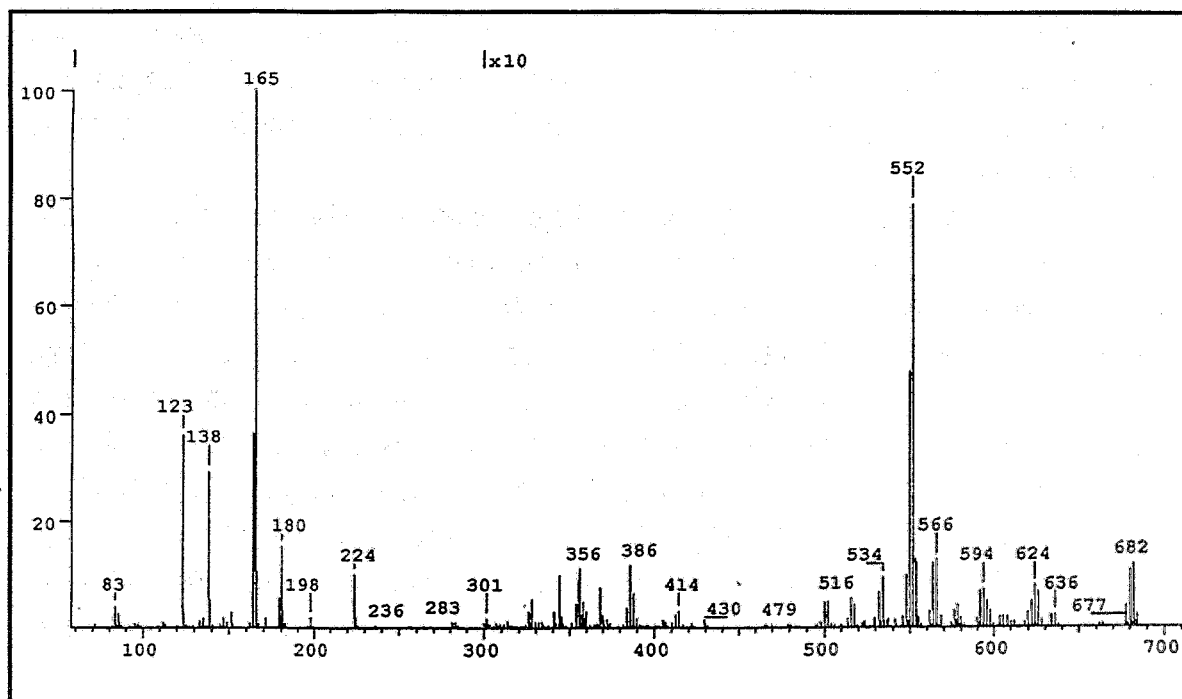

Fig. 2: Electron impact mass spectrum (15 eV) of **3**

An X-ray crystal structure determination of **3** is described in the following part 2. Binding studies of **3** on dopamine D1 receptors in the striatum of Wistar rats were carried out both in striatum homogenates and in slices of the striatum and will be described in part 3.

References

[1] Coenen, H.H. et al., Life Sci. **40** (1987) 81

[2] Mach, R.H. et al, Nucl.Med.Biol. **20** (1993) 269

[3] Ballinger, J.R. et al., Appl.Radiat.Isot. Part A **40** (1989) 547

[4] Pietzsch, H.J. et al., Inorg.Chim.Acta **165** (1989) 163

11. TECHNETIUM AND RHENIUM COMPLEXES DERIVED FROM SPIPERONE
2. X-RAY CRYSTAL STRUCTURE OF (3-THIAPENTANE-1.5-DITHIOLATO)(p-FLUOROPHENYL-1-OXOBUTANETHIOLATO-4)-OXORHENIUM(V)

H Spies, P. Leibnitz[1], St. Noll, B. Noll

[1] Bundesanstalt für Materialforschung, Berlin

The X-ray crystal structure of the title compound was determined. Preparation and spectroscopical characterization are described in the preceding article [1]. The X-ray data of the compound were collected at room temperature (296 K) with an ENRAF-NONIUS CAD 4 diffractometer, graphite monochromatized Mo Ka radiation (A = 0.71073 Å). (Crystal system: triclinic, space group no. P1, Z = 2, R =3.5 %, selected bond lengths and angles are listed in Table 1).

The structure of $[ReO(SSS)(S(CH_2)_3COC_6H_4F-(p))]$ consists of discrete monomolecular units. A perspective view of the complex (Fig. 1) shows that the compound has a distorted square-pyramidal arrangement. The metal atom lies about 0.7 Å above the plane of the four basal donor atoms S_1 - S_4. The observed square-pyramidal arrangement is found for a large number of five-coordinated technetium as well as for rhenium complexes. (Data of selected mononuclear rhenium compounds with a square-pyramidal geometry are listed in Table 2). The structure of the tridentate/monodentate mixed-ligand complex is related to $[ReO(S_3)(SR)]$, where R is ethyl or $C_6H_4OCH_3-(p)$, the latter described in [2].

Data in Table 2 show that the $Re-O_1$ bond lengths are in the range 1.63 to 1.74 (1.68 Å on average). The $Re-O_1$ bond length of 1.686(7) Å is within this range. All other bond lengths and angles are normal. The data reveal also that there are no special interactions between the substituent fluorobutyrophenone and the complex unit.

Abbreviations

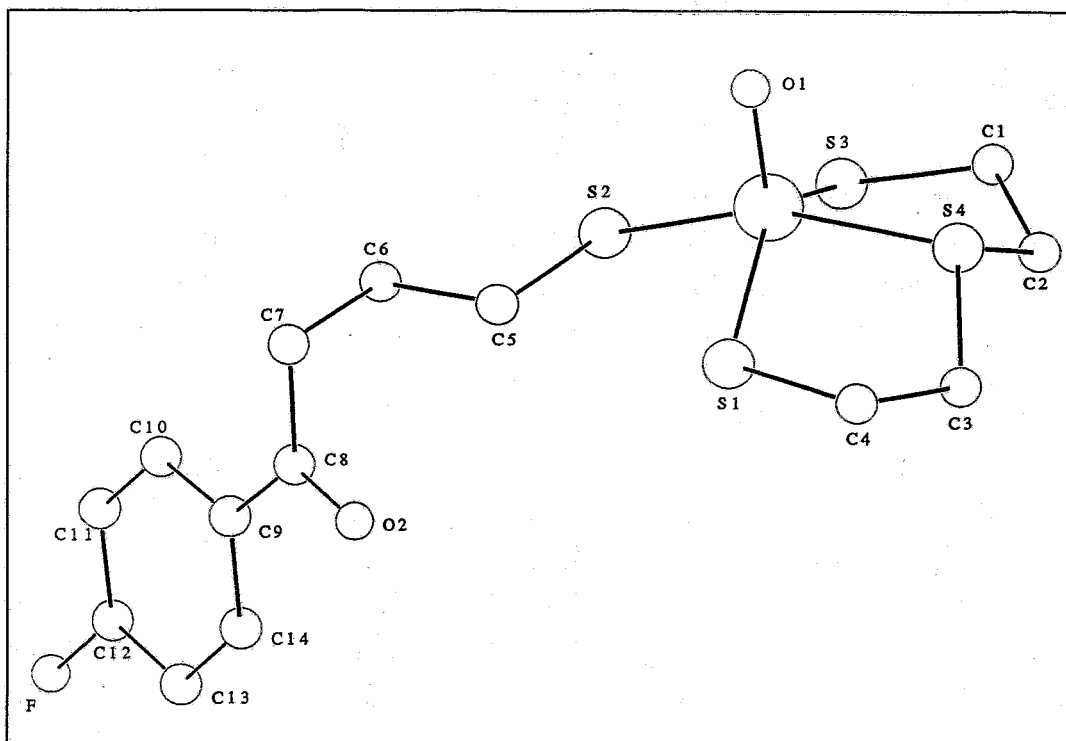|	
SSS	$SCH_2CH_2-S-CH_2CH_2S(2-)$
SOS	$SCH_2CH_2-O-CH_2CH_2S(2-)$
DMSA	*(meso)*$SCH(COOH)-CH(COOH)S(2-)$
tedadt	3,3'-[ethane-1,2-diylbis(iminomethylene)]bis(pentane-3-thiol)ato(3-)
map	2,3-bis(mercaptoacetamido)propanoate(S,N,N,S-)
MAG$_2$	mercaptoacetyl diglycine(S,N,N,O-)

Fig. 1: CELLGRAF drawing of [ReO(SSS)(S(CH$_2$)$_3$COC$_6$H$_4$F-(p))]

Table 1: Selected bond lenghts and angles of [ReO(SSS)(S(CH$_2$)$_3$COC$_6$H$_4$F-(p))]

Bond lengths (Å)

Re-O$_1$	1.686(7)	Re-(S$_1$-S$_2$-S$_3$-S$_4$) plane	0.7
Re-S$_1$	2.287(2)	Re-S$_3$	2.297(2)
Re-S$_2$	2.301(2)	Re-S$_4$	2.369(2)

Bond angles (^{o})

O$_{(1)}$-Re-S$_1$	115.5	S$_{(1)}$-Re-S$_{(2)}$	88.06
O$_{(1)}$-Re-S$_{(2)}$	105.7	S$_{(1)}$-Re-S$_{(4)}$	83.98
O$_{(1)}$-Re-S$_{(3)}$	114.3	S$_{(2)}$-Re-S$_{(3)}$	82.16
O$_{(1)}$-Re-O$_{(4)}$	99.9	S$_{(3)}$-Re-S$_{(4)}$	84.21

Table 2: Mononuclear rhenium compounds with a square-pyramidal geometry

Complex	Core	Re=O (Å)	Re-S (mean) (Å)	δ (Å)	Reference
[ReO(SC$_6$H$_5$)$_4$]$^-$	ReOS$_4$	1.686(9)	2.34	0.732	[3]
[ReO(SC$_6$H$_2$Me$_3$)$_4$]$^-$	ReOS$_4$	1.651	2.32	0.71	[4]
[ReO(SCH$_2$CH$_2$S)$_2$]$^-$	ReOS$_4$	1.742	2.31		[5]
[ReO(DMSA)$_2$]$^-$	ReOS$_4$	1.699(8)	2.31		[6]
[ReO(DMSA)$_2$]$^-$	ReOS$_4$	1.672	2.31		[7]
[ReO(SOCCOS)$_2$]$^-$	ReO$_3$S$_2$	1.674	2.33	0.752	[8]
[ReO(SSS)(SEt)]	ReOS$_4$	1.633	2.29		[9]
[ReO(SOS)(SC$_6$H$_4$OMe)]	ReO$_2$S$_3$	1.659	2.28		[2]
[ReO(tedadt)]	ReON$_2$S$_2$	1.709$^{1)}$	2.28		[10]
[ReO(map)]$^-$	ReON$_2$S$_2$	1.662	2.28	0.747	[11]
[ReO(MAG$_2$)]$^-$	ReO$_2$N$_2$S		2.267		[12]

δ is the displacement (Å) of the rhenium atom from the square base

[1)] Bond lengthening due to intermolecular O···H···N hydrogen bond

References

[1] Spies, H. et al, this report, p. 37

[2] Spies, H. et al, FZR 93 - 12 (1993) 94

[3] McDonell A. C. et al., Aust. J. Chem. **36** (1983) 253

[4] Blower, P. P. et al., Inorg. Chim. Acta **90** (1984) L27

[5] Blower, P. J. et al., J. Chem. Soc., Dalton Trans., **1986**, 1339

[6] Singh, J. et.al., J. Chem. Soc.,Chem. Commun. **1991**, 1115

[7] Seifert, S.et al., this report, p. 91

[8] Mattes, R. et al., Z. Anorg. Allg. Chem., **474** (1981) 216

[9] Spies H. et al., FZR 93 - 12 (1993), 94

[10]Jackson, W. et al., Austr. J. Chem. **46** (1993) 1093

[11]Rao, T. N. et al., Am. Chem. Soc. **112** (1990) 5798

[12]Johannsen, B. et al., Inorg. Chim. Acta **210** (1993) 209

12. TECHNETIUM AND RHENIUM COMPLEXES DERIVED FROM SPIPERONE
3.BIOLOGICAL EVALUATION OF A 4-FLUOROBUTYROPHENONE-CONTAINING NEUTRAL RHENIUM COMPLEX

R. Syhre, U. Wenzel, R. Berger

Introduction

Dopamine receptor agents are very important for diagnosis of diseases of the central nervous system. A ^{99m}Tc-SPECT tracer for imaging these receptors does not yet exist in spite of numerous efforts. This is due to the high demands which receptor imaging agents have to meet in terms of basic requirements, especially as regards their biological quality. For instance, they must be able to pass through the intact blood-brain barrier following i.v. injection, show no or little in vivo metabolism and exhibit high affinity to the specific receptor [1].

The biological screening of potential imaging agents has priority for an assessment of receptor binding properties. With a suitable choice of experimental conditions such an assessment is possible in vitro on the brain of the rat [2,3].

The first Re-coordinate compound is at present ready for use in biological screening. The test substance is described in the chemical part (Part 1) of this volume. Re-complex 3 is a model of an analogeous structure of the planned ^{99m}Tc radioligand. The structure of this complex shows similarity to the dopamine D_2 receptor binding ligand spiperone.

In the preliminary experiments it shall be tested whether this substance has an influence on the uptake of [3H]-spiperone into rat brain sections. The precursors have also been investigated in comparison with the test substance to recognize possible effects caused by the partial structures of the molecule.

Principle of receptor binding studies

Dopamine D_2 receptors are proved to be different regions of the brain (Fig.1a,b),especially in:

Principle of receptor binding studies

D_2 receptors are proved to be in different regions of the brain (Fig. 1a,b), especially in:

- basal ganglia (caudate/putamen, nucleus accumbens)
- olfactory system (olfactory tubercle)
- cortical areas like entorhinal- and frontal cortex, cingulum
- hippocampus (CA1 field and gyrus dentatus)

These receptors are not found in the cerebellum.

For the described investigations a level of rat brain horizontal sections is chosen in which the main regions are registered. (Fig. 1b)

The principle of the binding studies is the following:

Binding (total) - specific receptor binding = nonspecific binding

The total binding is measured by the uptake of [3H]spiperone into the brain section. When a substance with a high affinity to the receptor (competitive ligand; displacer substance) is added to the radioligand, then the [3H] uptake is reduced by the amount of specific binding and represents the nonspecific binding.
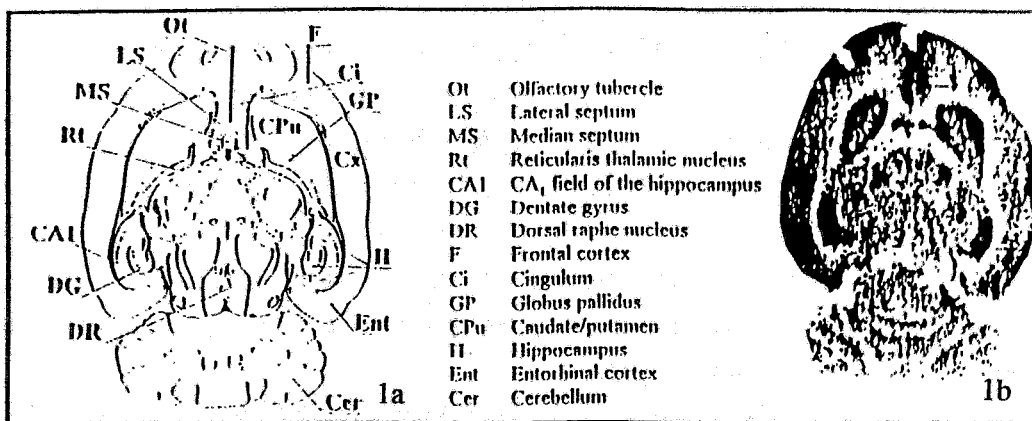

Ot	Olfactory tubercle
LS	Lateral septum
MS	Median septum
Rt	Reticularis thalamic nucleus
CA1	CA₁ field of the hippocampus
DG	Dentate gyrus
DR	Dorsal raphe nucleus
F	Frontal cortex
Ci	Cingulum
GP	Globus pallidus
CPu	Caudate/putamen
H	Hippocampus
Ent	Entorhinal cortex
Cer	Cerebellum

Fig. 1a: Schematic representation of a horizontal section of rat brain , modified from
M.C. MIQUEL [4]
1b: Autoradiograph after incubation with [3H]spiperone /
the same region as 1a

In the first part of the studies for testing the evidence of a potential dopaminergic substance the compounds are used as competitive ligands.
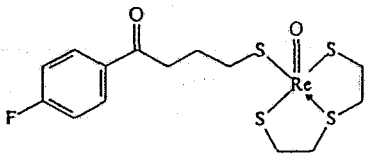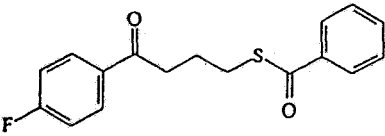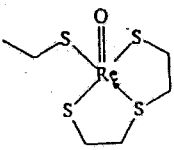
Reference substances

The dopaminergic radioligand [3H]spiperone (specific radioactivity [3.55 TBq/mmol]) is used as a reference substance for measuring the total binding. The dissociation constant (K_D) and the maximal binding (B_{max}) of this receptor/ligand system, depending on the experimental conditions were described to be between 1.2 and 4.3 x 10^{-10} mol/l and 80 fmol/mg tissue [5]. (+)-Butaclamol is used as a reference substance to prove the displacement. Its dissociation constants using [3H]spiperone as a radioligand are described in the literature with large variations (0.4 - 4.4 nmol) [6].

Test substance

The test substance (Re-complex **3**) is used as a competitive ligand like (+)-butaclamol. The partial structures of the test substance were also investigated (Table 1).

44

Table 1: Structure of the Re complex and its precursors

RE-COMPLEX 3		(3-Thiapentane-1,5 dithiolato)(fluorophenyle-1-oxobutanthiolato-4)oxorhenium
PARTIAL STRUCTURE 1		4-Benzoylmercapto(p-fluoro)butyrophenone
PARTIAL STRUCTURE 2		Ethanethiolato-3-thiapentanethiolato-1,5-oxorhenium

Studies of receptor binding

Receptor binding studies were carried out on brain sections of rats. Details of the method are described in this report [7]. The uptake and distribution pattern of radioactivtiy were measured after incubation with solutions 1 - 5 in Table 2.

Table 2: Solutions for incubation

1	[^{3}H]spiperone	(A)
2	[^{3}H]spiperone and (+)-butaclamol	(B)
3	[^{3}H] spiperone and Re-complex 3	(C)
4	[^{3}H]spiperone and partial structure 1	
5	[^{3}H]spiperone and partial structure 2	

In the first part of the studies only one concentration (5 μmol/l) of the test substance was used. K_D and B_{max} results cannot be given at the present time. Since these constants are missing, the following results can only be evaluated in qualitative terms as regards the affinity of the Re-complex to the dopamine D_2 receptor.

Results and discussion

The results of the LSC measurements of brain sections after incubation with solutions 1 - 5 are shown in Fig. 2. The uptake of radioactivity after incubation with [^{3}H]spiperone is the reference value (100 % uptake of radioactivity). This was reduced to 37 % uptake of radioactivity by using (+)-butaclamol as a competetive ligand. The Re-complex reduced the

[^{3}H] uptake to 56 %. In comparison, the partial structures 1 and 2 influenced the [^{3}H] uptake only insignificantly (Fig. 2).
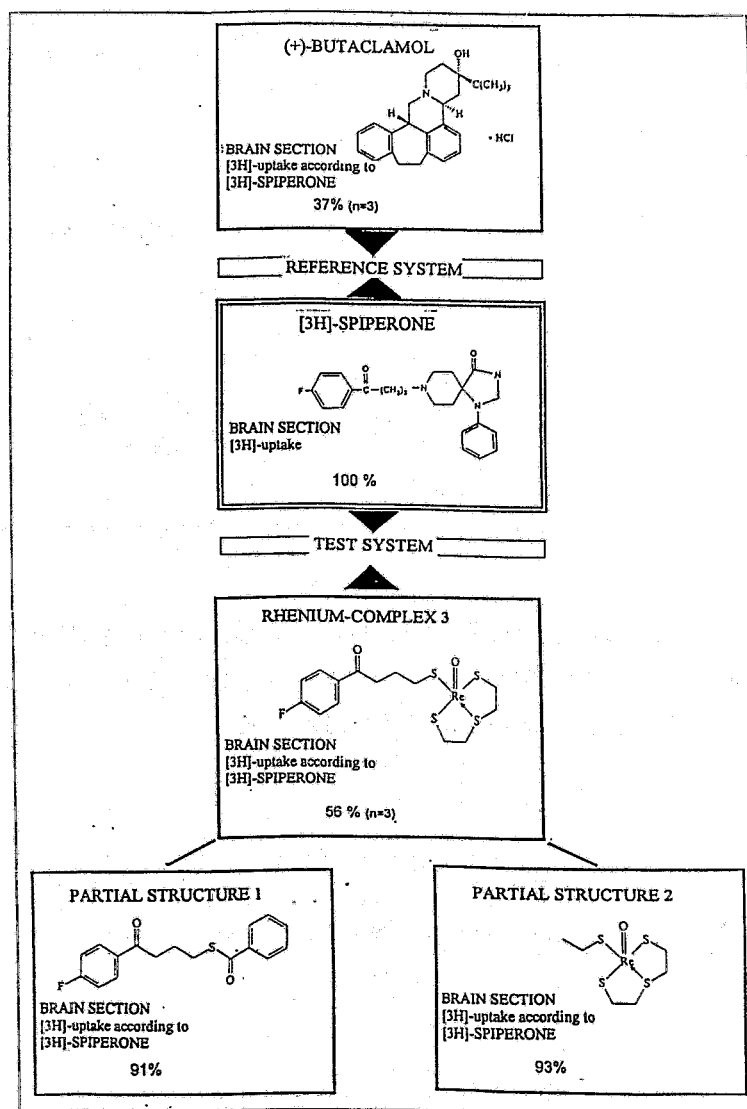

Fig. 2: [^{3}H] uptake into brain sections after incubation with test solutions 1 -5 /
LSC- measurements (Liquid Scintillation Counting)

Similar results were obtained by autoradiographic studies. These studies were carried out with test solutions 1, 2, and 3. The results of a representative experiment are shown in Fig. 3.
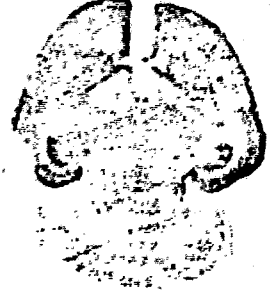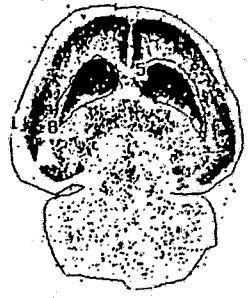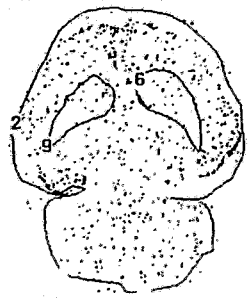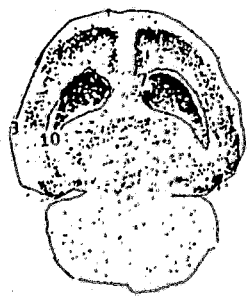
	REFERENCE SUBSTANCE	DISPLACER SUBSTANCE	TESTSUBSTANCE
	[3H]-SPIPERONE (A)	BUTACLAMOLE (B)	RE-COMPLEX (C) e
BRAIN SECTION [3H]-DISTRIBUTION PATTERN			
BRAIN SECTION [3H]-DISTRIBUTION PATTERN	STRIATUM 1 STRIATUM 2	STRIATUM 1 STRIATUM 2	STRIATUM 1 STRIATUM 2
	UPTAKE OF RADIOACTIVITY	UPTAKE OF RADIOACTIVITY ACCORDING TO [3H]-SPIPERONE	UPTAKE OF RADIOACTIVITY ACCORDING TO [3H]-SPIPERONE
BAS 2000			
BRAIN SECTION (TOTAL)	100 %	25 %	55 %
STRIATUM 1	100 %	10 %	67 %
STRIATUM 2	100 %	12 %	56 %
LSC MEASUREMENT			
BRAIN SECTION (TOTAL)	100 %	24 %	45 %

Fig. 3: Representation of autoradiographs (film) as well as pictures and quantitative data of $[^3H]$ uptake (BAS 2000) in comparison with LS counting / horizontal rat brain sections

The pattern of $[^3H]$ distribution in brain sections demonstrates a significant differentiation in the

$$[^3H]SPIPERONE \ (A) \ > \ Re \ COMPLEX \ (C) \ > \ (+)\text{-}BUTACLAMOL \ (B)$$

The quantitative interpretation of the $[^3H]$ distribution in the brain sections (BAS 2000) is shown in the table (Fig. 3). $[^3H]$spiperone is also the reference for radioactivity uptake (100 %) . The Re complex **3** reduces the $[^3H]$ uptake to 55 % and (+)-butaclamol to 25 %. In further investigations (determination of K_D and B_{max}.) it will be determined whether the displacing effect repesents a significant dopamine D_2 receptor binding of Re complex **3**.

References

[1] Kung, H. F. et al., Nucl. Med. Biol. **17/1** (1990) 85

[2] Repke, H. et al., Membranrezeptoren und ihre Effektorsysteme
Akademie-Verlag Berlin (1987)

[3] Yamamura, H. J, Methods in Neurotransmitter Receptor Analysis
Raven Press New York (1990)

[4] Miquel, M.-C. et al, Neurochem. Int. **19** (1991) 453

[5] Palacios, J. M. et al, in: Dopamine Receptors Alan R. Liss. Inc.,
New York (1987) 175

[6] Seeman, P., Neurophsychopharm. **7** (1992) 261

[7] Wenzel, U. et al , this report, p. 142

13. N-ALKYLATED MERCAPTOACETYL GLYCINE DERIVATIVES AS MULTIPURPOSE LIGANDS IN RADIO TRACER DESIGN PART I: SYNTHESIS OF LIGANDS

St. Noll, B. Noll, H. Spies, B. Johannsen, L. Dinkelborg[1], W. Semmler[1], P.E. Schulze[1], M. Findeisen[2]

[1] Institut für Diagnostikforschung Berlin, [2] Universität Leipzig

Mercaptoacetyl glycine (MAG) derived ligands represent a small-sized highly reliable chelate system that offers potential for various purposes of technetium and rhenium radiotracer design. The potential grows with chemical diversity in terms of charge and variable substituents of the metal complexes. In exploring such a variability, we found that a very advantageous option is N-alkylation of one of the amide groups present in a MAG peptide chain, such as MAG_3. N-alkylation has considerable consequences for the MAG_n ligand, which normally forms a monoanionic core and provides a pendent carboxylic group.

48

Since the alkylated amide group is no longer able to contribute negative charge to the metal, formation of a neutral oxometal(V) core results. With such an elimination of the charge at the core, one is able to drastically increase the lipophilicity of the complexes. In addition, the chain length of the alkyl group enables us to fine-tune lipophilicity.

The following two papers provide information on synthesis and labelling with technetium-99m of N^1-alkylated mercaptoacetyl glycine ligands and analytical characterization of the formed products. Biodistribution patterns were determined in Wistar rats. The ability of the resulting species to be accumulated in arteriosclerotic plaques was tested in rabbits.

Synthesis of ligands

N-alkyl-MAG$_n$ ligands **5** were prepared by reaction of the various chloroacetylamino acids or chloroacetyl peptides **1** with the required alkyl amines to give the N-alkyl glycines **2**. These were chloroacetylated, yielding the precursors **3** for reaction with thiobenzoic acid to the S-protected compound **4**. This procedure was followed by splitting off the benzoyl group according to a synthesis described in [1].

5   n = 0,1,2   R = methyl, hexyl, octyl, dodecyl
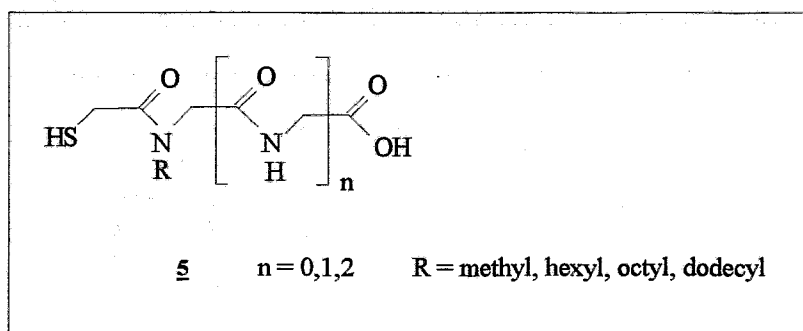
All prepared substances **5** and the S-benzoylated compounds **4** are listed in Table 1.
Compounds **5** are white or pink solids of widely differing solubility in water and organic solvents.
TLC of the compounds was carried out in the Silufol//n-butanol/acetic acid/water 2:1:1 chromatographic system (*) and in the RP18//methanol chromatographic system (**). Chloroacetylated compounds were detected by spraying with iodine, amino acids, alkylated compounds and mercaptoacetyl derivatives were sprayed with ninhydrine and benzoyl-protected substances were detected at 254 nm.
HPLC characteristics of **4a-d** are shown in Fig. 1.

Tab.1: Data of compounds **4** and **5**

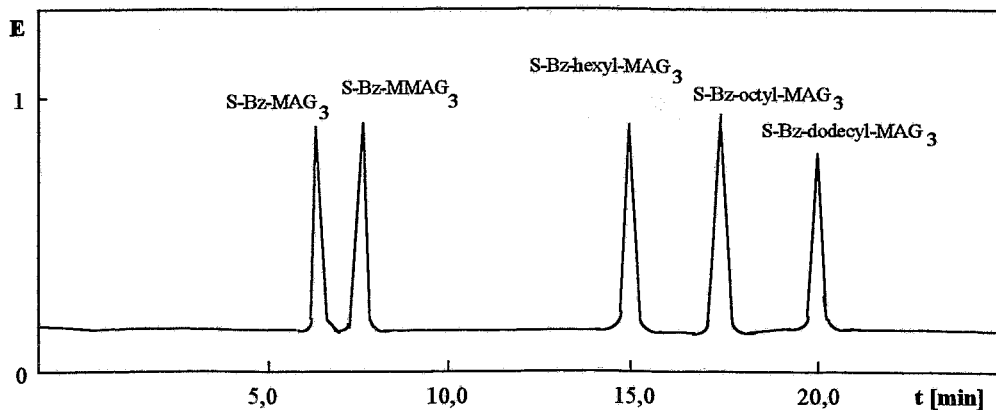| Compound			yield [%]	m.p. [°C]	TLC	
	n	R			R_f^*	R_f^{**}
4a	2	methyl	32	134	0.8	
5a	2	methyl	19		0.4	0.8
4b	2	hexyl	5		0.8	
5b	2	hexyl	2		0.8	
4c	2	octyl	5	191	0.84	
4d	2	dodecyl	4	122	0.8	
4e	1	methyl	30		0.75	
5e	1	methyl	28		0.48	
4f	0	methyl	45		0.85	
5f	0	methyl	35		0.7	0.85
4g	0	hexyl	14	69	0.85	
5g	0	hexyl	7		0.8	0.75

Fig. 1: HPLC characteristics of compounds **4a-d** (Hypersil ODS, phosphate buffer pH 7.0/ methanol, 1 ml/min)

Reaction scheme and preparation of a typical representative of **5** is shown in Fig. 2 and described below.

Synthesis of mercaptoacetyl-hexylglycyl diglycine (N^1-hexyl-MAG₃) 5b

Chloroacetyl-diglycine

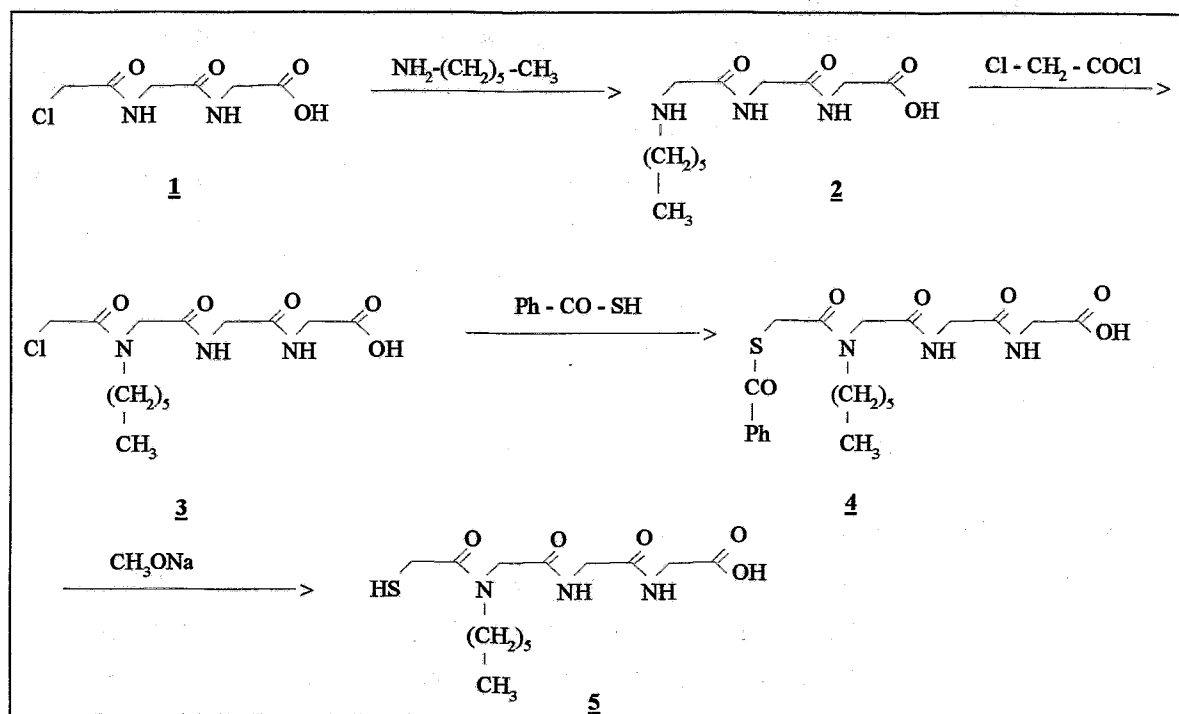was prepared according to a procedure described in [2]

Fig.2: Reaction scheme

Hexylglycyl-diglycine

1 g (4.8 mmol) chloroacetyl diglycine and 5 g (50 mmol) hexylamine were dissolved in 5 ml of ethanol. The solution was allowed to stand at room temperature for 6 days and then the solvent was removed by rotary evaporation. The oily residue was dissolved in 50 ml of boiling acetone. After cooling to 5 °C, the residue was separated, washed with cooled acetone and dried.

Yield: (610.5 mg, 47 %)

TLC: (Silufol//n-butanol/acetic acid/water 2:1:1) R_f 0.3 (ninhydrine),
        (RP 18//methanol) R_f 0.7 (ninhydrine)

Chloroacetyl-hexylglycyl-diglycine

0.61 g (2.2 mmol) hexylglycyl-diglycine was dissolved in 5 ml of 1 N sodium hydroxide at room temperature, while stirring. After cooling the solution to 0 °C while stirring, 0.3 ml (3.7 mmol) chloroacetylchloride and 4 ml of 1 N sodium hydroxide were added. The ice bath was removed and stirring was continued for 30 min. After acidification with 5 N hydrochloric acid the solvent was evaporated. The yellow oil was extracted twice with hot acetone, the acetone was distilled and the white residue was vacuum-dried.

Yield: (311 mg, 40 %)

TLC: (Silufol//n-butanol/acetic acid/water 2:1:1) R_f 0.75 (iodine)

Benzoylmercaptoacetyl-hexylglycyl-diglycine **4b**

311 mg (0.89 mmol) chloroacetyl hexylglycyl diglycine was dissolved in 70 ml of anhydrous methanol while stirring under a nitrogen atmosphere. 0.26 g (1.9 mmol) thiobenzoic acid dissolved in 5 ml of methanol and neutralized with sodium methylate was slowly added to this solution under nitrogen, and stirring was continued for 12 h. The methanol was evaporated and the residue dissolved in 2 N hydrochloric acid. After removing the hydrochloric acid, the residue was washed with water. The oily reaction product was treated with a small amount of methanol and the product crystallized. The crystals were washed with acetonitrile and dried.

Yield: (253.3 mg, 63 %)

TLC: (Silufol//n-butanol/acetic acid/water 2:1:1) R_f 0.8 (UV)

Mercaptoacetyl-hexylglycyl-diglycine **5b**

27.3 mg (0.06 mmol) benzoylmercaptoacetyl hexylglycyl diglycine and 2.7 mg Pd/CaCO$_3$ (5 %) were suspended in 2 ml of methanol. 0.04 ml (0,19 mmol) sodium methylate in 1 ml of methanol was added while stirring under a nitrogen atmosphere at 63 kPa. Stirring was continued for 15 min and then the mixture was acidified with methanolic cation exchange resin DOWEX 50WX8. The resin and the catalyst were filtered off and the solvent was evaporated. The residue was three times extracted with 12 ml of benzene for and freeze-dried from methanol.

Yield: (9.4 mg, 45 %)

TLC: (Silufol//n-butanol/acetic acid/water 2:1:1) R_f 0.5 (ninhydrine)

Elemental analysis: (Found: C, 48.65; H, 7.16; N, 12.20; S, 9.38, $C_{14}H_{25}N_3O_5S$
   requires C, 48.40; H, 7.25; N, 12.09; S, 9.23 %)

^{1}H NMR data: δ_H(250 MHz; solvent DMSO; standard TMS) 1.2 (3 H, -CH$_3$), 3.1 (1 H, SH), 3.2 (10 H, N-CH$_2$), 3.7 (6 H, -CH$_2$), 3.8 (2 H, CH$_2$-SH), 8.2 - 8.5 (2 H,-NH)

References

[1] Noll, St. et al., this report, p. 63

[2] Noll, B. et al., FZR 93 - 12 (1993) 104

14. N-ALKYLATED MERCAPTOACETYL GLYCINE DERIVATIVES AS MULTIPURPOSE LIGANDS IN RADIO TRACER DESIGN
PART II: FORMATION AND BIODISTRIBUTION OF TECHNETIUM COMPLEXES

B. Noll, St. Noll, H. Spies, B. Johannsen, L. Dinckelborg[1], W. Semmler[1]
[1] Institut für Diagnostikforschung Berlin

N^1-alkylated mercaptoacetyl glycine ligands were labelled with technetium-99m and the formed products analyzed by chromatographic methods. Biodistribution patterns of the resulting species were determined in Wistar rats. The compounds were tested with regard to their ability to be accumulated in arterioclerotic plaques.

Experimental
Methods
TLC: Silicagel (Kieselgel 60/Merck)// ethanol/water // 95/5.
HPLC: RP 18 column (Nucleosil, 25 cm), 0.5 M phosphate buffer pH 7.4 .
Thin layer electrophoresis on special sheets coated with silicagel and phosphate buffer solution pH 7.0 respectively glycine buffer pH 2, electric field strength of 20 V/cm.

Biodistribution
74 kBq of the complexes were intravenously injected into mice. The animals were sacrificed after 0.5, 1, 3 and 5 h. The percentage of the injected dose (% ID) as well as the percentage of the injected dose per gram of tissue (% ID/g) were determined.

The accumulation was in ateriosclerotic lesions was determined in aortae derived from WHHL rabbits. 74 MBq of the complexes were intravenously injected into WHHL rabbits. 5 h later the rabbits were sacrificed, the aorta was removed and a sudan-III-staining as well as an autoradiography were performed. The ratio of accumulation between the arteriosclerotic lesions and normal vessel walls for the various N-alkyl-MAG derivatives was estimated by autoradiography.

Procedures
^{99m}Tc gluconate
2.0 ml eluate of a $^{99}Mo/^{99m}Tc$-generator was added to 2 ml 0.1 M sodium gluconate solution. Pertechnetate was reduced with 10 ml 0.01 M stannous chloride and the completeness of the reduction was proved by TLC.

^{99}Tc gluconate was prepared by addition of 1 x 10^{-6} mol stannous chloride to 1 x 10^{-6} mol potassium pertechnetate in 2 ml 0.05 M sodium gluconate solution.

Labelling procedures for animal studies

Labelling of N-alkyl-MAG$_n$ was accomplished by reaction of the appropriate ligand with Tc gluconate. Ligands, reaction conditions and TLC/HPLC data are listed in Table 1.

Table.1: Labelling conditions of MAG$_n$ derivatives according to the general procedure

Ligand	weight [mg]	solvent [μl]	S-protection/ saponification	neutralization [μl 0.1 N HCl]	reaction time [min]
S-benzoyl-N-dodecyl-MAG$_3$	2.2	EtOH [250 μl]	1M NaOCH$_3$ [50 μl]	45	30/30
S-benzoyl-N-octyl-MAG$_3$	2.0	EtOH [200 μl]	1M NaOCH$_3$ [50 μl]	45	15/15
S-benzoyl N-hexyl-MAG$_3$	0.5	0.1 N NaOH [400]	-	400	40
S-benzoyl N-methyl-MAG$_3$	0.4	H$_2$O [500]	-	-	60
S-benzoyl N-methyl-MAG$_2$	1.0	H$_2$O [200]	-	-	25
S-benzoyl N-hexyl-MAG$_1$	1.0	EtOH [200]	-	-	20
S-benzoyl N-methyl-MAG$_1$	1.0	H$_2$O	-	-	20

Determination of the molar ratio at the c.a. level (general procedure)

A small volume of the N-alkyl-MAG$_n$ solution was dropped into 2 ml Tc gluconate solution (c_{Tc} = 5 x 10^{-4} M) causing a significant change in volumes. After about 20 min the spectra of the solutions were recorded by the UV/VIS spectrometer. 100 ml 1 N sodium

hydroxide were added and measurement was repeated. The solutions were neutralized with 100 ml 1 N hydrochloric acid.

Results and discussion

The reaction conditions for labelling N-alkyl-MAG$_n$ ligands according to the general procedure are listed in Table 1. The resulting preparations were used for animal studies.

The analytical data of the species formed by the reaction of ligands $\underline{4}$ with Tc gluconate are summarized in Table 2.

Experiments at c.a. level are described for two typical representatives, N-methyl-MAG$_3$ and N-methyl-MAG$_1$.

Tc N-methyl-MAG$_3$

Gradual addition of the ligand to Tc gluconate under UV/VIS spectral control showed a peak with an absorption maximum at 422 nm. Varying the ligand/Tc ratio, the maximum extinction was reached at 4:1. A pH shift from pH 7 to approx. pH 10 caused a drastic chanch of the absorption maximum to 360 nm; the extinction coefficient remained unchanged. This reaction is reversible, a changing of the pH value back to 7 shifts the absorption to 422 nm. Both absorption maxima coexist in the pH region 8 - 9. In electrophoresis the complex with the absorption maximum at 422 nm migrated as an anion.

Ligand exchange in alkaline solution was not successful. Only after gradual neutralization of the alkaline reaction mixture did a ligand exchange take place; the complex occured with an absorption maximum at 350 nm. Further neutralization led to a double peak.

Table 2: Characterization of the Tc complexes with N-alkyl-MAG$_n$ ligands prepared by ligand exchange with Tc gluconate

Ligand	TLC [R$_f$] (system 1)	electrophoresis [u$_{rel}$]	molar ratio ligand : Tc	UV/VIS
N-dodecyl-MAG$_3$	0.5 (90 %) 0..0.2 (10 %)	pH 7* 0 (> 90 %) (part.decomp. →TcO$_4^-$)	no values	-
N-octyl-MAG$_3$	0.1 (20 %) 0.3 (45 %) 0.4 (20 %) 0.55 (15 %)	pH 7 0 (70 %) 0.8 (30 %)	1:1	λ_{max} = 355 nm
N-hexyl-MAG$_3$	0.7 (85 %) 0..0.2(15 %)	pH 7 0.4 (85 %) pH 2 0.4 (95 %)	1:1	pH > 7 λ_{max} = 358 nm
N-methyl-MAG$_3$	0.1 (40 %) 0.8 (60 %)	pH 7 0.4 (70 %) 0.6 (30 %)	1:1	pH > 7 λ_{max} = 355 nm
N-methyl-MAG$_2$	0.1 (90 %) 0.4 (10 %)	pH 7 0.2 (70 %) 0 (30 %) pH 2 0 (100 %)	could not be clearly deter-mined (1:1 or 2:1)[1]	pH < 7 λ_{max} = 420 nm pH > 7 λ_{max} = 358 nm
N-hexyl-MAG$_1$	0.75 (95 %)	pH 7 0 (> 95 %) pH 2 0 (100 %)	no values	-
N-methyl-MAG$_1$	0.1 (80 %) 0.2 (10 %) 0.4 (10 %)	pH 7 0.2 pH 2 0	(4 : 1)[2] 2 : 1	pH < 7 λ_{max} = 422 nm pH > 7 λ_{max} = 357 nm

* electrophoresis was done both with phosphate buffer and phosphate buffer//MeCN 1:1

[1] see Fig. 1

[2] ligand exchange is only complete in excess of ligand ($\approx$ 8-fold)
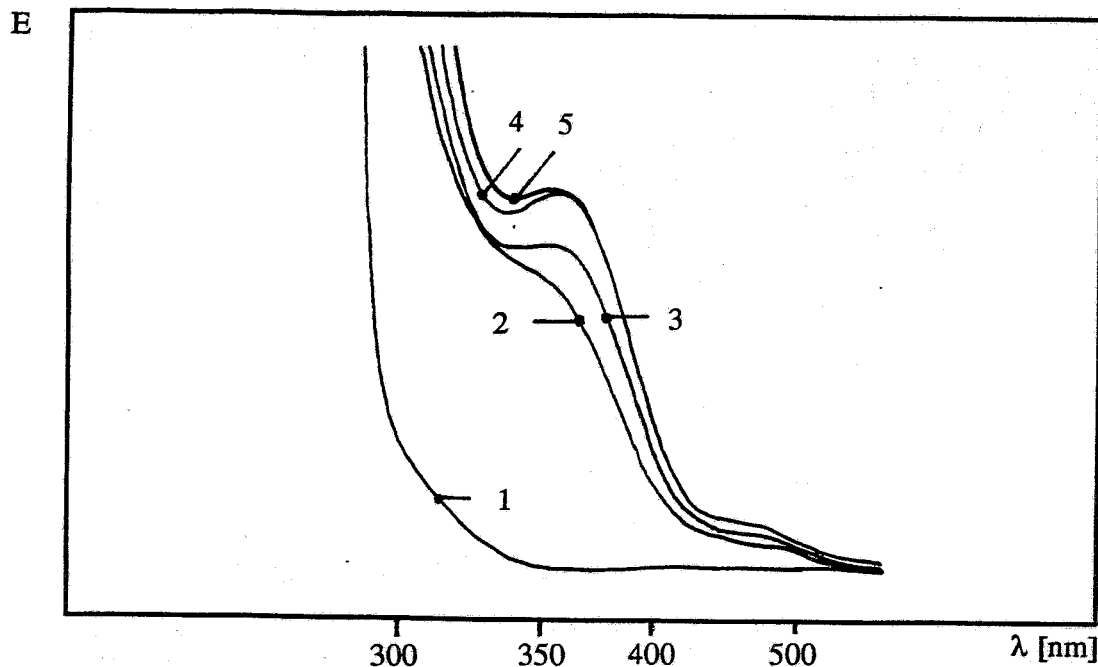
Fig. 1: UV/VIS spectra of the reaction mixture Tc gluconate/N-methyl-MAG$_3$ at various
ligand/metal molar ratios prepared in neutral solution after raising pH > 11
1: Tc gluconate; 2: molar ratio ligand Tc 1:1; 3: 2:1; 4: 4:1; 5: 8:1

Tc N-methyl-MAG$_1$

In neutral solution a yellow species was chiefly formed with an absorption maximum at 410
nm. However, we were unable to determine a defined molar ligand/Tc ratio. The product
decomposes during the electrophoresis both at pH 7 and pH 2. Increasing of pH values up
to pH 10 results in a shift of the absorption maximum to λ = 357 nm. With a sufficient ex-
cess of ligand (molar ratio ligand/Tc > 4) the pH-dependent shift of the absorption maxi-
mum is reversible.

In alkaline solution (pH > 11) only the complex with the absorption maximum at 357 nm
was formed, the molar ratio ligand/Tc of 2:1 was well defined.

Anionic mobility was detected in alkaline buffer solution at pH 10 only, because the com-
plex is not stable at pH 2 and pH 7, and only Tc gluconate was found.
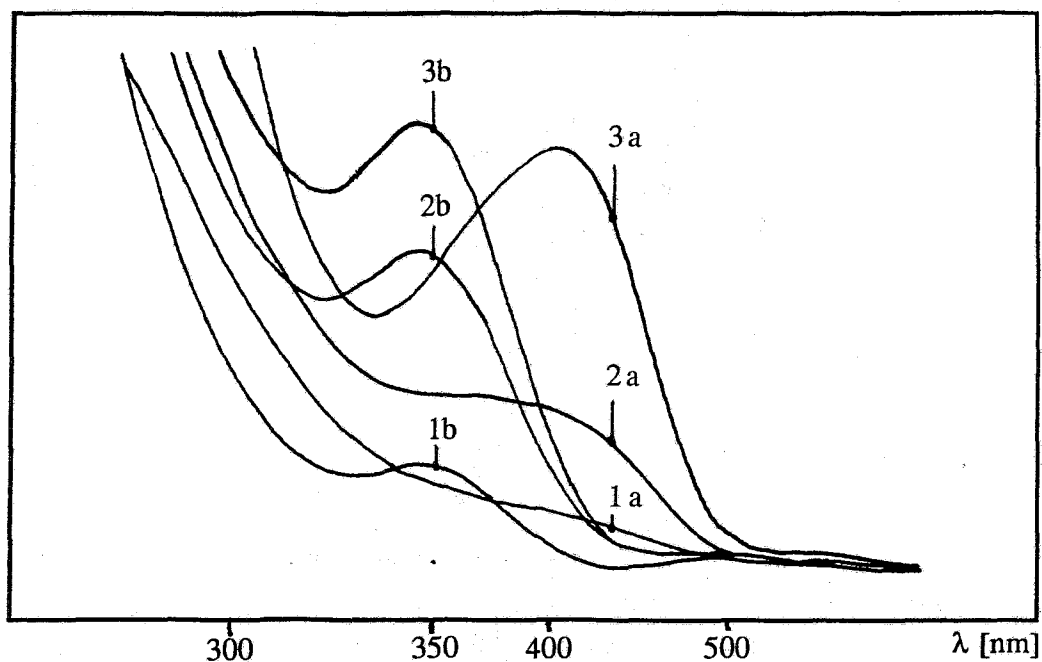
E

Fig. 2: UV/VIS spectra of the reaction mixture Tc-gluconate/N-methyl-MAG$_1$ at various
ligand/metal molar ratio both in neutral (a) and in alkaline solution (b)
1: 1:1; 2: 2:1; 3: 8:1

Discussion of biodistribution studies

The ratio of accumulation of N-hexyl-MAG$_3$ between the arteriosclerotic lesions and
normal vessel walls was 4, as estimated by autoradiography. Renal excretion of N-hexyl-
MAG$_3$ is fast (5 h p.i.: 56 % ID) The renal excrection of N-octyl-MAG$_3$ (5 h p.i.: 8 %
ID) is much less, compared with N-hexyl-MAG$_3$. The accumulation of N-octyl-MAG 3 in
the liver (5 h p.i.: 28 % ID) is significantly higher than that of N-hexyl-MAG$_3$ (5 h p.i.: 1
% ID). Because of a lower accumulation of Tc N-octyl-MAG$_3$ in normal vessel walls, the
ratio of accumulation between the arteriosclerotic lesions and normal vessel walls (> 10) is
higher to that of Tc N-hexyl-MAG$_3$.

Shortening the N-alkyl side chain to N-methyl leads to a renal excretion of 65 % ID (5 h
p.i.) and an accumulation in the liver of 2 % ID (5 h p.i.) which is comparable to N-hexyl-
MAG$_3$. Hence the elongation of the alkyl side chain from methyl to N-hexyl has no pro-
nounced effect on the biodistribution and elimination of the Tc labelled MAG$_3$ complex.
But a further elongation of the alkyl side chain from hexyl to octyl leads to a significant ac-
cumulation of the Tc-MAG$_3$ complex in the liver. The renal excretion of tc N-dodecyl-
MAG$_3$ amounts to 16 % ID and hepatobilary excretion to 6 % ID 5 h p.i.. Accumulation of
N-dodecyl-MAG$_3$ in the liver (5 h p.i.: 10 % ID) was lower if compared to Tc N-octyl-
MAG$_3$. The concentration of Tc N-dodecyl-MAG$_3$ in the blood was high (5 h p.i.: 31 %
ID).

Compared with N-methyl-MAG$_3$, N-methyl-MAG$_1$ shows an increased accumulation in the liver (5 h p.i.: 11 % ID) and a decreased renal excretion (5 h p.i.: 30 % ID). This tendency is even more pronounced when the biodistribution and elimination values of N-hexyl-MAG$_3$ are compared with those of Tc N-hexyl-MAG$_1$. 5 h p.i. the accumulation of Tc N-hexyl-MAG$_1$ in the liver amounts to 75 % ID (5 h p.i.) and the renal excretion amounts to 6 % ID. The higher accumulation in the liver as well as the lower renal excretion of Tc N-alkyl-MAG$_1$ derivatives compared with the Tc N-alkyl-MAG$_3$ derivatives could be due to the fact that N-alkyl-MAG$_1$ derivatives form 2:1 complexes so that two alkyl groups present in the molecule make the complex more lipophilic.

Conclusions

N-alkyl-MAG$_n$ (n = 1, 2, 3) ligands may act as monodentate, bidentate or, in the case of N-alkyl-MAG$_3$, as tetradentate ligands and form various complexes at the Tc(V) oxidation stage.

N-alkylation of MAG$_n$ favoures the formation of 2:1 species, MAG$_3$ is lower than that of the "alkyl-free" Tc MAG$_3$.

Some of the representatives tested in animals show a significant accumulation in arteriosclerotic plaques.

15. LIGAND EXCHANGE REACTION OF TECHNETIUM GLUCONATE WITH MERCAPTOACETYL GLYCINE (MAG$_1$) AND N-METHYL MERCAPTOACETYL GLYCINE (CH$_3$-MAG$_1$)

B. Noll, B. Johannsen, St. Noll, H. Spies

^{99m}Tc labelling of derivatives of mercaptoacetyl triglycine (MAG$_3$) having fewer than three amide functions has been carried out by several authors [1,2]. The influence of a methyl substitution at the amide nitrogen on complex formation with technetium was studied by comparing the reaction of mercaptoacetyl glycine and N-methyl-mercaptoacetyl glycine (N-methyl-MAG$_1$) with Tc gluconate. Synthesis of N-methyl-mercaptoacetyl glycine is described in [3].

UV/VIS spectra depending on the molar ratio Tc gluconate/MAG derivative were recorded by means of the spectrophotometer Specord M40. The chromatographic behaviour was determined by thin layer chromatography on silica gel with acetone or 95 % ethanol as the solvent. The charge of the complexes was determined by thin layer electrophoresis with phosphate buffer solution pH 7 and glycine buffer solution pH 2.0 at an electric field strength of 20 V/cm.

Tc-MAG₁

With molar ratios (ligand:Tc) ranging, the UV/VIS spectrum shows one maximum at 360 nm with a shoulder at 480 nm. The extinction at 360 nm increases up to a molar ratio of 2:1. At a ratio of 1:1 50 % of the Tc gluconate remains unreacted. In TLC (silica gel/95 % ethanol) the Tc gluconate remains at the starting point, the main component has the R_f value of 0.5 and is extractable in methylene chloride after addition of tetrabutylammonium bromide. Anionic mobility is the same both at pH 7 and 2. This fact may be explained by assuming the carboxylic group to be involved in binding technetium.

At a molar ratio of 100:1 a second component (about 15 %) occurs with R_f 0.1.

Tc-N-methyl-MAG₁

Gradual addition of an aqueous solution of N-methyl-MAG₁ to a neutral Tc gluconate solution gives a peak at 422 nm, the maximum extinction is found at a molar ratio of 4:1 (ligand/Tc). The absorption maximum in the UV/VIS-spectrum is shifted to 360 nm with the same extinction coefficient by adding 0.1 M NaOH. The pH-dependent conversion is reversible. In contrast to Tc MAG₁ the methylated species Tc methyl-MAG₁ cannot be extracted into organic solvents either in neutral or in alkaline solution. The exchange reaction of N-methyl-MAG₁ and Tc gluconate did not proceed in an alkaline solution but after gradual neutralization of the solution it was completed, with conversion to the same species as found above.

A small variation of the complexing agent thus results in quite different Tc-complexes. While the unsubstituted MAG₁ forms a 2:1 complex, N-methyl-MAG₁ forms predominantly a species which we consider to be a 4:1 complex. This behaviour may be explained by the lack of the N-H proton (methyl substituted), resulting in a lower tendency of the amide group to coordinate.

References

[1] Okarvi, M.S. et al.; Eur.J.Nucl.Med. **18** (1991) 605

[2] Vandebrouck, T. et al.; Eur.J.Nucl.Med.**18**(1991) 674

[3] Noll, B. et al., this report, p. 48

16. SYNTHESIS AND X-RAY CRYSTAL STRUCTURE OF AsPh4[ReO(MAG2)]

B. Noll, P. Leibnitz[1], St. Noll, B. Johannsen, G. Reck[1], H. Spies

[1] Bundesanstalt für Materialforschung, Berlin

Formation and structures of rhenium complexes with mercaptoacetyl glycine are of interest in the context of our studies of technetium and rhenium complexes of mercapto-containing peptides [1].

The Re complex of the S,N,N,O-ligand mercaptoacetyl diglycine (MAG2) was prepared and characterized by X-ray structure determination.

The ligand exchange reaction of a molar excess of MAG2 with Re gluconate in a neutral solution produces up to three species, whereas a single 1:1 complex [ReO(MAG2)]⁻ is obtained when Re(V) gluconate [2] is allowed to react with an equimolar amount of mercaptoacetyl diglycine (MAG2). The complex was isolated as tetraphenylarsonium salt and identified by elemental analysis, ^{1}H NMR, and infrared spectroscopy.

The crystals formed are suitable for X-ray crystal structure determination.

Procedure

21 mg MAG2 (0.1 mmole) dissolved in 1 ml 0.1 N NaOH was dropped to 3 ml (0.1 mmole) aqueous Re(V) gluconate solution while stirring. After standing for 15 minutes, 42 mg (0.1 mmole) tetraphenylarsonium chloride dissolved in 0.5 ml water was added. The reaction mixture was extracted with methylene chloride (3 x 2 ml), the combined extracts were dried over sodium sulphate and evaporated to dryness. The residue was recrystallized from acetone to give 54 mg (0.07 mmol = 70 %) of dark brown crystals.

M.p.203 - 205 °C.

Elemental analysis: (Found: C, 45.74; H, 3.30; N, 3.56; S, 4.07, $C_{30}H_{26}N_2O_5SAsRe$
requires C, 45.80; H, 3.31; N, 3.55; S, 3.86 %.

^{1}H NMR: 7.80 ppm (m, 20 H) phenyl, 4.83/4.16 ppm (AB, 2 H) and 4.01 ppm (s, 2 H) 2x N-CH2, 3.89/3.62 ppm (AB, 2 H) S-CH2.

IR (KBr): 976 cm^{-1} (Re=O)

UV-VIS absorptions: λ_{max}/nm(EtOH) 412 (log ε/dm^3 mol^{-1} cm^{-1} 2.15)

X-ray crystal structure

The structure of AsPh4[ReO(MAG2)] was confirmed by X-ray crystallography. The crystal structure consists of discrete [ReO(MAG2)]⁻ anions and AsPh4⁺ cations. The geometry of the AsPh4⁺ cation is normal and requires no further discusssion. A perspective view of the complex anion (Fig. 1) shows that the compound has a distorted square-pyramidal arrangement.
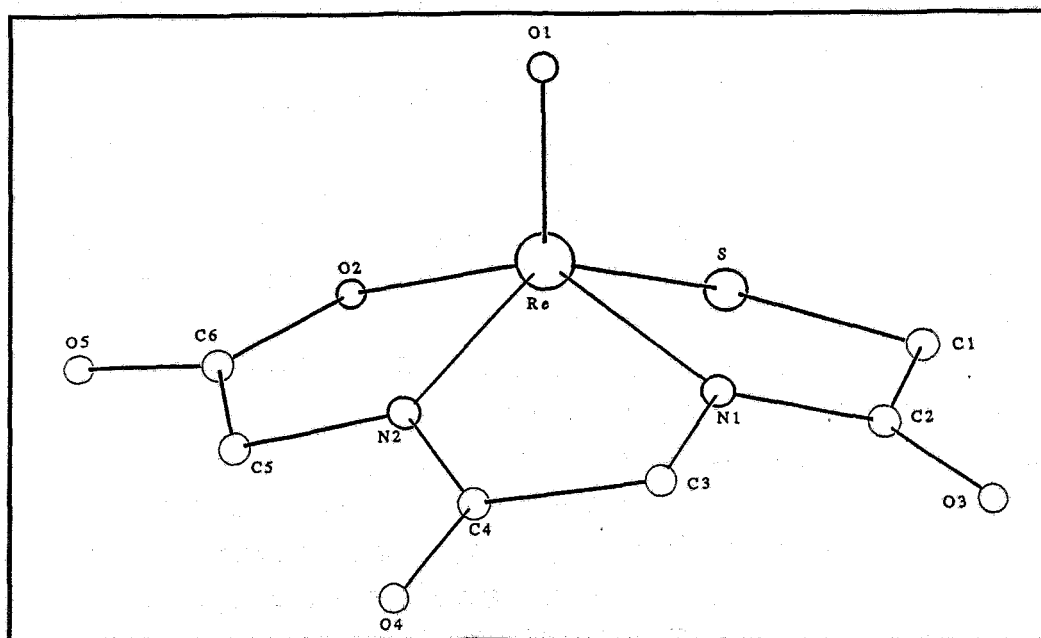
Fig. 1: CELLGRAF drawing of the [ReO(MAG₂)]⁻ anion

It is distorted in the sense that the metal atom lies above the plane of the four basal ligands. (The rhenium atom is displaced towards the oxo ligand from the plane formed by the equatorial S,N,N,O atoms. The corresponding value for $[TcO(MAG_2)]^-$ is 0.756 Å [1]).

The observed square-pyramidal arrangement is found for a large number of five-coordinated technetium complexes as well as for rhenium complexes. The Re-O_1 bond length of is equal to that observed for the Tc=O structure element [3]. $[ReO(MAG_2)]^-$ is related to the known technetium complex, and selected bond distances and angles (summarized in Table 1) are very close to $[TcO(MAG_2)]^-$. Most values of bond lengths in the coordination sphere differ only in the third decimal place.

Table 1: Selected bond distances and angles for $[ReO(MAG_2)]^-$

Bond lengths (Å)					
Re-O_1	1.661	Re-N_1	1.964	C_1-S	1.825
Re-O_2	2.013	Re-N_2	1.962	C_6-O_2	1.308
Re-S	2.267			C_6-O_5	1.228
Bond angles (°)					
$O_{(1)}$-Re-S	110.2	S-Re-$N_{(1)}$	83.7		
$O_{(1)}$-Re-$N_{(1)}$	110.1	S-Re-$O_{(2)}$	88.2		
$O_{(1)}$-Re-$N_{(2)}$	116.1	$N_{(1)}$-Re-$N_{(2)}$	78.7		
$O_{(1)}$-Re-$O_{(2)}$	110.1	$N_{(2)}$-Re-$O_{(2)}$	78.8		

References

[1] Johannsen, B. et al., Inorg.Chim.Acta **210** (1993) 209

[2] Noll, B., et.al., FZR 93 - 12 (1993) 115

[3] Mazzi, U. et al., Polyhedron **8** (1989) 1638

17. HYDROGEN-MEDIATED CLEAVAGE OF S-PROTECTED MERCAPTO-ACETYL TRIGLYCINE DERIVATIVES

St.Noll, B.Noll, H.Spies

Having in mind a more general use of mercaptoacetyl glycine derived ligands as multifunctional chelators for technetium and rhenium, a suitable procedure for the removal of the protective group from the corresponding S-protected ligand precursor is required. This procedure should be applicable not only to the parent compound MAG3, as already used in kit-based radiopharmaceutical preparation [1], but also to more sensitive derivatives without any change of structure.

Several methods have been published for splitting the protective substituent from the sulphur atom of mercaptoacetyltriglycine (MAG3) derivatives [2]. Our current procedure involves saponification of S-benzoyl-protected MAG3 with sodium methylate, which produces some amount of MAG3-SS-MAG3 disulphide and other by-products [3]. Catalytic hydrogenation could be an alternative, superior method for removal of the protective substituent, as previously described [4]. To optimize the reaction conditions for catalytic hydrogenation, the influence of the catalyst was studied under the following reaction conditions:

Solvent: 50 % aqueous ethanol

Hydrogen pressure: 53 kPa

Temperature: 18 °C

Reaction time: 3 h

The results are summarized in Table 1, showing the behaviour of benzoyl-MAG3 and derivatives (Nos.1 - 8) and of MAG3 (Nos. 9, 10).

Initially, hydrogenation was carried out at 0.02 mmol benzoyl-MAG3-ergoline with both 150 mg and 50 mg Pd-black. By decreasing the amount of catalyst, we achieved a small increase in splitting rate, but NMR spectroscopic investigation demonstrated that nearly 50 % of the sulphur had been removed from the molecule.

Further tests with benzoyl-MAG3 also resulted in an unsatisfactory amount of unprotected MAG3. Regardless of the type of catalyst used, we obtained acetylglycine as the main

product as well as some decomposition products. A similar product spectrum was obtained after hydrogenation of MAG_3, benzoyl-MAG_2 and benzoyl-MAG_1.

Table 1: Results of catalytic hydrogenation of protected mercaptoacetyl triglycine derivatives changing the catalyst

No.	substance	catalyst	results
1	benzoyl-MAG_3-ergoline	150 mg Pd-black	20 % MAG_3-ergoline
2	benzoyl-MAG_3-ergoline	50 mg Pd-black	30 % MAG_3-ergoline
3	benzoyl-MAG_3	150 mg Pd-black	5 % MAG_3 95 % acetylglycine
4	benzoyl-MAG_3	50 mg Pd-black	10 % MAG_3 90 % decomp.prod.
5	benzoyl-MAG_3	150 mg Pd/$CaCO_3$ (5 %)	10 % MAG_3 90 % acetyltriglycine
6	benzoyl-MAG_3	10 mg Pd/$CaCO_3$ (5 %)	unreacted
7	benzoyl-MAG_3	150 mg PdO/$BaSO_4$ (10 %)	10 % MAG_3 90 % acetyltriglycine
8	benzoyl-MAG_3	50 mg PdO/$BaSO_4$ (10 %)	unreacted
9	MAG_3	150 mg Pd-black	5 % MAG_3 95 % acetyltriglycine
10	MAG_3	50 mg Pd-black	15 % MAG_3 85 % decomp.prod.

In view of these results it seems to be pointless to further optimize the catalyst; instead we should change the solvent and decrease the reaction time.

A better method of splitting the protective substituent from the MAG derivatives without changing the structure of the molecule seems to be combining saponification with sodium methylate under hydrogen with the use of a catalyst.

Thus, we developed the following procedure for splitting the protective group of MAG derivatives.

The protected derivative was solved in anhydrous methanol in a round bottle. After addition of Pd/CaCO$_3$ (5 %) the bottle was connected to a vacuum apparatus, evacuated and then hydrogen was added to a pressure of 50 kPa. While stirring the reaction mixture vigorously, sodium methylate in anhydrous methanol was dropped into the solution over 15min. After neutralization with methanolic cationic exchange resin, the mixture was filtered and freeze-dried. The residue was extracted twice with benzene and purified by liquid chromatography on Sephadex G10.

With this method we succeeded in splitting the protective group from a series of investigated MAG derivatives, with high yields and a small amount of by-products.

References

[1] Noll, B. et al., Appl. Radiat. Isot. **43** (1992) 899

[2] Bormans, G. B. et al., J. Lab. Comp. Radiopharm. **20** (1989) 50)

[3] Hoffmann, I. et al., ZfK - 711 (1990) 47

[4] Noll, St. et al., FZR 93 - 12 (1993) 113

18. A NEW OXORHENIUM(V) COMPLEX CONTAINING A STABLE RHENIUM-CHLORINE BOND. X-RAY STRUCTURE ANALYSIS OF (3-THIAPENTANE-1,5-DITHIOLATO)(CHLORO)OXORHENIUM(V)

Th. Fietz, H. Spies, H.-J. Pietzsch, K. Klostermann[1], D. Scheller[1], P. Leibnitz[2], G. Reck[2]

[1] Technische Universität Dresden, [2] Bundesanstalt für Materialforschung, Berlin

Introduction

A large number of precursors for ligand exchange reactions at transition metal cores contain chlorine as the leaving group. In many cases these metal-chlorine bonds are very sensitive to hydrolysis. Oxides and oxide hydrates of lower valences are obtained when these compounds come into contact with humid air or water-containing solvents.

However, we have synthesized the new neutral stable oxorhenium(V) complex $ReO(S-CH_2-CH_2-S-CH_2-CH_2-S)(Cl)$ from $[BzNEt_3][ReOCl_4]$ and bis(2-mercaptoethyl)-sulphide, with one chlorine atom still left at the core. The metal-chlorine bond in this complex is even stable to boiling water. Another ligand exchange reaction is strongly retarded. This is similar to other oxorhenium(V) complexes containing very stable Re–Cl bonds after a particular ligand exchange, cf. the stability of the thioether complexes $ReO(R-S-CH_2-CH_2-S-R)(Cl)_2$ [1]. The stability found in **5a** enables us to transform the normal one-pot "3+1" reaction into a two-step one. This may be important when the reactivities of the tridentate and monodentate ligands differ too much to guarantee a simultaneous attack of the ligands on the precursor.

Experimental

(3-Thiapentane-1.5-dithiolato)(chloro)oxorhenium(V)

5a: A solution of 27.8 mg (180 μmol) of "HS$_3$H" in 5 ml chloroform is added over 15 minutes to a stirred and cooled (0 °C) solution of 214.5 mg (200 μmol) of [NBzEt$_3$][ReOCl$_4$] **1** in 10 mL chloroform and 1 ml methanol. After stirring for another 30 minutes, the solvent is removed by rotary evaporation. The dark residue is washed several times with chloroform to give a blue powder. The product is recrystallized from acetonitrile to give dark-blue needles.

Yield: 48 mg (68 % of the "HS$_3$H"), m.p.: 221 - 223 °C (decomp).

UV/VIS absorptions: λ_{max}/nm (CH$_3$CN) 572 (log ε/dm^{-1} cm^{-1} 2.0), 348 (3.2), 258 (3.9), 232 (3.8).

^{1}H NMR data: solvent CD$_3$CN; 4.22 ppm (m); 3.12···3.42 ppm (triplet of doublets); 2.64 ppm (m).

(3-Thiapentane-1.5-dithiolato)[1.2-bis(ethoxycarbonyl)ethanethiolato]oxorhenium(V):

10.6 mg (27.2 μmol) of **5a** is dissolved in 1 ml of acetonitrile. 28 mg (136 μmol) of thio-malic acid diethyl ester is added and the mixture left at room temperature for four days. The colour of the mixture changes from blue to violet. The solvent is evaporated in a vac-uum without heating the mixture and the residue dissolved in chloroform. 6.4 mg (16.4 μmol; 60.4 %) of the starting **5a** is recovered. 4.9 mg (8.8 μmol; 32.5 %) of the complex is isolated from the chloroform solution.

(3-Thiapentane-1.5-dithiolato)(ethanethiolato)oxorhenium(V):

400 μl (5.4 mmol) ethane-thiol is dropped into a refluxing solution of 33.9 mg (87 μmol) of **5a** in 5 ml acetonitrile. The mixture is refluxed for 10 minutes. Then the clear reddish-brown solution is evaporated to dryness and the residue dissolved in chloroform. The pro-duct is purified by column chromatography with silica gel 60 (0.063 - 0.1 mm) and chloro-form. Only a small amount of material remains at the starting point. One millilitre of etha-nol is added to the eluate. 28.8 mg (80 %) of brown needles are obtained on slow evapo-ration.

Results and discussion

Our 3+1 concept is based on the idea of achieving small changes in the properties of the complexes (e.g. lipophilicity) by saturating three of the four free coordination sites (the co-ordination of a ligand into the *trans*-position towards the oxo group is unlikely) of the $Re=O^{3+}$ core with a relatively constant tridentate ligand **2** (X=S; O; NCH$_3$) and "tuning" the properties with a widely variable monodentate coligand **3** (R= [substituted] alkyl, [substituted] aryl) (see Fig. 1) [2].

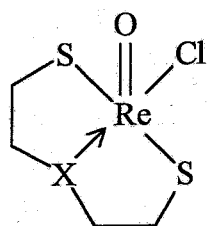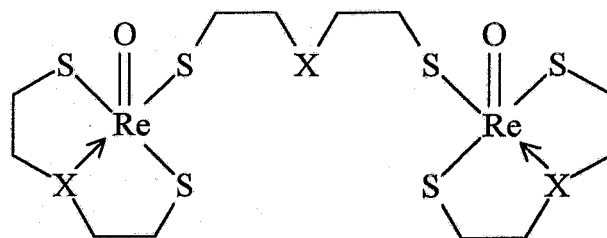1 (M=Re;Tc)   2a (X=S)   3   4 (M=Re;Tc)
                     2b (X=O)
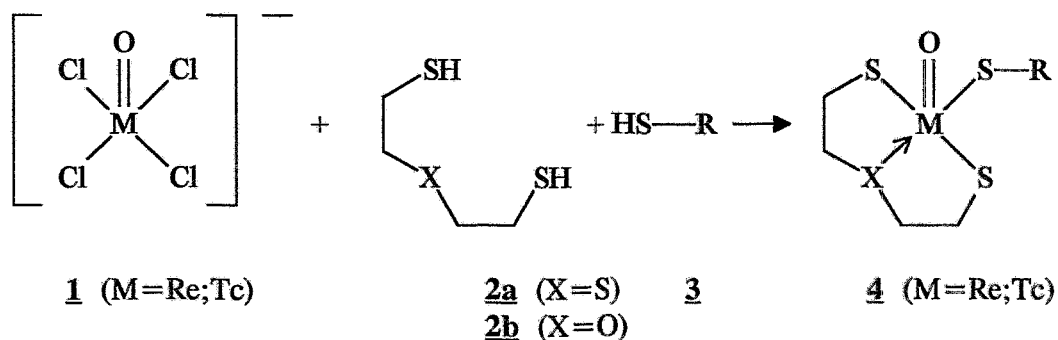
Fig.1: Reaction scheme for the preparation of "3+1" complexes

When **1** (M=Re) is reacted with **2a** and several monothioles **3**, a light-blue by-product can sometimes be isolated. The same compound **5a** is obtained in high yields when the mon-odentate co-ligand is omitted and only 0.9 equivalents of bis(2-mercaptoethyl)sulphide (HS–CH$_2$–CH$_2$–S–CH$_2$–CH$_2$–SH; **2a**) are dropped into the solution of ReOCl$_4$$^-$. When an excess of **2a** is used, a brown oily compound is formed instead of **5a**. This should be **6a**, but no further examination was carried out due to failure of crystallization.

5a X=S
5b X=O

6a X=S
6b X=O

5a was found to be (3-thiapentane-1.5-dithiolato)(chloro)oxorhenium(V). **5a** is soluble in acetonitrile, acetone and dimethylsulphoxide, sparingly soluble in chloroform and dichloromethane and insoluble in diethylether, hexane, water and methanol. On slow evaporation of its solution in acetonitrile, **5a** is obtained in the form of dark-blue needle-shaped crystals. Its IR spectrum exhibits the known strong Re=O valence band at $v = 968$ cm^{-1}. Elemental analysis of **5a** gives the proposed formula $[C_4H_8ClOReS_4]_n$. The electron impact mass spectrum shows the mol peak at m/z = 390; there are no signs of any structures with n > 1 (see Fig. 2).

Fig. 2: Electron impact mass spectrum of **5a**

The electron impact mass spectrum of **5a** shows the molar mass of the complex to be M=390 g/mol. Further peaks of interest are seen at m/z = 362 (first loss of –CH$_2$–CH$_2$–), m/z = 334 (second loss of an ethylene unit), m/z = 302 and 270 (losses of one and two sulphur atoms). There are also interesting images of binuclear Re species with m/z values higher than the molar peak of **5a**.

68

Attempts to react **5a** with a monothiol **3** in acetonitrile under the conditions of the classic 3+1 reaction (equivalent amount of **3**; 0 °C) as well as allowing it to stand for three days at room temperature were unsuccessful. For instance, 60 % of the **5a** used can be recovered after standing for three days with a fivefold excess of thiomalic acid diethyl ester. The reaction can be completed by adding a heavy excess of the monothiol **3** and briefly heating of the mixture (see Experimental). Then the 3+1 complex is formed in a high yield and purity. Since **5a** does not react with a monothiol under the conditions used for reactions according to Fig. 1, we assume that **2a** and **3** are attached to the core simultaneously and not, as postulated before, one after another.

The oxygen analogue **5b** cannot be isolated after the reaction of **1** (M = Re) with 0.9 equivalents of **2b** in acetonitrile. Immediately on addition of **2b**, a blue colour is observed but after some ten seconds a reddish-brown precipitate is formed, which is completely insoluble in acetonitrile. Elemental analysis of this precipitate gives approximately the theoretical C, H and S values of the binuclear complex **6b**.

X-ray crystal structure of 3-(thiapentane-1.5-dithiolato)(chloro)oxorhenium(V)

The X-ray crystal structure of 3-(thiapentane-1.5-dithiolato)(chloro)oxorhenium(V) **5a** shows a longer Re=O double bond (1.74 Å) than (3-thiapentane-1.5-dithiolato)(ethane-thiolato)oxorhenium(V), where a bond length of 1.66 Å was measured. Compared with the latter, the rhenium–sulphur distances are shorter in **5a** (mean lengths of the Re–S$_{thiol}$ bonds is 2.251 Å in **5a** vs. 2.293 Å; Re–S$_{thioether}$= 2.269 Å in **5a** vs. 2.363 Å). The Re atom is situated 0.673 Å above the plane of the sulphur and chlorine atoms.

Table 1: Selected bond lenghts and angles

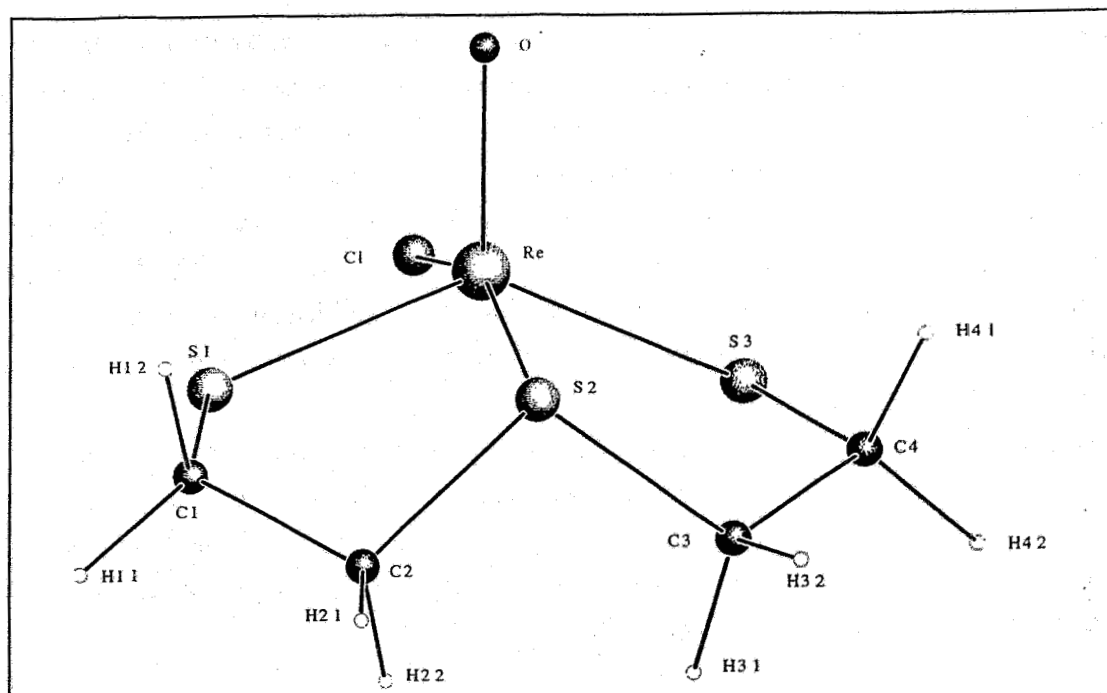| Bond	distance [Å]	angle	[°]
Re=O	1.74	O–Re–Cl	100.9
Re–Cl	2.397	O–Re–S1	111.9
Re–S1	2.257	O–Re–S2	101.3
Re–S2	2.269	O–Re–S3	115.0
Re–S3	2.245	Cl–Re–S1	83.0
		Cl–Re–S2	157.7
		Cl–Re–S3	84.5
		S1–Re–S2	87.4
		S1–Re–S3	132.9
		S2–Re–S3	87.4

Fig. 3: X-ray crystal structure of compound **5a**.

References

[1] Pietzsch, H.-J. et al., this report, .p. 78

[2] Pietzsch, H.-J. et al., Inorg. Chim.Acta **161** (1989) 15

[3] Spies, H. et al., FZR 93 - 12 (1993) 94

19. TRICHLORO-BIS(TRIPHENYLPHOSPHANE)RHENIUM(III) COMPLEXES CONTAINING ONE ISOCYANO LIGAND

M. Glaser, H. Spies, F. E. Hahn[1], D. Scheller[2]

[1] FU Berlin, [2] TU Dresden

Rhenium complexes [ReCl$_3$(CNR)(PR$_3$)$_2$] may be useful as precursors for preparation of rhenium isocyanide/chelate mixed-ligand complexes [1].

Because only [ReCl$_3$(CNMe)(PPh$_3$)$_2$] had been previously reported by RICHARDS and ROUSCHIAS [2], we sought to prepare and characterize further representatives of this class of compounds.

Experimental

General procedure for the preparation of **3a-d**

233 µmol [Re(MeCN)(PPh₃)₂Cl₃] **2** were dissolved in 10 ml of degased benzene and 348 µmol of the appropriate isocyanide were added under nitrogen atmosphere. The mixture was boiled under reflux for about 30 minutes and reduced in volume. Yellow-orange products precipitated (otherwise the product was dissolved in 2 ml of methylene chloride and 5 ml of ethanol were added). The raw materials were washed by diethyl ether and recrystallized from ethanol/methylene chloride to give yellow crystals.
Yields: 70 to 80 %

NMR data of **3a-d**

3a δ_H(90 MHz; solvent CDCl₃; standard SiMe₄): 7.89 (9 H, s, C-(CH₃), 8.47 (6 H, "t", para-H), 8.72 (12 H, "t", meta-H) and 15.40 (12 H, "d", ortho-H) ppm

3b δ_H(90 MHz; solvent CDCl₃; standard SiMe₄): 3.74 (2 H, d, ortho-H), 4.65 (1 H, t, para-H), and 8.84 (18 H, m, meta and para-H in PPh₃) ppm

3c δ_H(90 MHz; solvent CDCl₃; standard SiMe₄): 4.25 (3 H, s, CH₃), 7.7 (2 H, s, CH₂), 8.93 (18 H, m, meta- and para-H) and 15.65 (12 H, m, ortho-H) ppm

3d δ_H(90 MHz; solvent CDCl₃; standard SiMe₄): 2.94 and 3.94 (8 H, m, broad, morpholine-CH₂), 5.65 and 7.35 (8 H, m, very broad, ethylene-CH₂), 8.95 (18 H, m, meta-and para-H) and 15.50 (12 H, m, ortho-H) ppm

Synthesis of [ReCl₃(CNR)(PPh₃)₂] **3** has been accomplished both by reduction of [trans-ReOCl₃(PPh₃)₂] **1** and by selective exchange of the acetonitrile ligand in **2** against the appropriate isocyanides RNC as shown in Scheme 1. Considering the reaction of **1** to **3**, triphenylphosphane seems to be essential as a reducing agent. Attempts to reduce the Re(V) core by means of the isocyanide failed. Using an excess of isocyanide instead of triphenylphosphane, the originally obtained blue species was decomposed. The substitution reaction of **2** produced about 80 % of the theoretical yield and should be the preferred method of preparation.

The structure of **3a** was investigated by X-ray crystal structure analysis. A perspective view of the complex (Fig. 1) shows that the compound has an octahedral arrangement. Selected bond lengths and angles are listed in Table 1. It is worthy of note that there is no linearity between C-1, N and C-2 as usually found in comparable compounds [3]. The Re-Cl-1 and Re-Cl-2 distances are in agreement with the values found in the literature [4]. The coordinated t-butyl-isocyanide obviously causes stretching of the third chlorine bond.

The infrared spectra of **3a-d** show very broad ν-(CN) absorptions. The hypsochromic shifts of the coordinated CN-function - compared with the free isocyanide - in **3a** and also in the case of N-morpholinyl-2-ethyl-isocyanide (**3d**) are unexpected and inexplicable (see Table 2). All complexes **3a-d** are paramagnetic detected by unusual chemical shifts in the ¹H NMR spectrum.

To sum up, one can say that the Re(III) complexes presented could serve as precursors for the preparation of complexes containing a tripod ligand as shown for tris-(2-mercaptoethyl)amine in [1]. In view of the additional coupling of rhenium with "anchor groups", precursor **3c** is of special interest: the presence of the ester group is expected to allow functionalizations and to become biochemically important.
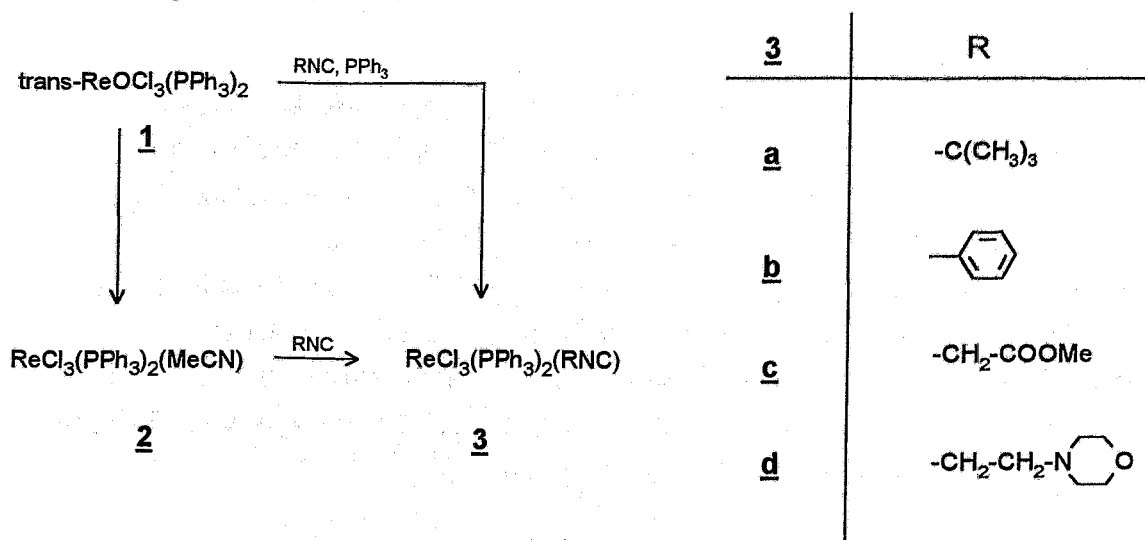
Scheme 1. Synthesis of **3**

3	R
a	$-C(CH_3)_3$
b	(phenyl)
c	$-CH_2-COOMe$
d	$-CH_2-CH_2-N{\overset{\frown}{\underset{\smile}{}}}O$

Table 1: Selected bond lengths (Å) and angles (deg) for **3a**

Re-Cl1	2.335(3)	Re-P1	2.465(3)	Re-C1	1.99(1)
Re-Cl2	2.335(3)	Re-P2	2.472(3)	N-C1	1.14(1)
Re-Cl3	2.432(2)				

Cl1-Re-Cl2	173.13(9)	P1-Re-P2	177.54(7)
Cl1-Re-C1	81.7(3)	P1-Re-C1	91.7(3)
Cl2-Re-C1	91.7(3)	P2-Re-C1	90.6(3)
Cl3-Re-C1	171.1(3)	C1-N-C2	166.0(1)
		Re-C1-N	176.6(9)

Fig. 1: X-ray structure of <u>3a</u>

Table 2: IR and UV/VIS data of <u>3a-d</u>

<u>3</u>	$\tilde{\nu}$(CN) in cm^{-1} [a) (KBr)	λ_{max} in nm [b) (CH$_2$Cl$_2$)
<u>a</u>	2144 (2136.7 [5])	304 (3.68) 448 (3.35)
<u>b</u>	2104 (2126.7 [5])	254 (4.04) 313 (4.04) 462 (3.02)
<u>c</u>	2112 (2150 [6])	455 (3.31)
<u>d</u>	2152 (2150 [6])	252 (3.37 303 (3.95) 451 (3.29)

[a] Data for vibrations of the free isocyanides are given in parentheses.
[b] Values of lg ε are given in parentheses.

73

Table 3. Melting points and elemental analysis of 3a-d

3	Formula	m. w.	m. p. in °C	calc./ found			
				C	H	N	Cl
a	$C_{41}H_{39}Cl_3NP_2Re$ x CH_2Cl_2	985.21	188-194 (EtOH/MeCl$_2$)	51.20 51.31	4.19 4.26	1.42 1.49	17.99 17.99
b	$C_{43}H_{35}Cl_3NP_2Re$	920.27	200-209 (MeOH/MeCl$_2$)	56.12 56.10	3.83 3.89	1.52 1.65	11.56 11.35
c	$C_{43}H_{35}Cl_3NP_2O_2Re$	916.24	184-188 (n-hexane/MeCl$_2$)	52.44 52.66	3.85 3.81	1.53 1.56	11.61 11.29
d	$C_{43}H_{42}Cl_3N_2OP_2Re$	957.33	195-200 (EtOH/MeCl$_2$)	53.95 53.53	4.42 4.45	2.93 2.99	11.11 11.08

References

[1] Spies, H. et al., this report, p. 74

[2] Richards, R. J. et al., Am. Chem. Soc **98** (1976) 5729

[3] Hahn, F. E., Angew. Chem. **105** (1993) 681

[4] Drew, M. G. B. et al., J. Chem. Soc., Chem. Com. (1970) 600

[5] Stephany, R. W. et al., Org. Magn. Reson. **6** (1974) 45

[6] Obrecht, R. et al., Synthesis (1985) 400

20. RHENIUM COMPLEXES WITH TRIS-(2-THIOLATOETHYL)AMINE

H. Spies, M. Glaser, F. E. Hahn[1]

[1] FU Berlin

The chemistry of technetium and rhenium tracers can be considered to be mainly a chemistry of oxo compounds. In order to gain access to alternative "oxo-free" metals capable of being coupled to anchor groups, on complex formation studies were carried out with a tripodal tetradentate "umbrella ligand" which to correspond with a monodentate neutral ligand in trans-position.

Experimental

Tris(2-thiolatoethyl)amine-t-butylisocyanide-rhenium(III) **3a**

24 μl (233 μmol) **1** in 2 ml MeCl$_2$ were slowly added to a solution of 100 mg (156 μmol) ReL(PPh$_3$) in 5 ml MeCl$_2$ at room temperature. TLC of the mixture (silica gel, MeCl$_2$) in-

dicates PPh$_3$ (R$_f$ = 0.75), **1** (R$_f$ = 0.59) and the olive green coloured **3a** (R$_f$ = 0.41). **3a** was isolated by column chromatography (Merck Kieselgel 60, Ø 0.063 - 0.1 mm, column 15 x 250 mm, MeCl$_2$).

Yield: 46 mg (64 %); rhomboedric plates suitable for X-ray analysis from EtOH;
m.p. 238 - 242 °C (decomp.)

Elemental analysis: Found   C, 28.77; H, 4.60; N, 5.86; S, 20.80,
C$_{11}$H$_{21}$N$_2$S$_3$ requires C, 28.49; H, 4.56; N, 6.04; S 20.74 %

IR absorptions: $\tilde{v}_{max}$/cm^{-1} (KBr) 1976 br. v(NC)

UV/VIS absorptions: λ/nm (MeCl$_2$) 250 (log ε/dm^3 mol^{-1} cm^{-1} 4.23), 312 (3.98), 350
(3.11) and 448 nm (3.26)

NMR data: δ$_H$(90 MHz; solvent CDCl$_3$; standard SiMe$_4$) 1.54 (9 H, s, CH$_3$) and 2.98 ppm
(12 H, m, CH$_2$)

Tris(2-thiolatoethyl)amine-isocyanoacetic acid-methylester-rhenium(III) **3b**

3b was prepared as described for **3a**.

Yield: 62 % of the theory; rhomboedric plates; (crystals for X-ray analysis from
Et$_2$O/MeCl$_2$); m.p. 205 - 212 °C

Elemental analysis: Found   C, 25.37; H, 3.56; N, 5.68; S, 19.79,
C$_{10}$H$_{17}$N$_2$O$_2$S$_3$Re requires C, 25.04; H, 3.57; N, 5.84; S, 20.05 %

IR absorptions: $\tilde{v}_{max}$/cm^{-1} (KBr) 1940 br. (vNC)

UV/VIS absorptions: λ/nm (MeCl$_2$): 251 (4.20), 314 (3.84), 355 (2.98) and 437 nm (3.12)

NMR data: δ$_H$(90 MHz; solvent CDCl$_3$; standard SiMe$_4$): 3.02 (12 H, m, CH$_2$), 3.81 (3 H,
s, OCH$_3$) and 5.46 ppm (2 H, s, CH$_2$)

The best results were obtained with tris-(2-mercaptoethyl)amine **LH$_3$** [1]. Five-coordinated Re(III) complexes [ReL(PR$_3$)] and [ReL(CNR)] were prepared and their structure determined by X-ray crystal structure analysis (Figs. 1 and 2). Scheme 1 shows all important pathways finally leading to complexes **1** and **3**.

Reduction of NH$_4$ReO$_4$ by treatment with **LH$_3$**, an excess of conc. hydrochloric acid and a phosphane resulted in formation of the green compounds **1a-d** in EtOH. The obviously fastest reaction occurred in the case of PPh$_3$.

The isocyanides are stronger π-acids than the phosphanes. It is therefore very easy to replace the phosphane by the isocyanide to prepare **3a-f** (room temperature). We found a significant equilibrium reaction when we exchanged PPh$_3$ as verified by TLC (silica gel, chloroform). Working up the reaction mixture by column chromatography resulted in a high proportion of the starting product (30 %). Better yields we obtained using [ReL(PPhMe$_2$)] **1c** (i. e. 93 % formation of **3c**).

Scheme 1. Synthesis of **1** and **3**

$$ReO_4^-\qquad trans\text{-}ReOCl_3(PPh_3)_2\qquad ReCl_3(PPh_3)_2(MeCN)$$

R´NC

$$ReCl_3(PPh_3)_2(R´NC)$$

2

LH_3/PR_3

LH_3

$LH_3/R´NC$
R´NC

$$ReL(PR_3)\xrightarrow{\quad R´NC\quad} ReL(R´NC)$$

1   **3**

$$L = N(CH_2CH_2S^-)_3$$

$$LH_3 = N(CH_2CH_2SH)_3$$

1	PR_3
a	PPh_3
b	PPh_2Me
c	$PPhMe_2$
d	PBu_3

3	R´NC
a	$CNC(CH_3)_3$
b	$CNCH_2COOMe$
c	$CNCH_2COOEt$
d	CN–⟨H⟩
e	CN–⟨⟩
f	CN–CH₂CH₂–N(morpholine)O

By the second route **3** was produced from **2** in the presence of LH_3 - also under moderate reaction conditions. Finally, **3** can be synthesized by reaction of $[ReCl_3(PPh_3)_2MeCN]$ with an equimolar mixture of the tripod ligand and an isocyanide. But the most convenient route is the use of the phosphane/tripod substituted "precursor" **1**.

Complexes **3b, c** permit the formation of further derivatives by subsequent reaction at the ester group. They might thus have some potential in the design of bifunctional rhenium tracers. For instance, we prepared the amides by reaction with ammonia, morpholine and benzyl amine. Saponification experiments and others are still in progress.

Fig, 1: X-ray structure of **1**

3a   **3b**

Fig. 2: X-ray structure of **3a** and **3b**

The X-ray structural analysis of **1a** and **3a, b** confirmed the supposed coordination of the trigonal bipyramidal type (see Figs. 1 and 2).

Only two technetium compounds of comparable structures have so far been described: [Tc(PS$_3$)(CN-i-Pr)] (PS$_3$ = tris(o-thiolatophenyl)phosphine) and [TcL(PPh$_3$)] [2,3].

References

[1] Harley-Mason, J. J. Chem. Soc. (1946) 320

[2] de Vries, N. et al., Inorg. Chem. **30** (1991) 2662

[3] Pietzsch, H. J. et al., FZR 93 - 12 (1992) 86

21. TECHNETIUM AND RHENIUM COMPLEXES WITH THIOETHER LIGANDS
4. SYNTHESIS AND STRUCTURAL CHARACTERIZATION OF NEUTRAL BINUCLEAR OXORHENIUM(V) COMPLEXES WITH BIDENTATE THIOETHERS

H.-J. Pietzsch, H. Spies, K. Klostermann[1], P. Leibnitz[2], G. Reck[2], J. Beger[3], R. Jacobi[3]

[1] TU Dresden, [2] Bundesanstalt für Materialforschung Berlin, [3] Bergakademie Freiberg

Recently we found that neutral oxotechnetium(V) complexes are formed when TcOCl$_4^-$ reacts with bidentate thioethers in methanolic solution [1,2].

In view of the fact that the rhenium nuclides [186]Re and [188]Re emit β^- particles with therapeutically useful energies, rhenium is included in our efforts to evaluate novel thioether complexes as potential tracers for radiodiagnostic and radiotherapeutic purposes.

In this paper we describe the synthesis and structure of binuclear oxorhenium(V) complexes derived from bidentate thioethers.

Neutral, bidentate dithiaalkanes such as 5,8-dithiadodecane and 3,6-dithiaoctane ("S$_2$") react with ReOCl$_4^-$ in acetone/methanol with a partial exchange of chloride ligands by the S atoms of dithia ligands.

Analytically pure, dark green oxo complexes of the composition [ReO("S$_2$")Cl$_2$]$_2$O **1, 2** precipitate from the reaction mixtures by slow evaporation of the solvent.

$$\text{ReOCl}_4^- \xrightarrow[\text{acetone/methanol}]{\text{"S}_2\text{"}} [\text{ReO("S}_2\text{")Cl}_2]_2\text{O}$$

1 "S$_2$": C$_4$H$_9$SCH$_2$CH$_2$SC$_4$H$_9$

2 "S$_2$": C$_2$H$_5$SCH$_2$CH$_2$SC$_2$H$_5$

The neutral complexes are stable on exposure to air and, except for acetone and acetonitrile insoluble in the common organic solvents. Elemental analyses are consistent with the proposed formulations.

In the infrared spectra broad absorptions between 650 and 700 cm^{-1} indicate the O=Re-O-Re=O moiety. Peaks which can be assigned to the Re=O^{3+} cores are not observed.

The structure of complex $\underline{1}$ was determined by X-ray structure analysis. Suitable crystals were obtained from acetone/methanol. Drawings of $\underline{1}$ are shown in Figs. 1 and 2. Selected bond angles and distances are listed in Table 1.

The crystal structure of $\underline{1}$ consists of two independent ReO("S$_2$")Cl$_2$ units bridged by an oxygen atom.

The characteristic feature is the presence of the O=Re-O-Re=O group. In this respect the structure of $\underline{1}$ is comparable to those of [ReO(pyr)$_2$Cl$_2$]$_2$O (pyr = pyridine) [3], [TcO("S$_2$")Cl$_2$]$_2$O ("S$_2$" = bidentate thioether) [1], [TcO(salpd)]$_2$O (salpd = N,N'-propane-1,3-diylbis-(salicylideneiminate) [4], and [TcO(N$_2$S$_2$)]$_2$O (N$_2$S$_2$ = N,N'-ethylenebis(thio-acetylacetone-iminate) [5].

Fig. 1: CELLGRAF[6]-drawing of [ReO(5,8-dithiadodecane)$_2$Cl$_2$]$_2$O

Fig. 2: Molecular geometry of [ReO(5,8-dithiadodecane)$_2$Cl$_2$]$_2$O viewed perpendicular (on the left) and parallel to the O$_1$, Re$_1$, O$_3$, Re$_2$, O$_2$ axis

The rhenium atoms are centred in a flattened octahedron with the equatorial plane formed by a S$_2$Cl$_2$ donor set, in which the rhenium atoms Re1 and Re2 are 0.12 Å out of plane towards O1 and O2 respectively. The S$_2$Cl$_2$ planes are almost parallel with a small deviation of 0.013 Å; the dihedral angle is 2.6 °. The sulphur and chlorine donor atoms of the units are in the anti position with respect to the bridging oxygen.

The bond lengths of the Re=O cores with 1.705 and 1.735 Å, are in the range generally found for these units (1.61- 1.75 Å), but they are in between those in the octahedral O=Re=O compounds and in square-pyramidal Re=O complexes. This corresponds to the relatively low value of Re=O absorption in the infrared spectrum.

The bridging Re-O distances (Re1-O3 1.908 Å and Re2-O3 1.946 Å) are intermediate between the average Re=O length and the average Re-O bond distance which are observed being in the range 1.98- 2.09 Å [3,7-10].

This new class of rhenium complexes is worthy of special interest as manifolde subsequent reactions can be anticipated. Diversity is given in ligand exchange reactions by various leaving groups in the coordination sphere. New radiopharmacologically relevant compounds may thus become accessible. Studies on the reactivity of the described complexes will follow.

Tab. 1: Bond lengths (Å) and angles (°) for [ReO(5,8-dithiadodecane)$_2$Cl$_2$]$_2$O

Re1-Cl1	2.405(2)	Re2-Cl3	2.401(2)
Re1-Cl2	2.395(2)	Re2-Cl4	2.395(2)
Re1-S1	2.439(2)	Re2-S3	2.419(2)
Re1-S2	2.410(2)	Re2-S4	2.420(2)
Re1-O1	1.705(8)	Re2-O2	1.735(4)
Re1-O3	1.908(9)	Re2-O3	1.946(3)
Cl1-Re1-Cl2	89.53(7)	Cl3-Re2-Cl4	89.63(9)
Cl1-Re1-S1	91.27(7)	Cl3-Re2-S3	93.10(9)
Cl1-Re1-S2	173.82(6)	Cl3-Re2-S4	173.36(7)
Cl1-Re1-O1	100.7(3)	Cl3-Re2-O2	93.8(3)
Cl1-Re1-O3	89.1(3)	Cl3-Re2-O3-	87.7(3)
Cl2-Re1-S1	173.82(6)	Cl4-Re2-S3	174.16(7)
Cl2-Re1-S2	93.54(7)	Cl4-Re2-S4	90.12(8)
Cl2-Re1-O1	92.3(3)	Cl4-Re2-O2	106.1(4)
Cl2-Re1-O3	94.5(3)	Cl4-Re2-O3	95.3(3)
S1-Re1-S2	85.11(7)	S3-Re2-S4	86.58(8)
S1-Re1-O1	93.6(3)	S3-Re2-O2	78.9(4)
S1-Re1-O3	79.4(3)	S3-Re2-O3	79.7(3)
S2-Re1-O1	84.5(3)	S4-Re2-O2	92.6(3)
S2-Re1-O3	85.3(3)	S4-Re2-O3	85.7(3)
O1-Re1-O3	168.1(4)	O2-Re2-O3	158.6(5)

References

[1] Pietzsch, H.J. et al., Polyhedron, **12** (1993) 187

[2] Pietzsch, H.J. et al., FZR 93-12 (1993) 66

[3] Lock, C.J. et al., Can. J. Chem. **56** (1978) 179

[4] Bandoli, G. et al., J. Chem. Soc. Dalton Trans. (1984) 2505

[5] Tisato, F. et al., J. Chem. Soc. Dalton Trans. (1991) 1301

[6] Reck, G. et al., CELLGRAF- a program for representation of organic and inorganic crystal structures, Analytical Centre Berlin (1989/1991)

[7] Davison, A. et al., Inorg. Chem. **19** (1980) 1988

[8] McDonell, A.C. et al., Aust. J. Chem. **36** (1983) 253

[9] Blower, P.J. et al., J. Chem. Soc. Dalton Trans. (1986) 1339

[10] Luna, S.A. et al., Inorg. Chem. 31 (1992) 2595

22. TECHNETIUM AND RHENIUM COMPLEXES WITH THIOETHER LIGANDS
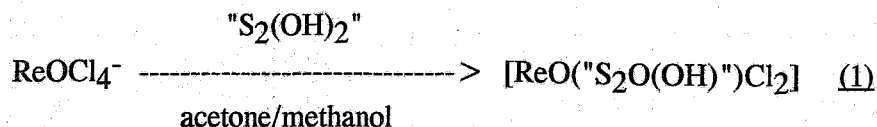## 5. SYNTHESIS AND STRUCTURAL CHARACTERIZATION OF NEUTRAL OXORHENIUM(V) COMPLEXES WITH POTENTIALLY TETRADENTATE THIOETHERS

H.-J. Pietzsch, H. Spies, K. Klostermann[1], P. Leibnitz[2], G. Reck[2], J. Beger[3], R. Jacobi[3]

[1] TU Dresden, [2] Bundesanstalt für Materialforschung Berlin,

[3] Bergakademie Freiberg

Ligand exchange reaction of the potentially tetradentate ligand 1,8-dihydroxy-3,6-dithiaoctane ("$S_2(OH)_2$") with $ReOCl_4^-$ leads to the formation of a violet microcrystalline compound which precipitates from the reaction mixture. The elemental analysis is consistent with the formulation $[ReO("S_2O(OH)")Cl_2]$.

$$ReOCl_4^- \xrightarrow[\text{acetone/methanol}]{\text{"}S_2(OH)_2\text{"}} [ReO("S_2O(OH)")Cl_2] \quad \underline{(1)}$$

"$S_2(OH)_2$": $HO\text{-}CH_2CH_2SCH_2CH_2SCH_2CH_2\text{-}OH$

The complex is practically insoluble in all common organic solvents; attempts to obtain crystals suitable for X-ray structure analysis were therefore unsuccessful.

The infrared spectrum shows the characteristc strong absorption at 940 cm^{-1} indicating the $Re=O^{3+}$ core.

By analogy with the appropriate technetium complex [1] compound $\underline{(1)}$ should consist of discrete monomolecular units containing the $O=Re\text{-}O\text{-}$ core as illustrated in Fig. 1.

Fig. 1: Proposed structure of $[ReO\{8\text{-hydroxy-}3,6\text{-dithiaoctan-}1\text{-olato-}(O,S,S)\}Cl_2]$ $\underline{(1)}$

82

The proposed structure of (1) is supported by the FAB mass spectrum (Fig. 2). It is charac-
terized by typical metal-containing fragment ions. The parent peak is found at m/z = 455
(M+H).
The isotope patterns caused by the metal and the Cl⁻ ligands correspond to the calculated
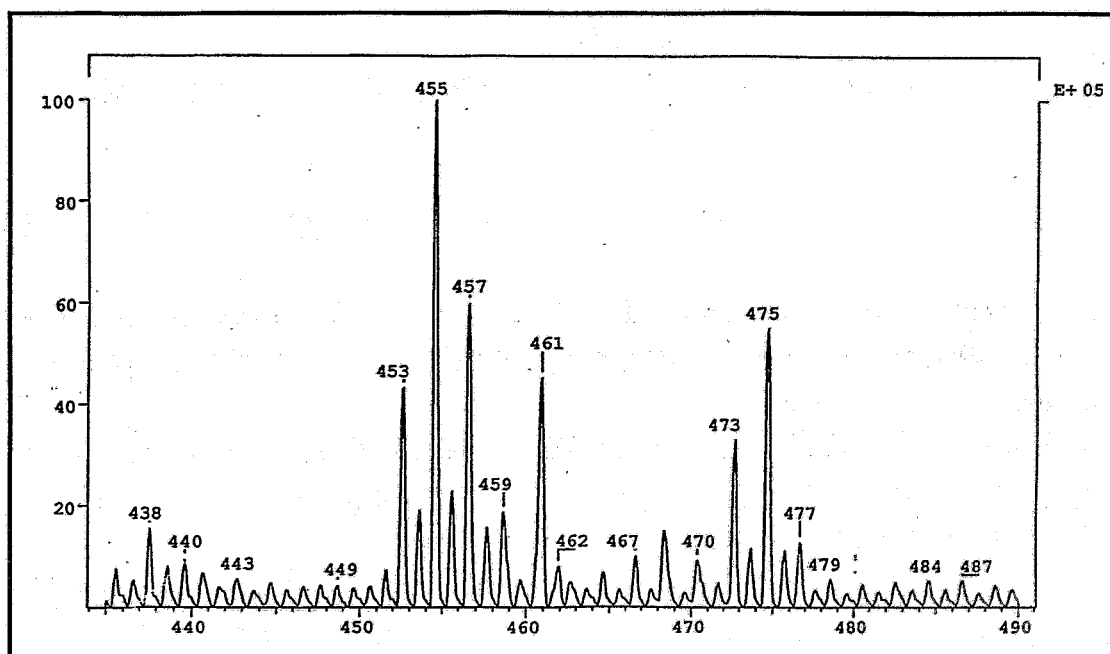isotope pattern shown in Fig. 3.

Fig. 2: FAB mass spectrum of [ReO{8-hydroxy-3,6-dithiaoctan-1-olato-(O,S,S)}Cl$_2$] (1)
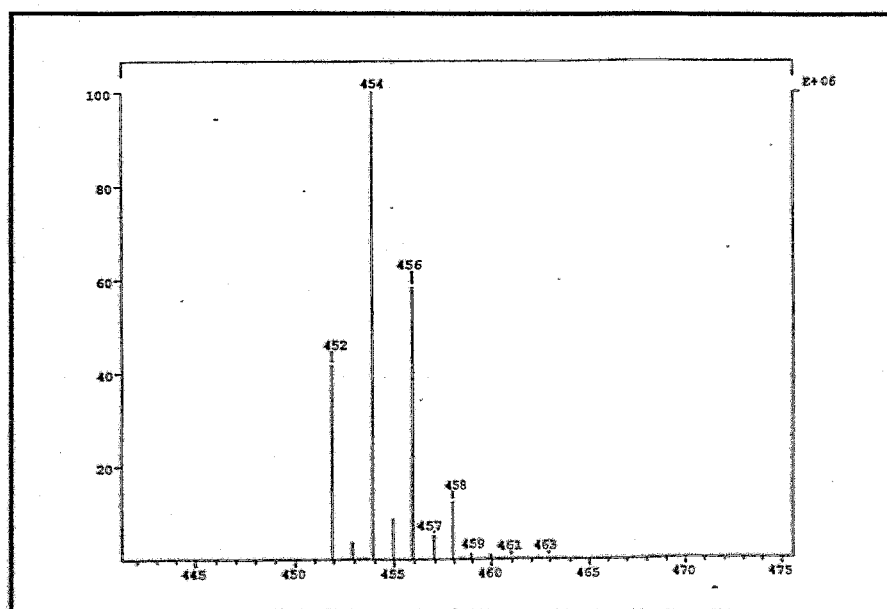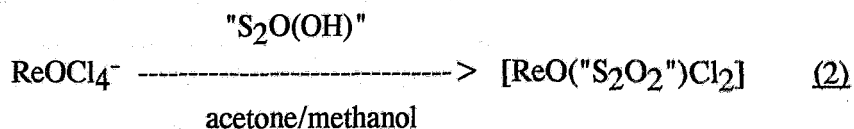(region between m/z= 435 and 490)

Fig. 3: Calculated isotope pattern of C$_6$H$_{13}$S$_2$Cl$_2$O$_3$Re (1)

Rhenium complex with 1-hydroxy-3,6-dithia-9-oxaundecane

Ligand exchange reaction of $ReOCl_4^-$ with 1-hydroxy-3,6-dithia-9-oxaundecane ("$S_2O(OH)$") in acetone/methanol leads to the formation of a violet compound which can be precipitated from the reaction mixture by diethylether. The complex recrystallizes from chloroform/diethylether as violet needles.

$$\text{"S}_2\text{O(OH)"}$$
$$ReOCl_4^- \text{ ----------------------------} > [ReO(\text{"}S_2O_2\text{"})Cl_2] \quad \underline{(2)}$$
$$\text{acetone/methanol}$$

$$\text{"S}_2\text{O(OH)": } CH_3CH_2O\text{-}CH_2CH_2SCH_2CH_2SCH_2CH_2\text{-}OH$$
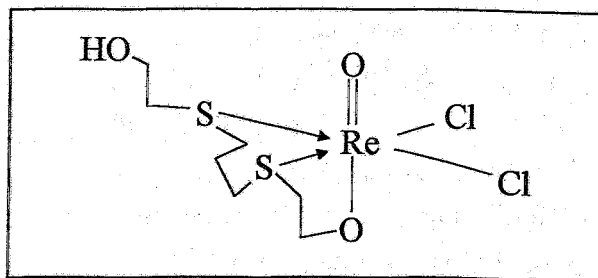
According to the elemental analysis and the infrared spectrum which shows an absorption at 948 cm^{-1}, indicating the $Re=O^{3+}$ core, compound $\underline{(2)}$ is a mononuclear complex of the formulation $[ReO(\text{"}S_2O_2\text{"})Cl_2]$.

This is confirmed by the FD mass spectrum (Fig. 4) and the X-ray structure analysis. Suitable crystals were obtained from chloroform/diethylether. Drawing of $\underline{(2)}$ is shown in Fig. 5. Selected bond angles and distances are listed in Table 1.
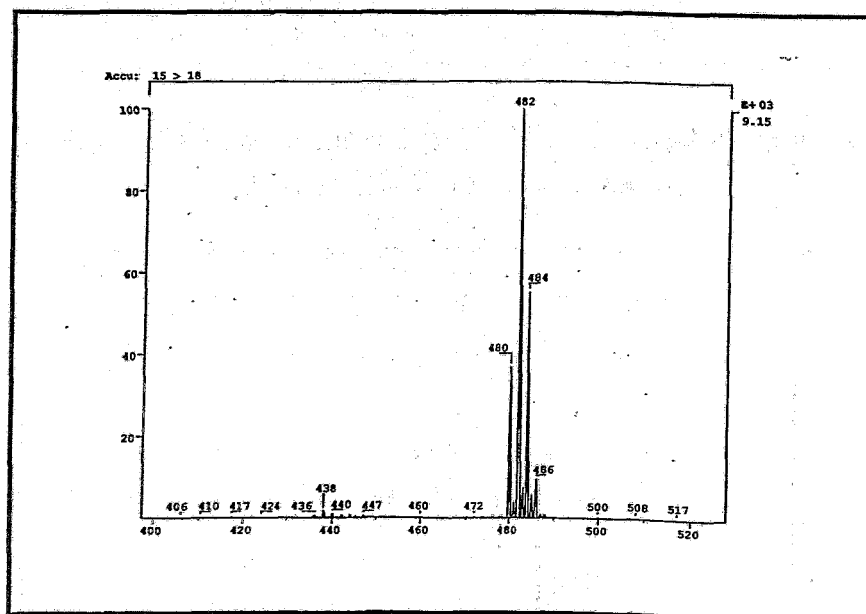
Fig. 4: FD mass spectrum of $[ReO\{3,6\text{-dithia-9-oxaundecan-1-olato-}(O,S,S)\}Cl_2]$ $\underline{(2)}$ showing the characteristic isotope pattern of a ReS_2Cl_2 complex and the parent peak at m/z = 482.
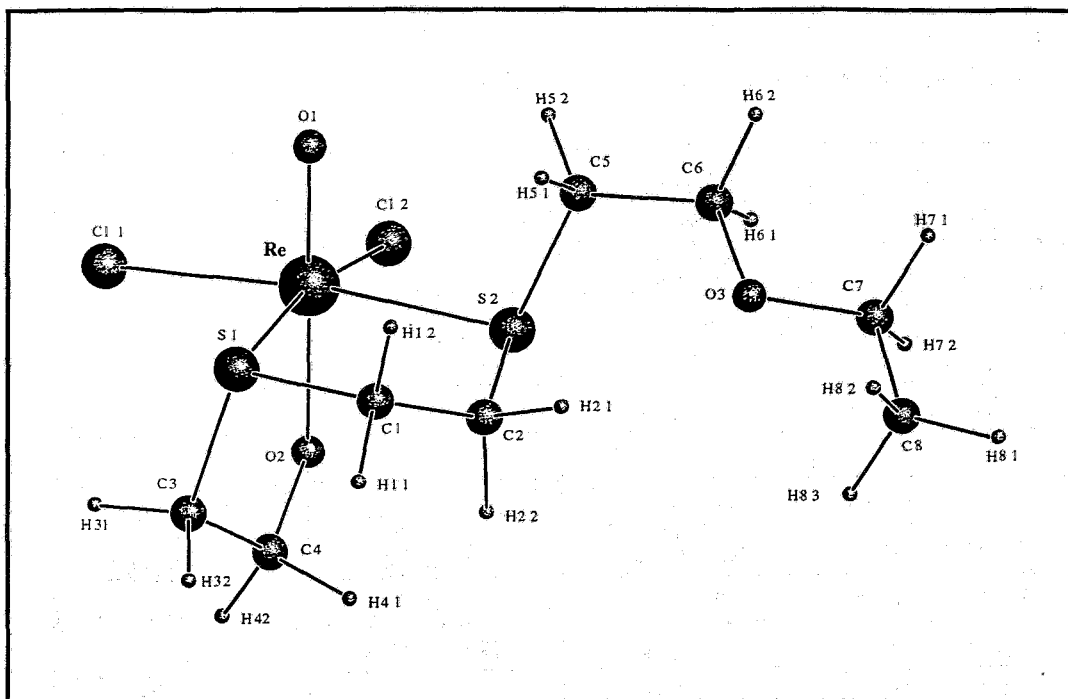
Fig. 5: CELLGRAF [4] drawing of [ReO{3,6-dithia-9-oxaundecan-1-olato-(O,S,S)}Cl₂] (2)

Complex (2) consists of discrete monomolecular units containing the O=Re-O- core.

In general, the structure strongly resembles that of the technetium [1,2] and rhenium complexes derived from dithiaoctane [3].

However, while in the dinuclear species the trans-position is occupied by a bridging oxygen which may come from traces of water present in the reaction mixture, the trans position in complex (2) is occupied by the oxygen of the terminal hydroxy group.

The S atoms of the dithioether and the two Cl atoms which remain at the metal due to the incomplete exchange at the tetrachlorooxotechnetium ion form a cis-arrangement in the equatorial plane.

Such compounds with a single bonded oxygen trans to the M=O core (M=Tc, Re) have been hardly described so far.

The length of the Re-O bond (1.912 Å) is comparable to that found in other trans-O=M-O⁻ groups (M=Tc, Re) [5-8].

Table 1: Bond lengths (Å) and angles (°) for
[ReO{3,6-dithia-9-oxaundecan-1-olato-(O,S,S)}Cl₂] (2)

Re-Cl(1)	2.405(3)		
Re-Cl(2)	2.360(3)		
Re-S(1)	2.428(2)		
Re-S(2)	2.422(3)		
Re-O(1)	1.686(6)		
Re-O(2)	1.917(6)		
Cl(1)-Re-Cl(2)	91.2(1)	Cl(2)-Re-O(2)	89.5(2)
Cl(1)-Re-S(1)	90.74(9)	S(1)-Re-S(2)	86.59(8)
Cl(1)-Re-S(2)	172.6(1)	S(1)-Re-O(1)	88.3(2)
Cl(1)-Re-O(1)	94.4(2)	S(1)-Re-O(2)	78.8(2)
Cl(1)-Re-O(2)	89.7(2)	S(2)-Re-O(1)	92.4(2)
Cl(2)-Re-S(1)	168.2(1)	S(2)-Re-O(2)	83.0(2)
Cl(2)-Re-S(2)	90.03(9)	O(1)-Re-O(2)	166.5(3)
Cl(2)-Re-O(1)	103.2(2)		

References

[1] Pietzsch, H.J. et al., Polyhedron **12** (1993) 187

[2] Pietzsch, H.J. et al., FZR 93-12 (1993) 66

[3] Pietzsch, H.J. et al., this report, p.

[4] Reck, G. et al., CELLGRAF- a program for representation of organic and inorganic crystal structures, Analytical Centre, Berlin (1989/1991)

[5] Lock, C.J. et al., Can. J. Chem. **56** (1978) 179

[6] Blower, P.J. etal., J. Chem. Soc. Dalton Trans. (1986) 1339

[7] Franklin, K. et al., Inorg. Chem. **21** (1982) 1941

[8] Fackler, P. et al., Inorg. Chem. **23** (1984) 3968

23. ELECTROCHEMICAL INVESTIGATIONS INTO RHENIUM(V) THIOETHER COMPLEXES

I. Hoffmann, H.-J. Pietzsch

Introduction

Rhenium complexes of the general formula $Re_2O_3X_4(L)_4$ are known with several ligands L, and electrochemical studies have been carried out, for examples, with complexes where L = pyridine [1]. Analogous rhenium complexes with thioethers have now been prepared by us [2] (Fig. 1). Their electrochemical behaviour was characterized by cyclic voltammetry, d.c. polarography and coulometry. Special attention was devoted to similarities and differences between Re-S-(thioether)- and Re-N-(pyridine) compounds.
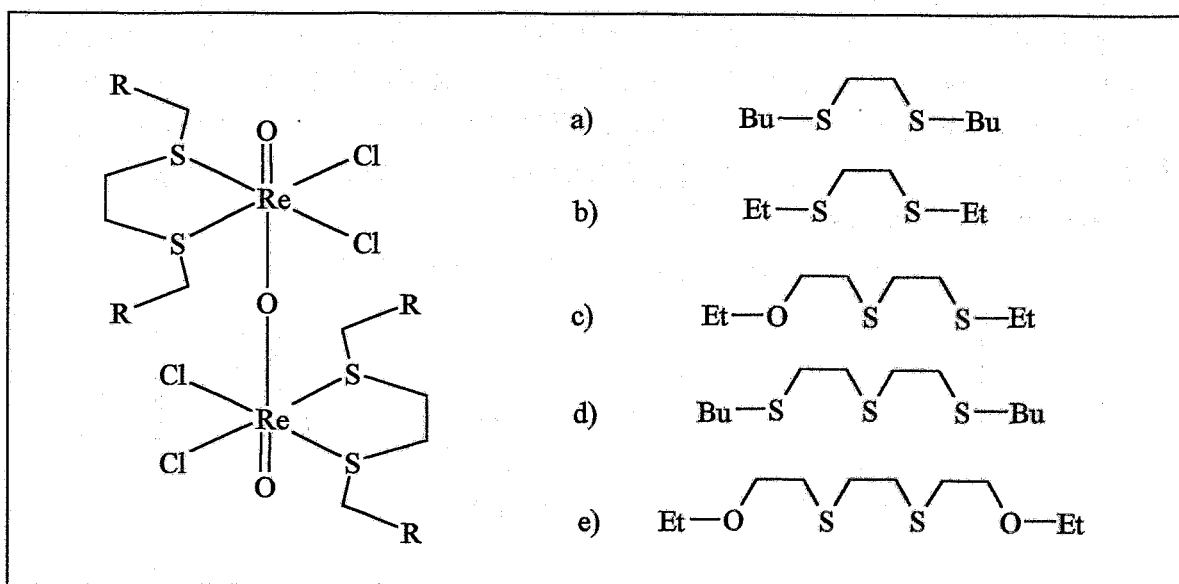
Fig. 1: General formula of the rhenium(V) thioether complexes

Experimental

Chemicals

Supporting electrolyte: 0.1 M Bu_4NPF_6 in anhydrous dichloromethane (Aldrich Chem.)
Re complexes with thioethers were prepared according to [2] (Fig. 1).
All solutions were deoxygenated by argon (99.998 %).

Apparatus

Cyclic voltammograph (CV - 27, BAS), DC/AC polarograph (GWP 673, ZWG Berlin)

Electrodes

Working electrode: Pt button electrode, static mercury drop electrode (GQE 100, ZWG Berlin)

Reference electrode: saturated calomel electrode

Counter electrode: Pt electrode or Hg-pool

Results and discussion

Five rhenium thioether complexes (Fig. 1) were electrochemically investigated in the supporting electrolyte of 0.1 M Bu_4NPF_6 in CH_2Cl_2 at Pt electrodes. The supporting electrolyte used allows measurements within the potential range from +1500 to -1800 mV vs. SCE. The cyclic voltammograms of all compounds investigated are nearly identical. In comparison with the Re(V) pyridine compounds [1] the investigated complexes show a similar reduction behaviour. Two reduction steps (A,B) are observed in this potential range (see Fig. 2). The first reduction peak at -790 mV vs. SCE (A) indicates a reversible 1-electron process because the voltage difference to the corresponding anodic peak (C) is about 60 mV. The peak magnitude of the first reduction process (A) depends on the potential sweep rate in accordance with the theory of a reversible electron transfer. The second cathodic peak at -1600 mV vs. SCE (B), close to cathodic decomposition of the supporting electrolyte, has no counterpart in anodic direction. This electrode reaction is therefore irreversible. In the case of the corresponding pyridine compounds, the reduction peak at this potential has a reversible oxidation peak [1].
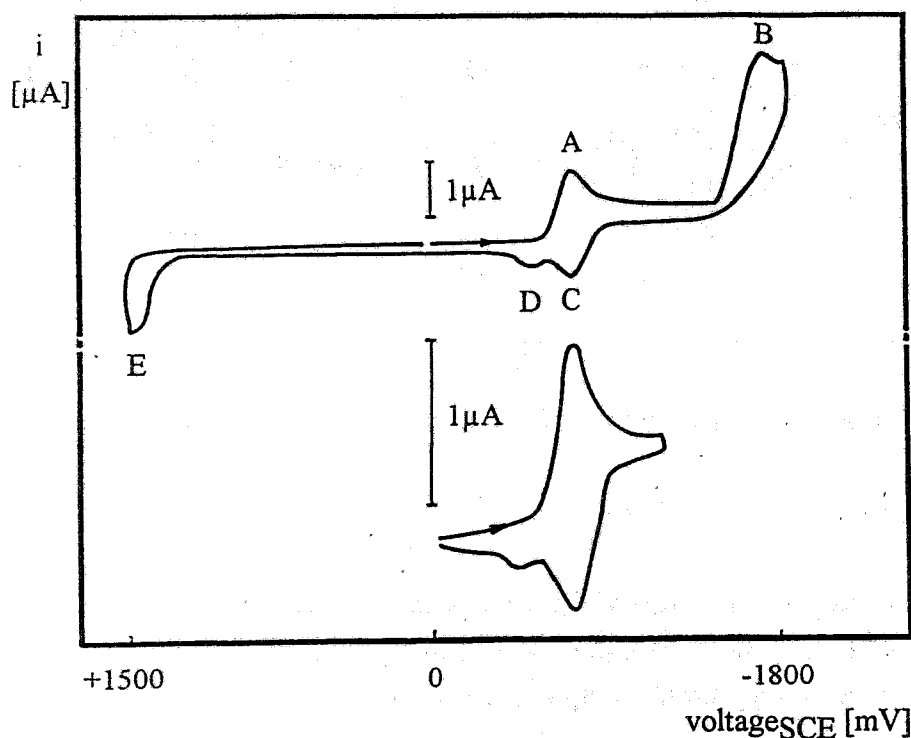

Fig. 2: Cyclic voltammogram of complex (b) in 0.1 M Bu_4NPF_6/CH_2Cl_2
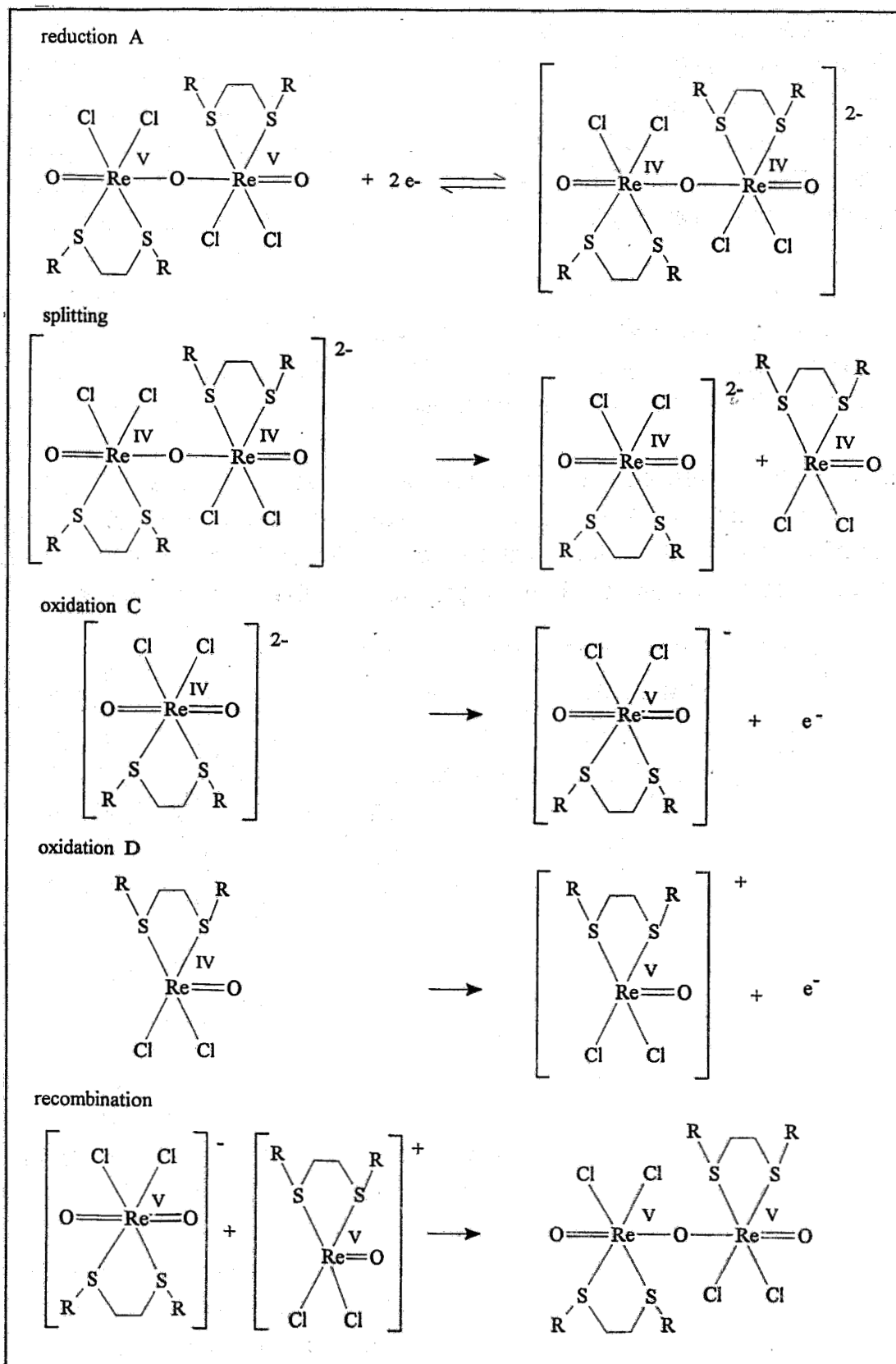($c_{(b)}$ = 1.5 x 10^{-3} M, scan rate = 100 mV/s)

Fig.3: Proposed mechanism for reduction

During the anodic scan a second oxidation peak (D) was found near the above-mentioned reversible oxidation peak (C). That means that the reduced compound consists of two electrochemically different forms. As shown in the lower part of (Fig. 2) these peaks (C, D) exist without a previous scan up to -1800 mV vs. SCE and are therefore independent of reduction step (B). This process differs from the reduction of Re dioxo complexes with pyridine. Pyridine complexes only split into two parts after the reduction step at more negative potentials [1].

Despite the splitting of the oxidation process into two parts (C, D) the original amount of the complex is formed again by recombination. That was concluded from the observation that the peak magnitude (A) did not decrease after some potential runs.

This behaviour can be interpreted as both Re atoms being reduced at the same potential by 1- electron transfer and split into two parts with different potentials for reoxidation (C, D). The mechanism (formulated in Fig. 3) can be discussed on the analogy of the rhenium pyridine complexes [1]. The data obtained are in accordance with this scheme (Fig. 3).
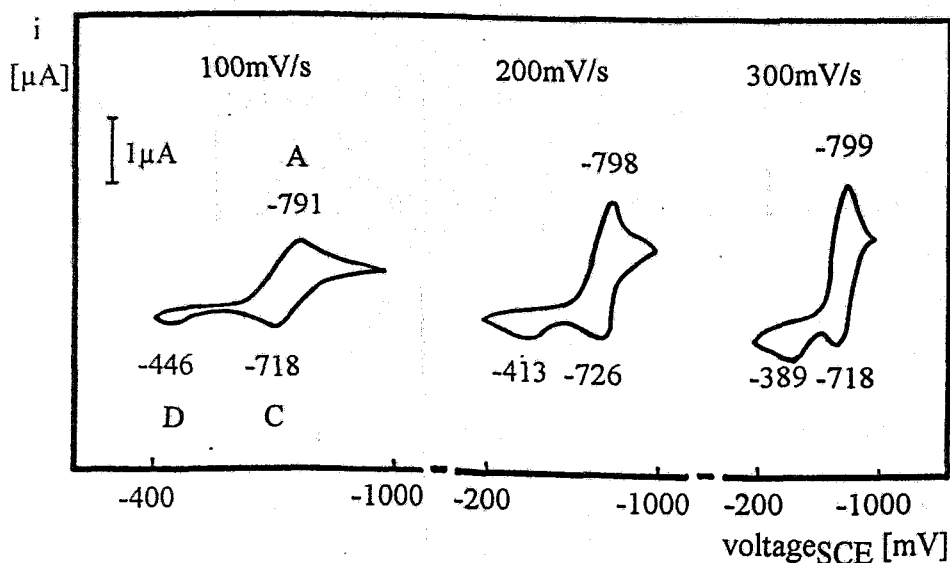

Fig. 4: Cyclic voltammogram of complex (c) in 0.1 M Bu_4NPF_6/CH_2Cl_2 at different scan rates, $(c_{(c)} = 1.5 \times 10^{-3}$ M)

Fig. 4 shows the cyclic voltammograms of the complex compound (c) at various potential sweep rates. The peak magnitude (A) increases with increasing sweep rate. The peak potentials of A and C are nearly constant but that of peak (D) depends on sweep rate, and the peak distance (C/D) increases. That means that the reaction will be more irreversible. The relation of the peak magnitudes (D) and (C) changes with the potential sweep rate and the

reaction time. The magnitude of peak (D) increases with sweep rate and time in the same measure as peak (C) decreases.

At potential B (Fig. 2) rhenium (IV) is probably reduced to rhenium (II). The height of the wave in the DC polarograms suggests a 2-electron process. Coulometric measurements at the mercury pool are disturbed by other reactions.

Oxidation of Re(V) thioether complexes is more difficult than oxidation of pyridine complexes because the oxidation peak is up to 300 mV more positive than that of pyridine complexes. In the potential range only one oxidation peak was found at +1300 mV. This oxidation seems to be irreversible.

References
[1] Holder, G. N. et al., Inorg. Chim. Acta **194** (1992) 133
[2] Pietzsch, H.-J., this report, p. 81

24. RHENIUM(V) COMPLEXES WITH *meso*-DMSA PART III: X-RAY CRYSTAL STRUCTURE OF Ph$_4$As[ReO(DMSA)$_2$] x 2 ACETONE AND IDENTIFICATION OF THE POSSIBLE ISOMERS

S. Seifert, H. Spies, P. Leibnitz, G. Reck

186/188Re(V)*meso*-DMSA, a potential therapeutic tumour seeking agent, exists in three stereoisomeric forms (syn-endo, syn-exo, anti) which can be detected by HPLC and[1]H NMR analyses as described in several articles [1,2,3]. Previous studies [4] showed that an equilibrium exists between the three species, depending on the solvent, pH value, temperature, and the age of the complex solution.

The time dependence of formation of an anti and another syn isomer from a pure isolated syn isomer in aqueous solution was studied by HPLC and ^{1}H NMR analyses [5,6].

For a complete assignment X-ray crystallography of at least one isomer is required. One such assignment was carried out by [5] using a preparation of Et$_4$N[ReO(DMSA)$_2$] in aqueous solution. We determined X-ray crystal structure of Ph$_4$As[ReO(DMSA)$_2$] obtained from an acetonic solution.

Experimental

Ph$_4$As[ReO(DMSA)$_2$] was prepared in an acetonic solution starting from [ReOCl$_4$]$^-$ and characterized by elemental analysis, IR and UV/VIS spectroscopy, HPLC and ^{1}H NMR analysis [6]. An alternative route uses ReOCl$_3$(PPh$_3$)$_2$ as the precursor.

X-ray analysis was carried out on orange-red crystals obtained by fractional crystallization of the tetraphenylarsonium salt from acetonic solution.

Crystal data: C$_{39}$H$_{32}$O$_9$S$_4$AsRe x 2 CH$_3$COCH$_3$, molecular weight 941.92, triclinic, space group P1, a = 12.792(2) Å, b = 13.953(2) Å, c = 14.842(3) Å, α = 116.40(1) °, β = 101.63(1) °, γ = 104.28(2) °, V = 2146.48 Å^3; Z = 2, D$_c$ = 1.456 g/cm^3,

Data collection: The intensity data of an orange crystal (size 0.13 x 0.45 x 0.45 mm) were recorded at room temperature by means of an automatic Enraf Nonius CAD4-diffractometer with graphite filtered Mo K$_\alpha$ radiation (λ = 0.71073 Å, μ = 38.556 cm^{-1}, F(000) = 1148) using the ω-2θ scan procedure with a variable scan rate of 1.1 - 4.8 °/min. A total of 6239 unique reflections were measured and 5628 were used for structure determination. Refinement converged with R = 0.026.

Results and discussion

The molecular structure of the complex anion with the atomic numbering scheme is given in Fig. 1. Selected interatomic distances and angles are summarized in Table 1.

In the crystal the complex anion adopts an approximate square-pyramidal configuration as expected from known data [5]. The pure isomer II of Ph$_4$As[ReO(DMSA)$_2$] according to elution order in HPLC reveals a syn-endo configuration of the carboxylic acid groups of both DMSA ligands. The correct configuration of the possible *meso* isomers of [ReO(DMSA)$_2$]$^-$ can be assigned as follows:

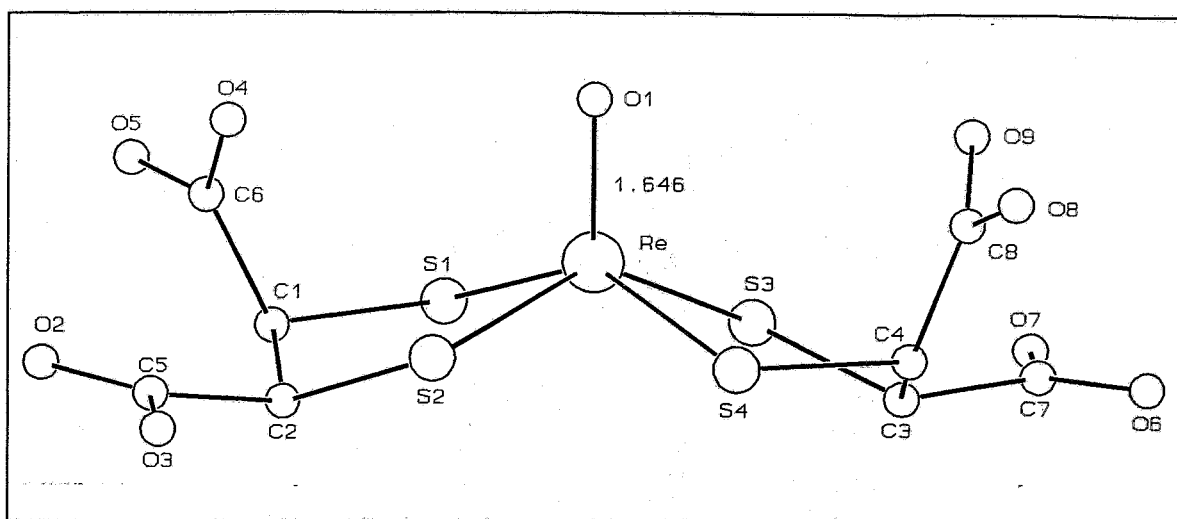**Isomer I: anti, isomer II: syn-endo, isomer III: syn-exo.**

Fig. 1: X-ray analysis of the pure isomer II of [ReO(DMSA)$_2$]$^-$

Tab. 1: Selected bond distances (Å) and angles (°) for Ph$_4$As[ReO(DMSA)$_2$] x 2 acetone

Re-S1	2.314(1)	O8-O10	2.676
Re-S2	2.294(1)	O4-O11	2.691
Re-S3	2.313(1)	O2-O7	2.605
Re-S4	2.319(2)	O3-O6	2.631
Re-O1	1.672(3)		
S1-Re-S2	86.33(5)	S1-Re-O1	108.1(2)
S1-Re-S3	82.41(5)	S2-Re-O1	109.1(1)
S1-Re-S4	143.58(4)	S3-Re-O1	110.0(1)
S2-Re-S3	140.92(3)	S4-Re-O1	108.3(2)
S2-ReS4	81.96(5)	O10-C34-C36	121.0(8)
S3-Re-S4	85.30(5)	C35-C34-C36	117.1(6)

Fig. 2 confirms the bonding of two acetone molecules per complex anion by hydrogen bridges and shows the arrangement of the pertinent tetraphenylarsonium cation.
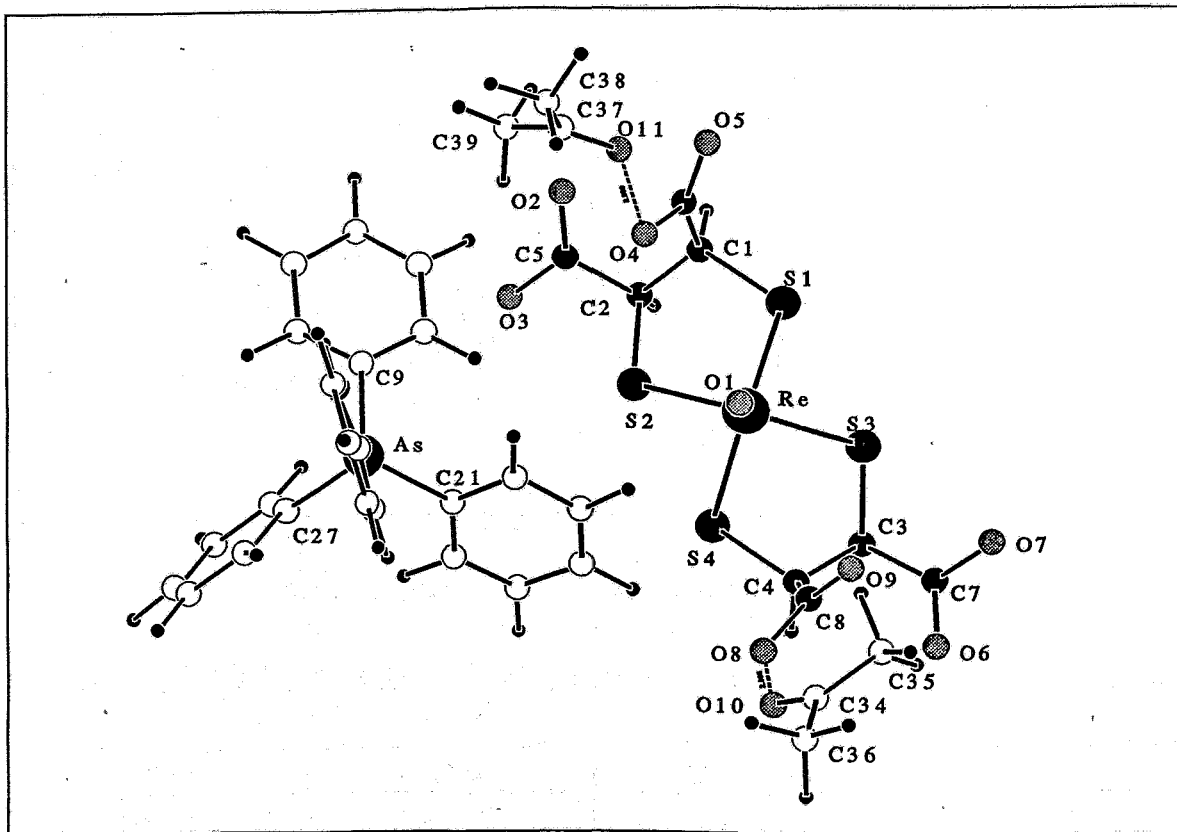
Fig. 2: Molecular structure of Ph$_4$As[ReO(DMSA)$_2$] x 2 acetone

The differences in the O-Re-S angles are smaller (108-110 °) than described by [5] for Et$_4$N[ReO(DMSA)$_2$] x 11/2 H$_2$O (105 - 113 °). However, the Re-O distance (1.699 Å) and also the Re-S bond lenghts (2.286 - 2.329 Å) are comparable. Weak but significant contacts were found between the rhenyl oxygen atom and two methylene hydrogens of the tetraethylammonium ion forming a loose ring structure with O--H contacts of 2.434 and 2.460 Å. The crystal structure of the complex under investigation shows hydrogen bonds between the acetone molecules and the carboxylic acid groups on the one side and between the carboxylic acid groups of two molecules on the other. The distances of the O--H contacts are slightly longer (2.605 - 2.691 Å) than described for the Et$_4$N[ReO(DMSA)$_2$] complex. This results in an arrangement of "endless" chains of complex anions as shown in Fig. 3. The acetone molecules are situated between these chains. The tetraphenylarsonium cations, omitted in the figure for clarity's sake, are also located between the complex anion chains.
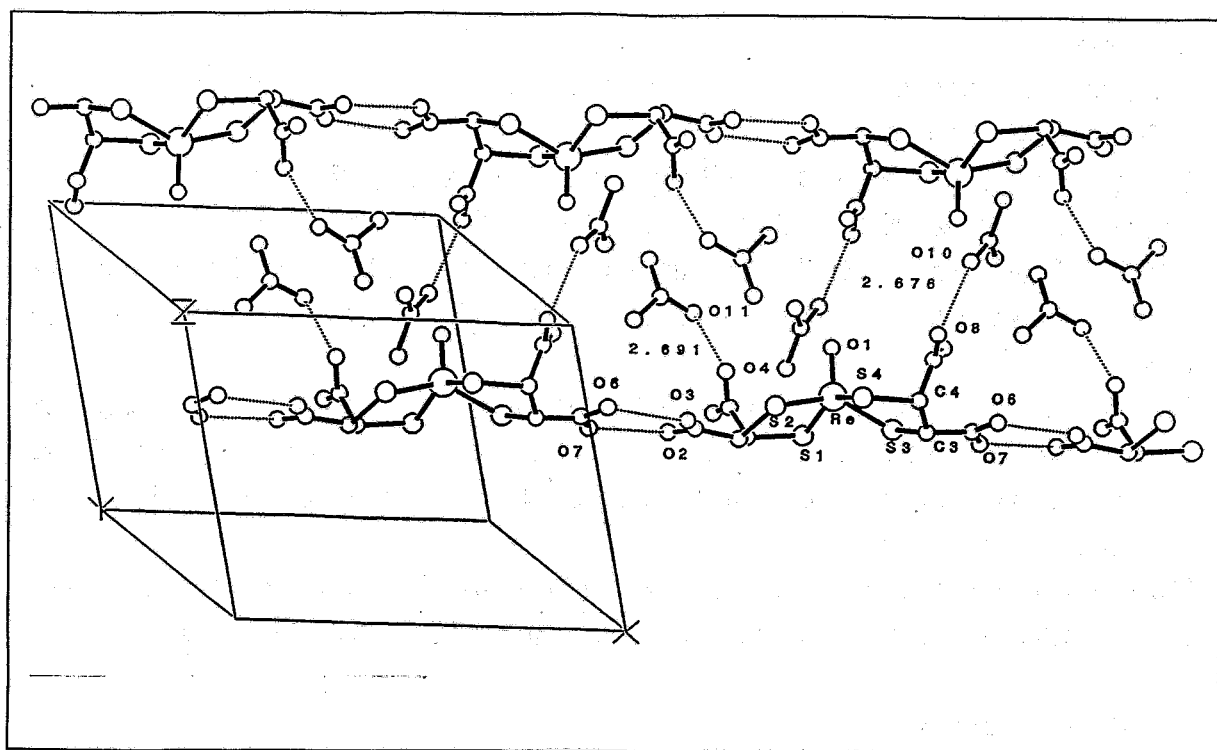
Fig. 3: Crystal structure of Ph4As[ReO(DMSA)2] x 2 CH3COCH3

References

[1] Bisunadan, M. M. et al., Appl. Radiat. Isot. **42** (1991) 167

[2] Lisic, E. C. et al. J. Lab. Comp. Radiopharm. **XXXIII** (1993) 65

[3] Singh, J. et al., Nucl. Chem. Commun. **14** (1993) 197

[4] Seifert, S. et al., FZR 93-12 (1993) 55

[5] Singh, J. et al., J. Chem. Soc., Chem. Commun. (1991) 1115

[6] Seifert, S. et al., FZR 93-12 (1993) 49

25. PREPARATION AND CHARACTERIZATION OF NITRIDORHENIUM(V) DMSA COMPLEXES

S. Seifert, F. Schneider, H.-J. Pietzsch, H. Spies

In connection with our work on ReO- and TcO-DMSA and DMS ester complexes attempts were made to prepare and characterize the corresponding ReN- and TcN-compounds of the same ligands.

The studies involve preparation of ReN-DMSA and ReN-DMS ester complexes as well as spectroscopic and chromatographic characterization and elemental analysis.

95

Experimental

The ReN-complexes were obtained by reaction of $ReNCl_2(Me_2PhP)_3$ with the DMSA ligands in acetonic solution.

35 mg $ReNCl_2(Me_2PhP)_3$ (5.1×10^{-5} mol) were dissolved in 5 ml dry acetone while stirring and 23 mg *meso*-DMSA (1.2×10^{-4} mol) **(A)** or 40 mg *meso*-DMS dimethylester (1.9×10^{-4} mol) **(B)**, also dissolved in acetone, were added. After stirring for 3 h at room temperature, the reaction was completed and the colour of the solution turned from yellow to brown.

The solutions were filtered and concentrated by bubbling nitrogen through the acetonic complex solution. Recrystallization from acetone/methanol gave microcrystalline products, which were characterized by elemental analysis, ^{1}H NMR, HPLC, UV/VIS and IR spectroscopy, and electrophoresis.

The orange brown reaction products are soluble in DMSO, hot methanol, ethanol, acetonitrile, CH_2Cl_2 and acetone. They are insoluble in water, ethers and hydrocarbons.

Results and discussion

The formation of the ReN-DMSA complexes has to proceed in dry organic solvents, preferably acetone, and at room temperature. Higher temperatures and the presence of water result in the formation of ReO-DMSA complexes as found by HPLC.

HPLC studies were performed using a PRP-1 column (Hamilton, 150 x 4.1 mm) in conjunction with a linear gradient system (+1.0) of 0.1 % trifluoroacetic acid in water (A)/0.1 % trifluoroacetic acid in acetonitrile (B). [t(min),B(%)]: [5,0], [10,20], [5,30], [1,50], [5,50]. The effluent from the column (flow rate 2.0 ml/min) was monitored by UV absorbance at 300 nm.

In accordance with the HPLC analyses of the ReO-DMSA complexes, three peaks of the possible stereoisomers are expected to occur in the ligand exchange reaction of $ReNCl_2(Me_2PhP)_3$ and DMSA or DMS dimethylester.

Fig. 1 shows the expected chromatograms obtained from the reaction solutions after filtration. When such solutions are concentrated a brown precipitate is formed and can be separated by centrifugation. Further concentration and addition of cold methanol or water to the remaining complex solution results in further precipitation of the complex without decomposition. The isomeric compositions of these precipitates differ clearly from each other as shown in Fig. 2.
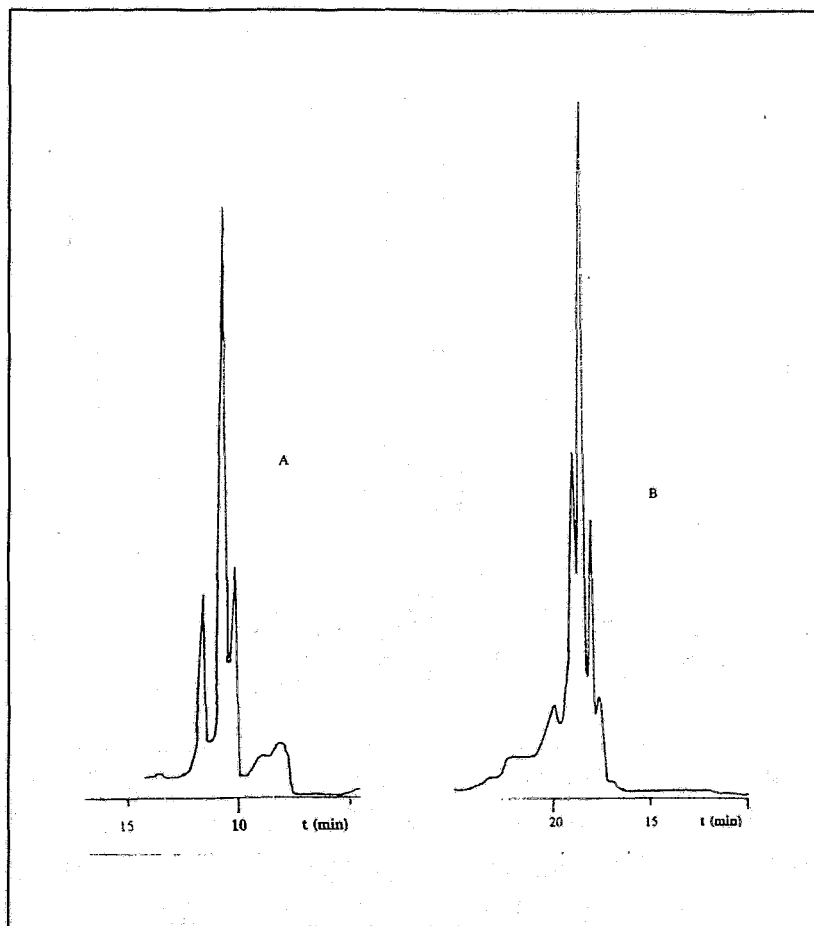
Fig. 1: HPLC chromatograms of reaction solutions of ReN-*meso*-DMSA (A) and
ReN-*meso*-DMS dimethylester (B) complexes

Elemental analyses:

[ReNHC(CH$_3$)$_2$(DMSA)$_2$PMe$_2$Ph] (A): (Found: C, 29.0, H, 3.5, N. 2.0, S, 15.7,
C$_{19}$H$_{26}$O$_8$NS$_4$PRe requires C, 29.4, H, 3.4, N, 1.8, S, 16.5 %)

[ReNHC(CH$_3$)$_2$(DMS dimethylester)$_2$PMe$_2$Ph] (B): (Found: C, 35.3, H, 4.3,
N, 1.7, S, 15.8, C$_{23}$H$_{34}$O$_8$NS$_4$PReCl requires C, 34.6, H, 4.1, N, 1.8, S, 16.1 %)

UV/VIS absorptions: λ_{max}/nm (acetone) 268 and 302

IR absorptions v_{max}/cm^{-1} (A): 3432, 2920, 1708, 1630, 1480, 1440, 1312, 1280, 1184,
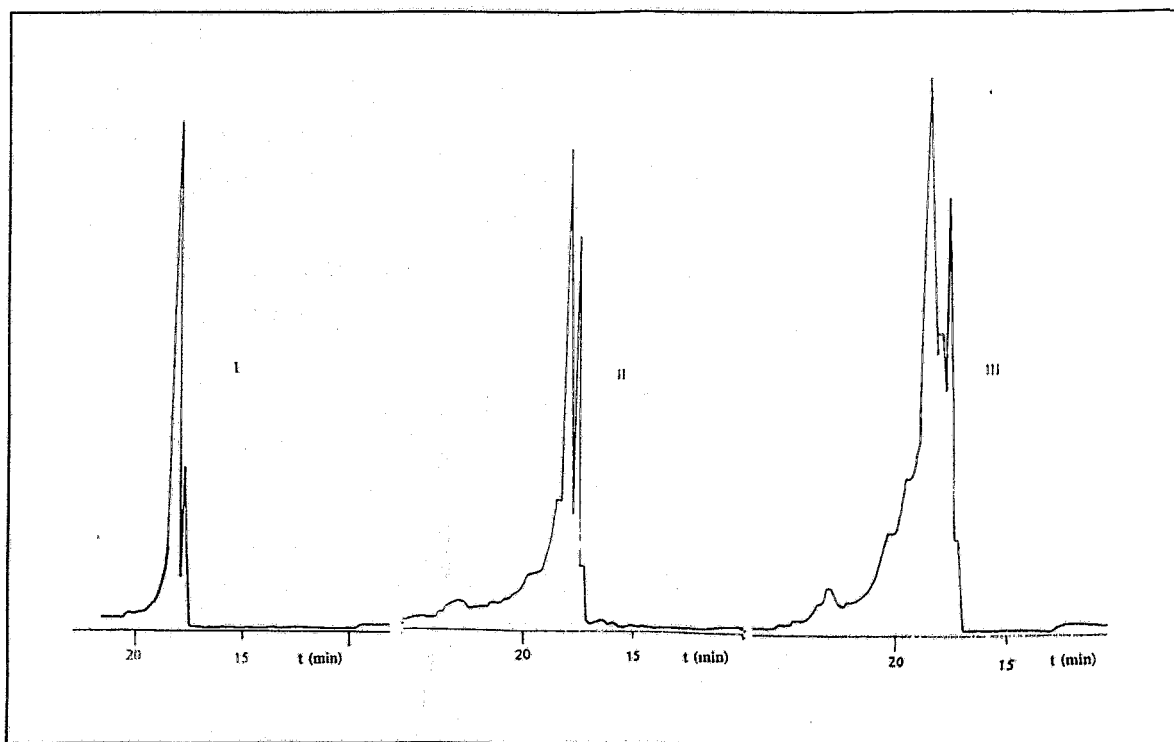1080, 1000, 916, 744, 688, 592, 464

Fig. 2: HPLC analyses of precipitates of ReN-DMS dimethylester complex dissolved in acetonitrile: I: 1st precipitate, II: 2nd precipitate (sample for elemental analysis and ^{1}H NMR), III: 3rd precipitate

Electrophoretic studies on silica gel in DMSO/1 % $NaClO_4$ solution (20 V/cm) revealed the surprising fact that the yellowish-brown complex does not migrate.

Elemental analysis shows an unexpected remaining coordination of a phosphine molecule in the complex. This result is confirmed by ^{31}P and ^{1}H NMR studies carried out in DMSO. Fig. 3 shows the ^{1}H NMR spectrum of (B). The sharp signals indicate that the Re(V) compound is diamagnetic. The five phenyl protons at 7.6 - 7.8 ppm indicate the coordination of one dimethylphenylphosphine molecule. The sum of all integrated protons shows that in addition to the C-H and O-CH_3 protons of the DMS dimethylester ligands and the CH_3 protons of the phosphine another constituent containing 6 methyl protons must still be coordinated. A possible explanation is that reaction of the solvent acetone with the ReN core leads to a Schiff base coordination sphere ReN=$C(CH_3)_2$. However, this formulation is still rather speculative and will be clarified by mass spectrometry and X-ray analysis.
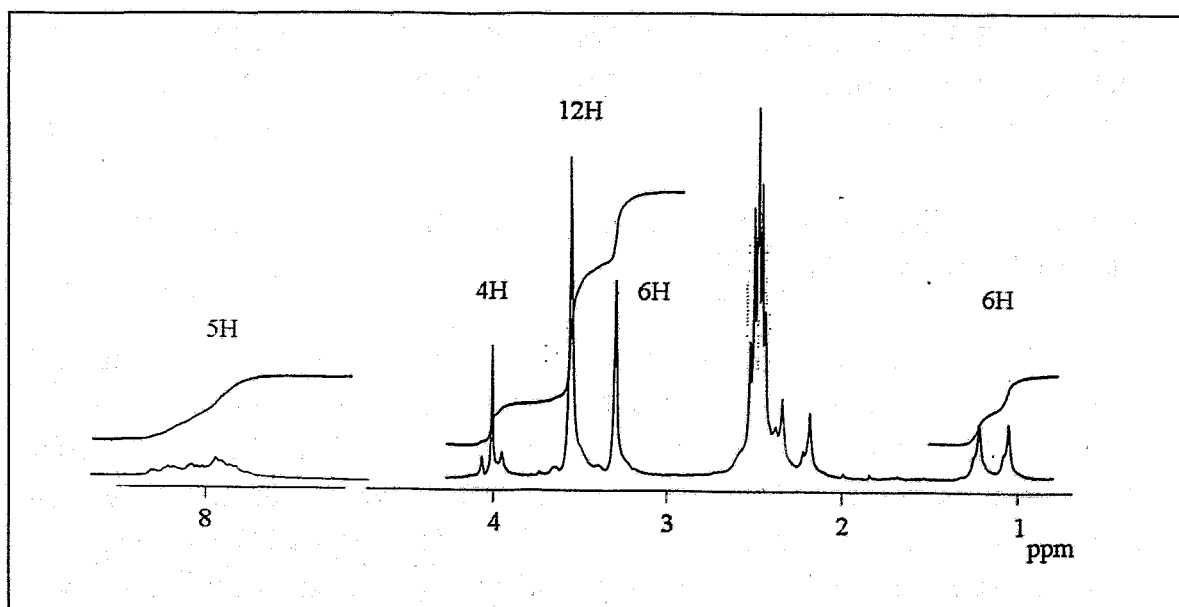
Fig. 3: ^{1}H NMR spectrum of **B** in DMSO-D$_6$

Alternatively, a nucleophilic attack by the free triphenylphosphine ligand on the nitrido group could be assumed. Such a reaction has been observed between an Re(V)nitrido compound and triphenylphosphine [1]. However the concomitant ν(N-P) vibration at 1134 cm^{-1} was not found for the complex under investigation.

References

[1] Winckler Tsang, B. et al., Inorg. Chim. Acta **211** (1993) 23

26. TECHNETIUM(V) COMPLEX WITH MESO-2,3-DIMERCAPTOSUCCINIC ACID MONOHEXYLESTER FOR ARTERIOSCLEROTIC PLAQUE ACCUMULATION

B. Noll, H.-J. Pietzsch, H. Spies, L. Dinkelborg[1], B. Johannsen, W. Semmler[1]
[1]Institut für Diagnostikforschung Berlin

Proceeding from the assumption that the presence of a carboxylic group and a longer alkyl chain in the ligand molecule of complexes fulfil the requirements of arteriosclerotic plaque accumulation, the complexation reaction of 2,3-dimercaptosuccinic acid (DMSA) mono-hexyl ester with technetium and the biodistribution of the resulting product were investigated. Since DMSA forms stereoisomers of a 2:1 Tc^VO complex $[TcO(DMSA)_2]^-$ with sulphur coordination and four unbounded carboxylic groups [1], a corresponding Tc(V) complex with two lipophilic alkyl ester groups is expected when the monoester of DMSA containing a lipophilic alcohol is used as ligand.

The Tc^VO complex with 2,3-dimercaptosuccinic acid monohexylester was tested for its ability to be accumulated in arteriosclerotic plaques.

Synthesis involves conversion of meso-DMSA into its anhydride by acetyl chloride and subsequent reaction with n-hexanol.
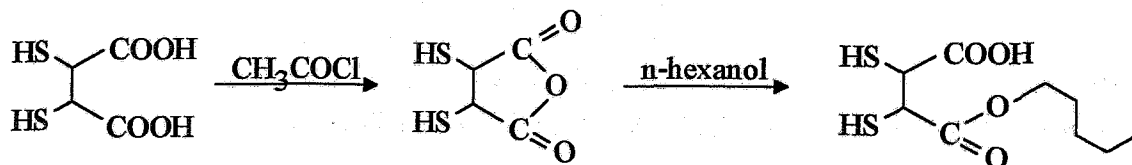
Experimental

2,3-dimercaptosuccinic acid anhydride:

1 g 2.3-dimercaptosuccinic acid (DMSA) is suspended in 250 ml acetylchloride and refluxed for 16 hours. Over this period the acid dissolves. Subsequent evaporation of acetylchloride and lyophilization of the yellow residue gives the crude product.

2.3-dimercaptosuccinic acid monohexylester:

1 g of the crude 2.3-dimercaptosuccinic acid anhydride is suspended in 40 ml n-hexanol. The reaction mixture is heated at 100 - 110 °C for 4 hours while stirring vigorously.

Over this period the product dissolves. After standing overnight the solvent is evaporated in vacuo. The residual oil is treated with n-heptane. As a result a white wax product is obtained. After washing with n-heptane the substance is dried in vacuo.

Yield: 30 % related to DMSA

Elemental analysis (Calc./Found, %): C 45,1/45,6; H 6,8/6,9; S 24,1/24,2

^{1}H NMR (chloroform):
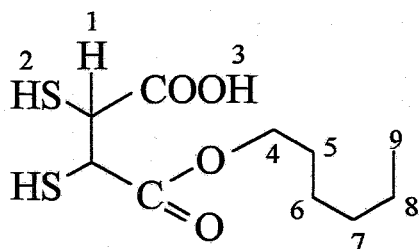
1	3,6 ppm (2H)
2	2,4 ppm (2H)
3	10,6 ppm (1H)
4	4,2 ppm (2H)
5	1,7 ppm (2H)
6-8	1,3 ppm (6H)
9	0,9 ppp (3H)

Complex formation with technetium(V) at c.a. level

Complexes were prepared at $1,3 \times 10^{-4}$ M by ligand exchange reactions starting from the Tc(V) gluconate precursors with varying molar ratios ligand / Tc in the range from 1:1 to 10:1. Thin layer chromatography, electrophoresis and UV/VIS spectroscopy were used to investigate the complexation and to characterize the products in solution.

Ligand exchange reaction with technetium(V) gluconate at n.c.a. level

1 mg monohexyl ester of DMSA dissolved in 100 μl ethanol is added to 2 ml ^{99m}Tc gluconate prepared according to [3]. After 15 min. the reaction mixture is ready for injection.

Biodistribution of ^{99m}Tc DMSA monohexylester

Biodistribution and elimination were investigated in mice. 74 kBq of the complexes were intravenously injected into mice. The animals were sacrificed after 0.5, 1, 3 and 5 h. The percentage of the injected dose (% ID) as well as the percentage of the injected dose per gram of tissue (% ID/g) were determined. Accumulation in ateriosclerotic lesions was determined in aortae derived from WHHL rabbits. 74 MBq of the complexes were intravenously injected into WHHL rabbits. 5 h later the rabbits were sacrificed, the aorta removed and a sudan-III-staining as well as an autoradiography were performed.

Results and discussion

Ligand exchange of Tc(V) gluconate with an excess of 2.3-dimercaptosuccinic acid monohexyl ester gives two products with a ligand/Tc ratio of 2:1 having an absorption maximum in the UV/VIS spectrum at 420 nm ($\varepsilon = 2680$ l/mol·cm). With a molar ratio of 1:1 about 50 % of the Tc gluconate complex ($R_f = 0$) was found because of an incomplete exchange. The occurrence of two components separated by TLC (silicagel//ethanol/water 95:5 (Fig. 1)) may be explained by the formation of isomeric forms. Isomers are expected to be either cis-trans forms regarding the position of the ester groups or stereoisomers, as observed earlier for Tc complexes with DMSA and its ester [1]

101

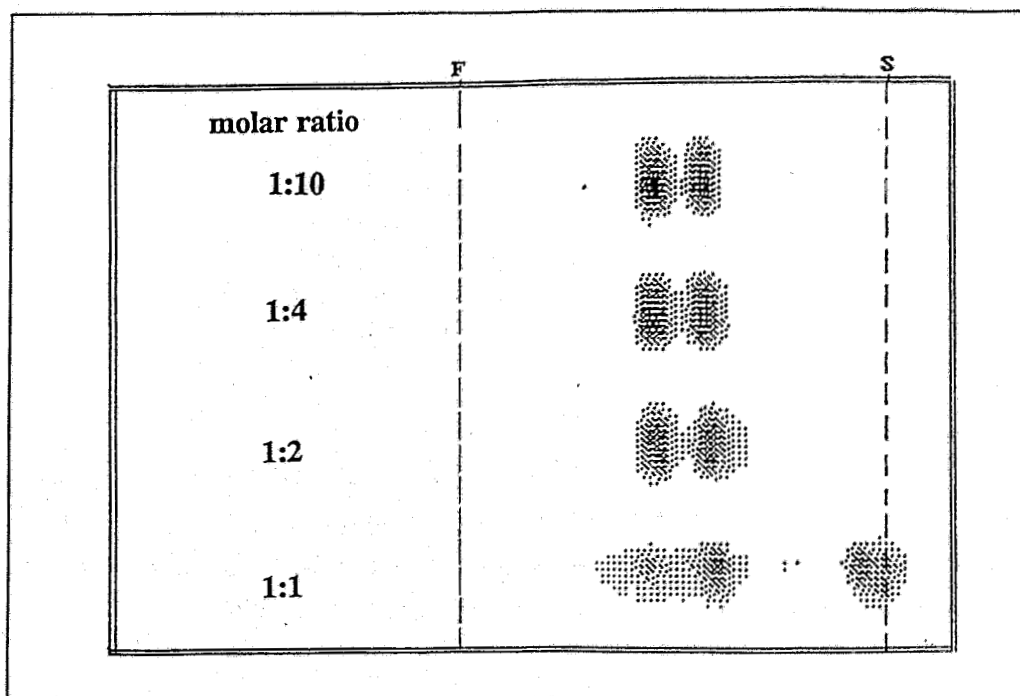There is no difference in composition between the complexes prepared at c.a. and n.c.a. level.

Fig.1: Separation of the reaction mixtures of ligand exchange Tc-gluconate / DMSA monohexyl ester for various molar ratios, by thin layer chromatography on silica gel(Kieselgel 60/Merck) and ethanol/water 95/5 (v/v) as the eluent.

The ^{99m}Tc tracer is poorly eliminated via the kidneys (5 h p.i.: 3 % ID). 5 h p.i. accumulation in the liver (5 h p.i.: 32 % ID) and in the intestines (5 h p.i.: 24 % ID) is high. The ratio of accumulation of the DMSA monohexylester between the arteriosclerotic lesions and normal vessel walls was > 10, as estimated by autoradiography. The total amount of Tc-99m-DMSA monohexylester in the arteriosclerotic lesions was not significantly higher than it was with our alternative tracer candidates, such as the Tc-N-alkyl-MAG$_n$ complexes [4].

References
[1] Spies, H. et al., Inorg.Chim.Acta **116** (1986) 1
[2] Johannsen, B. et al., Radiobol.Radiother. **20** (1979) 356
[3] Noll, B. et al., ZFK-739 (1990) 36
[4] Noll, B. et al., this report, p. 53

27. ESTER-BEARING OXORHENIUM(V) COMPLEXES – SYNTHESIS, CHARACTERIZATION AND REACTIONS

H. Spies, Th. Fietz, H.-J. Pietzsch, D. Scheller[1]
[1] Technische Universität Dresden; Institut für Analytische Chemie

Introduction

The biodistribution of Tc/Re tracers may be influenced by built-in ester groups provided the ester is capable of being cleaved enzymatically in vivo [1]. It is therefore necessary to carry out studies on enzymatic cleavage in order to enlarge our rather limited knowledge of the conditions and structural requirements essential for cleavage of this special type of compounds, where the ester groups are linked to metal complexes.

This article describes the preparation and characterization of a series of rhenium complexes as substrates for hydrolysis experiments with esterases. The neutral oxorhenium (V) compounds contain mercaptoacetic $\underline{1}$ and thiomalic acid esters $\underline{2}$ as constituents. The alcohol component is systematically altered from C_1 to C_6.

$\underline{1a}$	R= C_2H_5
$\underline{1b}$	R= $n\text{-}C_3H_7$
$\underline{1c}$	R= $i\text{-}C_3H_7$
$\underline{1d}$	R= $n\text{-}C_4H_9$
$\underline{1e}$	R= $sec\text{-}C_4H_9$
$\underline{1f}$	R= $i\text{-}C_4H_9$
$\underline{1g}$	R= $n\text{-}C_5H_{11}$
$\underline{1h}$	R= $n\text{-}C_6H_{13}$
$\underline{1i}$	R= H
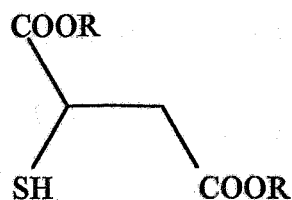
$\underline{2a}$	R=CH_3
$\underline{2b}$	R=C_2H_5

Experimental

(3-Thiapentane-1.5-dithiolato)[(ethoxycarbonyl)methanethiolato]oxorhenium(V) $\underline{3a}$:

28.8 mg (186 μmol) "H_2S_3" and 22.4 mg (186 μmol) $\underline{1a}$ are mixed in about 1 mL acetonitrile and added to a cooled (0°C) and stirred solution of 100 mg (186 μmol) [NBzEt$_3$][ReOCl$_4$] in 1 mL acetonitrile. Then one drop of triethylamine is added to the reaction mixture. The colour of the mixture turns dark brown. Some insoluble by-products are deposited. After further two hours of stirring, the solvent is completely removed and the raw product dissolved in a small volume of heated chloroform. The insoluble residue is re-

103

moved and the solution purified by column chromatography (silica gel, chloroform). On reducing the solvent to a small volume, 50 mg (57 %) of the pure product is obtained.

In the same way the compounds **3b-3i**, **6a** and **6b**. are obtained in yields from 30 to 55 %.

(3-Thiapentane-1.5-dithiolato)[(N-morpholinocarbonyl)methanethiolato]oxorhenium(V) **5**:
100 mg **3a** is dissolved in 5 mL chloroform, 10 drops of morpholine are added and the mixture is refluxed for 15 hours. The product is purified by preparative thin-layer chromatography using silica gel and chloroform/ethanol 3:1. The yield of the pure compound was 33 mg (35 %).

Results and discussion

The ester complexes **3a-3h** as well as **3i**, which contains mercaptoacetic acid, were obtained as analytically pure solids by reacting tetrachloro-oxorhenate(V) with bis(2-mercaptoethyl)sulphide ($HS-CH_2-CH_2-S-CH_2-CH_2-SH$; "$H_2S_3$") and the respective mercaptoacetic acid ester **1**. When using bis(2-mercaptoethyl)ether ($HS-CH_2-CH_2-O-CH_2-CH_2-SH$; "$H_2SOS$") and **1**, the corresponding complexes **4a** and **4b** are formed. However, attempts to isolate the latter compounds in crystalline form have failed up to now.
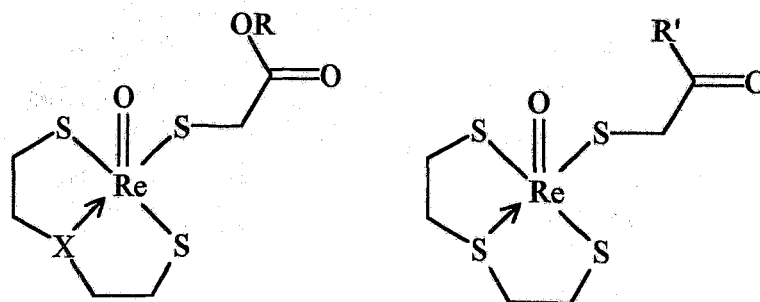

3a-3i X=S   **5**   R' = N-morpholino
4a, **4b** X=O
(For nomenclature of R see **1a-1i**)

For examination of the reactivity of the ester function, mainly to establish the possibility of coupling the chelate to the amino group of biomolecules, we tried to convert the compounds into amides. For this purpose, we added an excess of morpholine to a solution of complex **3a** in chloroform and left it at room temperature for a few days. When thin layer chromatography (chloroform/ethanol 3:1 v/v) showed insignificant changes of the ester complex, the mixture was refluxed. After a few hours no more **3a** was detectable by TLC. The morpholide **5** was purified by preparative TLC (chloroform/ethanol 3:1 v/v) to give light brown plates. Refluxing oily **4a** with morpholine resulted in decomposition of the complex.

104
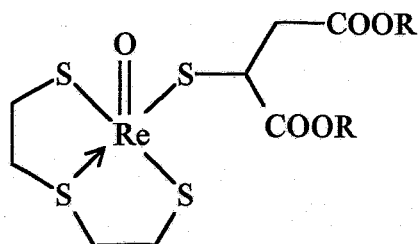
6a	R = CH$_3$
6b	R = C$_2$H$_5$
6c	R = H

A second group of complexes **6** derives from thiomalic acid. The esters **2a** and **2b** were synthesized by bubbling dry HCl into solutions of the diacid in the respective alcohol and purified by vacuum distillation (**2a**: b.p.$_8$: 97 °C; **2b**: b.p.$_3$: 95 - 100 °C). Reactions of the esters with "H$_2$S$_3$" and ReOCl$_4^-$ give the products **6a** and **6b** which were purified by column chromatography with chloroform. Compared with **3a**, **6b** shows a significantly lower R$_f$ value due to its increased polarity. The diacid complex **6c** was eluated from the column by water. It has not yet been possible to crystallize this compound, but it can be used as a standard in saponification experiments.

Table 1: List of compounds and selected analytical data. All compounds listed in Table 1 have satisfactory elemental analysis.

Compound Nr.	formula	molar weight [g/mol]	m.p. [°C]	Re=O band in IR spectra [cm^{-1}]	C=O band in IR spectra [cm^{-1}]
3a	C$_8$H$_{15}$O$_3$ReS$_4$	473.65	148-150	960	1728
3b	C$_9$H$_{17}$O$_3$ReS$_4$	487.68	131-134	960	1720
3c	C$_9$H$_{17}$O$_3$ReS$_4$	487.68	114-117	960	1724
3d	C$_{10}$H$_{19}$O$_3$ReS$_4$	501.71	106-110	960	1720
3e	C$_{10}$H$_{19}$O$_3$ReS$_4$	501.71	118-121	960	1716
3f	C$_{10}$H$_{19}$O$_3$ReS$_4$	501.71	117-119	960	1720
3g	C$_{11}$H$_{21}$O$_3$ReS$_4$	515.73	94-96	960	1728
3h	C$_{12}$H$_{23}$O$_3$ReS$_4$	529.76	81-83	960	1724
3i	C$_6$H$_{11}$O$_3$ReS$_4$	445.60	147-149	964	1724
5	C$_{10}$H$_{18}$NO$_3$ReS$_4$	514.70	185-188	968	1636
6a	C$_{10}$H$_{17}$O$_5$ReS$_4$	531.70	181-185	964	1724
6b	C$_{12}$H$_{21}$O$_5$ReS$_4$	559.74	127-130	960	1724

The compounds **3a**-**3i**, **6a** and **6b** show very similar spectroscopical properties. Their UV/VIS spectra in acetonitrile exhibit four peaks between 498···504 nm (log ε = 2.1···2.3), 372···375 nm (log ε = 3.4···3.6), 258···262 nm (log ε = 3.8···3.9) and 228···230 nm (log ε= 4.0···4.2). In the spectrum of **5** in acetonitrile, only two peaks are visable at 502 nm (log ε = 2.2) and 378 nm (log ε = 3.5), whereas the other two bands are transformed into shoulders.

The ^{1}H NMR spectra of **3a** and **6b** have been recorded in CD_3CN. **3a** exhibits values for the protons of the tridentate ligand which are comparable to those of other "3+1" complexes: 1.98···2.05 ppm (2 H); 3.11···3.19 ppm (2 H); 3.93···3.97 ppm (2 H); and 4.28···4.33 ppm (2 H). The methyl group of the ester function is depicted at 1.27···1.30 ppm; the ester's methylene protons at 4.21···4.23 ppm (2 H) and the methylene protons of the mercaptoacetic acid at 3.76 ppm (s, 2 H).

The proton signals of the tridentate ligand in **6b** are exhibited at 1.85···2.25 ppm (2 H), among two large assemblies of signals between 2.80 and 3.40 ppm and 3.82 and 4.45 ppm, respectively; each accompanied with signals of the co-ligand's protons. The methyl protons of the two ester groups are seen at 1.16···1.35 ppm (triplet of doublets, 6 H) whereas the single proton near the sulphur atom of the co-ligand is depicted at 5.3···5.51 ppm (q; 1 H). The methylene protons of the ester functions are accompanied with signals of the tridentate ligand between 3.82 and 4.45 ppm; whereas the methylene protons of the thiomalic acid are very closed to another signal group of the tridentate ligand between 2.80 and 3.40 ppm.

References
[1] R. Syhre et al., FZR 93 - 12 (1993) 61

28. HYDROLYSIS STUDIES OF ESTER SUBSTITUTED OXORHENIUM(V) COMPLEXES

S. Seifert, R. Syhre, Th. Fietz, H. Spies

In connection with our work on technetium and rhenium tracers with metabolizable ester functions [1], preliminary studies were carried out preparatory to the proposed investigations into enzymatic cleavage of ester groups in Tc and Re chelates. This includes installation of an HPLC system suitable for evaluating the cleavage reaction and characterizing the

reaction products, chemical saponification experiments, and elaboration of a procedure for measuring enzymatic cleavage of the proposed chelate-bound ester groups. The compounds used (1-9) are neutral oxorhenium(V) complexes with tridentate/monodentate sulphur donor ligand coordination, having metabolizable ester functions at the monodentate ligand; they are listed alongside the structure of the complexes.
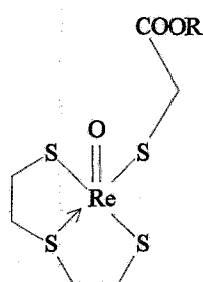
COOR Tridentate ligand: bis(2-mercaptoethyl)sulphide

$(HS-CH_2-CH_2-S-CH_2-CH_2-SH; "HS_3H")$

Monodentate ligand: mercaptoacetic acid (1) or its esters R (2)-(9)

$R = C_2H_5$ (2), n-C_3H_7 (3), i-C_3H_7 (4), n-C_4H_9 (5),
sec-C_4H_9 (6), i-C_4H_9 (7), n-C_5H_{11} (8), n-C_6H_{13} (9)

Experiments

The Re complexes were prepared by ligand exchange reaction starting with tetrachloro-oxo-rhenate(V) as described in [2].

For characterization by HPLC 1 - 2 mg of the pure complexes containing various ester groups were dissolved in 0.5 ml acetonitrile. The HPLC analyses were carried out with a PRP-1 column (Hamilton, 150 x 4.1 mm) using an isocratic mixture (A/B = 30/70) of 0.1 % trifluoroacetic acid in water (A) and 0.1 % trifluoroacetic acid in acetonitrile (B). The effluent from the column (flow rate 2 ml/min) was monitored by UV absorbance at 370 nm. For hydrolysis studies the pH of the samples was adjusted to 12 by adding 0.1 N NaOH.

To determine whether or not the ester bond in the Re complexes was susceptible to cleavage by esterases, we carried out incubation experiments with blood plasma of rats and humans, diluted 50/50 with phosphate buffer of pH 7.4, and pig liver esterase dissolved in the same buffer. 0.05 ml of the complex solution was generally added to 0.45 ml of the esterase-containing samples. The complexes were incubated at 37 °C for 10 - 120 minutes. After incubation the samples were filtered through a 0.22 μm cellulose acetate filter and analysed by HPLC.

Results and discussion

Fig. 1 shows chromatograms of (2) and the corresponding complex with mercaptoacetic acid (1) as the monodentate ligand This complex was obtained by direct preparation as well as hydrolysation in alkaline solution. For complete hydrolysation of the ester-group-containing ligand the solution has to be heated for several hours. For instance, at least 48 h at pH 12 and room temperature are required in order to convert about 50 % of (2) to (1).
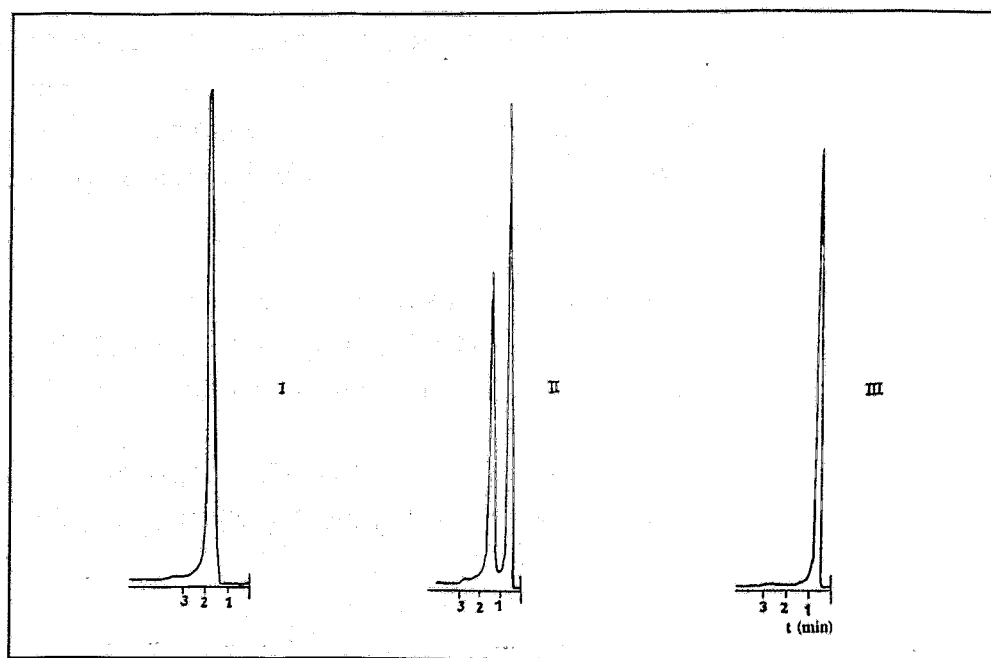
Fig. 1: HPLC chromatograms of (2) (I), a hydrolysation mixture
(48 h, pH 12, 22 °C) (II) and (1) (III)

The retention times of the various complexes parallel their lipophilicity on account of the
greater chain lengths of the ester groups (Table 1).

Table 1: R_t-values of the Re complexes as a function of the length of the alkyl residues

Re complex	R_t-value [min]
(1)	1.7
(2)	2.1
(3)	2.8
(4)	3.3
(5)	3.7
(6)	3.6
(7)	4.8
(8)	8.2
(9)	13.6

It is remarkable that complexes with n-alkyl groups are eluted faster than complexes containing the corresponding iso-alkyl residues. This behaviour could be caused by the steric configuration of the alkyl groups in the ester molecule and by their interaction with the col-

108

umn material. Whether the increasing retention time does, in fact, correlate with the lipophilicity of the compounds remains to be proved.

The enzymatic hydrolysis of the monodentate ligand was investigated using the ethyl, n-propyl, and n-butyl esters of mercaptoacetic acid. In rat plasma the cleavage of all ester complexes proceeds quickly. After five minutes of incubation the esters are quantitatively hydrolysed. In human plasma solutions, on the other hand, the complexes differ in their hydrolysis behaviour. The ethyl ester complex is only partially hydrolysed (~40 %) after two hours' incubation time, while a complete cleavage is observed for the propyl and butyl ester complexes as shown in Fig. 2.
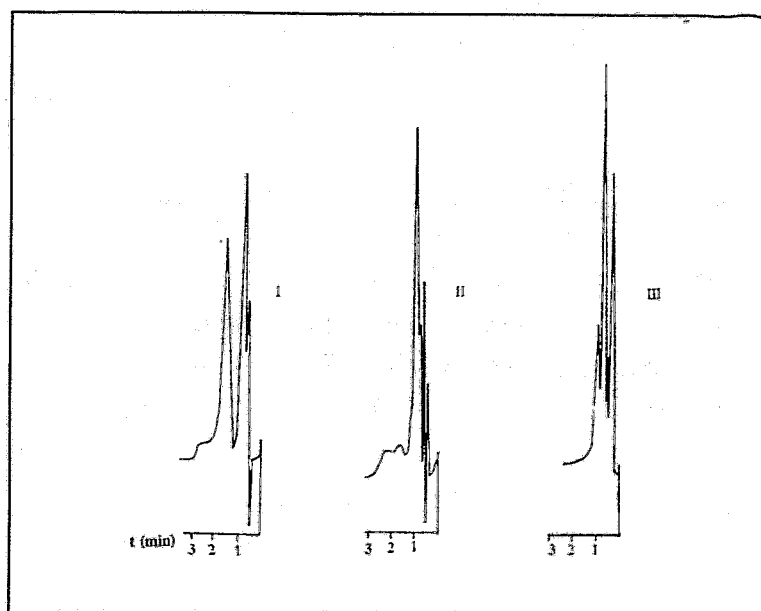
Fig. 2: HPLC chromatograms of the ethyl (I), n-propyl (II), and n-butyl (III) ester complexes after incubation in human plasma (phosphate buffer pH 7.4, 37 °C, 2 h)

Differences in hydrolysis are also observed after incubation with pig liver esterase (Fig. 3). While two hours after incubation all three ester complexes are quantitatively hydrolyzed, the HPLC chromatograms after 10 minutes still show portions of the ethyl and butyl ester complexes.

In summary, one can say that the investigated complexes with one ester group at the monodentate mercaptoacetic acid ligand are hydrolysed by the above-mentioned enzymes. Differences in the kinetics of the enzymatic hydrolyses studied in rat plasma, human plasma and pig liver esterase point to species-related differences between the enzyme systems used.
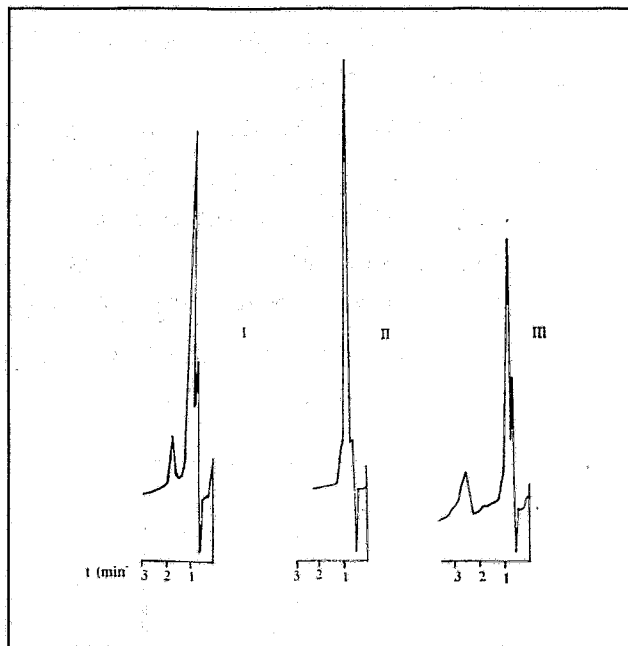
Fig. 3: HPLC chromatograms of ethyl (I), n-propyl (II), and n-butyl (III) ester
complexes after incubation with pig liver esterase
(phosphate buffer pH 7.4, 37 °C, 10 min)

References

[1] Syhre, R. et al., FZR 93 - 12 (1993) 61

[2] Fietz, Th. et al., this report, p. 103

29. THE LABELLING YIELD OF THE TECHNETIUM-MAG3 AS A FUNCTION OF THE CONTENT OF MERCAPTOACETYL TRIGLYCINE DISULPHIDE IN THE MAG3 KIT

B. Noll, St. Noll, B. Grosse, K. Landrock, A. Teich, H. Spies, B. Johannsen
O. Muth[1], K. Jantsch[1]
[1]Verein für Kernverfahrenstechnik und Analytik

Technetium-99m mercaptoacetyl triglycine (^{99m}Tc-MAG3) has been used extensively as a renal function agent for several years. The commercial available kit prepared in Rossendorf is based on S-unprotected mercaptoacetyl triglycine. The use of S-unprotected ligand makes it possible to avoid heating the radiopharmaceutical preparation during the labelling procedure [1]. However, sulphhydryl group in MAG3 may be oxidized by air during storage to give MAG3 disulphide. The presence of MAG3 disulphide may effect the quality of the re-

110

nal function agent, e.g. by decreasing the amount of stannous (II) chloride which acts as a reducing agent in the kit. For evaluation of the ^{99m}Tc-MAG$_3$ kit several impurities have to be taken into consideration:

- ^{99m}Tc tartrate which serves as the precursor of the ^{99m}Tc-MAG$_3$ complex in the kit formulation,
- Pertechnetate caused by incomplete reduction of the ^{99m}Tc generator eluate due to a decrease of the amount of stannous (II) chloride by oxidants like MAG$_3$ disulphide and
- Tc-MAG$_3$ complexes containing two or more ligands per technetium [Tc-(MAG$_3$)$_n$]. Their content depends on the reaction time, the pH value and the total amount of MAG$_3$ ligand [2].

The quality of the labelling product - the content of the desired Tc-MAG$_3$ complex should be greater than 90 % and it should be free from pertechnetate - will also depend on the purity of the MAG$_3$ ligand. The occurrence of pertechnetate may be due to the presence of MAG$_3$ disulphide. We therefore studied the influence of MAG$_3$ disulphide on the labelling yield and the formation of by-products in commercial kits.

The kit preparations were carried out at the kit production facility. The content of MAG$_3$ disulphide in MAG$_3$ ligand used was determined by polarography and HPLC. The radiochemical purity of the radiopharmaceutical preparations was determined by TLC on silica gel // ethanol/water 95/5 and by HPLC on RP18 column with phosphate buffer pH 5.85 // methanol 85/15 as the eluent.

Labelling procedure

A volume of 2 ml generator eluate was added to the kit vial containing a lyophilized mixture of 0.2 mg MAG$_3$, 22 mg sodium tartrate, 60 μg SnCl$_2$·2H$_2$O and 1.6 mg NaOH. After 10 minutes 2 ml isotonic sodium phosphate buffer solution, pH 7.4, was added to neutralize the solution.

The labelling yields and the contents of all radiochemical impurities of several kit series containing different amounts of MAG$_3$ disulphide are shown in Table 1. The radiochemical impurities found in the ^{99m}Tc-MAG$_3$ preparations are the ^{99m}Tc-(MAG$_3$)$_n$ (n > 1) and free pertechnetate/^{99m}Tc tartrate. ^{99m}Tc tartrate cannot be differentiated from pertechnetate either by TLC or by HPLC [2]

As shown in Table 1, there is no strong correlation beween the content of MAG$_3$ disulphide and the labelling yield. If the kit contains more than 40 % disulphide the amount of MAG$_3$ ligand is too small for a complete conversion of ^{99m}Tc tartrate into ^{99m}Tc-MAG$_3$.

The occurrence of ^{99m}Tc tartrate/pertechnetate in series 4 and 5 cannot be due to MAG3 disulphide because its content is low. More likely, the decrease in the content of stannous (II) chloride in the kits was caused by air being present during manufacture of the kit formulation.

Generally, it must be said that a high content of MAG3 disulphide decreases the labelling yield, while a low content of MAG3 disulphide (< 15 %) does not significantly influence the labelling yield of ^{99m}Tc-MAG3.

References

[1] Noll, B., EP 0427360 (1990)
[2] Noll, B. et al., Appl. Radiat. Isot.43 (1992) 899

30. AN EFFICIENT HPLC-METHOD FOR DETERMINATION OF THE CHEMICAL PURITY OF HM-PAO LIGAND AND KIT PREPARATIONS

S. Seifert, F. Schneider

^{99m}Tc-d,l HMPAO intravenous injection is used for regional cerebral blood flow scintigraphy. Commercially available kits (Ceretec, Neurospect) contain 0.5 mg of the ligand (RR,SS)-4,8-diaza-3,6,6,9-tetramethylundecane-2,10-dione bisoxime (d,l HM-PAO) per vial. The synthesis of the ligand HM-PAO results in a mixture of diastereoisomers, which are separated by repeated recrystallization from acetic acid ethyl ester.

Unlike Tc-d,l HM-PAO, the Tc complex with the stereoisomeric *meso* HM-PAO is weakly accumulated in the brain and the retention time is shorter [1]. A high stereochemical purity of d,l HM-PAO is therefore needed to ensure high quality kit preparations. The stereochemical purity of the samples of d,l HM-PAO obtained by recrystallization has to be determined quickly and reliably. HPLC analysis represents a suitable procedure as an alternative method to ^{13}C NMR analysis, which is also used for quality control. An HPLC procedure was previously developed [2], but no separation conditions have been reported.

We obtained good separation results using a normal phase NH$_2$-modified silica gel column (LiChrospher NH$_2$) and gradient elution with a mixture of isopropanol and hexane.

Separation conditions:

Column:	LiChrospher NH$_2$ (250 x 4 mm)
Eluant :	Isopropanol (A)/hexane (B), gradient -4
	10 min from 0 to 20 % A
	10 min 20 % A
	5 min 100 % A

Flow rate: 1.0 ml/min
UV detection at 210 nm

Fig. 1 shows the HPLC patterns of *meso* and *d,l* HM-PAO as well as a mixture of both. The separation allows a quantitative determination of the isomer composition of the fractions obtained by repeated recrystallization. A comparison of HPLC and ^{13}C NMR analyses of three samples of HM-PAO demonstrates good conformity of the results   (Table 1).
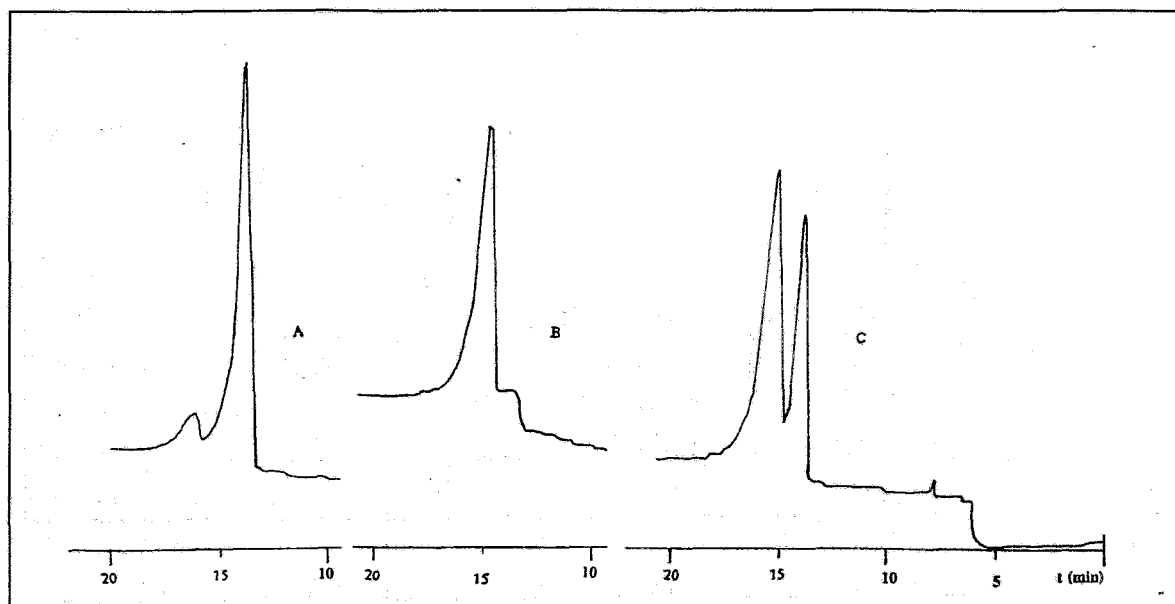

Fig. 1: HPLC chromatograms of *meso* (A), *d,l* (B) and a mixture (C) of HM-PAO

Table 1: Comparison of HPLC and ^{13}C NMR analyses for determination of d,l HM-PAO content [%] of various samples

Sample	HPLC	^{13}C NMR
1	76.1	78.0
2	77.5	79.4
3	64.6	66.4

The HPLC procedure makes it possible to determine the content of *d,l* HM-PAO of a kit vial. We now use this method for routine quality control of HM-PAO. In the case of our Neurospect preparations a ligand containing 94 % *d,l* HM-PAO was used. After lyophilization the same yield was found by dissolving the contents of the vial in 200 μl methanol, filtering the solution through a 0.22 μm cellulose acetate filter and performing HPLC analyses. This shows that the ligand does not change its isomeric composition. A comparison

with Ceretec kits from Amersham showed no difference in the quality of the HM-PAO ligand (Fig. 2).

In order to obtain a radiopharmaceutical with a high degree of accumulation in the brain, it is recommended that more than 90% of the HM-PAO ligand used for kit formulation be in the d,l form.
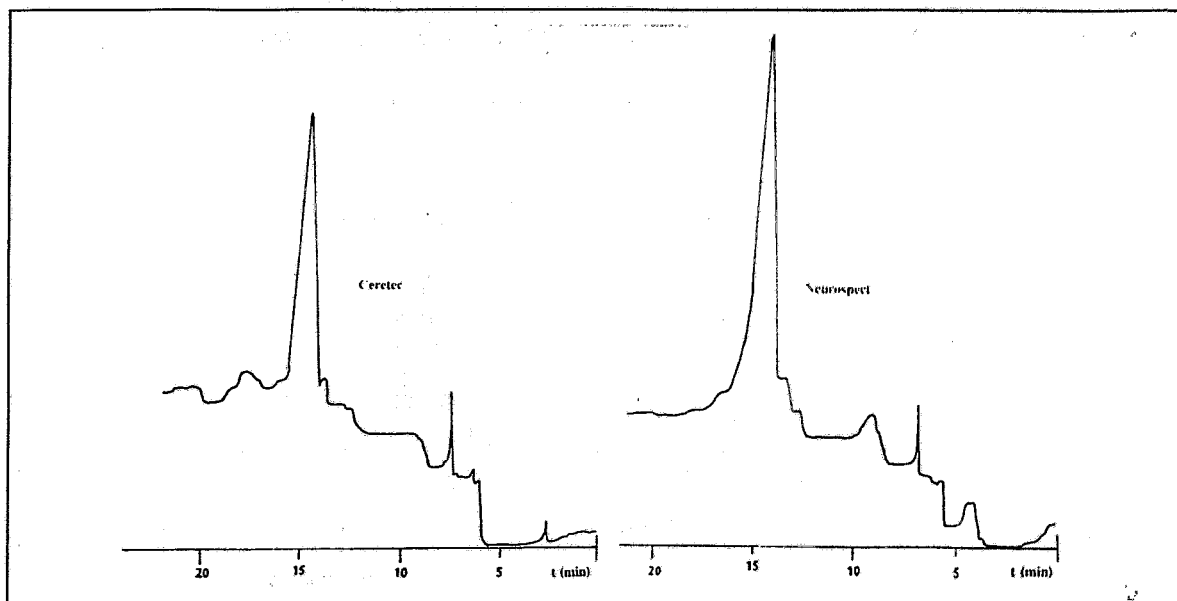

Fig. 2: HPLC analyses of the *d,l* HM-PAO content of Ceretec and Neurospect kit vials

References

[1] Gruner, K. R., Der Nuklearmediziner **5** (1986) 297
[2] Neirinckx, R. D. et al., J. Nucl. Med. **28** (1987) 191

31. POLAROGRAPHIC DETERMINATION OF TIN(II) IN HMPAO KITS

I. Hoffmann

Stannous chloride is an essential constituent in kits for preparation of ^{99m}Tc-HMPAO. Its content is very low. Each kit vial contains 5....7.6 μg stannous chloride. Because the quality of the radiopharmaceutical depends very much on the availability of "effective" stannous ions, a sensitive method is needed for selective determination of Sn(II) as distinct from Sn(IV). While general methods are available to determine the total of the stannous and stannic content, electrochemical methods are preferred because they make it possible to discriminate between the oxidized and reduced forms.

The article describes the determination of Sn(II) in the presence of Sn(IV) at low concentrations by DC polarography.

Experimental

Chemicals

Supporting electrolyte: phosphate buffer (Sörensen) pH = 7.7

For standard addition: 0.007 M solution of $SnCl_2 \cdot 2H_2O$ (p.a.) in 0.1 M HCl

HMPAO kits of varying Sn(II) content

All solutions were deoxygenated by argon (99.998 %).

Apparatus

DC/AC polarograph (GWP 673, ZWG Berlin)

Results and discussion

The half-wave potential of the Sn(II) reduction step depends on pH. In phosphate buffer (Sörensen) pH = 7.7 this potential was found at -750 mV vs. SCE. No influence of HMPAO can be observed because the half-wave potential of Sn(II)/Sn(0) is much more negative than that of HMPAO reduction. The Sn(II) content was determined by measuring the diffusion current. The proportionality of the Sn(II) concentration (concentration range from 10^{-6} M to 10^{-4} M) and the diffusion current was proved experimentally. At this low concentration it is especially important to work in the absence of any traces of oxygen.

For analysis about 5 ml of buffer solution are filled into the polarographic cell, and oxygen is removed with argon. The base line is recorded in the potential range from -400 to -1200 mV vs. SCE. The solution is bubbled with argon until no reduction wave of dissolved oxygen can be observed. 4 ml of this solution are injected into the kit. After solution of the substance 3.5 ml are transfered into the cell. Traces of oxygen are removed with argon, and the polarogram is recorded in the same potential range. By compensation of the load current the diffusion current of Sn(II) was made independent of potential. The Sn(II) content is determined by addition of small portions of Sn(II) standard solution (see Fig. 1).The Sn(II) content of the standard solution was determined iodometrically.

The results are summarized in Table 1. The $SnCl_2$ content of about 2.5 μg can be determined with an error of $\pm$ 10 %. The detection limit for the Sn(II) content was found to be about 0.2 μg/kit. The kits A, B, C contain additional Sn(II). The experimentally determined $SnCl_2$ content is about 5 μg lower than the original value at a concentration of 7.6 μg and higher (samples A, B, C and 1-9). With smaller original amounts of $SnCl_2$ (5 and 3.8 μg) the losses of Sn(II) are lower, as shown by Table 1. It can be assumed that the differences in content of Sn(II) are caused by oxidation during preparation of the kit. At this low concentration an additional small decrease can be observed during repeated measurements because Sn(II) is reduced at the dropping mercury electrode.
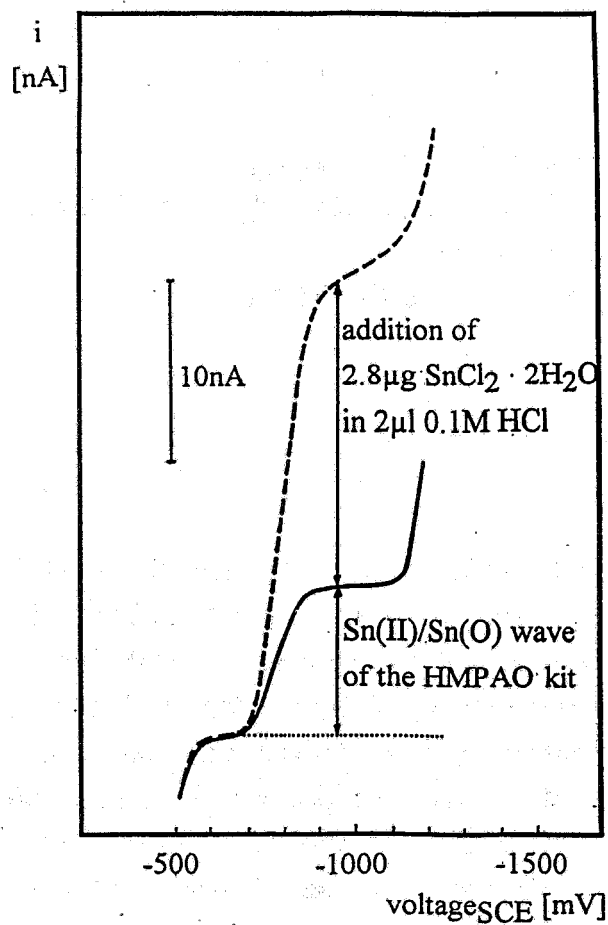
Fig. 1: DC polarogram of the reduction wave of Sn(II) in HMPAO kit (——) and after addition of Sn(II)-standard solution (-----) ($c_{Sn(II)} = 5 \times 10^{-6}$ M in phosphate buffer (Sörensen) pH = 7.7)

Table 1: Theoretical and polarographically determined Sn(II)-content in various vials of 7.6, 5.0, 3.8 μg batches (1-11) and of additional Sn(II) (A, B, C)

Preparation	Sn(II) content [μg SnCl$_2$ · 2 H$_2$O]	
	theoretical	polarographically determined
Kit A	17.6	12.6
Kit B	26.6	21.6
Kit C	45.6	41.5
Kit 1	7.6	2.5
Kit 2	7.6	2.6
Kit 3	7.6	2.6
Kit 4	7.6	2.5
Kit 5	7.6	2.3
Kit 6	7.6	2.44
Kit 7	7.6	2.44
Kit 8	7.6	2.78
Kit 9	7.6	2.44
Kit 10	5.0	1.5
Kit 11	3.8	0.85

32. ISOLATION AND CULTURE OF CELLS DERIVED FROM A BRAIN MICROVESSEL PREPARATION

S. Matys, U. Wenzel, G. Kampf [1], R. Bergmann, B. Ahlemeyer and P. Brust
[1] Dresden Technical University, University Clinics, Clinic of Nuclear Medicine

Introduction

Radiopharmaceuticals designed for studying the functions of the central nervous system have to pass the so-called "blood-brain barrier" (BBB) between the circulating blood into which the tracers are normally injected and the brain where they accumulate depending on the metabolism of the different brain cells. Morphologically, the BBB consists of brain endothelial cells which are joined together by tight intercellular junctions. In the past, information about the accumulation of radiopharmaceuticals in the brain was obtained from animal experiments, such as biodistribution studies or in vivo measurements of BBB transport. Recently, there have been attempts by several groups to study the function of the BBB in vitro [1]. The basic problem of these studies is the induction of tight junctions on cultured brain endothelial cells to obtain a high transendothelial resistance. Dehouck et al. [2] describe induction of tight junctions during co-culture of bovine brain endothelial cells with rat astrocytes. Using this model, the authors studied the transport of various pharmaceuticals and obtained a correlation between in vivo and in vitro data [3]. The present study was performed in order to establish a similar model for measurement of the BBB transport of radiopharmaceuticals. In most cases preparations of brain microvessels are used to obtain endothelial cell cultures [4 - 6]. Our method follows a similar strategy.

Materials and methods

Preparation of isolated capillaries from rat and pig brain

The experiments were undertaken in order to find the best method for isolation of brain microvessels. The experimental procedure was varied using different physiological buffers (sucrose, Krebs-Ringer salts) and medium 199 with 15 mM HEPES. Rat and pig brains were stored in ice-cooled buffer or medium 199 (Tecnomara) with 15 mM HEPES-buffer (Boehringer Mannheim). After weighing, the cortical tissue was homogenized in buffer or medium 199 in a volume 9 times greater than the initial volume of the tissue.

The tissue was homogenized using a syringe with a Luer-Lock conus and then pressed through nylon filters (SST Thal) of various pore sizes (125 μm - 225 μm).

The remaining capillaries on the filter were collected, diluted with fresh buffer or medium 199 and centrifuged at 150 x g for 5 - 10 minutes at 4 °C. The pellet was resuspended in DMEM, RPMI 1640 or medium 199 with 10 % fetal calf serum (Sigma) and seeded in plastic culture flasks (25 cm^2, Primaria, Falcon).

Fig. 1: Isolated capillaries from rat cerebral cortex (magnification 1:25).

Preparation of brain cells from rat cortical capillaries by enzymatic digestion

Isolated capillaries of rat cortex were centrifuged for 5 - 10 min at 150 x g and 4 °C and resuspended in medium 199 containing 200 U/ml penicillin, / 200 μg/ml streptomycin (Serva). The suspension was incubated at 37 °C in a shaker after addition of 1 % collagenase/dispase (Boehringer Mannheim) for 2 - 3 h. The digestion process was observed using a phase contrast microscope. The suspension was centrifuged for 5 - 10 min at 150 x g and 20 °C and the pellet was washed twice with 2 ml medium 199.

Following this, the pellet was resuspended in medium 199 with 10 % neonatal calf serum (Sigma) and 15 mM HEPES and layered onto a preformed 35 % percoll gradient (Sigma) [7] and then cautiously centrifuged for 10 min at 1000 x g and 20 °C . Two fractions were separated from the gradient, the lower band containing the brain cells was washed three times with medium 199 with neonatal calf serum (10 %). The upper band consisted of cell debris.

The mixture of brain cells was again centrifuged and resuspended in medium 199 containing 10 % fetal calf serum (Sigma), 2 ng/ml basic fibroblast growth factor (Sigma) and 100 U/ml penicillin/100 μg/ml streptomycin. The cells were seeded in 1 % gelatine (Sigma)-coated petri dishes (8 cm^2, Primaria, Falcon). Uncoated petri dishes were used as a control for cell attachment. The cell cultures were passaged weekly and examined using a phase contrast microscope. An immunohistochemical characterization of the cells with specific antibodies to detect contaminating cell types will be necessary before starting further experiments.
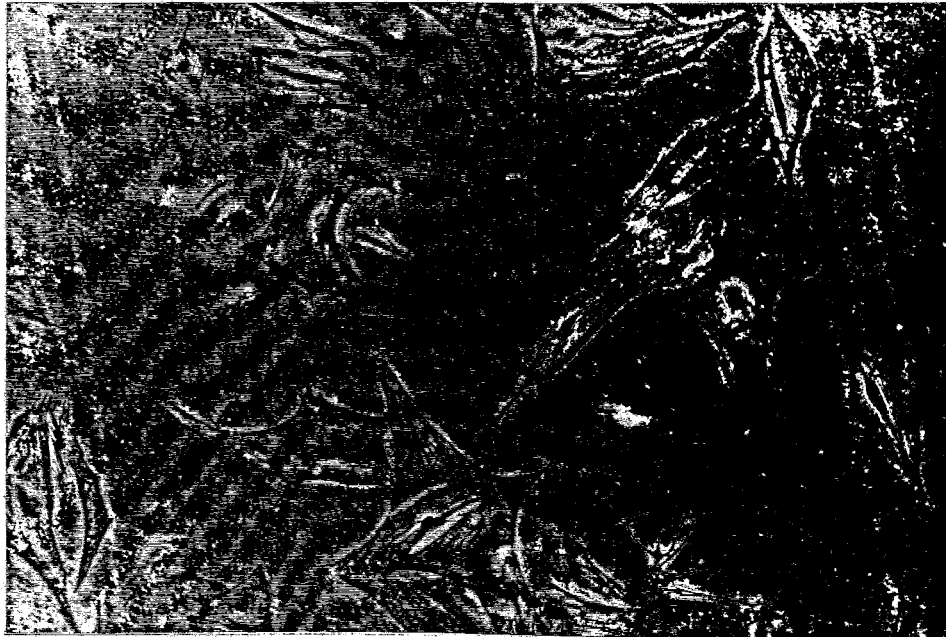
Fig. 2: Third passage of brain cells from rat cerebral cortex after 4 days in culture (magnification 1:4)

Results and discussion

In our studies the use of the percoll gradient proved to be suitable for separation of viable cells from cell debris. The best results in terms of tissue preparation and cell growth were obtained with medium 199. Coating the culture flasks with gelatine increased cell adherence and proliferation. Passage of the cell cultures was not always successful. Very low seeding densities led to a stagnation of cell proliferation. It is our intention to optimize the method of cell preparation and culture conditions, e.g. by addition of endothelial growth factor and heparin to the culture medium.

Further investigations will be aimed at growing cell cultures of pig endothelial cells with and without coculture of astrocytes and neurons to obtain an in vitro model of the blood-brain barrier.

References

[1] Joo, F., J. Neurochem. **58** (1992) 1

[2] Dehouck, M.-P. et al., J. Neurochem. **54** (1990) 1798

[3] Dehouck, M.-P. et al., J. Neurochem. **58** (1992) 1790

[4] Mischeck, U. et al., Cell Tissue Res. **256** (1989) 221

[5] Diglio, C. A. et al., Lab. Invest. **46** (1982) 554

[6] Bowman, P. D. et al., In vitro. **17** (1981) 353

[7] Gordon, E. L. et al., In Vitro Cell. Dev. Biol. **27 A** (1991) 312

33. DEVELOPMENTAL CHANGES IN ENZYMES INVOLVED IN PEPTIDE-DEGRADATION IN ISOLATED RAT BRAIN MICROVESSELS

P. Brust, A. Bech[1] and R. Bergmann

[1] University of Leipzig, Department of Biosciences

The endothelial cell layer of brain capillaries representing the blood-brain barrier (BBB) is a target for some endogenous peptides [for review see 1]. Circulating peptides interact with specific binding sites on brain endothelial cells [2,3], and the metabolism of peptides is a prerequisite for the BBB to be a regulatory interface. Several peptide-metabolizing enzymes have been detected in the cerebral microvasculature [for review see 4]. Membrane-bound peptidases may control the biological activity of peptide molecules when they contact the endothelial wall or pass through the BBB.

Recently, labelled somatostatin analogues have been used as an imaging modality for in vivo localization of somatostatin receptor-positive tumors, which were found also in the brain [5-7]. Stability against degrading enzymes is a prerequisite for these tracers to be of clinical interest.

In this study, we have measured peptidases expected to be involved in the degradation of somatostatin in the rat brain and in brain microvessels derived from the rat. Until now, it is still open whether the peptidases are equally distributed in the different cellular compartments of the brain (e.g. neurons, glial cells, endothelial cells). Therefore, we have chosen these two preparations. In addition, rats of different ages were used to find out whether developmental changes in the enzyme activities exist as has already been described for the BBB marker enzyme gamma-glutamyl-transpeptidase.

Materials and methods

Male and female Wistar rats (equally distributed) in groups of 4 different ages (6 - 8, 13 - 15, 26 - 30, 54 - 58 days) were used. Brain capillaries were isolated as described by Matys et al. (this volume). This preparation consisted primarily of capillaries but also contained minor amounts of small arterioles. The purity of each microvessel fraction was confirmed

by light microscopy and the enrichment in alkaline phosphatase and γ-glutamyl transpeptidase activities. Three different isolation procedures were performed for each group of animals. The number of brains pooled at various ages was for each experiment: 30 - 35 (days 6 - 8), 20 - 25 (days 13 - 15), 13 - 17 (days 26 - 30) and 12 at days 54 - 58.

Enzyme measurements

g-Glutamyltransferase (g-GT)

g-GT activity was measured at 25 °C, in Tris buffer (100 mmol/l) pH 8.25 with 6.0 mmol/l L-g-glutamyl-3-carboxy-4-nitroanilide as donor and glycylglycine (150 mmol/l) as acceptor. The increase in absorbance was measured continuously at 405 nm. The enzyme activities were calculated using an $e_{1=405\,nm} = 8.800$ mol^{-1} x cm^{-1}.

Alkaline phosphatase (ALP)

ALP activity was determined at 25 °C, in diethanolamine buffer (1.0 mol/l) pH 9.8 with Mg^{++} (500 mmol/l) and as substrate 10 mmol/l p-nitrophenylphosphate. The increase of absorbance was measured continuously at 420 nm. The enzyme activities were calculated using an $e_{1=420\,nm} = 17.300$ mol^{-1} x cm^{-1} of 4-nitrophenol.

Amino peptidase A (APA), amino peptidase M (APM), and dipeptidyl-dipeptidase IV (DPIV)

The different enzymes were measured using L-glutamic acid-4-methoxy-2-naphtylamide (APA), L-leucine-2-naphtylamide (APM) and glycyl-proline-4-methoxy-2-naphtylamide (DP IV), respectively, as substrate (40 mM) in phosphate buffer (100 mM, pH 7,4) for 120 to 240 min at 37 °C. After incubation (end volume 570 μl) the samples were mixed with 500 μl Fast Blue B (1 mg/ml) for 5 min at room temperature. The protein was precipitated with trichloro acetic acid (50 g/l). The same volume (1500 μl) of ethyl acetate was added to the supernatant, mixed and centrifuged. The organic phase was measured at 525 nm (d = 1 cm). The activity was calculated using standards of 4-methoxy-2-naphtylamid (MNA).

Protein determination

Protein was measured with the protein assay kit from SIGMA after solubilization with deoxycholate and precipitation with trichloroacetic acid according to Lowry.

Results and discussion

Alkaline phosphatase and GGT are known as BBB specific enzymes. Enrichment of these enzymes is used as a measure of the enrichment of the microvessel fraction obtained from brain tissue. The activities of GGT and ALP in the brain cortex and cortical microvessels of rats of different ages are shown in Tables 1 and 2. The enrichment of these enzymes in the microvessel fraction is between factor 7 and factor 33, which is in accordance with previous studies [8-10]. It confirms the suitability of our method for obtaining a highly enriched capillary fraction of the brain.

Developmental changes of the specific activity of GGT have already been described [10,11]. It was concluded that GGT might be considered an element involved in the matu-

ration of the BBB [10]. However, in that study the number of observations was too small to perform a statistical analysis. In our investigation we obtained similar results (Table 1). A significant increase of GGT activity during the first 30 days after birth was observed. In contrast, the ALP activity in microvessels increased between day 7 and day 14, and decreased between 2 and 6 weeks (Table 2). In the cortical tissue the ALP activity tended to decline.

Table 1: Specific activity of γ-Glutamyl transpeptidase measured at 25 °C in isolated rat brain microvessels and total brain homogenate

Age (weeks)	microvessels (nmol/min/ mg protein)	significance	brain (nmol/min/ mg protein)	significance	ratio microvessels/brain
1	33.1 ± 14.2 (6)	$p \leq 0.001$ (vs. 4)	2.8 ± 0.5 (6)	$p \leq 0.05$ (vs. 2)	11.8
2	46.1 ± 17.6 (6)	$p \leq 0.001$ (vs. 4)	3.4 ± 0.3 (5)		13.6
4	102.3 ± 7.5 (4)		3.1 ± 0.9 (4)		33.0
6	143.3 ± 4.3 (2)		10.8 ± 2.4 (2)		13.3

Results are expressed as mean ± S.D. Number of determinations is shown in parentheses.

Table 2: Specific activity of alkaline phosphatase measured at 25 °C in isolated rat brain microvessels and total brain homogenate

Age (weeks)	microvessels (nmol/min/mg protein)	brain (nmol/min/mg protein)	ratio microvessels/brain
1	406 ± 29 (4)	59 ± 11 (4)	6.9
2	793 ± 243 (4)[a]	57 ± 24 (4)	13.9
4	699 ± 28 (2)	36 ± 1 (2)	19.4
6	429 ± 16 (2)	26 ± 3 (2)	16.5

[a]$p \leq 0.01$

Results are expressed as mean ± S.D. Number of determinations is shown in parentheses.

Until now only a few data are available about developmental changes of the specific activities of peptidases in the brain. Thus, Dauch et al. [12] report that peptidases in the mouse brain displayed differential ontogenic profiles and speculate on a putative role of the enzymes in maturation or differentiation processes.

The distribution of the various peptidases measured in this study was similar in the cortical tissue and the microvessels. Only a small enrichment in the microvessel fraction was observed, in particular during later development (weeks 4 and 8) (Fig. 1-3).
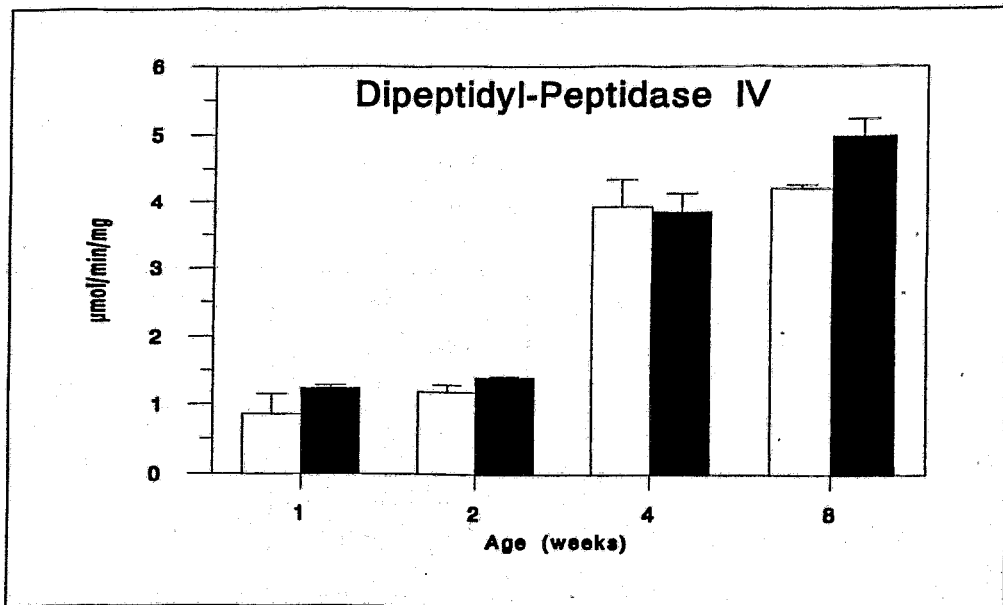

Fig. 1: Specific activity of dipeptidyl aminopeptidase IV measured at 37 °C in isolated rat brain microvessels and total brain homogenate of rats of different ages
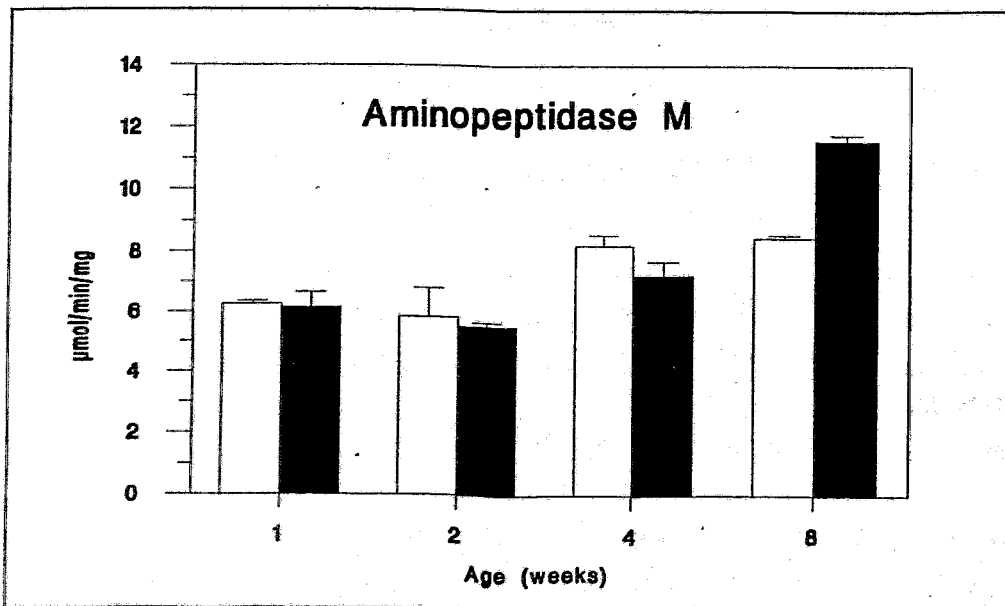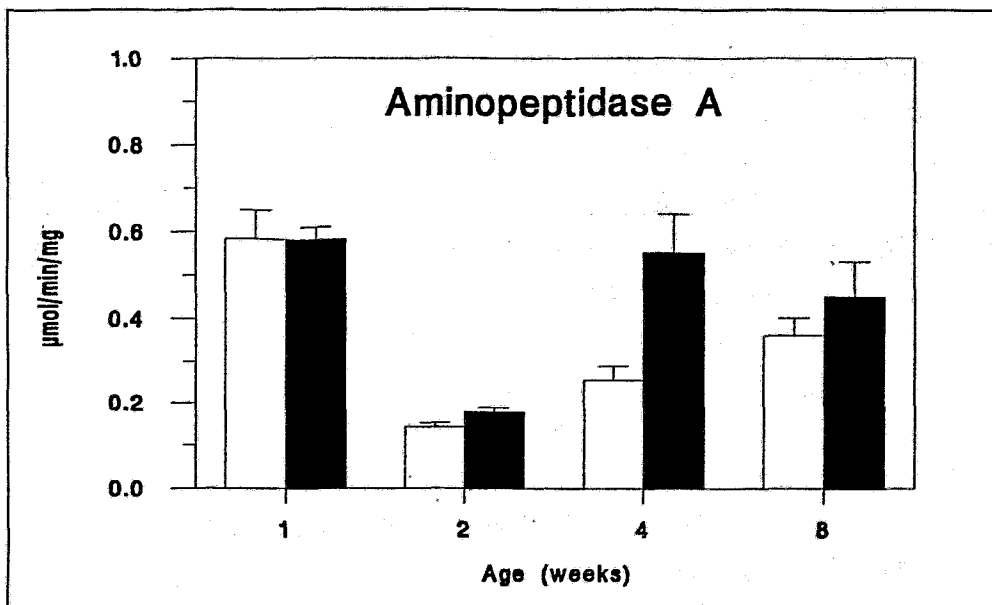

Fig. 2: Specific activity of aminopeptidase M measured at 37 °C in isolated rat brain microvessels and total brain homogenate of rats of different ages

Fig. 3: Specific activity of aminopeptidase A measured at 37 °C in isolated rat brain microvessels and total brain homogenate of rats of different ages

Also, the changes of the specific activities of these peptidases during development are similar in both preparations. We found a 5-fold increase in the activity of the membrane-bound serine peptidase dipeptidyl peptidase IV (DP IV; EC 3.4.14.5) during the first two months after birth (Fig. 1). This is in contrast to immunohistochemical studies in which the DP IV activity in brain capillaries appears to decline after birth in humans and rats [13,14]. In mice the specific activities of DP IV and the metalloenzyme aminopeptidase M (APM; EC 3.4.11.2) did not vary significantly from day 9 before to month 2 after birth [12]. The sensitivity of the various methods and species-related differences may account for this discrepancy. Fig. 2 shows that APM activity in brain tissue and microvessels increases by factor 1.5 and 2, respectively. The aminopeptidase A (APA) activity decreases between day 7 and day 14 after birth and increases thereafter.

Cerebrovascular APM and DP IV are probably involved in the metabolism of somatostatin [4,15], a peptide which has been found to have an inhibitory effect on the growth of various tumours [16]. The developmental changes of the activities of both enzymes may be of importance for the evaluation of the therapeutic and diagnostic use of somatostatin and somatostatin analogues.

References

[1] Ermisch, A. et al., Physiol. Rev. **73** (1993) 489

[2] Kretzschmar, R. et al., Brain Res. **380** (1986) 325

[3] Ermisch, A. et al., Brain Res. **554** (1991) 209

[4] Brownless, J. et al., J. Neurochem. **60** (1993) 793

[5] Bakker, W.H.et al., J. Nucl. Med. **31** (1990) 1501

[6] Bakker, W.H.et al., Life Sci. **49** (1991) 1593

[7] Mäcke, H.R. et al., Hormone Metab. Res. **27** (1993) 12

[8] Orlowski, M. et al., Science **184** (1973) 66

[9] Mooradian, A.D. et al., Neurochem. Res. **16** (1991) 447

[10] Buard, A. et al., Neurosci. Lett. **141** (1992) 72

[11] Budi Santoso, A.W. et al., Int. J. Devl. Neuroscience **4** (1986) 503

[12] Dauch, P. et al., Peptides **14** (1993) 593

[13] Bernstein, H.G. et al., Int. J. Dev. Neurosci. **5** (1987) 237

[14] Härtel-Schenk, S. et al., Histochem. J. **22** (1990) 567

[15] Pardridge, W.M. et al., J. Neurochem. **44** (1985) 1178

[16] Reichlin, S., N. Engl. J. Med. **309** (1983) 1495

34. CHARACTERIZATION OF SEROTONIN UPTAKE SITES ON ISOLATED BRAIN MICROVESSELS

R. Bergmann, R. Berger and P. Brust

The blood-brain barrier (BBB) represents a complex epithelial interface in vertebrates that separates the blood compartment from the extracellular fluid compartment of the brain [1]. Isolated microvessels represent a tool to study the function of this interface in vitro [2,3]. In the past they were used to characterize binding sites for different hormones and neurotransmitters [1,3,4].

It was shown that imipramin blocks the neuronal uptake of the neurotransmitter serotonin [5]. High affinity ^{3}H-imipramin binding was used to characterize the distribution of serotonin uptake sites in the mammalian brain [6,7]. However, until now there has been no data about the binding of ^{3}H-imipramin on brain endothelial cells. Here we report on attempts to characterize serotonin uptake sites on microvessel preparations from the pig hippocampus.

Materials and methods

The hippocampi of about 100 pig brain hemispheres were used for the study. Microvessels from this material were obtained by a similiar procedure as described by Matys et al. (this volume). The microvessels and hippocampal tissue were homogenized in 10 volumes of ice-

cold buffer (10 mM sodium phosphate containing 0.32 M sucrose, pH 7.4) with an Ultra-Turrax T25. The homogenate was centrifuged at 20.000 g for 10 min. The resulting pellet was resuspended with the Ultra-Turrax and centrifuged again at 20.000 g for 10 min. After repeating the same procedure the pellet was resuspended in 10 volumes of buffer and stored at -20 °C until use in the binding studies.
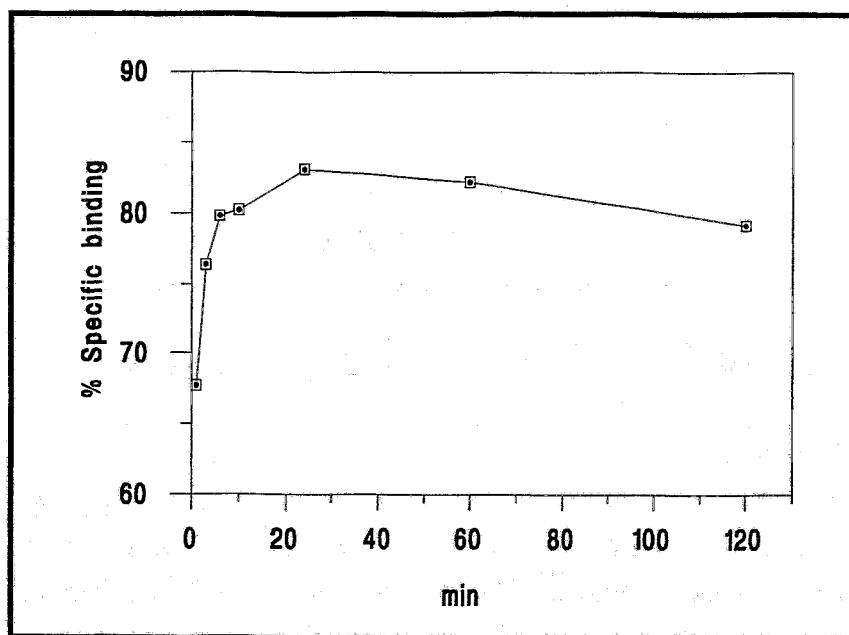

Fig. 1: Time dependency of ^{3}H-imipramin binding to membranes from pig hippocampus.

The time dependency of imipramin binding was studied on membrane preparations of hippocampal tissue (0.4 ml; 0.2 mg protein). The samples were incubated at 4 °C for various periods with [2,4,6,8-^{3}H]imipramin hydrochloride (888 GBq/mmol, Amersham) in the presence and absence of a 10,000-fold excess of unlabelled imipramin. For inhibition studies samples of microvessels (0.4 ml; 0.05 mg protein) and hippocampal tissue were incubated at 4 °C for 60 min. The binding assays were terminated by rapid filtration through GF/B glass fibre filters (Whatman, Maidstone, England). The filters were rapidly washed with four 4 ml portions of ice-cold buffer, transferred to 10 ml scintillation fluid (Ultima-Gold, Packard) and analyzed for radioactivity. Aliquots of the incubation fluid were measured as well. Corrections were made for binding of ^{3}H-imipramin to the filters. The protein content of the membrane suspensions was estimated according to the method of Lowry et al. [8]. The enrichment of the capillary fraction determined by measurement of alkaline phosphatase activity was 28-fold.
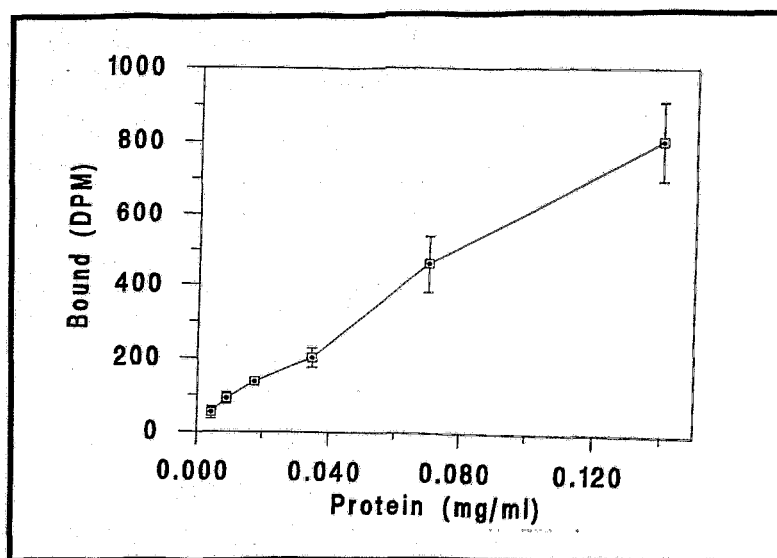
Fig. 2: Relationship between ^{3}H-imipramin binding and protein concentration

Results and discussion

The time dependency of ^{3}H-imipramin binding to membranes from the pig hippocampus is shown in Fig. 1. Equilibrium is reached at about 30 minutes. Therefore, in accordance with other studies [6,9] an incubation time of 60 min was chosen for the inhibition studies. Fig. 2 shows the dependency of the specific ^{3}H-imipramin binding on hippocampal membranes on the protein concentration. The binding increases linearly with increasing concentration of protein. Hence, we used lower protein concentrations for measurement of ^{3}H-imipramin binding on brain microvessels.

Table 1: Parameters of ^{3}H-imipramin binding

Parameter	hippocampus	microvessels
K_{D1} (nM)	1,4 ± 0,6	n.d.
K_{D2} (nM)	112 ± 25	100 ± 18
B_{max1} (pmol/mg)	1,15 ± 0,50	n.d.
B_{max2} (pmol/mg)	112 ± 19	140 ± 23

Different concentrations of unlabelled imipramin were used to inhibit the binding of ^{3}H-imipramin on hippocampal membranes and on microvessels (Fig. 3). In the hippocampus a two-site model gives a better fit to the data than a one-side model. In the microvessels only a one-side model fits the data. The parameters obtained are shown in Table 1. In accordance with studies in rats and humans [6,7,9] a high- and low-affinity binding site for ^{3}H-

imipramin was also detected in the pig hippocampus. However in the hippocampal mi-crovessels only the low-affinity site could be demonstrated.
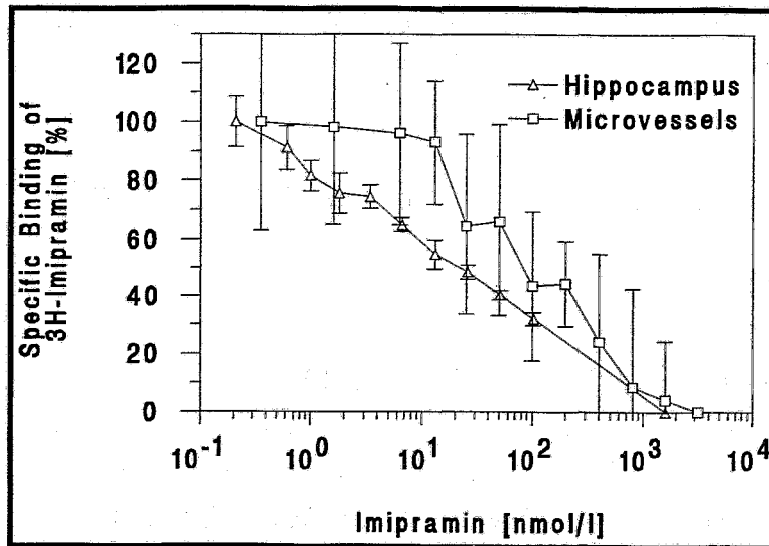

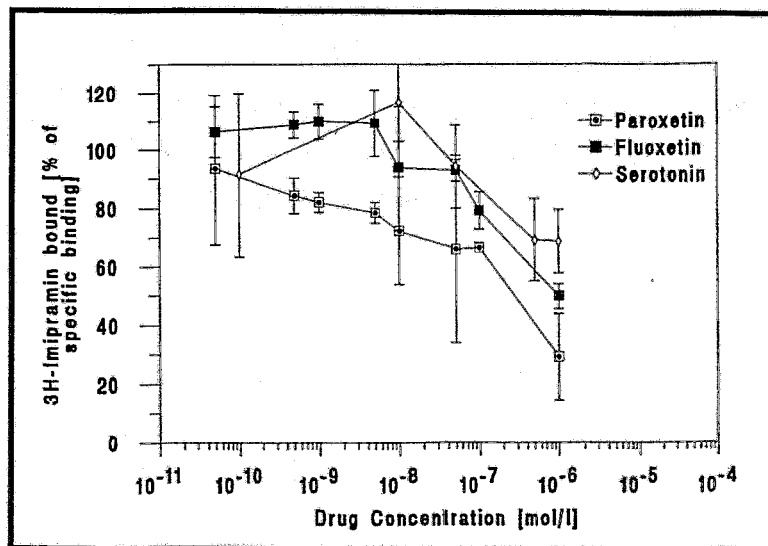Fig. 3: Inhibition of ^{3}H-imipramin binding by unlabelled imipramin.

Fig 4:Inhibition of ^{3}H-imipramin binding by various inhibitors of serotonin
uptake sites

Imipramin binding on this low-affinity site was inhibited by paroxetin, fluoxetin and sero-tonin (Fig. 4). Paroxetin and fluoextin are known as potent inhibitors of the serotonin transporter. Therefore we conclude that ^{3}H-imipramin labels serotonin uptake sites local-ized on the brain microvessels. This is the first indication of the presence of this transporter on brain endothelial cells while it was already demonstrated on endothelial cells derived

from pulmonary arteries [10,11]. As stated by several authors, use of ^{3}H-imipramin is complicated by the fact that part of the specific binding of this tracer on neuronal membranes is apparently not localized on the serotonin transporter [12]. ^{3}H-paroxetin is a better candidate for studying serotonin uptake. Therefore we intend to perform similar experiments using this tracer.

References
[1] Ermisch, A. et al., Physiol. Rev. **73** (1993) 489
[2] Joó F., Neurochem. Int. **7** (1985) 1
[3] Joó F., J. Neurochem. **58** (1992) 1
[4] Ermisch, A. et al., J. Cereb. Blood Flow Metab. **5** (1985) 350
[5] Langer,S.Z. et al., Science **210** (1980) 1133
[6] Reith, M.E.A. et al., J. Neurochem. **40** (1983) 389
[7] Cortes, R.et al., Neuroscience **27** (1988) 473
[8] Lowry, O.H. et al., J. Biol. Chem. **193** (1951) 265
[9] Moret C. et al., J. Neurochem. **47** (1986) 1609
[10]Lee S.-L. et al., Amer. J. Physiol. **250** (1986) C761 - C765
[11]Block E.R. et al., Amer. J. Physiol. **253** (1987) C672 - C678
[12]Mellerup, E.T. et al., Psychopharmacology **89** (1986) 436

35. A COMPARISON OF ANALYTICAL METHODS FOR DETECTION OF [^{14}C]TRICHLORO ACETIC ACID-DERIVED RADIOACTIVITY IN NEEDLES AND BRANCHES OF SPRUCE (*PICEA SP.*)

M. Kretzschmar, M. Bubner[1], M. Matucha[2], H. Uhlirova[3]
[1] Institute of Radiochemistry,
[2]Czech Academy of Science, Prague, Institute of Experimental Botany,
[3]Forestry and Game Management Research Institute, Prague

It is assumed that chlorocarbons as environmental pollutants will be oxidized by UV light or ozon into trichloro acetic acid. Their biotransformation can only be examined by tracer techniques. [^{14}C]trichloro acetic acid was therefore synthesized according to a previously described procedure [1]. This compound was added to the nutritional solution for cut-off

spruce branches with the aim of showing the uptake and distribution of trichloro acetic acid in these plant pieces.

Materials and methods

The branches (wood and needles) of spruces of varying age treated with [^{14}C]trichloro acetic acid (3.7 GBq/mmol) were studied, using the following methods:

Qualitative:

-conventional macroautoradiography with X-ray film and histological classification.

Quantitative:

-^{14}C combustion analysis with the sample oxidizer A 307 (Canberra/Packard) followed by measurement of radioactivity using the LS counter 6000 (Beckman Instruments)

- digital autoradiography with the Digital Autoradiograph LB 286 (Berthold GmbH)

- digital autoradiography with the Bio-imaging Analyzer BAS 2000 (Fuji Film Co.)

Conventional macroautoradiography and digital autoradiography with the BAS 2000 Analyzer were carried out as described in [2]. The needles were cut lengthwise and the wood crosswise. The slice thickness was 40 μm. The exposure time for conventional autoradiographs was 1.5 weeks for fresh needles and last year´s wood and 3 weeks for the last year´s needles and fresh wood. The same slices were exposed on the IP (imaging plate) of the BAS 2000 Analyzer for 18 hours.

Using digital autoradiography with the LB 286 device, a multiwire proportional counter, the radioactivity in the whole needle was measured.

In addition, the amount of volatile ^{14}C components in the needles was estimated from values measured after lyophilization in the vacuum apparatus and on frozen sections used for exposure on X-ray film.

Results

The autoradiographs in Figs. 1 and 2 show a high accumulation of ^{14}C radioactivity, especially in the tips of the needles and in the cork cambium of the branches. Also the epidermis, cork, phloem, cambium and xylem of the branches store the ^{14}C compound. Only the pith does not contain any radioactive material.

A different distribution of radioactivity was observed in needles from the same branch (Fig. 1).
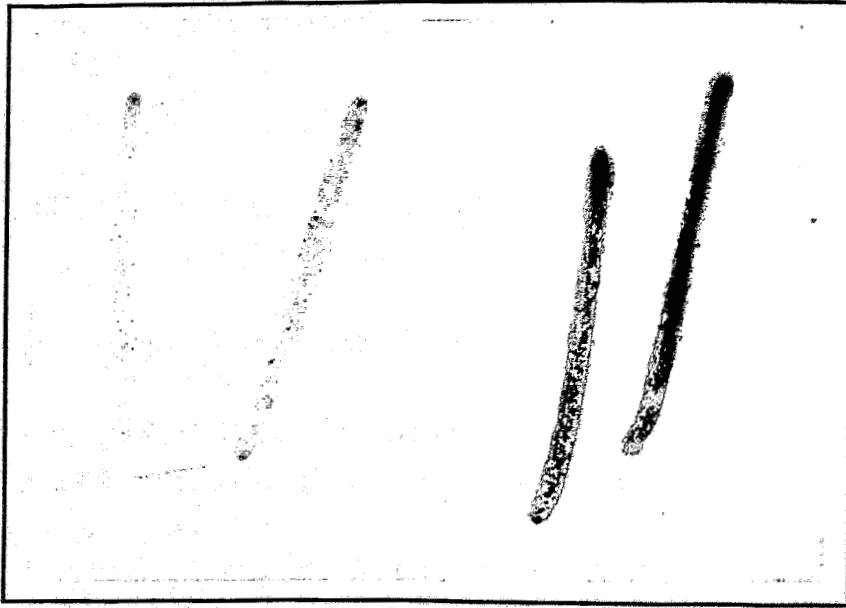
Fig.1: Conventional autoradiograph of whole spruce needles from one branch after incubation with a solution containing $[^{14}C]$trichloro acetic acid (magnification 3.7 fold)
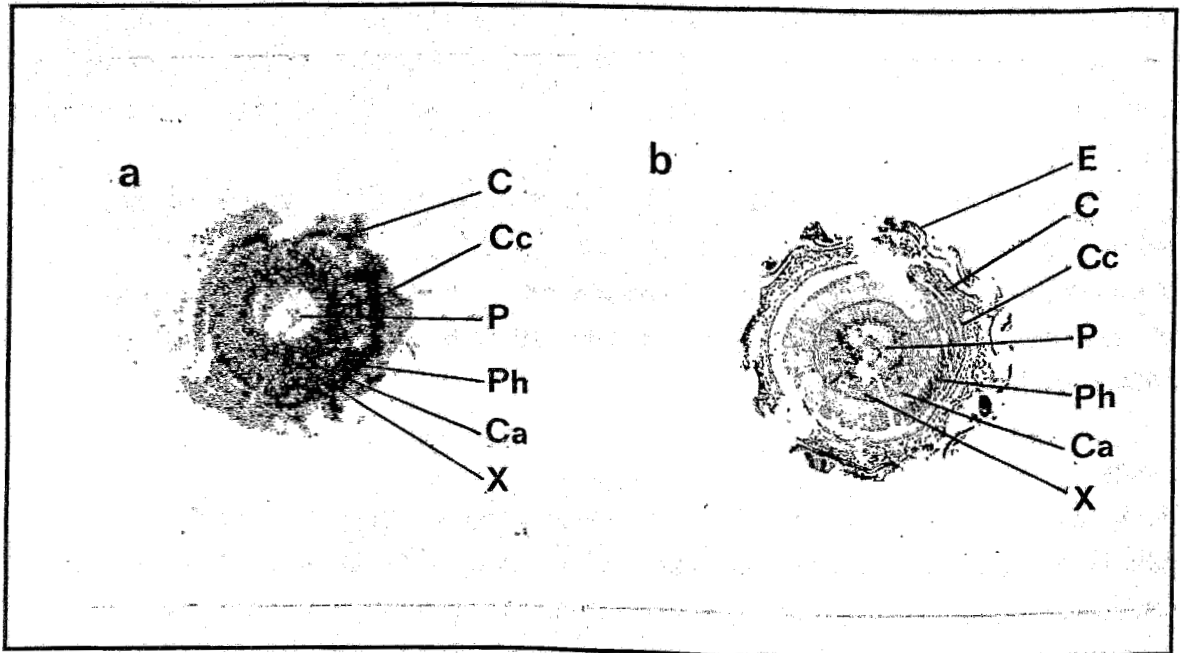

Fig. 2: a) Conventional autoradiograph from a cross-section of the branch, b) to a) accompanying histological section; E = epidermis, C = cork, Cc = cork, cambium, P = pith, Ph = phloem, Ca = cambium, X = xylem (magnification 9 fold)

The quantitative methods confirm the macroautoradiographic findings according to which a higher radioactivity uptake was found in the needle tip than in the needle base (see Fig. 3).

Combustion analysis showed a radioactivity concentration of 3100 Bq/g for fresh needles and 1000 Bq/g for last year´s needles. The ^{14}C uptake of this year´s wood was 1450 Bq/g and of last year´s wood 2600 Bq/g. The values obtained by the BAS 2000 analysis were similar (2800 Bq/g fresh needles, 2000 Bq/g last year´s wood). The radioactivity ratios between needle tip (one third of the needle) and needle base (two thirds of the needle) was 1 : 1.1 by combustion analysis and 1 : 1.2 using the BAS 2000 device.

Fig. 4 demonstrates the ^{14}C radioactivity distribution in the cross section of the same branch as shown in Fig. 2 but measured with the BAS 2000 Analyzer. Three ROI`s (regions of interest) were drawn. Only a small radioactive concentration was measured in ROI 1 (= 858 Bq/g) corresponding to the pith. Higher radioactivity accumulation was found in ROI`s 2 (= 2220 Bq/g) and 3 (= 1961 Bq/g) corresponding to the phloem, cambium, xylem and cork tissue. The highest uptake of radioactivity in the cork cambium (see Fig. 2) was not registered by the BAS 2000 Analyzer.
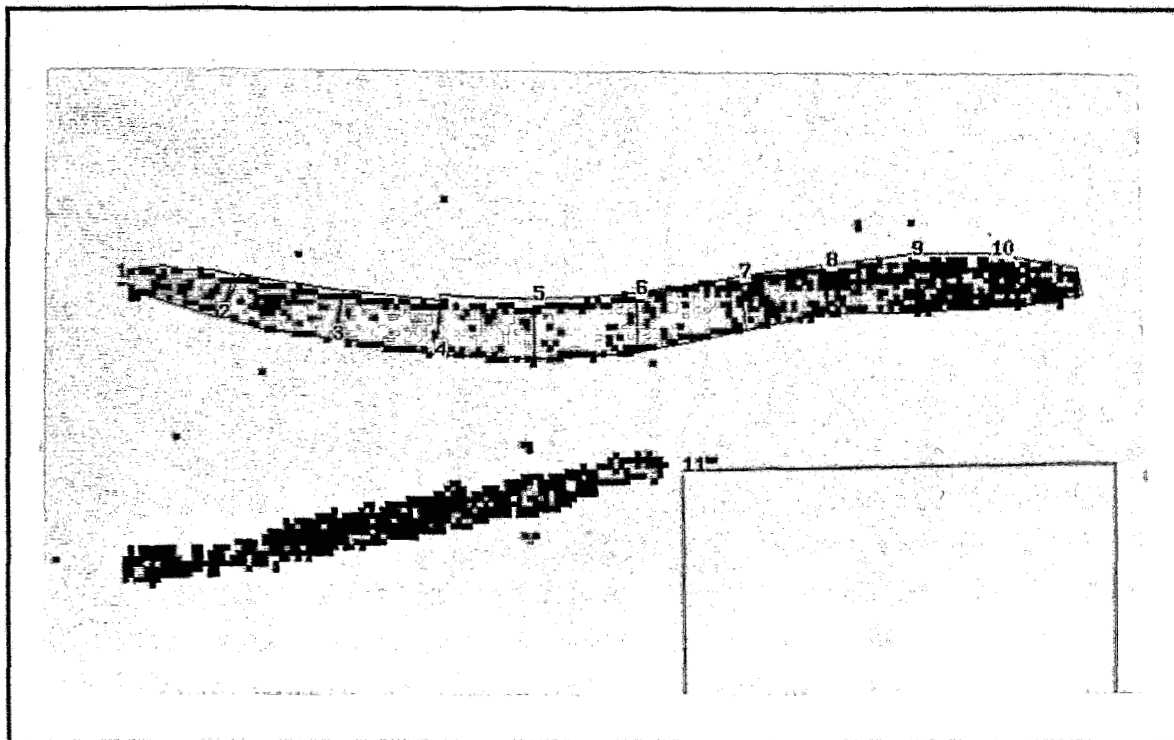
Fig. 3 : BAS 2000 autoradiographic representation of the ^{14}C-distribution in a 40 μm thick needle longitudinal section (magnification 7.5 fold). The radioactivity of the needle was measured in 10 segments between tip to base; 1 = 1568 Bq/g, 2 = 2098 Bq/g, 3 = 1861 Bq/g, 4 = 1743 Bq/g, 5 = 1528 Bq/g, 6 = 1454 Bq/g, 7 = 1202 Bq/g, 8 = 973 Bq/g ,9 = 751 Bq/g ,10 = 714 Bq/g .

The relative amount of volatile substances was less than 10 %. No radioactivity was measured by the Digital Autoradiograph LB 286. The ^{14}C concentration of the plant pieces was obviously below its limit of detection.
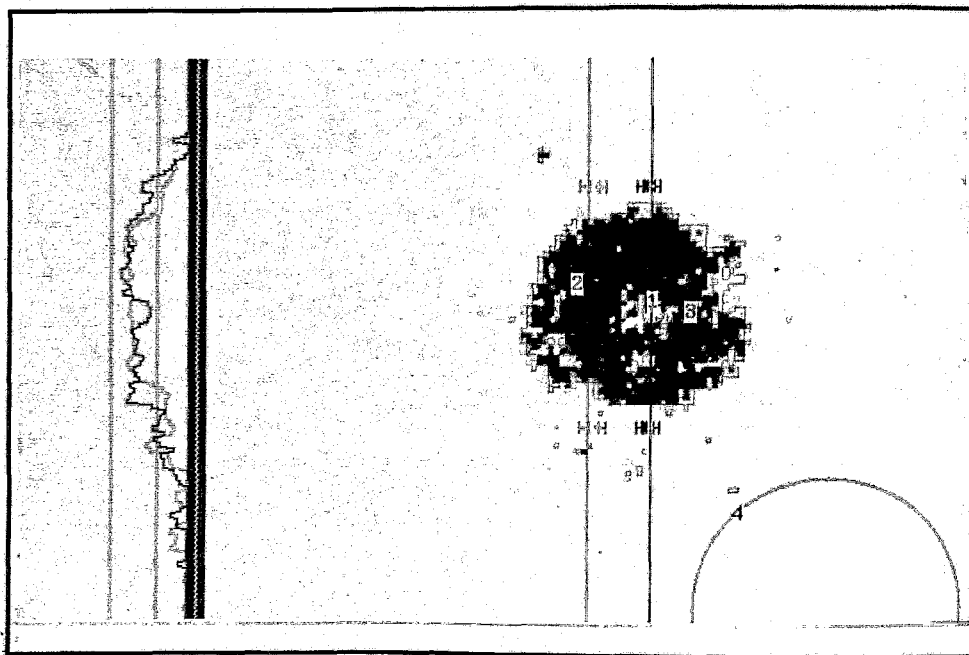

Fig. 4: BAS 2000 autoradiographic representation of the ^{14}C distribution in the cross-section of a branch as shown in Fig. 2 (magnification 8 fold), left side ^{14}C profile display of the section (1 = 858 Bq/g , 2 = 2220 Bq/g, 3 = 1961 Bq/g).

Discussion

This study demonstrated that [^{14}C]trichloro acetic acid or its metabolites are easily transmitted from the conducting vessels into branches and needles. A high accumulation was observed in the cork cambium and the tips of the needles. Conventional and digital autoradiography are suitable for measurement of this biodistribution. Nevertheless, the resolution of the BAS 2000 Analyzer is lower than that of the conventional autoradiography. Structures below 100 μm (cf. the cork cambium) were no longer distinguishable.

References

[1] Bubner, M. et al., FZR 93 - 12 (1993) 71
[2] Kretzschmar, M. et al., this report, p. 135

36. ATTEMPTS AT QUANTIFICATION OF ^{3}H AND ^{14}C DISTRIBUTIONS IN TISSUE SECTIONS USING VARIOUS METHODS

M. Kretzschmar, H. Mixtacki[1], R. Hahn[1]
[1]Raytest Isotopenmessgeräte GmbH,Straubenhardt 1

Introduction

Whole body and single organ autoradiography has been much improved and widely applied in the field of pharmacology and toxicoloy. Quantitative autoradiography (QAR) is a powerful tool for high spatial resolution determination of tissue concentrations of radiolabelled tracers. QAR provides values of the biodistribution of tracers in small histological structures within organs, especially in the neurosciences is the great heterogeneity of cerebral metabolic activity throughout the brain clearly visible.

Several methods have been developed in the last few years to determine the radioactivity concentrations in tissue sections. The traditional method is autoradiography with X-ray or ^{3}H film [1]. The principle of this type of QAR is densitometry. The degree to which a film is exposed to a radioactive substance determines the density of silver grains on the developed film. A densitometer measures the amount of light passing through the film compared with the amount of light transmitted through air. The unit of measurement is the optical density (OD). The OD of the autoradiograms produced from radioactively labelled thin tissue sections can be quantitatively converted into radioactive concentration by comparison with radioactive standard scales. The modern method is digital autoradiography [2]. The position and intensity of 2-dimensional radioactivity distributions are quantitatively measured by a device. The traditional X-ray or ^{3}H film has been replaced by a multiwire proportional counter or the phosphor imaging plate.

Materials and methods

Two different methods of quantification should be compared:
- densitometry with film and the Photo Finish^{TM} software, and
- digital autoradiography with the BAS 2000 bio-imaging Analyzer from the Fuji Film Co.

Using the densitometric method, the tissue sections were put on X-ray or ^{3}H-film and exposed for days or weeks. The resulting autoradiograms were scanned by the Hewlett Packard Scan Jet II c and handled by the image processing software PhotoFinish^{TM}. The ODs of the autoradiograms were analyzed as grey values on the display screen of the PC. The optical resolution of the Scan Jet amounted to 400 dpi. The influence of several system parameters, such as enhancement, brightness,contrast,transmission of scan area, emulsion side of the film, was determined.

Using digital autoradiography, the tissue sections were exposed in a brightly lit cassette on the imaging plate (IP) for several hours. The IP contained an image sensing layer with fine crystals of photostimulable phosphor (BaFBr: Eu^{2+}) on a polyester plate.When the exposed IP is inserted into an image reading unit and then scanned with a fine laser beam,it emits luminescence in proportion to the recorded radiation intensity .This luminescence (PSL = photostimulated luminescence) is collected in a photomultiplier tube and converted into electrical signals.The radioactive image recorded on the IP during exposure is read as high resolution digital data of 10 pixels/ mm and recorded in an analyzing unit. After reading ,all the image data recorded on the IP can be erased by exposing the IP to uniform light in an IP eraser attached. The IP can then be reused.

With both methods it is necessary to calibrate the grey values and the PSL data by means of radioactive standard scales and to convert them into radioactivity units. The commercial Amersham ^3H- microscales were used as radioactive standards. In addition ^{14}C standards of benzylic acid -1,1 [^{14}C] dimethylpiperidinylesteriodide were prepared in a radioactivity concentration from 277 Bq/g (7 nCi/g) to 296 kBq/g (8 μCi/g) [3].

The biodistribution in rats of ^3H -leucine and of the laxative ^{14}C-Rhein was measured 30 min after application. One male Wistar rat (120 g) was i.v. injected with 19.2 MBq (520 μCi) ^3H-leucine dissolved in 30 % ethanolic solution. Another Wistar rat (137 g) was given an oral dose of 888 kBq (24 μCi) ^{14}C-Rhein dissolved in sodium phosphate buffer pH 8. The rats were frozen in ethanol/dry ice solution and sectioned in a cryomicrotome at -20° C. The slice thickness was 40 μm and 50 μm in the case of ^{14}C-Rhein. The tissue sections were freeze-dried for 48 hours in the apparatus.

The ^3H-labelled sections were exposed to ^3H-Ultrofilm for 5 and 7 weeks and in the case of ^{14}C-Rhein to RF64 X-ray film for 2 and 4 weeks. In order to ensure identical exposure conditions and good contact of the films to the tissue sections, the exposure was carried out in a screwpress.

The same tissue sections were exposed on the IP for 15 hours (^3H-leucine) and 21.5 hours (^{14}C-Rhein).

Results

Fig. 1a and 1b show the standard curves of the ^3H-microscales. Fig. 1a demonstrates that the standard curves can only be used for calculation of tissue radioactivity from the measured grey values in the range between 0 - 370 kBq/g (10 μCi/g) in case of 5 weeks´ exposure, and in the range from 0- 185 kBq/g (5 μCi/g) in case of 15 weeks´ exposure.

The standard curve of ^3H-microscales obtained by the BAS 2000 (Fig. 1b) shows linearity in the whole range between 0 and 1224 kBq/g (0 - 33.1 μCi/g) using only a short exposure time of 15 hours.

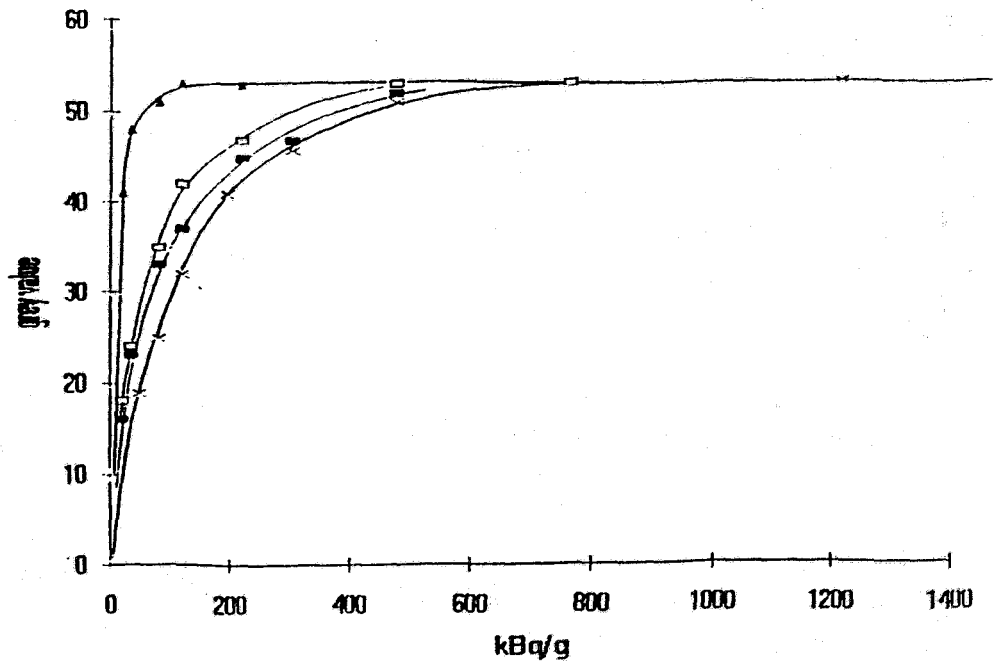Fig. 1a: ^{3}H-microscales standard curve for $\times = 5$ ■ $= 7$ □ $= 9$ and ▲ $= 15$ weeks exposure time. Abscissa represents tissue equivalent ^{3}H-concentration, and ordinate the corresponding grey values derived by Photo Finish.
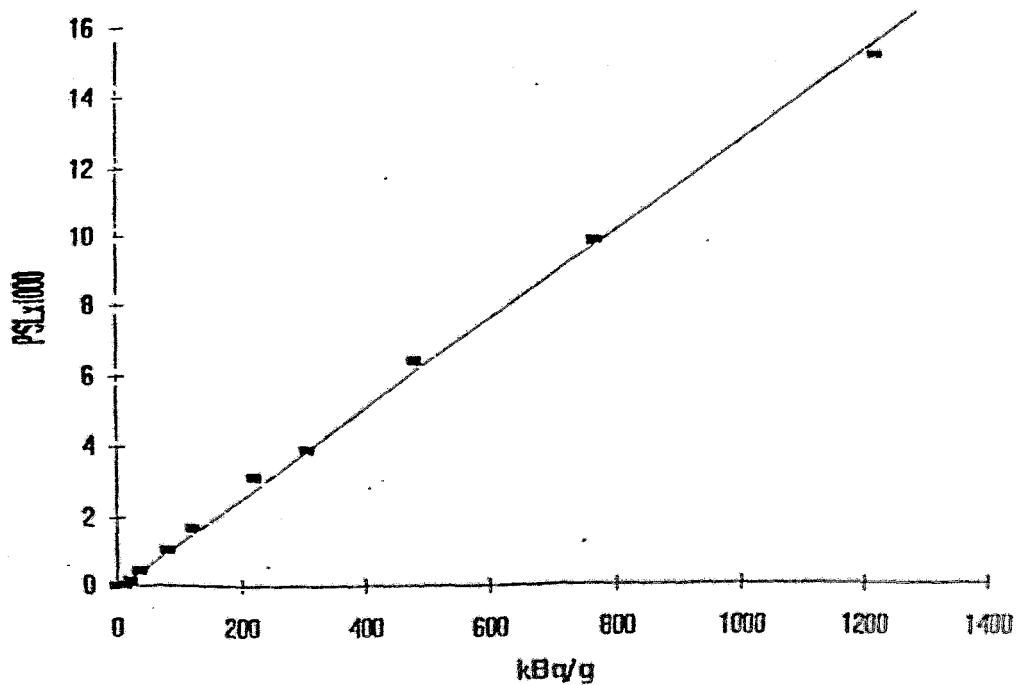

Fig. 1b: ^{3}H-microscales standardcurve for 15 hours exposure time. Abscissa represents tissue equivalent ^{3}H- concentration and ordinate the corresponding PSL values derived with the BAS 2000 device.
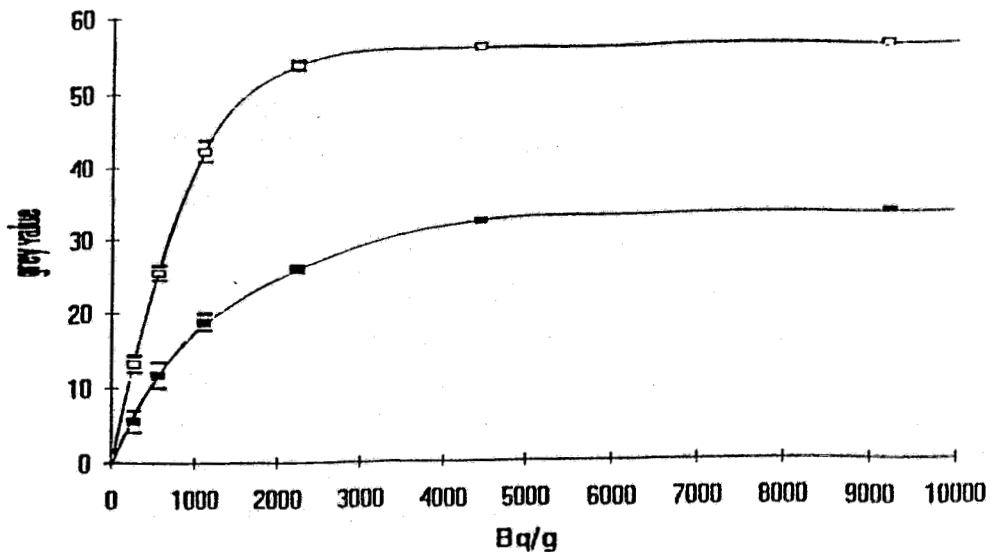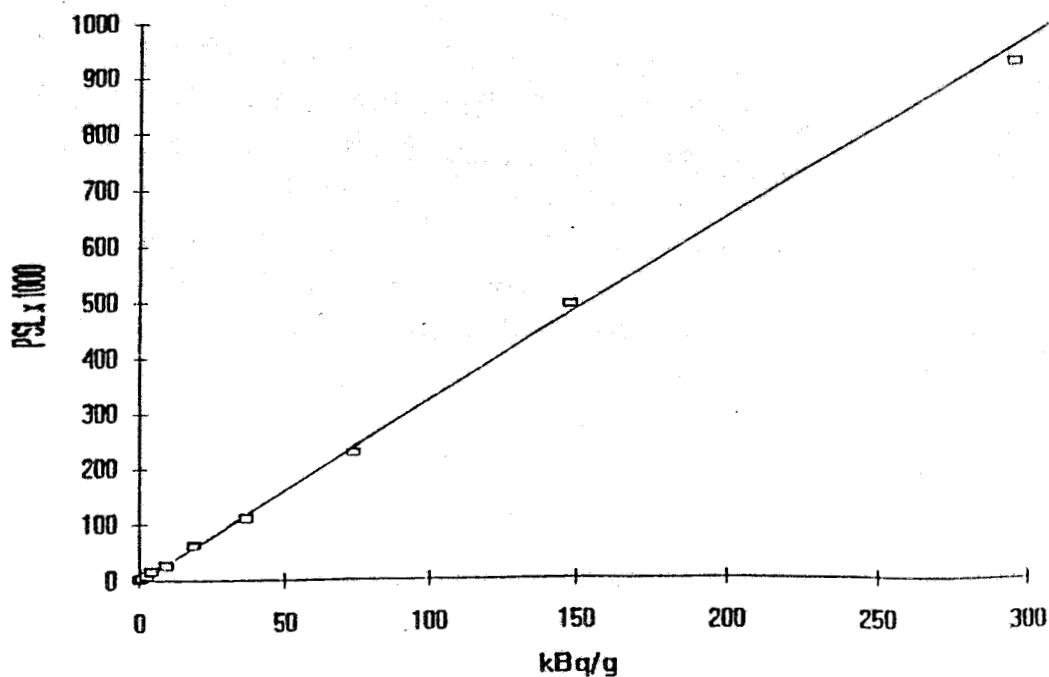
Fig. 2a : ^{14}C-standard curve for ■ = 2 and □ = 4.5 weeks exposure time. Abscissa represents the ^{14}C-concentration , and the ordinate the corresponding grey values derived by Photo Finish.

Fig. 2b : ^{14}C-standard curve for 21.5 hours exposure time. Abscissa represents the ^{14}C-concentration, and the ordinate the corresponding PSL values derived with the BAS 2000 device.

Fig. 2a illustrates the standard curves of the ^{14}C scale with an exposure time of between 2 and 4.5 weeks. A quantitative evaluation is only possible in the range between 0 and 4.4 kBq/g (120 nCi/g) .Beyond this radioactivity the film is overexposed and the grey values remain uninfluenced by an increase in radioactivity. The standard curve obtained by the BAS 2000 device (Fig 2b) shows linearity in the whole range between 277 Bq/g (7.5 nCi/g) and 296 kBq/g (8 μCi/g). The exposure time was only 21.5 hours .

Fig. 3b shows the ^{14}C radioactivity standard used. The profile across the standard (Fig. 3c) demonstrates that higher radioactivity cannot be measured under these conditions. The upper horizontal line in Fig. 3c represents the maximum PSL which is measurable. For higher radioactivity the exposure time must therefore be reduced.

Tables 1 and 2 show the radioactivity concentrations after application of ^{3}H-leucine and ^{14}C-Rhein, respectively in several organs of rats calculated from densitometric and luminescence measurements. With only a few exceptions (hippocampus) the values obtained with the BAS system lie between the values obtained by the densitometric method after 5 and 7 weeks.

Table 1: Comparison of the biodistribution of ^{3}H-leucine in rats 30 min after i.v. application , quantified by densitometry and luminescence measurement

Organ	tissue radioactivity with PhotoFinish (kBq/g)		tissue radioactivity with BAS 2000 (kBq/g)	% differences BAS 2000 and PhotoFinish	
	exposure time (weeks)		exposure time	exposure time (weeks)	
	5	7	15 hours	5	7
skeletal muscle	148.6 ± 10.0	155.4 ± 11.2	151.7	+ 8.6 -4.5	+ 4.7 - 9.0
stomach wall	424.4 ± 16.8	436.6 ±11.2	-	-	
liver	249.4 ± 16.9	259.0 ±10.1	255.3	+ 8.9 -4.3	+2.5 - 5.3
pancreas	overexposed		1350.5		
cardiac muscle	170.4 ±12.2	175.2 ± 7.2	177.6	+10.9 -2.8	+5.4 - 2.7
spinal medulla	131.0 ±11.3	140.6 ± 8.7	-	-	
brain gray matter hippocampus pyramidal and dentate granu- le cells	104.7 ± 8.6 167.6 ± 9.9	108.4 ±5.9 -	103.6 122.1	+ 7.2 -1.1 + 1.1 -10.3 + 45.3	
thymus	356.0 ± 6.7	-	351.5	+0.6 -3.2	-

Table 2: Comparison of the biodistribution of ^{14}C-Rhein in rats 30 min after oral application, quantified by densitometry and luminescence measurement

Organ	tissue radioactivity with PhotoFinish (Bq/g) exposure time (weeks)		tissue radioactivity with BAS 2000 (Bq/g) exposure time 21.5 hours	% differences BAS 2000 and PhotoFinish exposure time (weeks)	
	2	4.5		2	4.5
skeletal muscle	148.0 ± 14.1	166.5 ±12.8	159.1	+15.8 -1.9	+3.4 -12.7
stomach content	overexposed		177600.0	-	
liver	814.0 ±39.4	788.1 ± 45.0	777.0	+ 0.3 -9.8	+5.7 - 5.7
kidney					
medulla	2300.0±77.5	2328.0±47.0	2368.0	+ 6.2 -0.4	+ 3.7 -0.2
cortex	2923.0±83.5	overex.	2997.0	+ 5.3 -0.3	-
lung	647.5±32.8	666.0±29.7	662.3	+ 7.2 -2.7	+3.9 -5.0

Table 3: Comparison of conventional autoradiography and digital autoradiography with BAS 2000

	conventional autoradiography with Photo-Finish	digital autoradiography with BAS 2000 device
resolution	good 10-20 μm	good 100 μm
measuring value registration from the display	good with pixel, especially for small structures	good with ROIs, especially for large structures
exposure time for ^{3}H (20 kBq/g) ^{14}C (277 Bq/g)	long ~ 7 weeks ~ 3 weeks	short ~ 15 hours ~ 21 hours
image development process	~ 1 hour for development	~ 3 min for scanning and development
measuring value range	slow dynamic range of the order of ~ 10^1, several film exposures are necessary for the whole measuring range	wider dynamic range of the order of ~ 10^4, only one exposure is necessary for the whole measuring range
use of the film and IP	only once	IP for ^{3}H 5 - 10 x IP for ^{14}C ~ 1000 x
price	film for ^{3}H ~25 DM film for ^{14}C ~ 6 DM	IP for ^{3}H 540 DM IP for ^{14}C 1100 DM

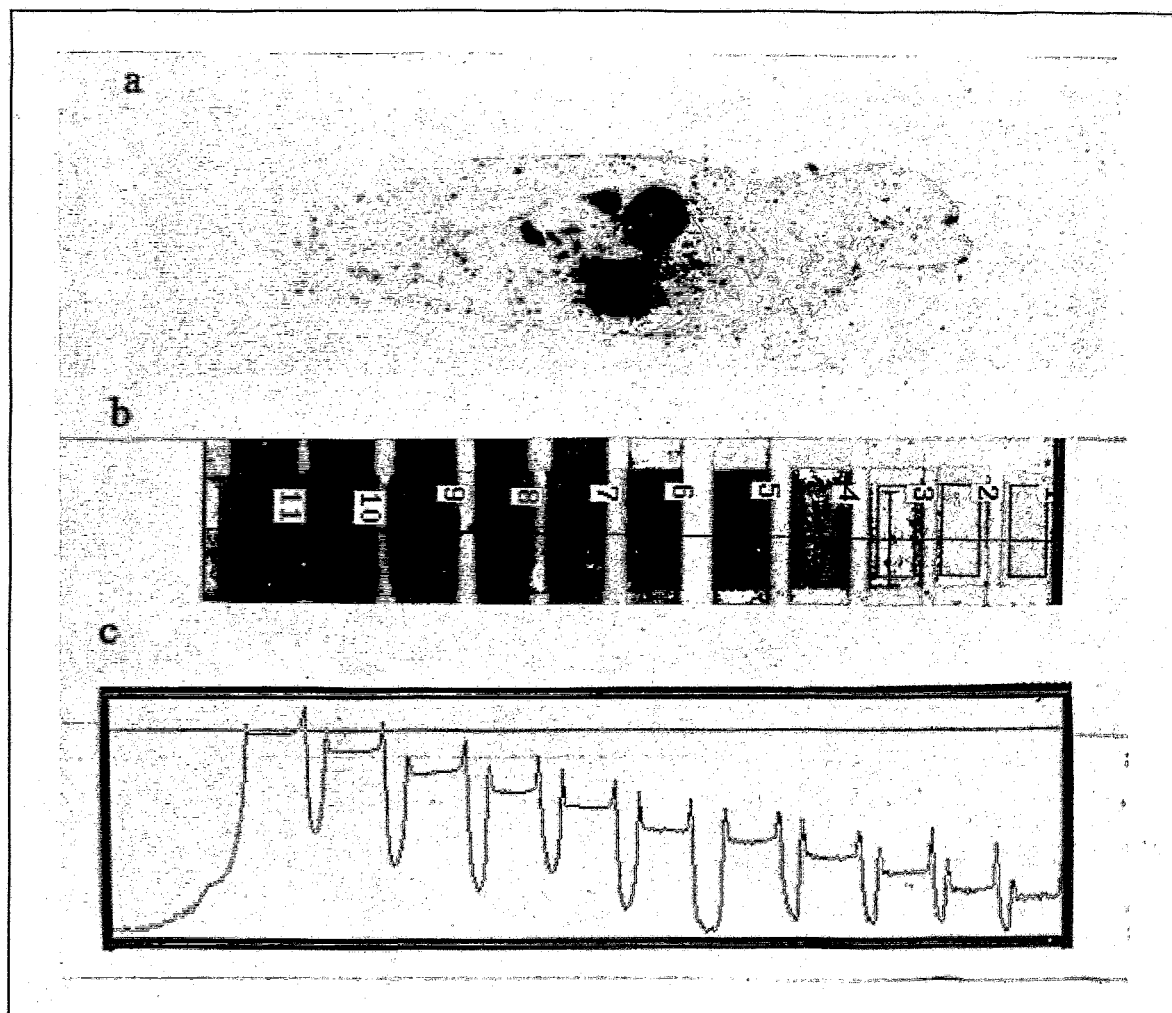Table 3 summarizes the advantages and disadvantages of both methods

Fig.3 : Representation from a) ^{14}C-Rhein biodistribution 30 min p.i. in rats, b) ^{14}C-radio-activity standard in the range between 277Bq/g (7.5 nCi/g) and 296 kBq/g (8 μCi/g) c) profile display of the ^{14}C-radioactivity standard in b)

Further studies are planned for the assessment of the methods.

References

[1] Lear, J.L. in : Positron emission tomography and autoradiography.Principles and applications for the brain and heart (ed. M.Phelps et al.) Raven Press, New York, (1986) 197

[2] Miyahara, J., Chemistry Today **223** (1989) 29

[3] Sobeslavsky, E. et al., FZR 93 - 12 (1993) 30

37. SUITABILITY OF INCUBATION OF RAT BRAIN SECTIONS FOR EVALUATION OF POTENTIAL DOPAMINERGIC Re- OR Tc-COORDINATION COMPOUNDS

U. Wenzel, R. Syhre, R. Berger, R. Bergmann

Introduction

One aim of radiotracer research is the design of receptorbinding substances to which ^{99m}Tc is coordinated. Some first steps are taken with the preparation of Re- and Tc-model compounds respectively, which are similar in chemical structure [1a,b]. Characterization of these substances requires methods of evaluation by which the affinity to receptors, in the present case to D_2 receptors, can be quickly and reliably established, first of all in the process of in vitro screening.

Several methods to perform these experiments in vitro have been described, among them investigations using homogenates of the receptorbearing brain regions and incubation [2]. In the present study we use in vitro incubation of brain sections. The advantages of this method are that it requires only minimal amounts of radioactive material and a very small number of test animals. The method was calibrated using [^{3}H]spiperone as the ligand and (+)butaclamol as a displacer. At the moment only nonradioactive Re complexes are available. Indications concerning any specific binding of Re-coordination compounds to D_2 receptors are therefore gained indirectly derived from competition with labelled spiperone, compared with the effect of (+)butaclamol.

Materials and methods

We modified the method described by M. J. Kuhar and J. R. Unnerstall [3]. In brief, after a short ether anaesthesia the animals (male Wistar rats, 150 - 200 g of weight) were sacrificed by decapitation. The brains were quickly removed and frozen in a mixture of dry ice and ethanol (-70 °C). After a short time at -20 °C brains were glued onto microtomic chucks by Compound (Leica Instruments, Nussloch, Germany). A number of consecutive horizontal sections were cut in the region of the Interaural line 2.9 - 6.4 mm (according to the rat brain atlas of Paxinos and Watson [4]) in 20 μm thickness and then thaw-mounted on microtomic glass slides, coated with gelatine-chrome alum (ORWO, Wolfen, Germany). The slides can be stored for two months at -20 °C [5]. One day before the tests, the test sections were dried at room temperature. In general, consecutive sections were incubated for 30 min at room temperature in a bath of:

A: Incubation buffer, containing 0.1 nM [^{3}H]spiperone (spec. act. 3.55 TBq/mmol, Amersham, Braunschweig, Germany) in tris-HCl, 10 mM ascorbic acid and 1μM pargyline (RBI, Cologne, Germany), pH 7.6

B: Incubation buffer as under A, containing 3 μM of the antagonist (+)butaclamol (RBI)

C: Incubation buffer as under A, containing the test substance, in this case 3 μM of derivative 3 of an Re-complex [1], dissolved in acetone/propyleneglycol

D: Incubation buffer as under B, containing the same solvents as C

In the last experiments, the sections were surrounded by a barrier of an inert material [PAP-PEN (Plano, Marburg, Germany)], for optimization of the incubation conditions. Everything points to the fact that surrounding the tissue section by a barrier rather than using a diving bath has the following advantages:

1. Minimizing the radioactivity applied

2. Exact dose of the labelled ligand

3. No contamination of the glass slides outside the barrier

After incubation the sections were washed twice for 5 min in the non-radioactive buffer at 4 °C, dipped shortly into distilled water at room temperature and dried in a stream of cold air. From each series some sections were wiped off (wet or dried) and, after shaking for several hours in the LS cocktail Ultima Gold (Canberra Packard, Frankfurt, Germany) they were measured by the LS spectrometer (Beckman, Düsseldorf, Germany). The radioactivity of the dried sections was measured together with [3H]micro-scales (RPA 510, Amersham), either directly by the Digital Autoradiograph (LB 286, Berthold, Wildbad, Germany) or indirectly. First by fixing them to Imaging Plates on light-tight cassettes (Raytest, Straubenhardt, Germany) for exposure overnight. The exposed Imaging Plates were then scanned by a laser beam and assessed by BAS 2000 (Raytest). For autoradiography, the same sections were brought into contact with [3H] Ultrofilm in autoradiographic film cassettes (Amersham) for up to 12 weeks' exposure. Development and fixation of the film plates follows standard procedures. In some of the resulting autoradiograms the optical density (OD) of regions of interest was measured for quantification by a CCD video camera coupled to a computerized image analysis system, using the PhotoFinish program.

Results and discussion

Reference substance: For comparison, the displacement of the [3H]spiperone binding to the D_2-receptors by the antagonist (+)butaclamol [2] as a reference substance was used as a measure of the unspecific binding in the four methods of quantification. LS measurement of the brain section is a rapid and simple method to estimate the range of inhibition in the whole brain (≈68 %, Fig. 1).
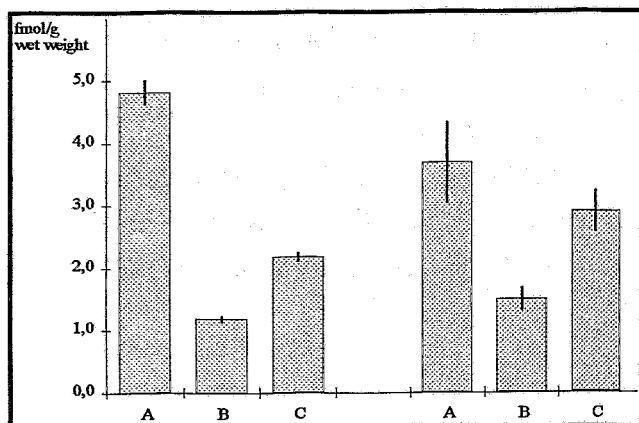
Fig 1: Two representative series of measurements by LSC (n = 5)
A = Incubation with [³H]spiperone
B = Incubation with [³H]spiperone in the presence of the reference substance
C = Incubation with [³H]spiperone in the presence of the test substance

The Digital Autoradiograph (DAR) serves for direct measurement of the radiation from the incubated section. However, the resolution of 1 mm is not sufficient for exact localization of the binding sites. The resolution of the indirect measurement by the Imaging Plates (Raytest) and the evaluation of autoradiographs on film by the PhotoFinish program is about 100 μm and 10 μm, respectively. Regions of interest inside the brain, in our case the caudate/putamen and the CA_1 field of hippocampus, which are rich in D_2-receptors [2], can thus be measured in detail. The results are shown in Fig. 2.
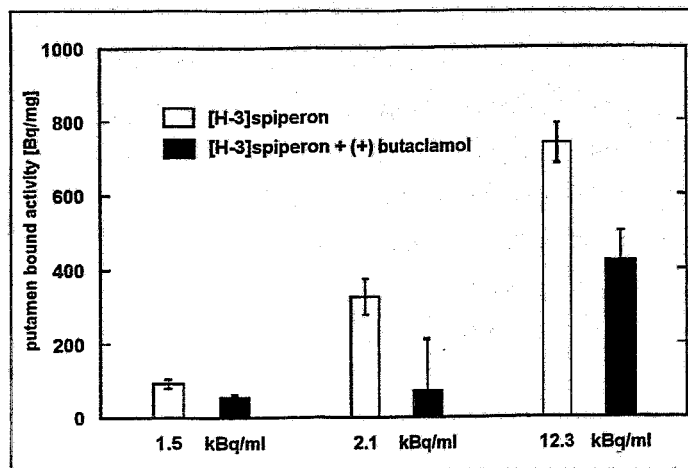
Fig. 2: Measurement of putamen bound activities of various concentrations [³H]spiperone by PhotoFinish. While the inhibition by (+)butaclamol in the whole brain section was nearly 80 %, in the caudate/putamen it was as high as 89 %, measured by BAS 2000.

In view of the number of series analysed (n = 6) we can assume that the results are representative.

Test substance: Using a Re coordination compound [1a,b] for inhibition, we found the displacement of the spiperone binding to be about 52 % in the whole brain section (see C, Fig. 3) and about 39 % for the caudate/putamen (see C, Fig. 3). Although inhibition by (+)butaclamol was higher than by the test substance (see B, b, Fig. 3), it can nevertheless be inferred that this method is suitable for characterization of Re complexes as regards their possible binding to D_2 receptors. Better results in terms of minimizing unspecific binding can be expected by preincubation of the sections with the same buffer [2].

The solution of (+)butaclamol in the same solvents as used for the Re complexes did not show any influence in our investigations (see D, materials and methods).
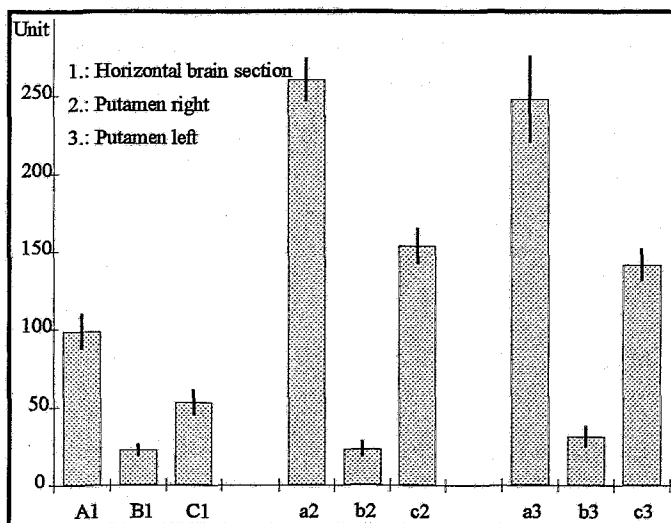
Fig. 3: Presentation of a typical experiment

A, B, C = whole brain section
a, b, c = caudate/putamen

A,a: Total binding of the ligand [³H]spiperone

B,b: Binding in the presence of (+)butaclamol

C,c: Binding in the presence of the Re coordination compound

Calibration: In all methods, [³H]micro-scales of known polymer activity and the estimated equivalent of tissue activity [6] were used for calibration. The standards were measured together with our labelled brain sections. The calibration results are shown in Fig. 4.
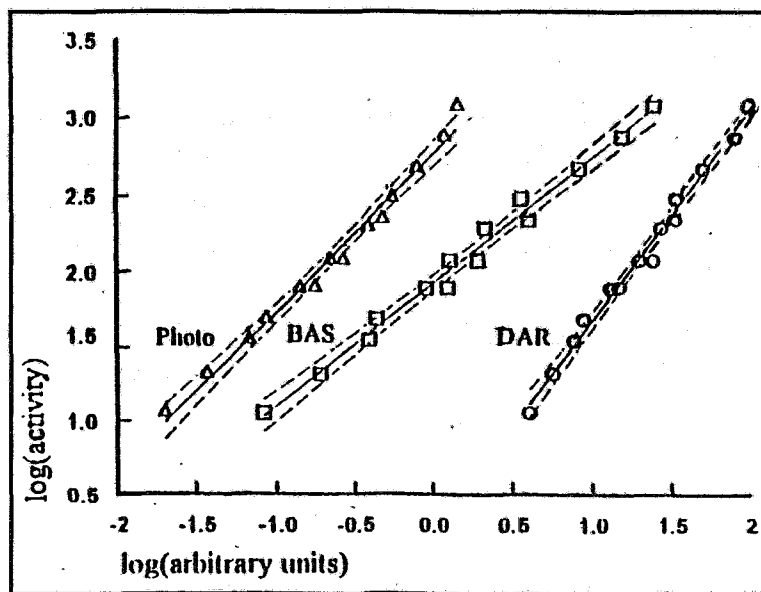
Fig. 4: Comparison of calibration curves of [³H]micro-scales
Photo = PhotoFinish
BAS = BAS 2000
DAR = Digital Autoradiograph

All curves permit statements concerning the measured activity of a substance of unknown biological behaviour. Measurement on BAS 2000 showed the best linearity also in the nonlogarithmic low range. In the other cases, the determination of radioactivity concentrations is less accurate for brain slices of high or low contamination.

In the future we intend to use this method as a standard procedure in conjuction with membrane binding studies [7]. In this way we hope to be able to select substances which are useful for SPECT investigations in the brain.

In the future we intend to use this method as a standard procedure in conjuction with membrane binding studies [7]. In this way we hope to be able to select substances which are useful for SPECT investigations in the brain.

References

[1] Spies, H. et al., this report, p. 37, 43

[2] Palacios; J. M. et al. in: Receptor Biochemistry and Methodology, Vol. 8, Alan R. Liss, Inc., New York (1987), p. 175

[3] Kuhar; M. J. et al. in: Methods in Neurotransmitter Receptor Analysis (ed. H. J. Yamamura et al.), Raven Press, New York (1990), p. 177

[4] Paxinos; G. et al., The Rat Brain in Stereotaxic Coordinates, Academic Press, New York (1986)

[5] Palacios, J. M. et al. in: Methods in Neurosciences, Vol. 12 (ed. P. M. Conn), Academic Press, San Diego (1993), p. 238

[6] Autoradiographic [^{3}H]micro-scales, Certificate, Amersham (1991)

[7] Berger, R. internal report

38. RELATIONS BETWEEN THE UPTAKE OF THE RADIOMETAL ^{169}Yb INTO NORMAL AND TUMOUR CELLS AND THEIR METABOLIC ACTIVITY DEPENDING ON THE LIGAND SPECIES

G. Kampf[1], G. Knop[1], S. Matys, G. Kunz, U. Wenzel[1], R. Bergmann, W.-G.Franke[1]

[1] Dresden Technical University, University Clinics, Clinic of Nuclear Medicine

Since some radioactive M^{3+} nuclides proved to be suitable for palliative therapy of bone metastases, several complexes of them were studied in our previous communications in respect of their biodistribution in rats under the special aspect of influencing their accumulation in various tissues by ligand variation, preinjection of other ligands, and variation of ligand concentration [1-4].

However, from these studies as well as from studies by other authors it was not possible to draw any conclusions as to the mechanism of uptake of the M^{3+} nuclides into the tumour cell. For gaining insights into such basic processes, experiments at cellular level are more appropriate, since the influence of the whole organism leading to superimposition of proc-

146

esses is absent in this case. We therefore decided to start experiments with cell cultures of normal and tumour cells in order to detect possible differences in the behaviour of these cell species and to find some indications concerning the uptake mechanism(s).

This direction of research is moreover favoured at present on account of the possibility of reducing - and, in part, eliminating - animal experiments.

This first study is aimed at detecting a relation between the metabolic activity of cells and their M^{3+} uptake using complexes with various ligands.

Material and methods

The radiometal ^{169}Yb has been used up to now in the form of M^{3+} compounds because of its easy availability and relatively long physical half-time. It is a nuclide which shows a chemical behaviour analogous to that of the therapeutically used yttrium and is representative of most of the lanthanides.

The following compounds were chosen as ligands: citrate (CIT), diethylenetriaminepentaacetic acid (DTPA), and ethylenediaminetetramethylenephosphonic acid (EDTMP), which are already used routinely in nuclear medical practice, as well as nitrilotriacetate (NTA) and ethylenediaminetetraacetic acid (EDTA), the biodistribution of which is known from studies on tumour-bearing mice [5]. The compounds were labelled using ^{169}YbCl$_3$ (Swierk, Poland, spec. act. 15 GBq/mg Yb), the chemical and radiochemical purity of the labelled complexes was checked by thin-layer chromatography and HPLC.

For comparison of the metabolic activities of the cell strains [^{18}F]-2-fluoro-2-deoxy-D-glucose ([^{18}F]FDG) produced by the Rossendorf department of positron emission tomography was used, the uptake of which provides information on the degree of glucose utilization by the cells.

The cell strains used were the hamster lung fibroblasts V79/4 (from the Max Delbrück Centre Berlin) for a non-malignant cell line, and a human adenocarcinoma of the kidney, KTCTL-2, from the tumour bank of the DKFZ (German Cancer Research Center) Heidelberg.

The cells were cultured on plastic surfaces in RPMI 1640 medium with 10 % of foetal calf serum in an atmosphere containing 5 % CO_2 for 46 - 48 hr before starting the experiments with the radioactive M^{3+} complexes. The labelled compound was added in a concentration of 1 μCi/ml ([^{18}F]FDG: 8 μCi/ml) together with fresh medium. The cell cultures were then incubated for various periods of time in the 5 % CO_2 atmosphere.

After incubation the monolayers were thoroughly rinsed with ice-cold buffer solution (all further steps were carried out at 4 - 6 $^{\circ}$C in order to minimize biochemical changes), dissociated with trypsin-EDTA, and washed 3 times with buffer. The radioactivity of the cell pellets was then measured in a COBRA II Auto-Gamma (Packard).

Results and discussion

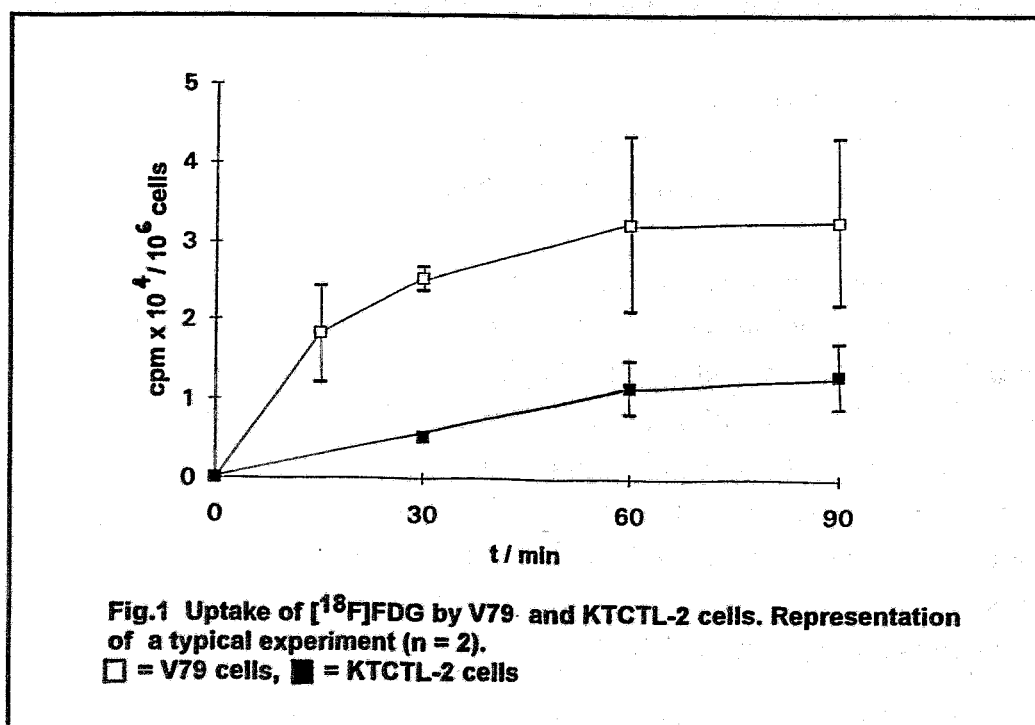### Uptake of the glucose analogue [^{18}F]FDG

Preliminary experiments with V79 cells showed - as expected - that [^{18}F]FDG was taken up to a much greater amount (by a factor of 3 - 4) by adherent cells in full metabolism than it was by cells in suspension. All following experiments were therefore performed with adherent cells.
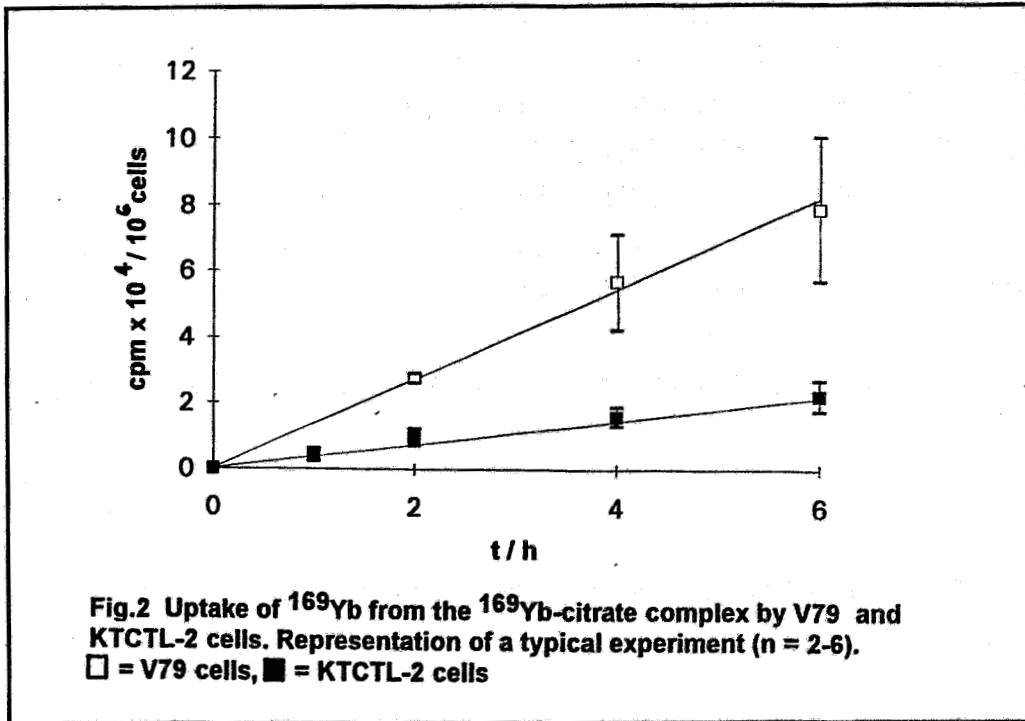
In spite of variations in the absolute amount of radioactivity taken up by the cells in the course of the various experiments it was observed that the well-established fibroblast cell line V79/4 always showed a higher glucose metabolism (i.e. [^{18}F] uptake) than the relatively young and still weakly growing tumour cell line KTCTL-2 (Fig. 1). The curves show a higher uptake during the first 15 min and then begin to flatten. Especially with the fibroblasts the shape of the curve as a function of time corresponds to that obtained by us in previous studies on the isolated perfused rat heart [6].

Uptake of ^{169}Yb from the complexes

Studying the uptake of the radiometal from the ^{169}Yb citrate complex, we observed a clear relation between the radioactivity concentration in the cells and their [^{18}F]FDG uptake, i.e. their metabolic activity: the V79 cells with their higher metabolic activity showed a higher ^{169}Yb uptake than the KTCTL-2 cells (Fig. 2).
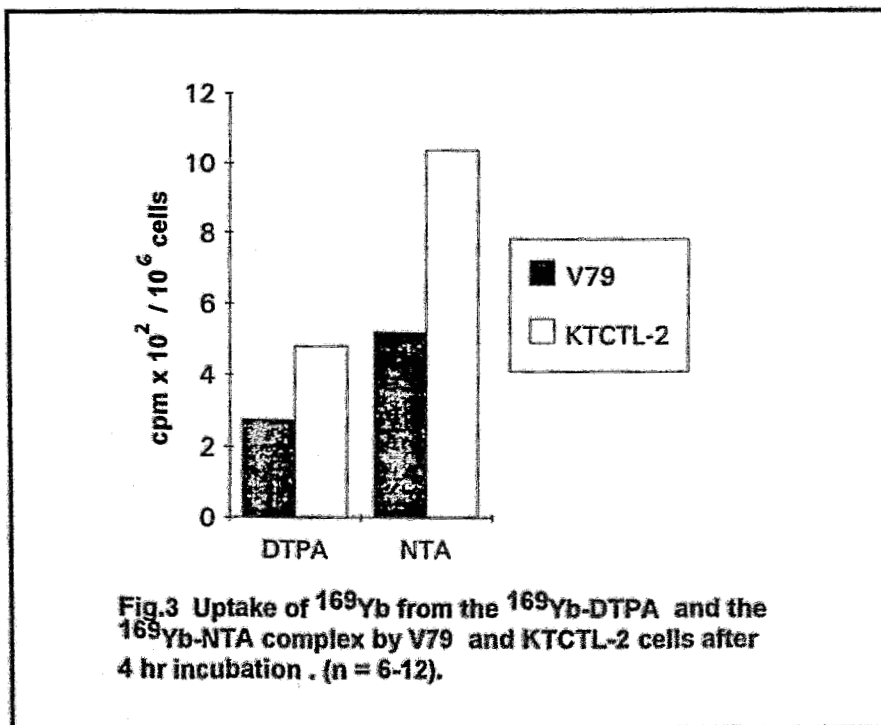
Quite another behaviour emerged when ^{169}Yb complexes with NTA, DTPA, or EDTMP were offered to the cells. Apart from the generally lower uptake level , in all these cases the tumour cells took up more radioactivity than the fibroblasts (Fig. 3, EDTMP not shown).

Fig.1 Uptake of [^{18}F]FDG by V79 and KTCTL-2 cells. Representation of a typical experiment (n = 2).
□ = V79 cells, ■ = KTCTL-2 cells

Fig.2 Uptake of ^{169}Yb from the ^{169}Yb-citrate complex by V79 and KTCTL-2 cells. Representation of a typical experiment (n = 2-6).
☐ = V79 cells, ■ = KTCTL-2 cells

Nor does the uptake of ^{169}Yb from these complexes depend on the metabolic activity of the cells as it does in the case of the citrate complex.

These results suggest the existence of different transport or uptake mechanisms for the radiometal from the citrate complex, on the one hand, and from the NTA, DTPA, and EDTMP complexes, on the other.

Fig.3 Uptake of ^{169}Yb from the ^{169}Yb-DTPA and the ^{169}Yb-NTA complex by V79 and KTCTL-2 cells after 4 hr incubation . (n = 6-12).

References

[1] Beyer, G. J. et al., FZR 92 - 13 (1992) 31

[2] Beyer, G. J. et al., Nucl. Med. Biol. **19** (1992) 201

[3] Beyer, G. J. et al., FZR 92 - 13 (1992) 34

[4] Beyer, G. J. et al., FZR 92 - 13 (1992) 37

[5] Schomäcker, K. et al., ZFK - 640 (1988) 68

[6] Kampf,G. et al., Isotopenpraxis **26** (1990) 162

39. INFLUENCE OF THE STABILITY OF [169]Yb LIGAND COMPLEXES ON THE UPTAKE OF THE METAL NUCLIDE IN CULTURED CELLS

G. Kampf[1], G. Knop[1], S. Matys, G. Kunz, U. Wenzel[1], R. Bergmann, W.-G. Franke[1]

[1] Dresden Technical University, University Clinics, Clinic of Nuclear Medicine

In connection with the preceding report this communication presents the results of experiments performed with [169]Yb ligand complexes of various stabilities. Materials and methods were exactly the same as described there.

The role of the complex stability for the bio-availability of M^{3+} nuclides in animals has been discussed in detail by Schomäcker [1]. In short, easily dissociating (labile) complexes lead to a greater amount of the metal being available for transport proteins in the blood.

The stability of the complexes can be influenced by varying the metal as well as the ligand. Concerning the metal, the complex stability increases with decreasing ion radius, ytterbium being the second smallest among the lanthanides, i.e. it forms relatively stable complexes. Concerning the ligands, those used by us form complexes of increasing stability in the order

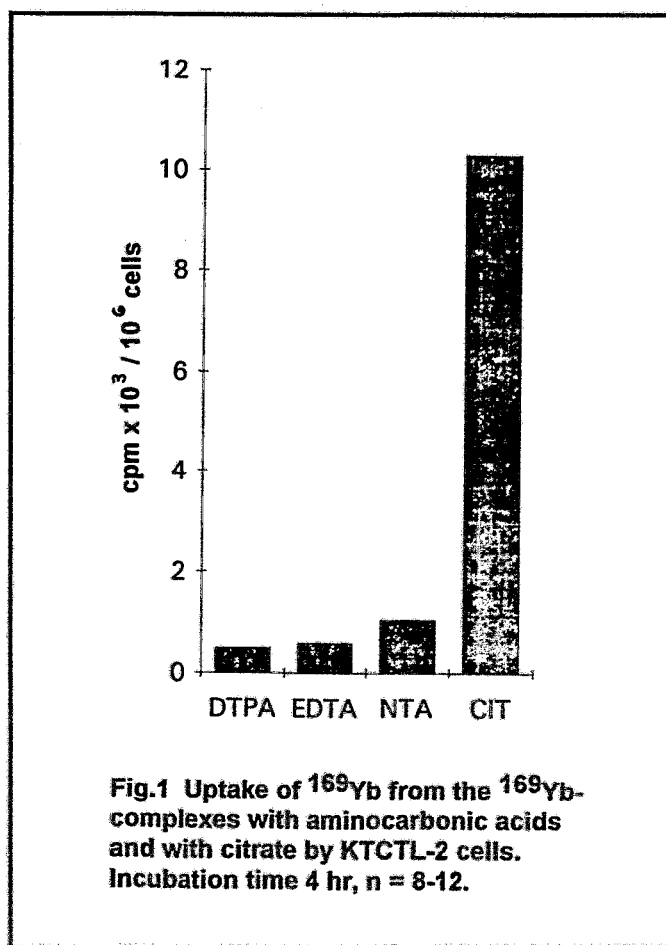CIT < NTA < EDTA < DTPA.
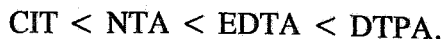
Results and discussion

Our experiments with cultured cells show that the metal complexes with tri, tetra, and pentaacetate belong to a group of compounds from which only a small amount of the metal nuclide is taken up by the cells. The use of carrier-added preparations did not enhance the [169]Yb uptake.

From the citrate complex the radiometal is taken up to a much greater extent. In Fig. 1 the uptake levels are shown for KTCTL-2 cells; analogous results were obtained with V79 cells.

In the complexes studied the ^{169}Yb uptake is clearly related to the complex stability: within the ligand group of the aminocarbonic acids DTPA, EDTA, and NTA the ^{169}Yb uptake into the cells increases with decreasing complex stability. The differences in uptake are not high in this group, but they were reproducible in several experiments.

The citrate complex has the lowest stability among the compounds tested, and it is from this complex that the greatest amount of the metal nuclide is taken up by our cultured cells. It is also known from numerous animal experiments that M^{3+} citrate complexes lead to high M^{3+} uptakes in tumours but also in many normal cells, especially in the highly metabolizing liver cells [2].

When only one metal nuclide is used, as in our case, the ligand species determines the complex stability; with decreasing complex stability the cellular uptake of the metal nuclide increases. This could perhaps be explained by better availability of the metal to the cell, possibly via a transporting compound.

Fig.1 Uptake of ^{169}Yb from the ^{169}Yb-complexes with aminocarbonic acids and with citrate by KTCTL-2 cells. Incubation time 4 hr, n = 8-12.

These results serve to confirm Schomäcker´s suggestion [1] at the cellular level.

References

[1] Schomäcker, K., Thesis, Akademie der Wissenschaften der DDR, 1987

[2] Beyer, G. J. et al., Nucl. Med. Biol. **19** (1992) 201

III.
PUBLICATIONS, LECTURES AND POSTERS

PUBLICATIONS

Uhlemann, E., H. Spies, H.-J. Pietzsch, R. Herzschuh
TcN- und ReN-Komplexe mit Thio-β-diketonen
Z. Naturforsch. **47b** (1992) 1441

Johannsen, B., B. Noll, P. Leibnitz, G. Reck, St. Noll, H. Spies
Technetium and rhenium complexes of mercapto-containing peptides
1. Tc(V) and Re(V) complexes with mercaptoacetyl diglycine (MAG$_2$) and X-ray structure
of AsPh$_4$[TcO(MAG$_2$)] x C$_2$H$_5$OH
Inorg. Chim. Acta **210** (1993) 209

Johannsen, B., B. Noll, P. Leibnitz, G. Reck, St. Noll, H. Spies
Occurence and nature of different Tc(V) and Re(V) complexes with mercapto/amide ligands
Radiochimica Acta **63** (1993) 133

Pietzsch, H.-J., H. Spies, P. Leibnitz, G. Reck, B. Johannsen
Technetium complexes with thioether ligands
Radiochimica Acta **63** (1993) 163

Pietzsch, H.-J., H. Spies, P. Leibnitz, G. Reck
Technetium complexes with thioether ligands
III. Synthesis and structural characterization of cationic nitridotechnetium(V) complexes
with thiacrown ethers
Polyhedron **12** (1993) 2995

LECTURES

Johannsen, B., H.-J. Pietzsch, H. Spies, P. Leibnitz, G. Reck
Technetium complexes with thioether ligands
Topical Symposium on the Behavior and Utilization of Technetium '93, Sendai,
18. - 20. März 1993

Johannsen, B.
Neue Ergebnisse an Technetium/S-Donorligandsystemen
Arbeitstagung IDF Berlin, 1. März 1993

Johannsen, B.
Positron emission tomography: The Rossendorf PET Center
Symposium der Deutschen Technion-Gesellschaft, Dresden,
29.- 30. April 1993,

Johannsen, B.
Review on radioisotope generator systems
IAEA Regional Training Course on Preparation and Control of Radiopharmaceuticals,
Algier, 26. - 30. Juni 1993

Johannsen, B.
Fundamentals and new aspects of technetium chemistry
IAEA Regional Training Course on Preparation and Control of Radiopharmaceuticals
Algier, 26. - 30. Juni 1993

Johannsen, B.
Technetium chemistry applied to radiopharmaceuticals
IAEA Regional Training Course on Preparation and Control of Radiopharmaceuticals
Algier, 26. - 30. Juni 1993

Johannsen, B.
99mTc radiopharmaceuticals: State of the art and forthcoming tracers
IAEA Regional Training Course on Preparation and Control of Radiopharmaceuticals
Algier, 26. - 30. Juni 1993

Johannsen, B.
Mechanisms of up-take
IAEA Regional Training Course on Preparation and Control of Radiopharmaceuticals
Algier, 26. - 30. Juni 1993

Johannsen, B.
Technetium chemistry in radiopharmacology
IAEA Interregional Training Course on Nuclear Medicine,
Berlin 20. Sept. - 15. Okt. 1993

Johannsen, B.
Studies of technetium(V) complexes as relevant to nuclear medicine. Part I.
University of British Columbia, Vancouver, 3. Dezember 1993

Johannsen, B.
The chemistry of Tc/thiol-amide ligand systems
University of Alberta, Edmonton, 6. Dezember 1993

Preusche, St.
Das Rossendorfer PET-Zentrum
Zyklotron-Workshop, FZ Rossendorf, 30. Sept. - 1. Okt. 1993

Spies, H.
Analytischer Bedarf bei der Entwicklung von Technetium-Tracern für die Medizin
BAM, Berlin, 27. Mai 1993

Steinbach, J., B. Johannsen
Das PET-Zentrum Rossendorf
Arbeitstagung "Radiochemie/Radiopharmazie", Deutsche Ges. f. Nuklearmedizin,
Bastei, 13. - 15. Mai 1993

Steinbach, J., B. Johannsen
Setting up a PET centre at Rossendorf
IAEA Interregional Training Course on Nuclear Medicine,
Berlin, 20. Sept. - 15. Okt. 1993

Wagner, G., S. Seifert, A. Eckardt
System for concentration and purification of pertechnetate solutions by chemical methods
IAEA Research Coordination Meeting, Budapest, 8. - 14. Februar 1993

POSTERS

Steinbach, J., B. Johannsen, W.-G. Franke
Radiopharmaceutical research and medical application at Rossendorf: The new PET project
Sixth Symposium on the Medical Application of Cyclotrons, Turku, 31. Mai - 5. Juni 1992

Syhre, R., S. Seifert
Ex-vivo-Bindungsuntersuchungen - eine Möglichkeit der Reduzierung von Tierversuchen im
biologischen Screening von Radiotracern
XXX. GV-SOLAS Tagung, Salzburg, 22. - 25. September 1992

Johannsen, B., B. Noll, P. Leibnitz, G. Reck, St. Noll, H. Spies
Occurence and nature of different Tc(V) and Re(V) complexes with mercapto/amide ligands
Topical Symposium on the Behavior and Utilization of Technetium '93, Sendai,
18. - 20. März 1993

Noll, B., B. Johannsen, St. Noll, H. Spies, P. Leibnitz, G. Reck
Technetium(V)- und Rhenium(V)-Komplexe mit Thiolat/Amid Koordination
24. GDCh-Hauptversammlung, Hamburg, 5. - 11. September 1993

Pietzsch, H.-J., S. Seifert, R. Syhre, H. Spies, B. Johannsen
Technetium(III) complexes with tetradentate thioether ligands: Preparation and preliminary
biological evaluation
Topical Symposium on the Behavior and Utilization of Technetium '93, Sendai,
18. - 20. März 1993

Pietzsch, H.-J., H. Spies, B. Johannsen
Neue kationische Technetiumkomplexe mit Thioether-Liganden: Charakterisierung und
erste biologische Bewertung
Deutsche Gesellschaft für Nuklearmedizin e.V., Jahrestagung, 15. - 17. April 1993

Pietzsch, H.-J., H. Spies, P. Leibnitz, G. Reck, B. Johannsen
Technetiumkomplexe mit mehrzähnigen Thioether-Liganden
24. GDCh-Hauptversammlung, Hamburg, 5. - 11. September 1993

Pietzsch, H.-J., M. Glaser, H. Spies, F. E. Hahn, A. Dittler-Klingemann
Technetium- und Rheniumkomplexe mit Tris-(2-mercaptoethyl)amin
24. GDCh-Hauptversammlung, Hamburg, 5. - 11. September 1993

Seifert, S., L. Lindemann, H. Spies, B. Johannsen, H.-J. Pietzsch, P. Leibnitz, G. Reck
The chemical identity and reactivity of individual technetium(V) and rhenium(V)-meso-
DMSA isomers
Topical Symposium on the Behavior and Utilization of Technetium '93, Sendai,
18. - 20. März 1993

Seifert, S., H.-J. Pietzsch, H. Spies, R. Syhre, B. Johannsen
Isomere Rhenium/Technetium-Komplexe mit 2,3 Dimercaptobernsteinsäure und deren Ester
24. GDCh-Hauptversammlung, Hamburg, 5. - 11. September 1993

Spies, H., H.-J. Pietzsch, R. Syhre, Th. Fietz, B. Johannsen
The 3+1 concept in the synthesis strategy of novel technetium and rhenium tracers
5. Europ. Symp. on Radiopharmacy and Radiopharmaceuticals, Cambridge,
21. - 24. März 1993

Spies, H., Th. Fietz, H.-J. Pietzsch, P. Leibnitz, G. Reck
Neutrale Oxorhenium(V)-Komplexe mit Gemischtligandkoordination
24. GDCh-Hauptversammlung, Hamburg, 5. - 11. September 1993

Spies, H., S. Seifert, B. Johannsen, H.-J. Pietzsch
Stereochemistry and unusual isomerization of DMSA complexes
4th Intern. Symp. Chelating Agents in Pharmacology, Toxicology and Therapeutics,
Pilsen, 3. - 5. August 1993

IV.
SCIENTIFIC COOPERATION

In multidisciplinary research such as carried out by this Institute, collaboration, the sharing of advanced equipment, and above all, exchanges of ideas and information obviously play an important role. Effective collaboration has been established with colleagues at universities, in research centres and hospitals.

Cooperative relations and joint projects

The *Technische Universität Dresden* (Dr. Scheller, Dr. Klostermann, Inst. of Analytical Chemistry) plays an essential part in SPECT tracer research by performing analytical characterization of new tracers and providing support with the synthesis of organic compounds (Dr. Habicher, Inst. of Organic Chemistry).

Common objects of radiopharmacological and medical research link the Institute with the *Universitätsklinikum "Carl Gustav Carus"*, above all with its Departments of Nuclear Medicine (Prof. Franke), Psychiatry (Prof. Felber), and Neurology (Prof. Kunadt). A joint team of staff members from both the Institute and the Clinic of Nuclear Medicine are currently working at the Rossendorf PET centre.

Very effective cooperation also exists with the *Bundesanstalt für Materialforschung Berlin* (Dr. Reck, Mr. Leibnitz) who have carried out X-ray crystal structure analyses of new technetium and rhenium complexes.

Our long-standing cooperation with the *University of Padua* (Prof. Mazzi) and the *"Demokritos" National Research Centre for Physical Sciences* in Athens (Dr. Chiotellis) has now been instrumental in advancing the chemistry of thioether complexes.

Joint work on technetium complexes with tripodal ligands has been carried out with the *Freie Universität Berlin* (Prof. Hahn, Inst. of Inorganic and Analytical Chemistry).

Cooperation on a special research topic concerning technetium tracers is in progress with the *Forschungszentrum Jülich* (Prof. Stöcklin).

Identification of common objects in radiopharmacy has led to collaborative research with the *Humboldt-Universität Berlin* (Dr. Michael of the "Charité" Hospitals, Clinic of Nuclear Medicine) and the *Universität Leipzig* (Dr. Günther, Radiology, Nuclear Medicine).

V.
MEETINGS HELD

First Meeting of the DGN Group of Radiochemistry and Radiopharmacy

In March 1992 the German Society of Nuclear Medicine, DGN, set up its Working Group of Radiochemistry and Radiopharmacy (headed by B. Johannsen, Rossendorf) to provide a suitable forum for scientists who are mainly engaged in the synthesis and characterization of radioactive compounds relevant to nuclear medicine. The objectives of the Group are dissemination of information, exchanges of ideas and specific radiochemical results, promotion of cooperation among individual members and institutions, particularly in Europe, addressing all radiochemical and radiopharmaceutical issues that may be relevant to nuclear medicine, and further education. To help achieve these objectives, regular meetings will be held under the auspices of the DGN.

The Group convened for the first time at the Bastei hotel near Dresden on 13 - 15 May 1993.

The meeting, sponsored by the radiopharmaceutical industry and by the Research Center Rossendorf, was attended by 75 participants from Germany, Austria and Switzerland. It covered three areas of work:

The first session was held under the aspect of education, with reviews on the pharmacological fundamentals of receptors, PET tracers for neurotransmitter systems, and clinical relevance of receptor SPECT, presented by G. Lambrecht (Frankfurt), K. Herholz (Cologne) and H.-J. Biersack (Bonn) as invited speakers.

The second scientific session, dealing primarily with halogen-labelled compounds for diagnostics and therapy, was opened by G. Stöcklin (Jülich) with an invited review on radiohalogenation-radiochemistry and pharmacology. Seven additional presentations and an intensive and fruitful discussion covered current activities - results and problems - in connection with ^{211}At, ^{123}I, and ^{18}F labelling. Seven free papers dealt with the setting up of a PET centre, ^{11}C precursors and products, synthesis of ^{73,75}Se compounds and ^{99m}Tc compounds, including ligand synthesis.

The third session, devoted to questions of quality control, documentation and the handling of radioactive waste in a radiochemical laboratory, addressed tasks and issues radiochemists are faced with in routine work.

IAEA Study Tour to Rossendorf

As a contribution to the IAEA Interregional Training Course on Nuclear Medicine for Developing Countries, held in Berlin between 20 September - 15 October 1993 (organized by H. Deckart), a visit to Rossendorf served to acquaint the participants with the Rossendorf research reactor and the set-up of a PET centre. The programme included lectures by B. Johannsen, P. Liewers and J. Steinbach, and visits to the facilities.

VI.
SEMINARS

Prof. H. Bartunik, MPG-Arbeitsgruppe Hamburg
Biologische und medizinische Anwendungen der Synchrotronstrahlung
16. Dezember 1992

Prof. M. Weiß, Maetin-Luther-Universität Halle
Anwendung der Verweilzeittheorie in der Pharmakokinetik
15. Januar 1993

OA Dr. R. Aurisch, Humboldt-Universität Berlin
Nuklearmedizinische Herzdiagnostik in der Vor-PET-Phase
26. Februar 1993

Prof. F. E. Hahn, FU Berlin
Koordinationschemie tripodaler Liganden
5. März 1993

Prof. E. Uhlemann, Universität Potsdam
Koordinationschemie des Vanadiums (aus bioanorganischer Sicht)
23. April 1993

Dr. Nebeling, KFA Jülich
Generelle Aspekte bei der Herstellung von PET-Tracern
21. Mai 1993

Dr. Knoop, Medizinische Hochschule Hannover
Neue Entwicklungstendenzen von PET-Scannern;
Leistungsparameter, Quantifizierbarkeit und Qualitätskontrolle
3. Juni 1993

Prof. C. Orvig, University of British Columbia, Vancouver
Medicine and Inorganic Chemistry - Vanadium and Diadetes
8. Juni 1993

Prof. Herrmann, Medizinische Akademie Dresden
Strahleneffekte der Lunge - Forschungsschwerpunkt und Kooperationsmöglichkeit?
24. Juni 1993

Prof. Diemer, Universität Kopenhagen
The role of glutamate transmission in focal and global ischemia
9. September 1993

Prof. Subramanian, State University of New York, Syracuse
What is new in radiopharmaceuticals?
1. Oktober 1993

Prof. H. H. Coenen, Universität Essen
Markierte Aminosäuren für PET und SPECT
11. Oktober 1993

Dr. K. Deutsch, Mallinckrodt Medical Inc., St. Louis
The chemistry underlying some new Mallinckrodt radiopharmaceutical products
18. Oktober 1993

Dr. K. Klostermann, TU Dresden
Massenspektrometrie: Grundlagen und Anwendung
19. November 1993

VII.

ACKNOWLEDGEMENTS FOR FINANCIAL AND MATERIAL SUPPORT